

UNIVERSITY OF OKLAHOMA

GRADUATE COLLEGE

A PROTOTYPE COMPUTERIZED SYNTHESIS METHODOLOGY
FOR GENERIC SPACE ACCESS VEHICLE (SAV)
CONCEPTUAL DESIGN

A DISSERTATION

SUBMITTED TO THE GRADUATE FACULTY

in partial fulfillment of the requirements for the

degree of

Doctor of Philosophy

By

XIAO HUANG
Norman, Oklahoma
2006

UMI Number: 3212013



UMI Microform 3212013

Copyright 2006 by ProQuest Information and Learning Company.
All rights reserved. This microform edition is protected against
unauthorized copying under Title 17, United States Code.

ProQuest Information and Learning Company
300 North Zeeb Road
P.O. Box 1346
Ann Arbor, MI 48106-1346

A PROTOTYPE COMPUTERIZED SYNTHESIS METHODOLOGY
FOR GENERIC SPACE ACCESS VEHICLE (SAV)
CONCEPTUAL DESIGN

A DISSERTATION APPROVED FOR THE
SCHOOL OF AEROSPACE AND MECHANICAL ENGINEERING

BY

Dr. Bernd Chudoba (Chair)

Dr. Alfred G. Striz (Chair)

Dr. Sesh Commuri

Dr. Zahed Siddique

Dr. Yunjun Xu

ACKNOWLEDGMENTS

I express my sincere thanks to my advisor Dr. Bernd Chudoba for his generous advice, encouragement, and continuous support throughout the progress of this research. His strong design knowledge and experience in aerospace vehicle conceptual design greatly accelerated my research. The available of extensive design data, information, experience, and knowledge of past and present aerospace projects in his personal database made my effort much easier. The quality of this research is significantly improved because of his thorough reading of the dissertation and open discussion of ideas.

Special thanks to Dr. Alfred G. Striz for kindly consenting to serve as co-chairman on my dissertation committee and providing valuable and constructive suggestions. Acknowledgments are also due Dr. Zahed Siddique, Dr. Yunjun Xu, Dr. Sesh Commuri, for serving as members of my doctoral advisory committee.

I would like to acknowledge the contributions of other Aerospace Vehicle Design (AVD) Laboratory members, and especially Paul Czysz for his guidance and valuable suggestions to the overall success of the research project. The students (Kiran Pippalapalli, Gary Coleman, Andy Huizenga, Andy N. Ferguson, Kristen N. Roberts, Amit R. Oza, Bradley D. Mixon, Bryan D. Mixon) have been with me throughout my graduate program and their friendship, and assistance have enriched my graduate study at The University of Oklahoma.

I would like to dedicate this dissertation to all members of my family, my dear father, Dr. Yubin Huang, my loving mother, Mrs. Songying Liu, my beloved wife, Min Luo, my brother, Dr. Xin Huang, and my cousin, Dr. Jiesheng Kang, who believe in me and provide unconditional support and constant encouragement. This work could not have been completed without their love, understanding, patience, and sacrifices.

This research was partially supported by TGV Rockets, Inc., Rocketplane, Inc., and SpiritWing Aviation. Financial assistance provided by the School of Aerospace and Mechanical Engineering (AME) at The University of Oklahoma is also gratefully acknowledged.

TABLE OF CONTENTS

ACKNOWLEDGMENTS	iv
LIST OF FIGURES	ix
LIST OF TABLES	xiv
NOTATION	xvi
ABSTRACT	xxiv
1. Introduction and Objectives.....	1
1.1 Introduction.....	1
1.2 Objectives.....	14
1.3 Research Strategy.....	20
2. Space Access Vehicle Design and Synthesis Systems.....	27
2.1 Space Access Vehicle (SAV)	27
2.2 Characteristics of Space Access Vehicle (SAV) Conceptual Design	27
2.3 Definition and Classifications of Design Synthesis Methodologies.....	30
2.4 An Assessment of Design Synthesis Systems	33
2.4.1 Mathematical Modeling of a Synthesis System	42
2.4.2 Multidisciplinary Analysis and Optimization	44
2.4.3 Knowledge-Based System.....	47
2.4.4 Generic Concepts	49
2.5 AVDS-SAV Development Requirements	51
3. Design Knowledge, Primary Design Disciplines and Methods Library.....	54
3.1 Design Knowledge Base - KBS^{DESIGN}	54
3.2 Primary Design Disciplines	62
3.2.1 Weight and Sizing.....	64
3.2.2 Propulsion	67
3.2.3 Aerodynamics	69
3.2.4 Stability and Control	74
3.2.5 Aerothermodynamics	77
3.2.6 Trajectory	80
3.2.7 Life-Cycle Cost	83

4. A Generic Space Access Vehicle Design Methodology	87
4.1 Generic Methodology Development.....	89
4.2 Alternative Methodology Concepts Towards a Generic SAV Synthesis System.....	91
4.3 Design Synthesis Methodology for Baseline Vehicle – HTHL.....	94
4.3.1 Takeoff.....	104
4.3.2 Ascent.....	130
4.3.3 Reentry	154
4.3.4 Approach and Landing.....	180
4.3.5 Design Space Screening and Design Convergence.....	200
4.4 Extension of the HTHL Methodology to VTVL Vehicles	210
5. Application of HTHL Design Methodology	214
5.1 HTHL Baseline Vehicle Description.....	219
5.1.1 Geometry Estimation	219
5.1.2 Weight Estimation.....	220
5.2 Disciplinary Analysis	225
5.2.1 Atmosphere	225
5.2.2 Aerodynamics	226
5.2.3 Stability and Control	228
5.2.4 Propulsion	230
5.2.5 Aerothermodynamics	231
5.3 Design Synthesis Process	232
5.3.1 Takeoff.....	232
5.3.2 Ascent.....	238
5.3.3 Reentry	243
5.3.4 Approach and Landing.....	247
5.3.5 Design Space Screening.....	252
5.4 Cost Analysis.....	255
6. Contribution Summary and Recommendations.....	260
6.1 Summary	260
6.2 Recommendations	265
Appendices.....	282
Appendix A Geometric Characteristics of OU XP Configuration.....	283
Appendix B SAV Design Methodologies.....	288

Appendix C Aerodynamic Method.....	296
Appendix D Cost Models – Transcost and Suborb-Transcost.....	299
Appendix E VDK Sizing Code.....	303
Appendix F SpaceShipOne Case Study.....	307
Appendix G Program User’s Guide.....	310

LIST OF FIGURES

Figure 1: Space transportation infrastructure.	2
Figure 2: Design status of the emerging generation of reusable space access vehicles.	7
Figure 3: Qualitative design space comparisons.	8
Figure 4: Design freedom, knowledge, cost of change, and MDO at CD, PD, and DD levels	10
Figure 5: A typical non-consistent SAV conceptual design methodology.	11
Figure 6: Space access vehicle (SAV) concepts.	14
Figure 7: AVDS ^{HYP} - a generic CD methodology approach	16
Figure 8: Generic configuration concept capability characteristics of the prototype SAV synthesis methodology.	17
Figure 9: Overview and interrelation of the (a) “Hands-on” and (b) Computer-integrated SAV design synthesis methodology.	19
Figure 10: Concentric evolution spheres representing the research strategy selected.	21
Figure 11: Roadmap for generic SAV conceptual design methodology.	25
Figure 12: Evaluation process of design synthesis systems.	34
Figure 13: Number of synthesis systems vs. development time period	35
Figure 14: Synthesis system vs. developers.	35
Figure 15: Synthesis system vs. design applications	36
Figure 16: Design methodology of spacecraft and its launch vehicle by K.D. Wood	37
Figure 17: Hypersonic vehicle design methodology by Paul Czysz	38
Figure 18: Design methodology for space transportation systems by Walter E. Hammond	39
Figure 19: Hypersonic air-breathing vehicle design methodology by James L. Hunt.	40
Figure 20: A ‘cockpit’ product development framework environment.	55
Figure 21: DBS – a dedicated aerospace conceptual design dynamic data-base system.	56
Figure 22: IBS – a dedicated aerospace conceptual design dynamic information-base system.	59
Figure 23: ML – a dedicated aerospace methods library integrated into AVDS-PrADO	61
Figure 24: Methodology for developing a generic SAV design synthesis system	90
Figure 25: Generic SAV mission profile.	93
Figure 26: Top level mission type approach design methodology for a HTHL SAV.	96
Figure 27: Detailed design methodology for each mission segment; shown here the take-off methodology.	97
Figure 28: Detailed break-down of analysis methods utilized for the take-off mission segment example.	98

Figure 29: SAV concepts from NASA hypersonic research programs.	100
Figure 30: Definition of takeoff field length.....	105
Figure 31: Ground run of aircraft takeoff phase.....	111
Figure 32: Takeoff rotation and transition	113
Figure 33: Takeoff geometry at vehicle rotation velocity	115
Figure 34: Design synthesis process for takeoff phase of a HTHL SAV vehicle.....	119
Figure 35: Drag polars of four wings from MDC methods.	121
Figure 36: Two engine jet aircraft FAR25 takeoff field length with engine failure.....	123
Figure 37: Variation of takeoff distance requirement with different wings.	124
Figure 38: Required takeoff thrust for different trim mechanisms.....	124
Figure 39: Takeoff length sizing of Supersonic Vehicles.	125
Figure 40: Variation of takeoff field length with wing sweep angle.	126
Figure 41: Variation of wing loading with sweep angles.....	127
Figure 42: Takeoff speed and nose wheel lift-off speed for different swept wings.....	128
Figure 43: Takeoff climb gradient requirement.	128
Figure 44: Angle of climb with altitude for OU XP Jet and Rocket Engines (GE engine).....	129
Figure 45: Rate of climb with altitude for OU XP Jet and Rocket Engines (GE engine).	130
Figure 46: Typical human tolerance to directions of acceleration	136
Figure 47: Structural materials for high speed aircraft.....	138
Figure 48: Energy height contour and design constraints.	139
Figure 49: Energy height contour for suborbital space tourism mission.....	142
Figure 50: CD design synthesis process for sizing of suborbital space tourism vehicle	144
Figure 51: Contours of minimum fuel energy climb trajectory for OU XP utilizing rocket power .	147
Figure 52: Contours of minimum fuel energy climb trajectory for OU XP utilizing jet power.	147
Figure 53: Comparison of minimum fuel trajectory and maximum q trajectory.	148
Figure 54: Variation of dynamic pressure with altitude for minimum fuel trajectory	149
Figure 55: Variation of flight speed with altitude for minimum fuel trajectory	149
Figure 56: Iterations of propellant weight.....	150
Figure 57: Variation of weight with flight speed for minimum fuel trajectory.....	151
Figure 58: Variation of fuel consumption with altitude for minimum fuel trajectory	151
Figure 59: Variation of altitude with time for minimum fuel trajectory and maximum q trajectory.	152

Figure 60: Variation of axial acceleration with time for minimum fuel trajectory.....	153
Figure 61: Variation of flight speed with time for minimum fuel trajectory	153
Figure 62: SpaceShipOne flight trajectory. ¹⁶⁷	154
Figure 63: Typical human tolerance to directions of accelerations by FAA-CAMI.....	160
Figure 64: Aerodynamic forces and thrust in inertial frame.	164
Figure 65: Ballistic entry of space tourism vehicle.....	166
Figure 66: Ground flight path of space tourism vehicle.	169
Figure 67: Gliding of space tourism vehicle.....	169
Figure 68: Design synthesis process for re-entry phase of suborbital space tourism vehicle.....	172
Figure 69: Variation of deceleration with altitude for ballistic entry of suborbital vehicle.....	174
Figure 70: Variation of velocity with altitude for ballistic entry of suborbital vehicle.	174
Figure 71: Lift/drag ratios and ballistic coefficient values for typical lifting vehicles.	175
Figure 72: Variation of deceleration with altitude for different flight paths.	176
Figure 73: Variation of deceleration with altitude for different ballistic parameter $m/(C_D * S)$	177
Figure 74: Variation of velocity with altitude for different ballistic parameter $m/(C_D * S)$	177
Figure 75: Design space for ballistic entry of suborbital vehicle.....	179
Figure 76: Approach and landing of the Space Shuttle.	182
Figure 77: FAR landing field length requirements.	183
Figure 78: Typical landing trajectory of space vehicles.	188
Figure 79: Landing flare approximation as circular arc.....	191
Figure 80: Design synthesis process for landing phase of a HTHL SAV.	193
Figure 81: Wing loading vs. maximum lift coefficient.....	196
Figure 82: Wing loading vs. aspect ratio based on Peckham method.....	197
Figure 83: Wing loading vs. aspect ratio based on Krienes method.	197
Figure 84: Wing loading vs. aspect ratio with consideration of leading edge vortex lift.	198
Figure 85: Thrust to weight ratio vs. wing loading.	198
Figure 86: Design space contours of transonic, supersonic and hypersonic configuration concepts by D. Kücherman.....	201
Figure 87: Torenbeek's general design procedure	202
Figure 88: Feasible design space example	206
Figure 89: Overall design space possibilities of SAV concepts.....	208
Figure 90: Design space for specific configuration example	209

Figure 91: Capability extension of HTHL methodology to combined HTHL/VTVL and HTHL/VTVL/VTHL methodologies	211
Figure 92: Comparison of analysis complexity throughout the abstract mission profile for HTHL and VTVL space access vehicle configuration concepts	213
Figure 93: Nominal trajectory with 3 minutes micro-gravity at 100 km apogee	215
Figure 94: Baseline OU XP based on Learjet 24. Status: March 2004	216
Figure 95: Design process of hands-on methodology.	218
Figure 96: SAV_HASA Excel program for geometry and weight estimations.	223
Figure 97: Aerodynamics analysis using MDC handbook methods	226
Figure 98: Drag polar of OU XP with 70° LE sweep.	227
Figure 99: Wind tunnel results of two supersonic fighters	228
Figure 100: Analysis process of digital DATCOM.....	230
Figure 101: Multidisciplinary design analysis of takeoff segment.....	233
Figure 102: Calculation of takeoff field length and nose liftoff speed	234
Figure 103: T/W requirement for initial climb and second segment climb	234
Figure 104: Required takeoff thrust for different trim mechanisms.....	235
Figure 105: Wing loading.	236
Figure 106: Takeoff field length.	236
Figure 107: Takeoff speed and nose wheel liftoff speed	237
Figure 108: Takeoff climb gradient requirement	238
Figure 109: Multidisciplinary design analysis of ascent segment	239
Figure 110: Minimum fuel trajectory and design constraints	240
Figure 111: Iterations of propellant weight of OU XP	241
Figure 112: Variation of dynamic pressure with altitude for minimum fuel trajectory of OU XP ..	242
Figure 113: Variation of flight speed with altitude for minimum fuel trajectory of OU XP	242
Figure 114: Variation of axial acceleration with time for minimum fuel trajectory of OU XP	243
Figure 115: Multidisciplinary design analysis of reentry segment	244
Figure 116: SAV_REENTRY program for reentry analysis	245
Figure 117: Design space for ballistic entry of OU XP	246
Figure 118: Variation of deceleration with altitude.....	247
Figure 119: Multidisciplinary design analysis of landing segment.	248
Figure 120: Excel programs for landing analysis	249

Figure 121: T/W requirement for the missed approach climb.....	250
Figure 122: Wing loading vs. maximum lift coefficient.....	251
Figure 123: Landing missed approach climb gradient requirement.....	252
Figure 124: Excel program for design space screening	253
Figure 125: Design space of two possible SAV concepts	254
Figure 126: Total launch prices for several suborbital vehicles.....	256
Figure 127: Total launch prices for several suborbital vehicles.....	257
Figure 128: Ticket prices for several suborbital vehicles	257
Figure 129: Overview of hands-on HTHL SAV design synthesis methodology.....	259

LIST OF TABLES

Table 1: Road map for development of design methodology	20
Table 2: Classification and characteristics of aerospace design synthesis approach.....	32
Table 3: Selected SAV concepts for the development of SAV HTHL design methodology	57
Table 4: Key disciplines involved in SAV design synthesis systems	63
Table 5: Weight and sizing analysis modules for SAV conceptual design	65
Table 6: Propulsion analysis modules for SAV conceptual design.....	67
Table 7: Aerodynamic analysis modules for SAV conceptual design.....	70
Table 8: Aerodynamic analysis methods for hypersonic aerospace vehicle design. ⁹⁰	73
Table 9: Stability and control analysis modules for SAV conceptual design	75
Table 10: Aerothermodynamics analysis modules for SAV conceptual design.....	78
Table 11: Trajectory analysis modules for SAV conceptual design.....	82
Table 12: Comparison of cost models	85
Table 13: Selected supersonic, hypersonic and SAV vehicles.....	103
Table 14: Design analysis methods for takeoff study.	106
Table 15: Design parameters required for reduced order model of takeoff design methodology.	109
Table 16: Design constraints imposed on vehicle takeoff requirements by FAR Part 25.....	110
Table 17: Takeoff performance data of some supersonic vehicles.	122
Table 18: Design analysis methods for ascent study.	131
Table 19: Design parameters required for reduced order model of ascent design methodology.	135
Table 20: Design constraints imposed on suborbital tourism vehicle ascent flight.	138
Table 21: Design analysis methods for reentry study.....	156
Table 22: Design parameters required for reduced order model of reentry design methodology.	159
Table 23: Design constraints imposed on suborbital tourism vehicle reentry flight.....	162
Table 24: Design analysis methods for landing performance study.	184
Table 25: Design parameters required for reduced order model of landing design methodology.	187
Table 26: Design constraints imposed on vehicle landing requirements by FAR Part 25.....	187
Table 27: Landing performance data of some space access vehicles	194
Table 28: Landing performance data of some supersonic vehicles	195

Table 29: A comparison study of analysis results with flight data of the Space Shuttle.....	199
Table 30: Geometry, mass, and propulsion parameters of six reference aircraft configurations	205
Table 31: Mission requirements and design requirements.....	219
Table 32: Geometry characteristics of OUXP.....	220
Table 33: Weight ratio of different propellant combinations.....	222
Table 34: Weight estimation of OUXP.....	224
Table 35: OU XP jet and rocket engines characteristics.....	231
Table 36: Industrial capability index, technology indices of OU XP and TGV Michelle-B.....	253
Table 37: Some suborbital flight vehicles.....	255
Table 38: Overall development contributions for the generic SAV design synthesis methodology.	264
Table 39: Design capability of PrADO	267

NOTATION

ABBREVIATIONS

AAA	Advanced Aircraft Analysis
CD	Conceptual Design
DD	Detail Design
DBS	Database System
DMS	Database Management System
DOC	Direct Operation Cost
ELV	Expendable Launch Vehicle
ESA	Energy State Approximation
FAA	Federal Aviation Administration
FAR	Federal Aviation Regulations
GBS	Gradient Based Method
HTHL	Horizontal Takeoff and Horizontal Landing
ICI	Industrial Capability Index
KB	Knowledge Base
KBS	Knowledge-Based System
LEO	Low Earth Orbit
LCC	Life Cycle Cost
MDO	Multidisciplinary Design Optimization
MSTO	Multiple Stages To Orbit
PD	Preliminary Design
PrADO	Preliminary Aircraft Design and Optimization
RLV	Reusable Launch Vehicle
RSM	Response Surface Method
SAV	Space Access Vehicle
SBA	Simulation-Based Acquisition
SBA-SE	Simulation-Based Acquisition Synthesis Environment

SSTO	Single Stage To Orbit
TAD	Technology Available Date
TPS	Thermal Protection System
TSTO	Two Stages To Orbit
VLM	Vortex Lattice Method
VTVL	Vertical Takeoff and Vertical Landing
VTBL	Vertical Takeoff and Ballistic Landing
VTHL	Vertical Takeoff and Horizontal Landing

SYMBOLS

a	acceleration
AR	aspect ratio
b	span
\bar{c}	mean aerodynamic chord
C_D	drag coefficient
C_{D_o}	drag coefficient for zero angle of attack
C_{D_α}	variation of drag coefficient with angle of attack
C_{D_q}	variation of aircraft drag coefficient with pitch rate
$C_{L_{T0}}$	lift coefficient at V_R on the ground in ground effect
C_{D_G}	drag coefficient at V_R on the ground in ground effect
C_l	rolling moment coefficient
C_{l_o}	rolling moment for zero angle of attack
C_{l_β}	variation of rolling moment coefficient with angle of sideslip
C_{l_p}	variation of aircraft rolling moment coefficient with roll rate

C_{l_r}	variation of aircraft rolling moment coefficient with yaw rate
C_L	lift coefficient
$C_{L,A}$	landing lift coefficient
C_{L_o}	lift coefficient for zero angle of attack
C_{L_o}	lift coefficient for zero angle of attack
$C_{L_{\max}}$	maximum lift coefficient
C_{L_q}	variation of aircraft lift coefficient with pitch rate
C_m	pitching moment coefficient
$C_{m_{cg}}$	pitching moment about c.g from pitch control surfaces
C_{m_o}	pitching moment coefficient for zero angle of attack
C_{m_α}	variation of pitching moment coefficient with angle of attack
C_{m_q}	variation of aircraft pitching moment coefficient with pitch rate
C_n	yawing moment coefficient
C_{n_o}	yawing moment coefficient for zero angle of attack
C_{n_β}	variation of yawing moment coefficient with angle of sideslip
C_{n_p}	variation of aircraft yawing moment coefficient with roll rate
C_{n_r}	variation of aircraft yawing moment coefficient with yaw rate
C_Y	side force coefficient
C_{Y_β}	variation of side force coefficient with angle of sideslip
C_{Y_o}	side force coefficient for zero angle of attack
C_{Y_p}	variation of aircraft sideforce coefficient with roll rate

C_{Y_r}	variation of aircraft sideforce coefficient with yaw rate
D	drag
E	energy per unit mass
f	fuel flow rate
F_T	component of the propulsive forces along the velocity vector
F_N	component orthogonal to it in the lift-drag plane
g	acceleration due to gravity
h	height absolute altitude
H	scale height of the atmosphere
I_p	propulsion technology index
I_{sp}	specific impulse
I_{str}	structure technology index
K_1	correction factor non-linear acceleration (≈ 1.04)
K_2	correction factor average drag during ground roll (≈ 0.3 to 0.5)
L	lift
L/D	aerodynamic efficiency
m	mass
$m/(C_D * S)$	ballistic coefficient
M	mach number
n	load factor
O/F	oxidizer/fuel ratio
p_0	sea level atmospheric pressure
q	vehicle dynamic pressure $= 1/2 \rho(V)^2$
p, q, r	scalar components of $\bar{\omega}$ in F_B

$\dot{p}, \dot{q}, \dot{r}$	rate of change of angular velocity in F_B
\dot{Q}	stagnation heat transfer rate
r	distance between the vehicle position and the origin of inertial system
R	radius of pull-up at rotation
R_e	radius of earth
R_n	a function of the vehicle's fineness ratio
S	wing reference area
S_F	flare distance
S_G	ground deceleration distance
S_L	landing distance
S_{plan}	planform area
S_{wet}	wetted area
t	time
Δt_R	time to rotate the aircraft
T	thrust
T / W	thrust to weight ratio
T_{VAC}	vacuum thrust
T_{SL}	sea level thrust
T_0	stagnation temperature
T_∞	atmosphere temperature
T_x, T_y, T_z	scalar components of \bar{T}
U, V, W	scalar velocity components of \bar{V}

\overline{V}	vehicle velocity vector
V_A	approach speed
V_L	landing speed
V_{LOF}	lift off velocity
V_{NWLO}	nose wheel lift off speed
V_R	rotation velocity
V_s	stall speed
V_{total}	vehicle total volume
V_{TD}	touch down speed
V_1	decision speed
V_2	takeoff safety speed
W	vehicle weight
W_f	payload weight
W_L	landing weight
W_{GT}	takeoff weight
W_E	operational empty weight
W_{str}	structure weight
WR	weight ratio
W / S	wing loading
\dot{W}	propellant flow rate
X	down range in the ground plane
X_g	ground run distance from rest to the point of lift-off
$X_{g to}$	takeoff ground distance

X_{OB}	distance from nose lift off over takeoff obstacle
$X_{R\ to}$	distance covered in the time to rotate the aircraft
ΔX_R	horizontal distance of pull-up rotation along the runway
X_{stop}	acceleration to stop distance
Y	cross range in the ground plane
ΔZ_R	vertical distance of pull-up rotation perpendicular to the runway
α	angle of attack
β	side slip angle
γ	flight path angle
ρ	air density
ρ_{ppl}	propellant density
ρ_{sl}	atmospheric density at sea level (0.002377 slug / ft ³)
ε	angle between thrust axis and zero-lift axis
σ	bank angle
σ'	ratio of atmospheric density at altitude to the density at sea level
ψ	heading angle
ϕ	rotation angle
ω	angular velocity
μ	braking coefficient
μ_{eff}	effective rolling coefficient
τ	küchemann tau, volume index

SUBSCRIPTS

VAC	vacuum value
SL	sea level value
Prop	propulsion value
0	initial condition
f	final condition

SUPERSCRIPTS

b	body frame system
E	inertial system

ABSTRACT

Today's and especially tomorrow's competitive launch vehicle design environment requires the development of a dedicated generic Space Access Vehicle (SAV) design methodology. A total of 115 industrial, research, and academic aircraft, helicopter, missile, and launch vehicle design synthesis methodologies have been evaluated. As the survey indicates, each synthesis methodology tends to focus on a specific flight vehicle configuration, thus precluding the key capability to systematically compare flight vehicle design alternatives. The aim of the research investigation is to provide decision-making bodies and the practicing engineer a design process and tool box for robust modeling and simulation of flight vehicles where the ultimate performance characteristics may hinge on numerical subtleties. This will enable the designer of a SAV for the first time to consistently compare different classes of SAV configurations on an impartial basis.

This dissertation presents the development steps required towards a generic (configuration independent) hands-on flight vehicle conceptual design synthesis methodology. This process is developed such that it can be applied to any flight vehicle class if desired. In the present context, the methodology has been put into operation for the conceptual design of a tourist Space Access Vehicle. The case study illustrates elements of the design methodology & algorithm for the class of Horizontal Takeoff and Horizontal Landing (HTHL) SAVs. The HTHL SAV design application clearly outlines how the conceptual design process can be centrally organized, executed and documented with focus on design transparency, physical understanding and the capability to reproduce results. This approach offers the project lead and creative design team a

management process and tool which iteratively refines the individual design logic chosen, leading to mature design methods and algorithms. As illustrated, the HTHL SAV hands-on design methodology offers growth potential in that the same methodology can be continually updated and extended to other SAV configuration concepts, such as the Vertical Takeoff and Vertical Landing (VTVL) SAV class. Having developed, validated and calibrated the methodology for HTHL designs in the ‘hands-on’ mode, the report provides an outlook how the methodology will be integrated into a prototype computerized design synthesis software AVDS-PrADO^{SAV} in a follow-on step.

1. Introduction and Objectives

1.1 Introduction

Space exploration requires a cost effective and efficient space transportation system which not only delivers people, equipment, and supplies to and from orbit for scientific study, but also serves as a platform for space commerce, such as space tourism. A space transportation infrastructure has to integrate various modes of space travel, requiring specific technologies, equipment, and transportation management strategies. A top-level space transportation infrastructure is illustrated in Figure 1. The three inter-related top level domains are the *management domain*, *technology domain*, and *operation domain*.

First, the *management domain* is required to plan improvements leading to a business plan, investment strategies and decision processes. In today's highly dynamic business environment, a space transportation system requires quick adaptation to competitive space exploration initiatives. The management domain is required to monitor the status of the operational and technology domains by defining investment strategies and processes.

The *technology domain* is primarily responsible to manage the design and manufacturing of the space access vehicle (SAV). Its focus is on utilizing available design experience, design methodologies and design tools leading to the manufacture of an affordable and safe SAV. Overall, the technology domain is the core element of the transportation infrastructure since it has to prove technical feasibility.

The *operation domain* is required to implement all activities related to ground handling, launch, and mission monitoring. Compared to other transportation systems such as railroad, shipping, and aviation, the operational processes characteristic for a space transportation system are complex and expensive. The current cost for transporting a payload via the space shuttle into orbit is around \$10,000/lb compared to \$1/lb for the Boeing 747 transporting goods over large distances in the atmosphere.

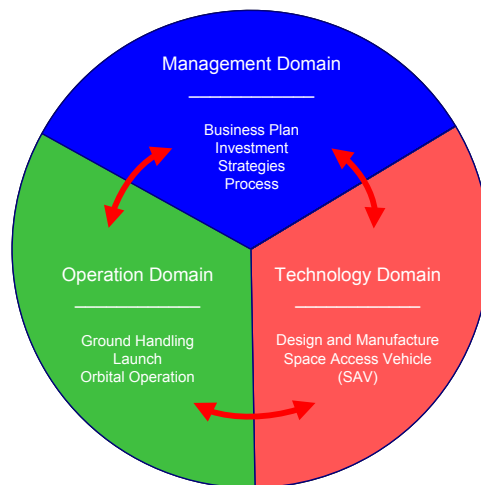


Figure 1: Space transportation infrastructure.

An efficient space transportation infrastructure requires the ability to rapidly define, create, and deploy flexible business solutions to meet the continually increasing space transportation demands through the integration of the three domains, see Figure 1. However, existing program management practices, funding procedures, personnel

practices, and non-integrated technical processes are not capable of supporting an efficient nationwide space exploration infrastructure. With the renewed emphasis on space exploration (President Bush's vision on Jan 14th, 2004), it is necessary to provide the decision making bodies with a top-level simulation tool capable of visualizing the interrelations among requirements, tasks, schedules, risks, investments, and budget. In general, the Simulation-Based Acquisition (SBA) process aims to provide industries, operators and research environments with a robust collaborative simulation technology that is integrated across acquisition phases and programs. Thus, SBA is an integrated system acquisition model which can provide immediate and continuous process information throughout the system life cycle from initial mission requirements to system retirement.¹ The concept of SBA has successfully demonstrated to be a robust modeling and simulation environment across acquisition phases and projects, such as Boeing's 777 and JSF. Clearly, the next-generation space transportation infrastructure demands a well-integrated **Simulation-Based Acquisition Synthesis Environment (SBA-SE)**, which is capable of modeling the space transportation system life-cycle consisting of management, launch vehicle technology and operation. To achieve this goal, an advanced **Simulation-Based Acquisition Synthesis Environment (SBA-SE)** process is currently under development at the AVD Lab, The University of Texas at Arlington. The status of the SBA-SE is described in Ref. 2.

In this dissertation, only one key element of the **Simulation-Based Acquisition Synthesis Environment (SBA-SE)**, the design of the SAV in the technical domain, is discussed. Today, the managerial, technical, and operational domains of space

transportation become more refined. However, the development future of a reliable and affordable space access vehicle is still uncertain. Without the availability of a reliable and cost-effective SAV, it is not possible to build an efficient space transportation infrastructure which has to be compared against the metrics as experienced for commercial transport aircraft operation. Until now, expendable launch vehicles (ELVs) together with the partially reusable Space Shuttle system have been the primary space-access transportation means. One reason that the launch cost of the Space Shuttle is too high is because the flight rate is way too low. Taking those lessons learned into account, it is desirable to have a SAV available to enable safer, lower cost and faster turn-around missions. Consequently, today's and especially tomorrow's competitive launch vehicle design environments require the development of a dedicated generic space access vehicle design and synthesis methodology, capable of comparing expendable launch design alternatives with the family of reusable launch vehicle alternatives.

One century ago, Sir George Cayley (England, 1773-1857) established an aircraft design archetype which has been named *Cayley's Design Paradigm*.³ This paradigm assumes that all design functions such as lift, propulsion, stability & control, and payload volume are distributed over distinctly different hardware and subsystems. The premise has been that only first order, weak and linear couplings link these subsystems and their functions. Then, each subsystem can be optimized independently within its function. Overall, this approach has endured for more than a century in aerospace vehicle design; thus, it is now opportune to revisit and update his work today.

Modern aerospace flight vehicles have to respond to the continuous development pressure imposed by civil, military, and research customers. Only superior aerospace flying machines endure this unforgiving marketplace. Taking today's flight vehicle performance expectation into account, *Cayley's Design Paradigm* appears to have reached its limits of applicability. Those limitations materialize in the fact, that the traditional approach rather locks the majority of design decisions and solutions at subsystem level, thereby missing the opportunity to assess them in the global context at system level. For example, conventional aircraft of the dis-integrated B707 configuration concept type (distinct propulsion system, distinct lift-generation element, distinct volume-supply element, and distinct stability & control elements) can be designed by optimizing subsystems primarily in isolation. However, such approach misses the opportunity to explore top-level multi-disciplinary coupling-effects of subsystems at system level with the aim to 'close' or 'converge' the overall design. Until today, most aircraft and space access vehicle designs, processes and tools, are still following this rather limiting and therefore out-dated design principle. It is time for this to change!

As mentioned above, *Cayley's Design Paradigm* is still being applied to the design of today's highly evolved transonic aircraft configuration concepts, the new generation of highly demanding reusable space access vehicles, and consequently to the underlying design processes and tools. This, however, leads to an erroneous representation of the design solution space truly available. Clearly, a successful total system is not the assembly of a number of individually optimized sub-systems, but a system optimum is the sum of subsystems that yields the optimum system.⁴

$$\text{Optimum System} \neq \sum_i^j \text{Optimum Components}$$

This usually results into a significant interdependence between subsystems. Clearly, a seemingly trivial subsystem can significantly affect the overall system optimum. Having understood the importance of systems engineering for flight vehicle development⁵, it becomes obvious to devise and engage design processes capable of dealing with multi-disciplinary design decision-making beyond the design resolution central to *Cayley's Design Paradigm*.

The extensive design experience available with tube & wing transonic aircraft designs compensates, to some degree, for this apparent weakness seen with today's design approach. This, however, often leads to the definition of sub-optimal transonic designs obviously showing technical feasibility and performance in the overall design space, but having missed to respond with precision to the available business case. Then, according to the metrics of the aerospace business, the main distinguishing variable between competing designs finally becomes 'customer satisfaction', a design facet often not accurately represented and quantified with the available flight vehicle design space visualization capability. In contrast, the emerging class of reusable SAVs is far less forgiving. For those vehicles, only a limited design data-base is available directing the design team towards the feasible design space. To complicate matters, the design resolution required for future SAVs immediately invalidates *Cayley's Design Paradigm*, a paradigm which has been successfully applied throughout the first century of flight.

Having reviewed the state of the art in flight vehicle synthesis processes and tools as documented in Chapter 2 from References 6 and 7, the importance of advancing today's design practices towards truly integrated synthesis environments becomes obvious. Required is a capable flight vehicle design solution space screening and proof-of-design-convergence capability. For the class of highly integrated reusable space access vehicles, we observe the systematic failing of today's deficient conceptual design tool-box.^{6,8,9} Obviously, attempts to reliably quantify the design space for reusable SAVs have consistently failed, as the track-record of cancelled and failed SAV demonstrator projects indicates, see Figure 2. Although dated, Derek Wood's account on *Project Cancelled – British Aircraft That Never Flew*¹⁰ comes to mind in striking analogy, highlighting the enduring difficulty of the project management team to perform up-front and informed 'business case screening'!



Figure 2: Design status of the emerging generation of reusable space access vehicles.

Our failure to arrive at a successful SAV demonstrates our inability to reliably quantify the existence of the feasible solution design space. Figure 3 qualitatively

compares the design spaces of surface transportation with air and space transportation. In general, the available design space for two-dimensional surface-transportation, as exemplified with the car, tends to be largest due to its functional simplicity.¹¹ Compared with the aircraft class, which operates at a higher complexity level (operation in three dimensions), the feasible design space tends to be far more constrained, thus reduced in space. This fact is quickly understood when surveying the number of test flight crews lost per year testing rather ‘conventional aircraft’. In contrast, the design space for reusable SAVs shrinks significantly compared to all other man-made transportation vehicles. As mentioned earlier, the design sensitivities to design for a positive payload to orbit are driven by the corresponding relationships among subsystems, in particular numeric subtleties amongst design parameters.

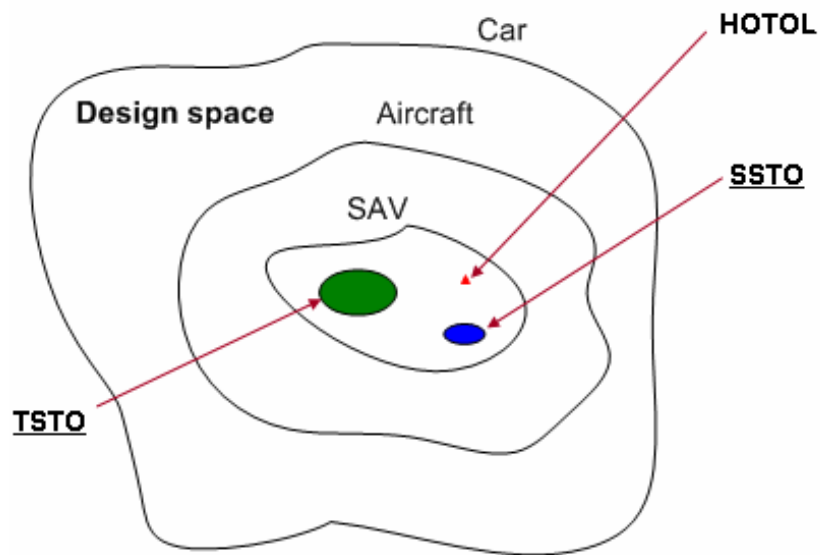


Figure 3: Qualitative design space comparisons.

Clearly, design methodologies and tools exploiting *Cayley’s Design Paradigm* are not capable of probing or approving inter-subsystem couplings, finally leading to a reliable

picture of the gross design space. We have seen too many space launcher studies and projects failing where the baseline configuration geometry has been drawn, frozen, and analyzed too early, eliminating the opportunity to trade different launch concepts against each other. In particular, amongst the SAV concepts, the single-stage-to-orbit (SSTO) notion obviously resides within the smallest design space, a potential which modern engineering has not yet been able to tab. Both, the British *HOTOL* and US *Venture Star* fell victim to the fact that the design apparently was outside the feasible design space possibly without being noticed by the design team due to the low resolution of the design synthesis process in place.¹¹

In general, the location, shape, and size of the design space of a prospective SAV design is initially not known to the design team. In general, it is the responsibility of the conceptual design group to reliably determine the feasible design space of either aircraft (e.g., UAV, transonic transport, SSBJ) or SAV (e.g., HTHL, VTVL, VTHL, SSTO, TSTO) as early as possible during the conceptual design phase. Still, what engineers do and how they do it largely determines the success rate of the product. Thus, we need to seriously rethink our engineering approach. As a consequence, the AVD Lab is developing a generic flight vehicle synthesis process consisting of (a) *hands-on methodology* and (b) *computer-integrated methodology*.

The flight vehicle design process is, in general, comprised of three sequential design phases: conceptual design, preliminary design, and detailed design. The sequence starts with a set of requirements for a new flight vehicle. The first step towards a flight worthy

vehicle is the definition of a configuration concept during the CD phase. This design phase is of utmost importance since around 80% of the configuration is determined at this stage. Most importantly, the life-cycle cost of the flight vehicle has to be calculated reliably during the CD phase due to adverse cost implications otherwise, see Figure 4. As the design evolves, the design freedom decays rapidly throughout the PD and DD phases while the knowledge about the product obviously continually increases.⁶ As a consequence, the present study describes one element of the design toolbox under development which focuses on the development of a hands-on generic design synthesis tool relevant for the CD phase.

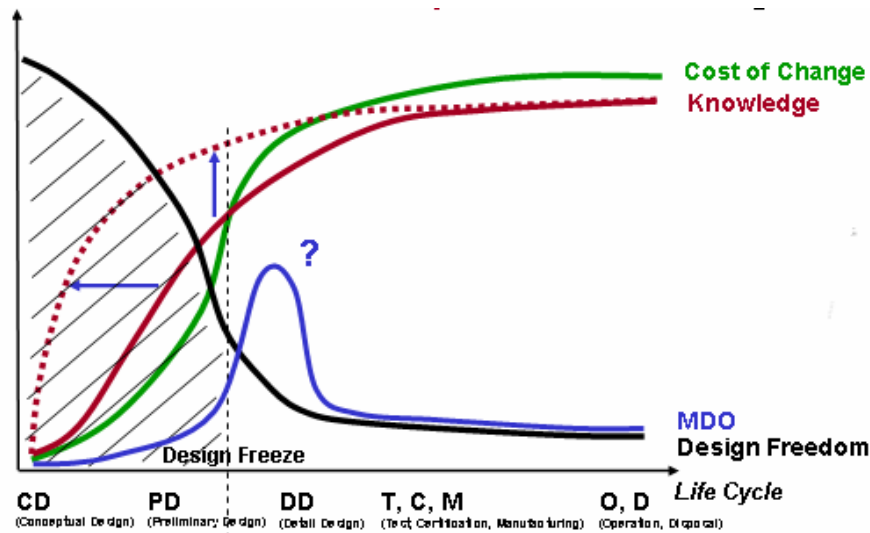


Figure 4: Design freedom, knowledge, cost of change, and MDO at CD, PD, and DD levels.²

A typical SAV conceptual design methodology scheme is exemplified with NASA Langley's approach shown in Figure 5. The current theme is to integrate readily available high-fidelity analysis tools into a software integration framework like *ModelCenter* provided by Phoenix Integration, Inc. As Figure 5 clearly indicates, the analysis tools assigned to distinct analysis disciplines are preliminary design to detail design software

packages, tools generally *not* suitable for the conceptual design (CD) task. Although the figure may indicate interrelations between analysis disciplines, there is an apparent weakness to precisely describe the design logic, the design process with a breakdown of sequence of events, the detailed data exchange between disciplines, and others. More importantly, the difficulty to systematically execute the prescribed design process in an organized manner results in the problem of not being able to reliably reproduce the final design deliverable. This, consequently, results in a high-risk product and low-transparency product evolution history, both for the design team utilizing the method, the method originators, and as well the project manager.

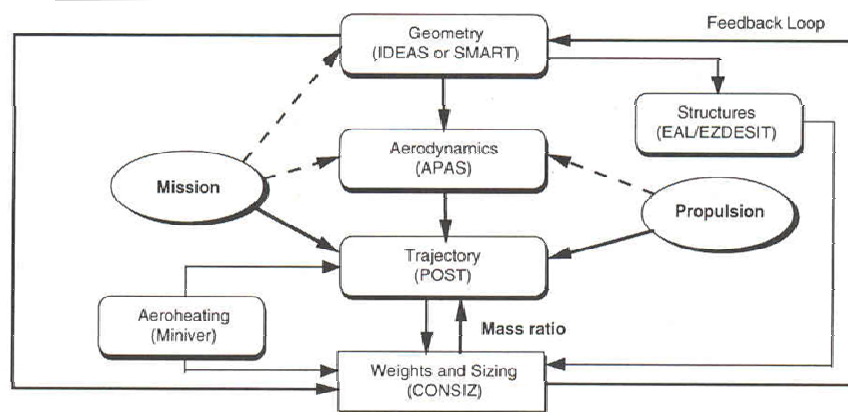


Fig. 2.10 Example of actual vehicle conceptual design process; APAS = Aerodynamic Preliminary Analysis System, CONSIZ = Configuration Sizing weights/sizing package, POST = Program to Optimize Simulated Trajectories, and SMART = Solid Modeling Aerospace Research Tool. (Courtesy: Vehicle Analysis Branch, NASA Langley Research Center.)

Figure 5: A typical non-consistent SAV conceptual design methodology.¹²

As identified earlier⁶, some level of design randomness appears to be a typical side-effect to the creative design process, ultimately hurting the credibility of the SAV design team as abbreviated with Figure 2. A well-known consequence of this deficiency is the attempt to compare the flight vehicle design process with *creative arts* when saying: “...

you know, aircraft design is an art ...”, ultimately a realization of the apparent shortcomings of the process involved and its compensation with the involvement of emotion and chance. It shows that the second century of flight demands a rationalization of the design process in order to produce an *Anatomy of Space-Access Vehicle Design Successes*.¹¹

Having reviewed more than 125 aircraft, helicopter, and SAV design strategies, methodologies, and processes^{6,7}, we have observed an apparent weakness to reliably communicate, document, and execute the design progression employed for aircraft, but in particular SAVs. This applies to both, the computer dis-integrated and computer integrated design processes. Also, the lack of modern conceptual design (CD) tools, particularly for SAV applications, unfortunately leads to the utilization of higher-fidelity analysis tools during the CD phase, processes not being capable of design space screening and incompetent to deliver a proof of design convergence. Clearly, under those circumstances, the design team has lost its opportunity to resourcefully trade configuration concepts using a consistent toolbox resulting in visualization of a narrow band of configuration trades only. We have seen too often design teams “... *falling in love with a flight vehicle geometry too early and successively analyzing it to death with high-fidelity tools.*”²

Since 1960, multidisciplinary optimization technology and computerized synthesis systems (such as Space Shuttle Synthesis Program, 1970) have been gradually adopted by aircraft design manufacturers particularly during the conceptual design phase. Experience

shows that the use and development of synthesis programs has greatly improved interdisciplinary communication since it has been shown to reduce design cycle time leading to deeper exploration of the design space.¹³ The synthesis and multidisciplinary optimization technology helps to converge the design. Today, the development of a computer-based integration platform or system is a highly demanding subject. Airbus has selected PACE¹⁴ to develop an integration tool common to all Airbus partners. NASA starts to develop a new synthesis system named CDS.¹⁵ Boeing and others are also very active in this field.²

It is a challenging task to develop a design synthesis system for space access vehicles due to the limited statistical data base available, a fact especially valid for the class of reusable launch vehicles (RLV). The development of a generic SAV synthesis methodology aims to assess and compare prospective SAV design configuration concepts by evaluating potential advances in technology and investigating different operational modes. Therefore, a large number of concepts need to be generated to meet the given mission requirements.¹⁶ As shown in Figure 6, several operational modes for Space Access Vehicle (SAV) concepts are developed: vertical takeoff and vertical landing (VTVL), *DC-X*; vertical takeoff and horizontal landing (VTHL), *X-33*; and horizontal takeoff and horizontal landing (HTHL) vehicle, *X-30*. Since future space access vehicles have to be more cost effective compared to today's generation of SAVs, a consistent and systematic design approach and system is required for the top level assessment of various SAVs, enabling true technical comparisons upfront.

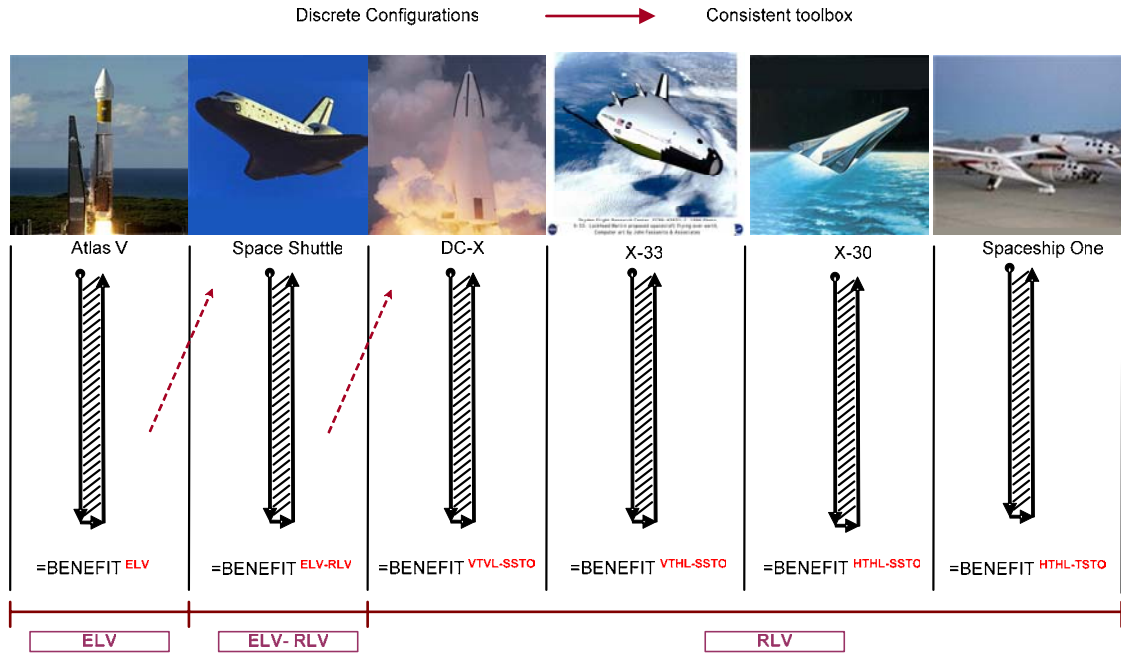


Figure 6: Space access vehicle (SAV) concepts.

1.2 Objectives

The future generation of space access vehicles has to be cost effective in comparison to today's family of expendable launchers and the remaining fleet of Space Shuttles¹⁷. A consistent and systematic design approach and design system is required for top level assessment of various SAV design and mission alternatives especially during the conceptual design phase. Developing a generic SAV conceptual design methodology, which allows for all vehicle types, is the key. In addition, it is the conceptual design phase which has the most profound effect on the success of the resulting SAV.¹⁸ A generic CD methodology will enable the designer to fully explore the design space available as early as possible in the design process, to ensure that the final product can

operate efficient by fulfill the mission specified.¹⁹ This idea of a generic CD methodology is the basis for the new design paradigm proposed.

Figure 7 prescribes a three-tier design space screening approach devised by the AVD Laboratory in order to solidify this foundation.²⁰ The *Tier 1* screening step is a technique which identifies the solution design space based on historical experience, key design parameters, and available industrial manufacturing and technology capability. It is used to assess the realm of possible solutions for an initial start configuration. In this way, the design space ('ballpark') for a particular configuration will be mapped. The output of Tier 1 is then subjected to an analysis from a physical perspective in *Tier 2*, which maps the design space based on physically correct and robust analysis techniques. Having reduced the solution design space with Tier 1 and 2, *Tier 3* is finally activated. This step offers a higher-fidelity computational analysis, further assessing and reducing the design space. Tier 3 will arrive at a converged conceptual design of the SAV start configuration. This logic 3-tier approach embodies a unique but highly effective conceptual design process leading towards successful SAVs.

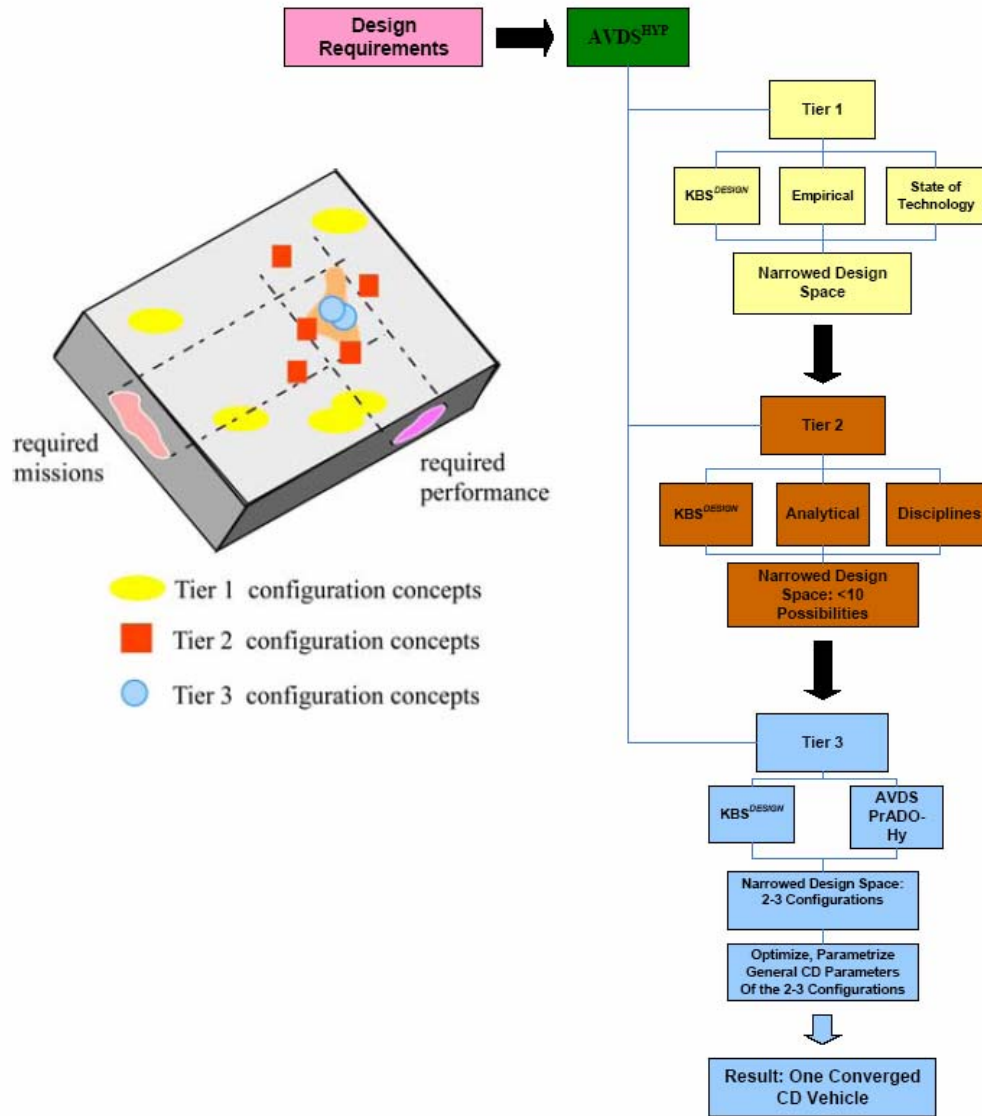


Figure 7: AVDS^{HYP} - a generic CD methodology approach.²⁰

In this context, the present research investigation focuses on the *Tier 2* step – a highly involved physical and analytical approach to narrowing the design space. To achieve this goal, a prototype hands-on and computerized synthesis methodology for the generic (configuration independent) design of SAVs was initiated at the AVD Laboratory at The University of Oklahoma and is currently under development at the AVD Laboratory, The

University of Texas at Arlington.^{17,21} Based on a given mission specification, this methodology is capable of assessing and comparing different SAV configuration concepts, is competent to define the design space required and available, and finally arrives at a converged design proposal for each configuration concept. As a result, characteristics like design features, operational implications, risk scenarios, and cost implications can be discussed for alternative SAV design proposals, providing the practicing engineer and project manager a transparent, thus, powerful decision tool. This will, for the first time, make available to the SAV design environment a structured multi-disciplinary decision support process and toolset, which enables a consistent comparison of different classes of SAV configuration concepts on an impartial basis as shown in Figure 8.

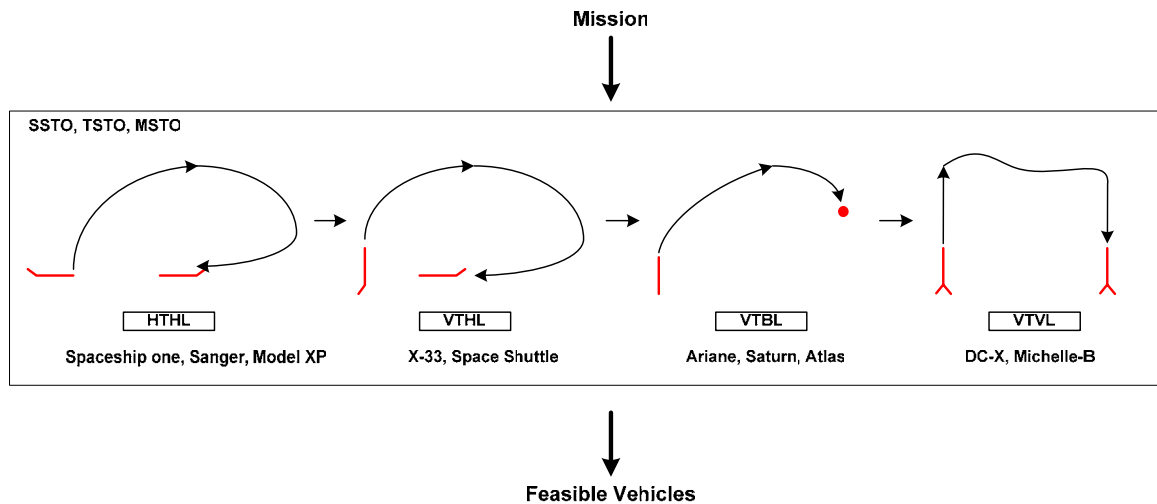


Figure 8: Generic configuration concept capability characteristics of the prototype SAV synthesis methodology.

The research objectives for the development of a generic SAV conceptual design methodology are:

1. Identify physical characteristics of possible SAVs and methodology concepts leading to a generic SAV design system
2. Evaluate current aerospace vehicle design synthesis systems
3. Compile a dedicated SAV design knowledge-based system KBS^{DESIGN}
4. Develop and validate a generic design methodology and algorithms for the conceptual design of SAVs which can efficiently define the design space and deliver a converged design
5. Implement the design algorithms to the standalone computer programs
6. Integrate the design methodology into a computerized design synthesis system - AVDS-PrADO

The development of the generic SAV methodology will be accomplished in two steps; the (a) ‘hands-on’ methodology, and (b) computer-integrated methodology, see Figure 9. Figure 9 illustrates the targeted generic design capability at the heart of the SAV design tool and process. First, the hands-on ‘manual’ methodology is developed and populated with relevant disciplinary methods. The individual methods are validated and calibrated using design case studies like those indicated in Figure 8. Having assembled a well documented and validated process, which can be executed in the traditional ‘hands-on’ mode, this algorithm will be integrated into the computerized design synthesis system AVDS-PrADO.^{7,17,22}, a task which is beyond the current research undertaking. This will lead to a dedicated synthesis system for the analysis and design of SAVs, where generic and more rigorous disciplinary engineering analysis methods are integrated into a truly multi-disciplinary synthesis environment offering state-of-the-art optimization and

visualization capability. Therefore, this dissertation describes the thought process, development steps, and validation of the *Hands-On Design Methodology* leading to the generic synthesis process for the conceptual design (CD) of space access vehicles (SAV).

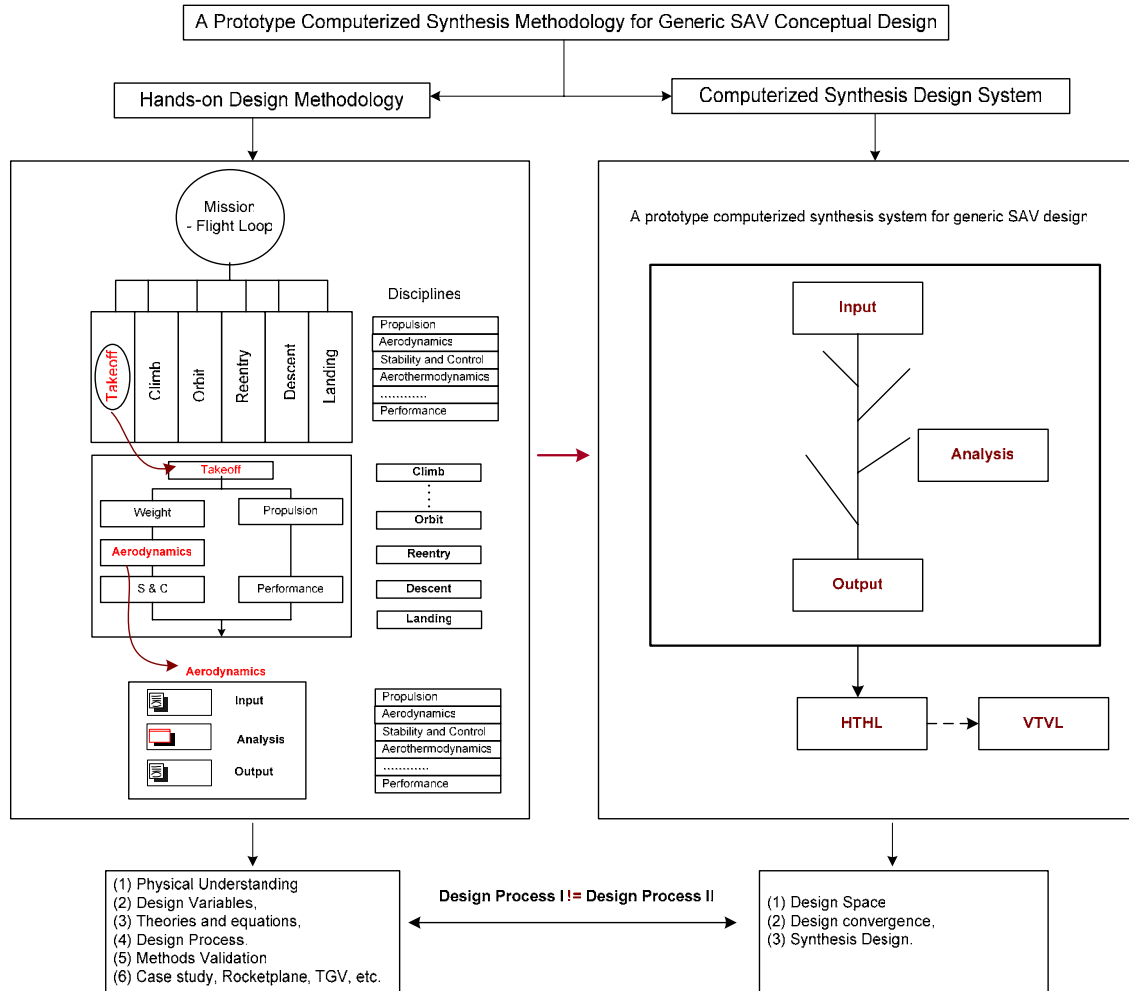


Figure 9: Overview and interrelation of the (a) “Hands-on” and (b) Computer-integrated SAV design synthesis methodology.

The systematic approach towards the development of the generic design synthesis methodology is presented in Table 1. For each engineering discipline of interest, the systematic approach addresses physical explanations, the survey of all relevant design methods, the identification of key design parameters, theory development, method

validation, and finally design case studies. The parameter identification and reduced-order method development processes are based on the knowledge-based system KBS^{DESIGN} which include 100 year design experience, references and validated methods relevant for the conceptual design of aerospace vehicles.

Table 1: Road map for development of design methodology

Development Process	Takeoff	Ascent	Reentry	Approach/Landing
Physical explanation	Chapter 4.3.1	Chapter 4.3.2	Chapter 4.3.3	Chapter 4.3.4
Design methods survey	Chapter 4.3.1 A	Chapter 4.3.2 A	Chapter 4.3.3 A	Chapter 4.3.4 A
Design parameter reduction	Chapter 4.3.1 A	Chapter 4.3.2 A	Chapter 4.3.3 A	Chapter 4.3.4 A
Design constraints	Chapter 4.3.1 A	Chapter 4.3.2 A	Chapter 4.3.3 A	Chapter 4.3.4 A
Theory development	Chapter 4.3.1 B	Chapter 4.3.2 B	Chapter 4.3.3 B	Chapter 4.3.4 B
Validation	Chapter 4.3.1 C	Chapter 4.3.2 C	Chapter 4.3.3 C	Chapter 4.3.4 C
Design case studies	Chapter 4.3.1 C	Chapter 4.3.2 C	Chapter 4.3.3 C	Chapter 4.3.4 C

1.3 Research Strategy

The research strategy selected adopts the approach devised for the development of the generic stability and control methodology for conventional and unconventional aircraft configurations as documented in Reference 6. We have learned from this research project that the challenge to develop a generic methodology, in the present context the generic conceptual design SAV synthesis methodology, is a highly demanding multi-disciplinary task. Only a decidedly disciplined approach to the problem can lead to the acclaimed objectives. In order to do so, we have to investigate SAV design processes, evaluate existing design synthesis systems, assemble SAV-related design knowledge, finally leading to the development of the generic SAV methodology. Figure 10 sketches the research strategy conceived for the present research investigation.

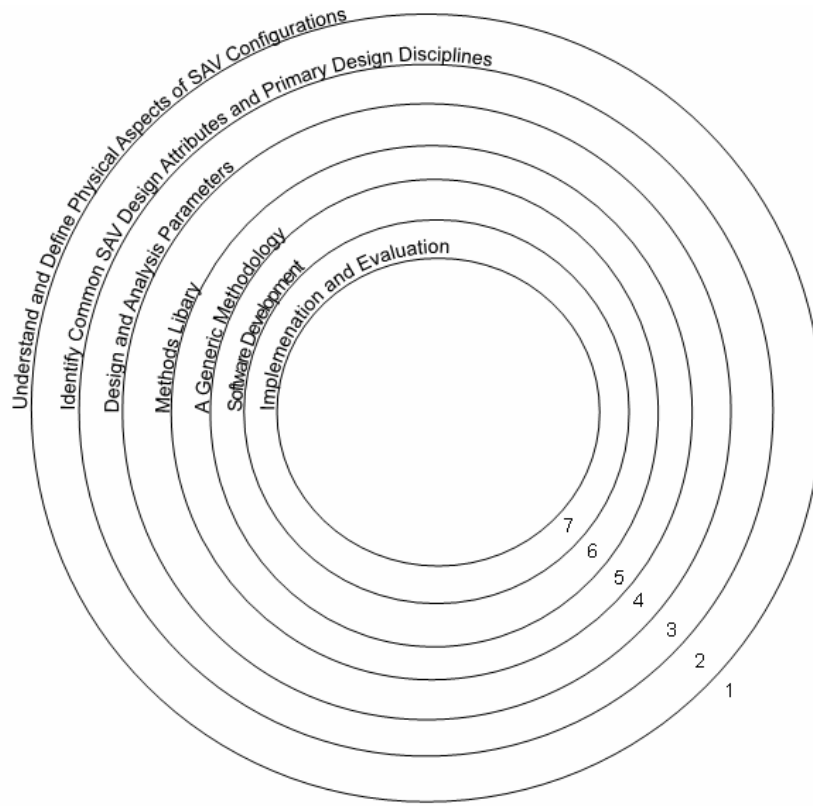


Figure 10: Concentric evolution spheres representing the research strategy selected

The modus operandi is presented via concentric spheres, where the work sequence proceeds from the outer to the inner layers. The process starts from the complete technology domain, passes in a pre-specified sequence various filtering levels until the space access vehicle conceptual design relevant knowledge is sufficiently assembled. The process ends when the methodology concept conceived will be evaluated against the research objectives specified above. Each layer of the concentric evolution sphere (parameter reduction process), as applied within the present research undertaking, is characterized below.

(1) Familiarization with Physical Aspects of SAV Configuration Concepts: The SAV design database system and dedicated design knowledge-based system are assembled during this phase. This step has to be considered the key preparatory activity since it aims to prepare for the integration of both, expendable launch vehicle and reusable launch vehicle design alternatives, into one generic model. The design commonalities and peculiarities of relevant SAV design alternatives are identified and documented at this point. The approach of utilizing first-order methods and procedures based on physical principles is adopted as follows. A comprehensive experience data base is available describing design and operation of modern ELVs. However, RLV design underlies the limitation of only having a sparse statistical database available. Therefore, it is necessary to clearly understand the basic physical characteristics of RLV design alternatives without prioritizing any specific RLV design configuration concept at this point. The focus is on physical correctness leading to simple reduced-order representations of gross design parameters from performance, propulsion, aerodynamics, and others, design disciplines common to all SAV alternatives. Such first order characterization is then translated into a consistent methodology concept relevant for the conceptual design level. This will enable the SAV designer *for the first time* to consistently assess SAV design alternatives leading to a final comparison of design configuration concept options. This leads to a first-order, physically correct, generic SAV sizing methodology capable of rapidly predicting the trends and sensitivities of competing SAV alternatives.

(2) Identify Common and Uncommon SAV Design Attributes and Individual Design Disciplines: Published SAV design approaches are analyzed to identify common and

uncommon SAV design attributes for individual design disciplines. The design logic selected for these individual approaches mirrors the variety in attempts towards a feasible SAV. Obviously it is of importance to have analyzed representative SAV alternatives (e.g., SSTO: X-33, Hotol; TSTO: Sanger) and to document them in the dedicated SAV DBS and KBS.

(3) Identification of Design and Analysis Parameters: The gross design parameters for the range of representative SAVs have been identified for building the generic analytical model according to the range of individual design disciplines (e.g., performance, aerodynamics, propulsion). The identification and extraction process of global design parameters represents a key activity throughout the research period. With completion of this level, an informed methodology development can be attempted.

(4) Methods Library: With the previous understanding of SAV designs, the input and output parameters of each primary design discipline are defined. For each discipline, a methods library is assembled consisting of either a generic method or rather more problem oriented stand-alone methods requiring method switching. The methods are the core of this engineering analysis process since they connect the earlier defined gross design parameters mathematically. Clearly, the method translates the physical design aspect into a problem solving process.

(5) Generic Methodology: For comparison of competing configurations, a consistent set of design and estimation methods is required. A generic design methodology is

developed applicable to all SAV alternatives. It can carry out consistent top level assessments of various SAVs enabling true technical comparisons. This allows designers to compare radically different alternative SAVs to achieve the goal of reduced cost and complexity, improved performance, efficiency, and reliability for space transportation.

(6) Software Development: The generic SAV methodology is developed and assembled in two successive steps: (a) ‘hands-on’ stand-alone software; (b) methodology integrated into AVDS-PrADO in a follow-on step.

(7) Validation and Calibration: The disciplinary analysis methods, modules, and overall methodology need to be validated before integration into the synthesis system AVDS-PrADO. The databases (DBS and KBS) compiled during Phase 1 have to provide data, information, and knowledge to support the validation effort for individual design disciplines and the synthesized SAV.

Figure 11 shows the roadmap which summarizes the key development steps of this research strategy. This roadmap is systematically followed throughout the present research investigation with the aim to arrive at a generic SAV design methodology. Further details and explanations are given in the individual chapters.

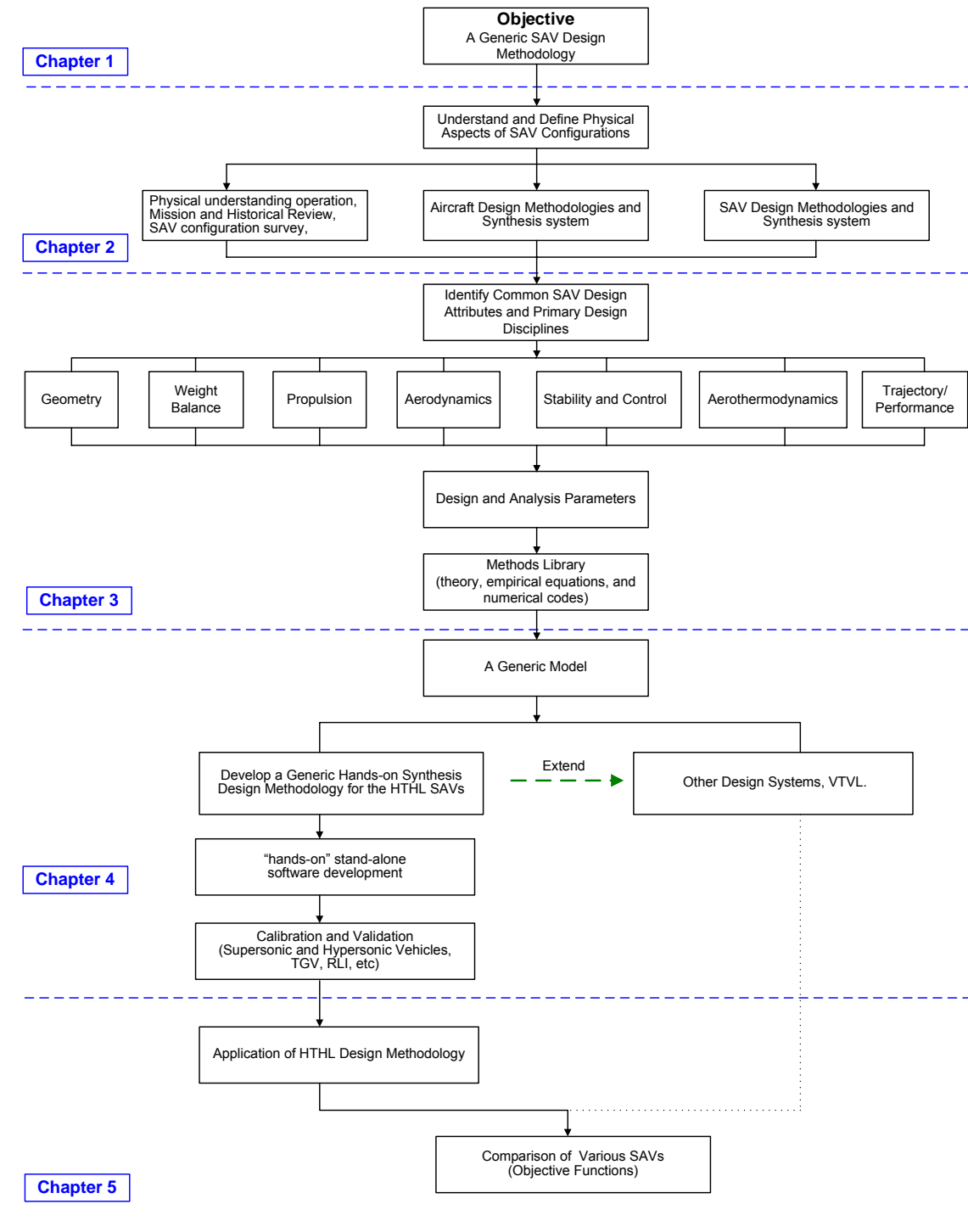


Figure 11: Roadmap for generic SAV conceptual design methodology.

The dissertation is organized as follows. Chapter 1 outlines the current SAV conceptual design problem, followed by the definition of research objectives and scope. A systematic research and development strategy towards the generic SAV design capability is presented. Chapter 2 provides at first an assessment of hypothetical and actual space access vehicles. The physical understanding related to the variety of SAV configuration concepts is obtained. A survey and discussion of aircraft and launch vehicle design methodologies makes it possible to identify the advantages and disadvantages of past and current synthesis systems. As a consequence, a specification for a dedicated generic SAV conceptual design methodology is formulated. The design knowledge, primary disciplines, associated method libraries, and design parameters related to SAV conceptual design are assembled in Chapter 3. Chapter 4 presents the thought process and necessary steps required for the development of a prototype synthesis methodology for generic SAV conceptual design. A hands-on generic synthesis methodology throughout the typical SAV flight loop (*takeoff, ascent, reentry, descent and landing*) is developed. An outlook towards the implementation of the VTVL logic into the ‘hands-on’ design methodology is provided. Chapter 5 shows a design case study which applied this methodology to an industrial tourist SAV *OUXP*. Finally, the dissertation concludes with the contributions summary in Chapter 6. The software development strategy is also presented to implement this hand-on design methodology into the synthesis environment AVDS-PrADO^{SAV}.

2. Space Access Vehicle Design and Synthesis Systems

2.1 Space Access Vehicle (SAV)

Currently, there are many hypothetical and actual space access vehicle concepts. The SAV concepts can be classified by the (a) types of flight mission like low earth orbit (LEO), orbital and interplanetary flights, or the (b) operational modes: horizontal takeoff and horizontal landing (HTHL), vertical takeoff and horizontal landing (VTHL), and vertical takeoff and vertical landing (VTVL), or the (c) number of stages: single stage to orbit (SSTO), two stage to orbit (TSTO), and multiple stage to orbit (MSTO) or the (d) reusability: reusable launch vehicle (RLV) and expendable launch vehicle (ELV).

All SAV design systems have two common objectives. The first is to design a feasible concept that can fulfill the flight mission. A space access vehicle uses propulsion power to overcome gravity and aerodynamic drag force in order to deliver a payload to orbit and return safely. Secondly, at the engineering level, it is necessary to optimize the vehicle for performance and cost figures of merit.

2.2 Characteristics of Space Access Vehicle (SAV) Conceptual Design

The flight vehicle design process is, in general, comprised of three sequential design phases: conceptual design (CD), preliminary design (PD), and detailed design (DD). The sequence starts with a set of requirements for a new flight vehicle. The first step towards a flight vehicle is the definition of a configuration concept during the CD phase. This design phase is key since it can be assumed that around 80% of the configuration is

determined at this phase. Most importantly, the life cycle cost of the flight vehicle has to be determined reliably during the CD phase since it is very costly to change the overall configuration beyond the CD stage.¹⁶ As the design evolves, the design freedom decays rapidly in the PD and DD phases while the knowledge about the product continually increases. As a consequence, the present study focuses on the development of a generic design synthesis tool relevant for the CD phase.

The conceptual design (CD) phase determines the general size and type of the configuration concept leading to the space access vehicle. In general, the next generation reusable launch vehicle, such as horizontal takeoff and horizontal landing (HTHL), is a highly integrated flight vehicle which does not anymore comply with Cayley's design theorem. As a result, this breed of highly integrated cost-effective launch vehicles requires an integrated synthesis approach where key disciplines such as geometry, weights, propulsion, aerodynamics and aerothermodynamics are balanced in a multi-disciplinary context. Overall, the conceptual design phase of a flight vehicle in general can be characterized as follows:

1. Trade studies are required to show correct trends and design sensitivities. Correctness is more important than absolute accuracy.
2. The early design concept generally determines the life cycle cost of the vehicle.¹⁶
3. The multi-disciplinary complexity and iterative nature of the launch vehicle design problem necessitates a computerized synthesis tools.

4. Simplified but transparent analysis is required to arrive at physically correct design information.
5. Rapid design feedback is required to avoid getting locked too early into a configuration concept.
6. Due to the limited experience database when discussing SAVs, the synthesis tool enables acceleration of the learning process. The final quality of the design is directly related to how much the design team has learned.

There is a lack of versatile design tools available for aerospace vehicle conceptual design environments. For example, conceptual design departments of commercial transport aircraft manufacturers lack adequate analysis and design methods to consistently assess and compare the performance potential and commercial feasibility of ‘novel’ aircraft configurations versus the classical shape.¹³ As a consequence, the present study targets the development of a configuration-independent methodology concept and tool capable of comparing traditional expendable launch vehicles and comparing them with relevant reusable launch vehicle design alternatives. The mission profiles and design processes of HTHL SAVs are comprehensive and complicated. Therefore, the HTHL SAV is considered as an underlying generic model for the development of a generic design synthesis methodology for the SAV conceptual design. A generic SAV design synthesis methodology with focus on an HTHL development approach is presented in this dissertation.

2.3 Definition and Classifications of Design Synthesis Methodologies

An aerospace vehicle design synthesis methodology is a systematic way to the design of complex aerospace vehicle systems where the interaction among several disciplines must be considered. Generally, a methodology includes a set of analysis methods, procedures, and the techniques used to collect and analyze information appropriate for evaluation of a particular program, project, or activity. The definition of 'synthesis' in the Concise Oxford Dictionary²³ is *"the process or result of building up separate elements, especially ideas, into a connected whole, especially into a theory or system"*. In aerospace vehicle design, it is the process of building a new concept, solution, and design for a purpose by assembling hardware together in a logical way. For example, design synthesis of the overall flight vehicle is usually based on achieving a minimum weight configuration or life cycle cost through parametric variation of critical design parameters. The process to arrive at a physically feasible and functional design is called to 'converge' the design. The computational approach established for converging the design has to be considered the 'heart' of the design process which will be developed and presented in Chapter 4.

A multitude of computerized design synthesis systems have been developed and used by aerospace design environments for the CD and PD phases, since most configuration synthesis occurs during these two key phases.²⁴ The utilization of modern computer technologies has greatly improved the flight vehicle design process. This applies particularly to disciplinary design analysis, but as well at a lesser degree to the capability to synthesize a design in the multi-disciplinary process. As an example, the following

design synthesis systems have been applied to the *disciplinary level analysis* of aerospace flight vehicles: SYNAC²⁵ for conventional takeoff and landing subsonic and supersonic aircraft employing air breathing engines, HESCOMP²⁶ for helicopter sizing and performance evaluations, POST²⁷ for launch vehicle trajectory optimization, and also *system level analysis*, such as FLOPS²⁸, for aircraft configuration optimization, TRANSYN²⁹ for a transport aircraft. Certain design synthesis systems have also been applied to *different types of flight vehicles* (commercial subsonic/transonic/supersonic aircraft, military aircraft, and space access vehicles, etc): PrADO³⁰ and CPDS³¹ are developed for commercial transport aircraft, HISAIR³² and MIDAS³³ for supersonic commercial transport aircraft, SSSP³⁴ for the space access vehicle Space Shuttle, CADE¹³ for low-aspect ratio F-15 type fighters, and FASTPASS³⁵ for advanced space systems. For more information on existing synthesis systems see Chapter 2.4.

The development of a generic conceptual design SAV synthesis methodology requires a thorough insight into the capabilities, limitations, and potential of vehicle synthesis environments in general. First, it needs to be decided which generation and type of synthesis system is desirable as a development platform. The results of a comprehensive survey of flight vehicle synthesis environments are presented. This enables the formulation of development guidelines (specification) for the the next-generation generic SAV design methodology AVDS-PrADO^{SAV}.

In order to distinguish the multitude of existing flight vehicle analysis and synthesis approaches, a classification scheme is proposed in the present context according to their

modeling complexity, expressing limitations and growth potential.⁶ According to this scheme, five different classes of design synthesis methodologies are defined as shown in Table 2.

Table 2: Classification and characteristics of aerospace design synthesis approach ⁶

Class	Design Definition	Develop Time	Characteristics
Class I	Early Dawn	Until 1905	Trial and error approach, experiment, no systematic methodology
Class II	Manual Design Sequence	1905 – 1955	Physical design transparency, parameter studies, standard aircraft design handbooks
Class III	Computer Automation	1955 – Today	Reduced design cycles, detailed exploration of the design space, discipline-specific software programs
Class IV	Multidisciplinary Integration	1960 – Today	Computerized design system, MDO, data sharing, centralizing design
Class V	Generic Design	Future Generation	Configuration independent, sophisticated design synthesis framework, detailed engineering analysis, synthesis of a user-defined aircraft, true inverse design capability, KBS

As shown by the classification scheme above, design synthesis has evolved from the early experimentalist's approach to today's highly computerized and analytical design system. It is noted that the design synthesis methodologies, from Class I to Class IV are still in use today. Class V design synthesis methodologies are currently under development, and not yet considered operational.

This classification illustrates that the next-generation of generic Class V systems will emphasize the integration of classical and generic-type computational analysis methods in all major analysis disciplines into a modern design synthesis environment. In particular, the generic design capability enables the design engineer to compare a wider range of design alternatives, in particular SAV configuration concepts like HTHL, VTHL, and VTVL. The major design variables are not frozen before the potential benefits of multidisciplinary interaction effects are explored. Integration of a multi-

disciplinary optimization capability enables the identification of counter intuitive solutions with local or global optima that can only be identified through inter-disciplinary design exploration. As a consequence, only such a capability can provide truly robust mathematical optimizations particularly meaningful during the early conceptual design phase. However, most of today's MDO implementations are focused on PD and DD phases. The proposed Class V design resolution and design capability are not seen with present day Class IV conceptual design methodologies.⁶

2.4 An Assessment of Design Synthesis Systems

A total of 115 aircraft, helicopter, missile, and launch vehicle design synthesis methodologies have been surveyed. Most of these systems have been developed by major aerospace companies, research, and academic environments. Their basic properties and development trends will be defined through this survey. A snap-shot of this extensive survey and evaluation process is provided in Figure 12. The survey was conducted through a review of existing literature documenting the systems. Each design synthesis system has been assessed and individually documented using a 'check-list' template report. The evaluation report of each design synthesis system provides an overview of the development history, design logic, module evaluation, and software development description for each system. At the end of each report, the advantages and disadvantages of the systems are discussed. The whole evaluation process is time consuming (around 8 months) and tedious. The specifications of each synthesis system have been documented in AVD reports³⁶ and there is no space for the detail descriptions of each system here. However, the top level assessment results of these systematic and unique evaluations are

provided below and the process to arrive at a specification for the development of a future Class V synthesis system will be shown.

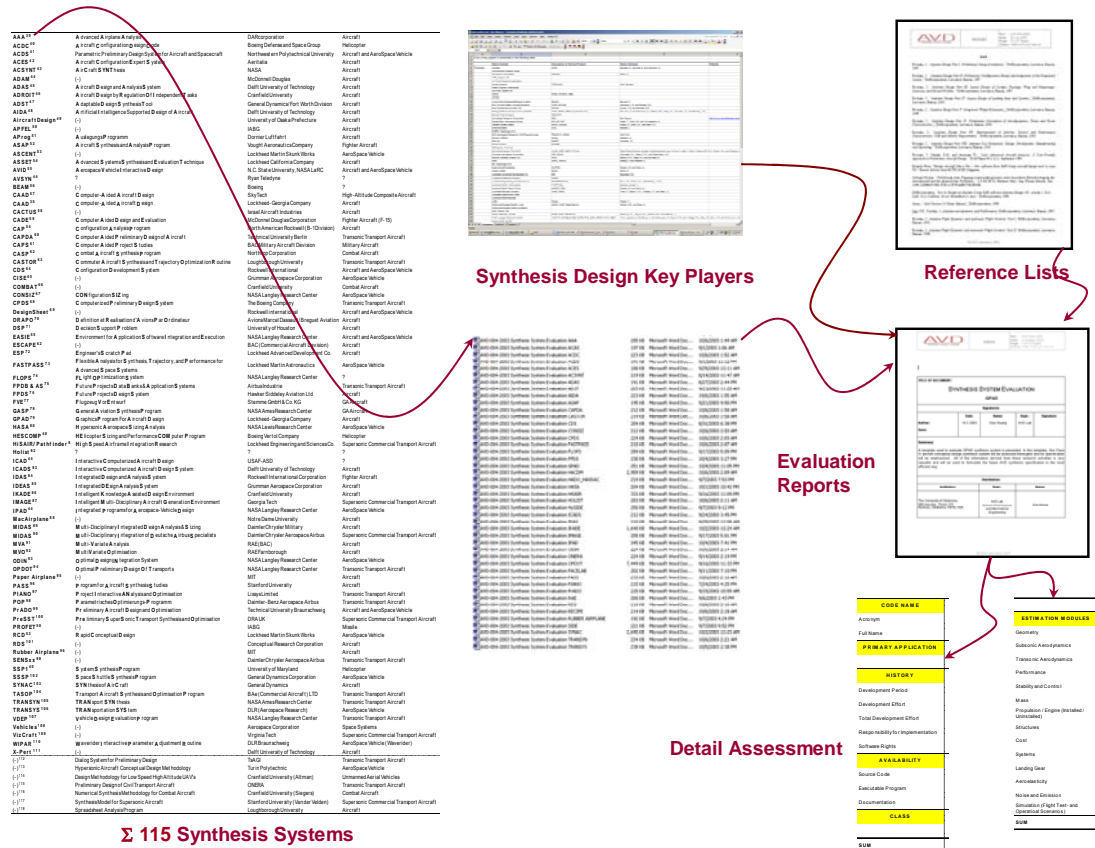


Figure 12: Evaluation process of design synthesis systems.

The survey shows that the development of computerized synthesis systems started in the early 1960's with the appearance of computer technology. The number of systems increased with the improvement of computer technology, and it reached a maximum in the 1990's as shown in Figure 13. It also shows that developing a well-integrated synthesis system is a demanding subject for designing today's highly integrated aircraft and aerospace vehicles. Recently, Airbus has appointed PACE¹⁴ to develop an Airbus internal synthesis system. NASA currently starts to develop a new synthesis system

called CDS¹⁵, Lockheed Martin advances since years RCD³⁷, and other airframe manufacturers are also very much active in this field. Figure 14 shows that most synthesis systems are developed by aerospace companies. These synthesis systems are mainly used for aircraft design, both civil and military, see Figure 15. Interestingly, only a few computer-based space access vehicle design synthesis systems are available, such as PrADO-Hy³⁰ and SSSP³⁴. These particular systems are specifically developed for space access vehicles.

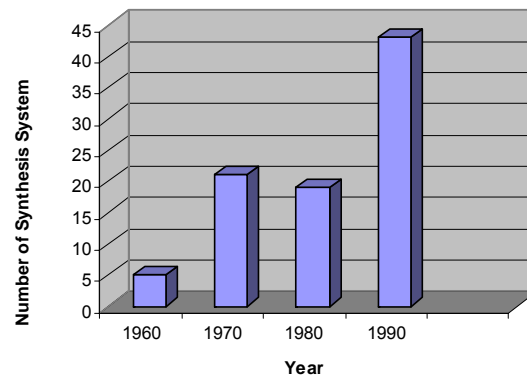


Figure 13: Number of synthesis systems vs. development time period

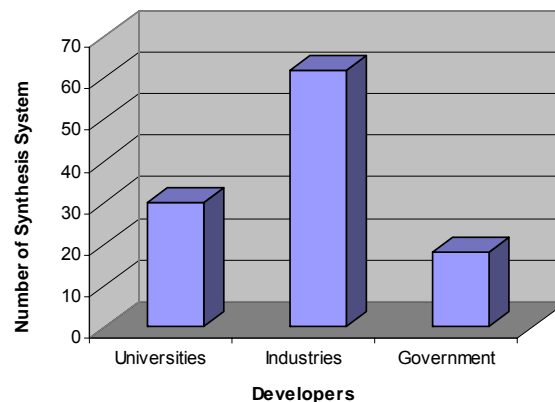


Figure 14: Synthesis system vs. developers

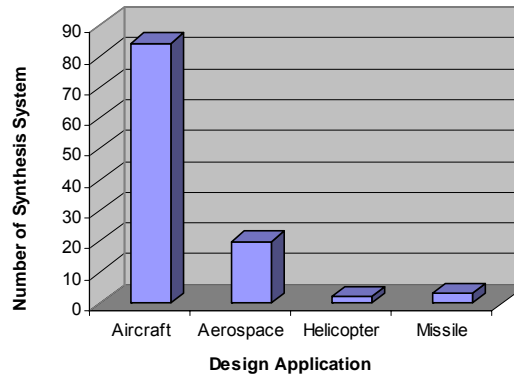


Figure 15: Synthesis system vs. design applications

Some non-integrated or manual space access vehicle (SAV) design methodologies are worth mentioning, particularly those of SAV design specialists K.D. Wood,³⁸ P. Czysz,³⁹ W.E. Hammond,¹² and J.L. Hunt.⁴⁰ The detailed descriptions of these SAV design systems are presented as flow charts in Figure 16 – Figure 19. The execution sequence and success rate of the manual approach very much depend on the individual engineer operating the system. The lack of automated design iterations prevents this system type from reliably converging a SAV in a multi-disciplinary context.

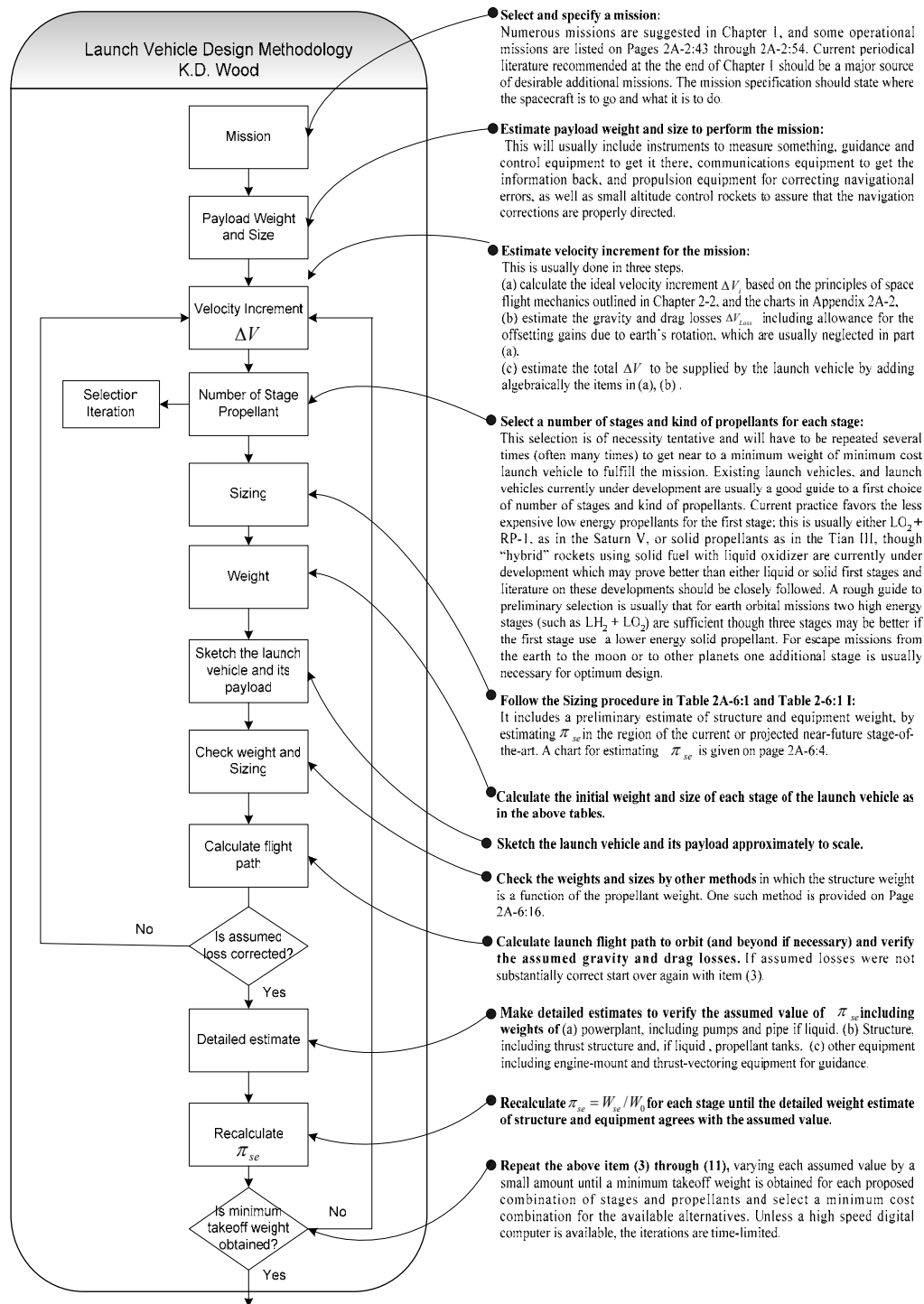


Figure 16: Design methodology of spacecraft and its launch vehicle by K.D. Wood ³⁸

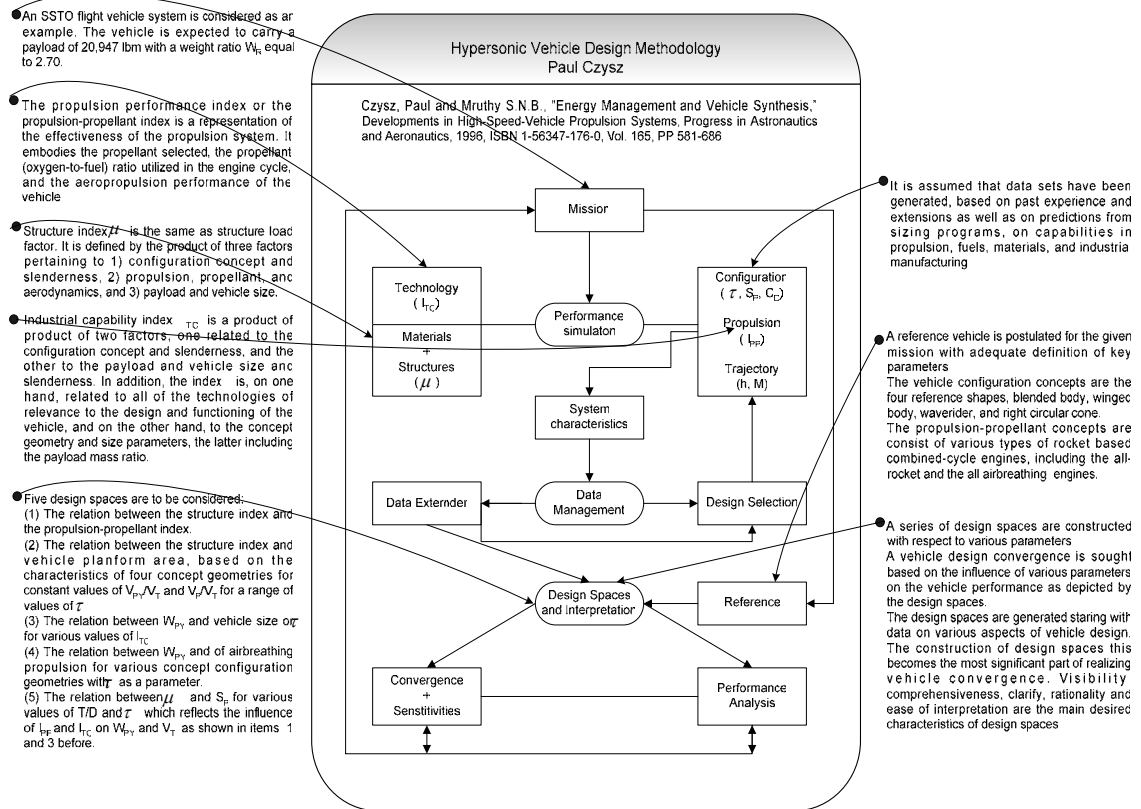


Figure 17: Hypersonic vehicle design methodology by Paul Czysz³⁹

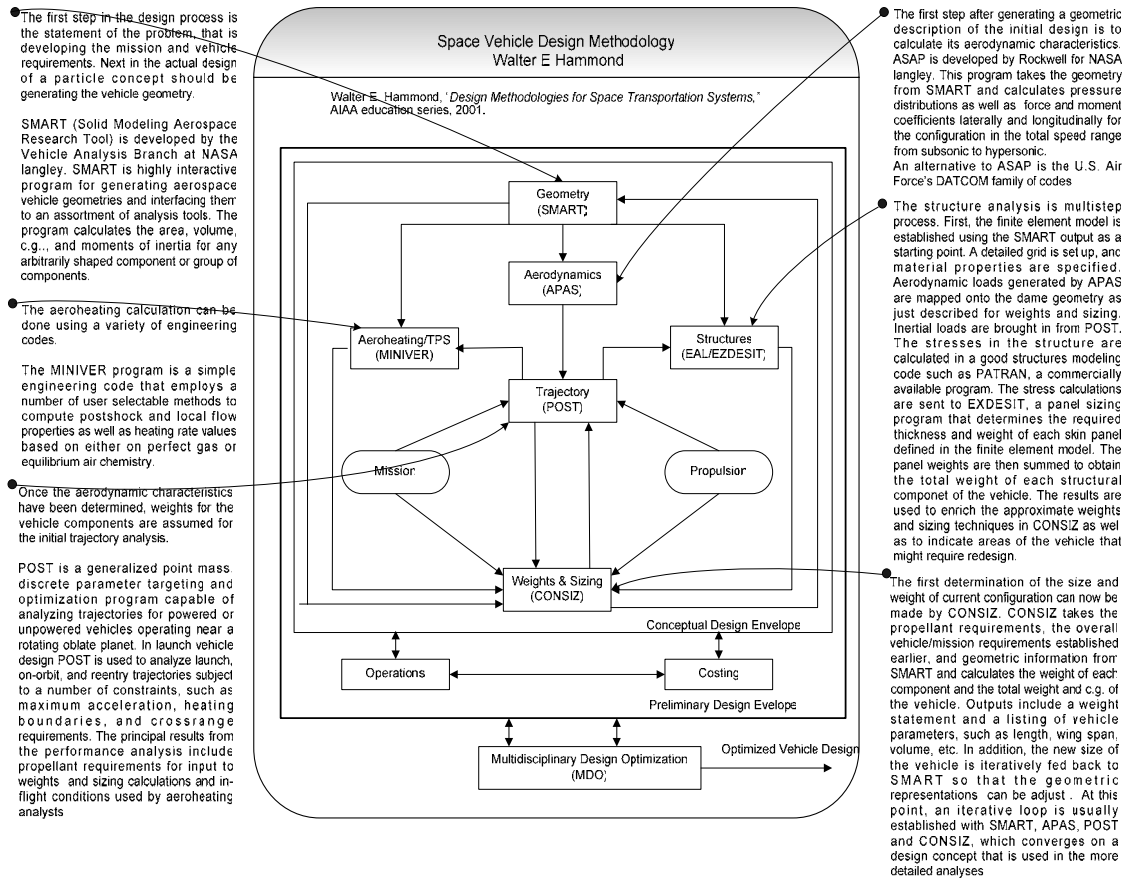


Figure 18: Design methodology for space transportation systems by Walter E. Hammond ¹²

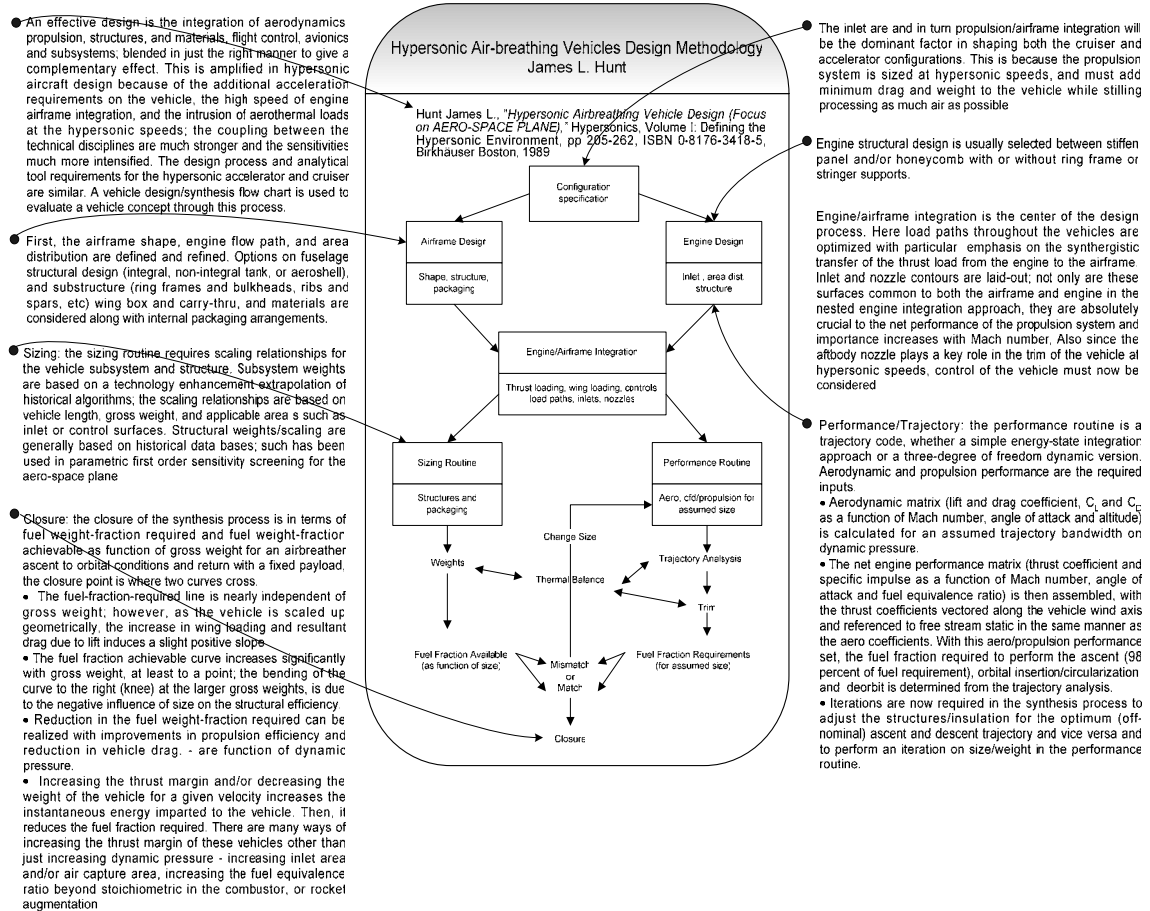


Figure 19: Hypersonic air-breathing vehicle design methodology by James L. Hunt ⁴⁰

These synthesis systems have been evaluated and as many key players in aerospace vehicle design organizations have been included as possible. It is inevitable to miss some synthesis systems not visible to the world (e.g. in-house synthesis systems at Gulfstream) and source codes not available for detailed evaluation. However, this unique and systematic assessment contains major synthesis systems and key design synthesis publications.³⁶ Therefore, this systematic assessment is considered a comprehensive survey to provide an overall philosophy of synthesis systems and offer the basic

specifications of current synthesis systems. Some top level conclusions can be drawn from the assessment as follows:

- Design synthesis systems are the heart of aerospace vehicle design organizations (Boeing, Lockheed Martin, Airbus, etc).¹³ The development of a synthesis system is a demanding task and requires large research activities.

- Most of the synthesis systems are developed for aircraft design. Very few SAV design synthesis systems exist. Especially, there is a lack of efficient design synthesis systems for highly integrated SAV-type vehicles because the Cayley's design paradigm is no longer valid.

- Synthesis is the key to close (converge) the design through iterations. Major synthesis systems estimate design sensitivities and support optimizing flight vehicle configurations, but only a few synthesis systems are capable of delivering a proof of convergence. The main drawback of current synthesis systems, especially for SAVs, is that they are not able to efficiently define the design space and prove design convergence.

- Many design synthesis systems tend to have a common structure with different computational procedures, see Chapter 2.4.1. However, the design methodologies of synthesis systems are not transparent. There is a lack of efficient computerized synthesis systems and multi-disciplinary interaction at the conceptual design level.

- Current design synthesis systems tend to develop a new system for each new application. There is no generic synthesis system for the SAV conceptual design.

- Some systems utilize *design statistics* (PIANO, AAA) but lack having available a dedicated *CD-Knowledge-Based System* for SAV design.

- Managerial decision-making power using a synthesis system is often underestimated and not understood.

The following survey of synthesis systems is organized by the architecture and distinguishing features of the synthesis systems. Accordingly, it includes sections on the mathematical model, multidisciplinary analysis and optimization, underlying generic concept, and the availability of a knowledge-based system (KBS).

2.4.1 Mathematical Modeling of a Synthesis System

The aim of the design synthesis methodology is to visualize the available solution design space of feasible flight vehicle configuration concepts, to deliver a proof of convergence for these flight vehicles, to estimate design sensitivities and design trends, to optimize relevant configurations, and to finally define and assess the impact of technology in order to reach the design targets specified. The methodology first screens the available design space, generates and evaluates new configuration concepts, then selects promising candidates for further design work and optimization. A typical mathematical model of a design synthesis methodology and software consists of one central synthesis module and several disciplinary analysis sub modules which perform dependent multi-disciplinary design studies. For the development of a generic SAV synthesis system, it is critical to investigate and select basic modular structure and individual modules which have generic character.

Modular Structure: There are several synthesis systems that have followed the software development aim leading to a top down modular program structure. Examples are SSSP³⁴ which consists of a synthesis driver providing the iteration logic and multi-disciplinary analysis capability required to ensure consistency among the weight, volume, geometry, trajectory, and mission constraints. ODIN⁴¹ has an executive program called DIALOG which controls the sequence and execution of independent programs representing various aerospace technology areas. ASSET¹³ is an analytical design program and data integration tool which analyses the vehicle configuration, weight, and cost implications through mission and performance analysis. MIDAS³³ integrates individual modular computer programs for effective use during the conceptual design phase. The benefit of such a synthesis system structure is shown with PACELAB⁴², since it is able to significantly reduce the design cycle time and cost, thus, improving design productivity and quality.

Individual Modules: Each analysis module represents a design discipline relevant to the flight vehicle. In industry and research organizations, these disciplinary modules tend to be developed by its respective disciplinary specialists; they have to be updated accordingly as new technology becomes available. For example, FASTPASS³⁵ allows the user to easily update and modify analysis modules with analysis tools of increasing fidelity level. PACELAB⁴² demonstrates user flexibility since it allows easy integration of customer-specific functionality. The modern concept of modular programming and the build-in tool-library avoids the primary drawback of some historically complex and aging codes like CADE¹³ (initially hard-coded system for F-15 development), since they were

custom-tailored to a predetermined set of design problems and are difficult to expand, modify, and maintain. As a result, this difficulty has eliminated 80% of legacy computer synthesis programs. CASDAT ⁴³ was carefully constructed from the best available analysis tools using a modular architecture. Modules should be integrated by task or functionality and not by programs.

Data Management System: The efficient coupling of individual analysis modules in a synthesis system requires consistent and efficient data transfer among modules. Therefore, the availability of an efficient data management system is key to improving the design process, reducing design cycle time, and allowing the engineers to concentrate on engineering rather than data manipulation. For example: IDEAS ⁴⁴ uses a central data bank to store all calculated data for more than seventy inter-related computer program modules. The database and file management system of RECIPE ⁴⁵ can facilitate inter-model and inter-platform communication and also widely distribute team analyses through the internet.

2.4.2 Multidisciplinary Analysis and Optimization

Multidisciplinary Design Optimization (MDO) is defined by the AIAA MDO Technical Committee (TC) as: *“A methodology for the design of complex engineering systems and subsystems that coherently exploits the synergism of mutually interacting phenomena. Optimal design of complex engineering systems requires multidisciplinary analysis that accounts for interactions amongst the disciplines (or parts of the system) and seeks to synergistically exploit these interactions.”* ⁴⁶ Multidisciplinary design

capability is the key feature for the success of any complex product. In this context, the SAV is one of the most complicated engineering applications as the track-record of failed projects confirms. Today, vehicle design optimization concentrates predominantly on single disciplines or on coupling of a few disciplines like CFD and FEM at higher fidelity level; typically, trades studies are conducted on individual components or subsystems only due to the enhanced computing cost at preliminary to detail design level.⁴⁷ Unfortunately, this approach is only capable to locate local optima compared to global optimal solutions, which have to be explored during the conceptual design of the vehicle.

Therefore, the synthesis analysis approach has to include not only disciplinary analysis and disciplinary sensitivity analysis, but also system level analysis to define a feasible design space and deliver a proof of design convergence. In contrast to disciplinary analysis, multidisciplinary analyses have the potential to evaluate the interactions between a multitude of disciplines and are capable of projecting the effects of important design parameters within the feasible design space, such as a complicated carpet-plot. Clearly, this coupling of analysis routines with multidisciplinary optimization will make the model more feasible, because any weakness of the model will be exploited. Six fundamental approaches to the problem of a system optimization are presented in Reference 48.

However, during the multidisciplinary design optimization (MDO) process, the number of analysis variables and design variables will increase with the addition of analysis disciplines and with an increase of the overall fidelity level. This requires

intensive data transfer between the modules. Even if each discipline can be reduced to a linear optimization problem, it is still hard to simplify the MDO process which by its very nature is highly interconnected and nonlinear. Finally, there might be single or multiple objective functions characterizing the MDO problem.⁴⁸ All of these factors dramatically increase the computational burden.

The investigation of multidisciplinary optimization is a vast field which is beyond the scope of this paper. Sobieski and Haftka⁴⁸ in 1996 provide a detailed survey and prospect of MDO techniques applied in aerospace design. The reference discusses several approaches valid for specific multidisciplinary optimization problems. One of these approaches is to use simple analysis tools at the conceptual design level. The simplicity of the analysis tools allows the integration of the various disciplinary analyses into a single, usually modular, computer program without increasing the computational burden. It uses less complex and less accurate models to reduce the computational cost. This ‘simple analysis tool approach’ can be seen in ACYNT⁴⁹ and FLOPS.²⁸

The survey shows that until 1996, very few aerospace vehicle systems have been optimized for their flight performance and vehicle total cost by taking all relevant disciplines into account.⁴⁸ However, there is a trend to continuously incorporate MDO techniques to couple legacy codes with new software integration tools. Several optimization methods are used to facilitate multidisciplinary design analysis and optimization at the conceptual level. The Response Surface Method (RSM) approach is used in IMAGE⁵⁰ and Gradient-Based Method (GBM) for PrADO³⁰ and SIEGERS⁵¹.

An optimization tool library can provide practical optimization algorithms with view to computational time and cost involved. LAGRANGE⁵² has ten different optimization codes, and users can customize their optimization in HOLIST⁵³.

MDO is still a developing area. It needs to be rigorously made transparent to the engineer, showing how the variety of disciplines and their assumed level of technology actually influence the design. CADE¹³ uses design surfaces to make optimization results transparent. This capability is of paramount importance to ensure the underlying physics, to enable so-called sanity or reasonableness checks. Overall, the mathematical optimizer has to be robust, suitable for a high number of variables, and has to operate with noisy and rough objective functions of complicated topography. The incorporation of non-linear optimization techniques into the design cycle realizes true multi-point design trade studies.

2.4.3 Knowledge-Based System

The conceptual design phase is an intense learning phase for the design team. As Hollowell and Bitten⁵⁴ comment: *“The final quality of design is directly related to how much the design team can learn. It can help the designer to quickly and well explore the design space. This is an extremely important observation relative the application of optimization techniques”*.

The development and integration objective of a dedicated flight vehicle Conceptual Design Knowledge-Based System (CD-KBS) is to make relevant design knowledge

effortlessly available. The particular strength of the system manifests in enabling the user to gain fundamental understanding of solution concepts realized in the past. In general, the design knowledge is comprised of data (raw material without implying any judgment or interpretation), information (data with meaning and value in various ways), and knowledge (a mixture of experience, values, contextual information, and expert insight that provides a setting for evaluating and incorporating new experiences and information).¹⁹ Currently, only very few systems utilize knowledge-based techniques but lack the dedicated CD-KBS. Examples are: PIANO⁵⁵, which is equipped with more than 150 existing or projected aircraft data for competitive analysis and development purposes; PASS⁵⁶, which is an aircraft synthesis code with an expert system to display warnings or provide design advice; AAA⁵⁷, which incorporates and coordinates the methods, statistical databases, formulas, and relevant illustrations, and drawings based on Roskam's Airplane Design book; and PACELAB⁴², which has the flexibility to integrate its KBS planform into new design applications.

As the assessment of synthesis systems shows, it would be advantageous to have a library of design knowledge which may be shared among the designers. A dedicated aircraft Conceptual Design Knowledge-Based System contains design decisions which truly accelerate the learning process of the conceptual design team. The learning capability of the KBS provides a dynamic and intelligent design information source with growth potential, which supports decision making while having design information available at the fingertips. However, there is no dedicated space access vehicle CD-KBS in existence.

2.4.4 Generic Concepts

The generic character of SAVs implies configuration independence. Until now, design synthesis systems have always been developed for specific design applications, and it is difficult to migrate them to other applications without major modifications. This fact prevents a more comprehensive exploration of the design space since it excludes a consistent comparison of conventional with unconventional design alternatives. Examples are: PIANO⁵⁵, which focuses on conventional transonic commercial aircraft certificated to FAR/JAR-25 or equivalent civil standards. This is not suitable for military (other than some transport) or unconventional (e.g., canard or three-surface) configurations. Initial synthesis efforts of ASSET¹³ have been applied to a specific application (FX study). This approach was very cumbersome and did not evolve a generic modular structure.

As shown in the section Mathematical Modeling of a Synthesis System, a synthesis system always includes all core disciplines required to represent the flight physics of the vehicle. However, there is not a consistent objective function common among different synthesis systems. For examples: FLOPS²⁸ uses flight optimization as its figure of merit, whereby other systems might use aerodynamic performance or cost as the main driver. In order to provide consistent design analysis, such a system is required to

- Avoid switching between different calculation routines to determine a parameter under different operating conditions (generic capability),
- Use the same fidelity or calculation accuracy throughout all disciplines (consistency). Method consistency ensures reproducibility of estimation results. On the

other hand, using a consistent set of estimation tools enables true comparison of different ideas (aircraft configurations, wing concepts, etc.).

Currently available software integration programs promise an open system architecture, e.g., PACELAB⁴² or ModelCenter⁵⁸ for developing computerized synthesis programs with unprecedented flexibility (new product focus), modularity (new design modules), and standardized interfaces (open system). This architecture allows unconstrained integration of existing analysis, design and optimization codes in a modular format. It enables exploitation of company-specific knowledge through standardized interfaces, in particular the integration of proprietary methods into the methods library, and integration of proprietary data. Also, advanced computing hardware provides high speed and parallel computing capability. Although these integrated design framework packages surely help to organize company's legacy codes, they can't offer a proof of design convergence or automatically identify the solution space. There are NO systematic methodologies established to integrate all these advanced technologies. PIANO⁵⁵ users requested to extend the program to unconventional and transonic, and supersonic aircraft. This was rejected by Dr. Simos, pointing out that Lissys neither has the resources nor the experience and methodologies for generic design. Due to the lack of modern conceptual design methods and tools applicable to the design of space access vehicles (SAV), high fidelity CFD and FEM tools are used instead during the conceptual design phase. Utilization of high fidelity tools increases design cycle time and cost. However, the main problem is that the input information required for those high fidelity tools is usually not available during the conceptual design phase, the design team is

loosing the opportunity to rapidly generate design trends, to visualize the multi-disciplinary solution space, and to provide a proof of design convergence.

Generic design capability is of particular importance for SAV design due to the lack of a comprehensive statistical database displaying real-life experience. A broad range of reusable SAV design configuration concepts have been discussed; none of those vehicles, varying from HTHL to VTVL, from winged vehicle to lifting body configurations, and others, have been tested in a real environment. As a result, it is mandatory to have a configuration independent, consistent, systematic, and physically correct design simulation system available for the top level assessment of prospective reusable and also expendable SAVs, enabling true technical comparisons at the conceptual design level.

2.5 AVDS-SAV Development Requirements

As the above survey indicates, there are only a few Class IV computer-integrated SAV synthesis systems in existence, such as PrADO-Hy,³⁰ and there are only a few SAV design approaches of the manual methodology type known. Each particular design synthesis system is inclined to be applied to a specific product and not capable to systematically compare various SAV design alternatives. The survey clearly shows that the current conceptual design capabilities available for the design of SAVs are design method and software limited rather than computer limited.

In general, a state of the art space access vehicle (SAV) design methodology requires a library of design methods, procedures, and standards that define an integrated synthesis

engineering approach for the multi-disciplinary design of SAVs. Consequently, the development of the dedicated generic SAV conceptual design synthesis methodology AVDS-PrADO^{SAV} requires the adoption of the following standards:

(1) Generic Design Capability: A generic design capability facilitates the initial configuration selection and definition phase during the conceptual design phase. Consequently, consistent SAV vehicle configuration comparisons are made possible for vehicles where the ultimate performance may hinge on numerical subtleties. It is required to consistently identify the convergence design space for total flight vehicles of different configuration concepts.

(2) Multi-Disciplinary Design Capability: Effective evaluation of a design at the conceptual level requires the integration of multiple disciplines. Each discipline has to be represented as a stand-alone module. Communication between modules (disciplines) has to be organized via the data management system (DMS). Multidisciplinary design plays a key role in the three main functions of design synthesis systems: (a) Arriving at a feasible design which means that a final design concept satisfies all the physical requirements in a multidisciplinary design context. The final design concept can be built and successfully fulfill the flight mission. (b) Identifying the boundaries of the feasible design solution space by multidisciplinary design space screening, and (c) Performing multidisciplinary design optimization (MDO) with objective functions such as a minimum direct operating cost (DOC). However, most of the current synthesis systems are not capable of defining feasible design space solutions by design space screening which is difficult and

challenging. In contrast, many designers start MDO before locating the feasible design space.

(3) Dedicated SAV Conceptual Design Knowledge-Based System (SAV CD-KBS): This dynamic design database contains the rationale and lessons learned from fundamental flight vehicle concepts realized in the past. The SAV CD-KBS provides, in particular, design lessons learned to accelerate the conceptual design learning process leading to informed decision making.

(4) Multi-Disciplinary Design Optimization (MDO): Being able to converge a single design multi-disciplinary followed by the visualization of all feasible designs in the solution space, MDO needs to be utilized as a tool using global sensitivity analysis and other MDO methods to find the best design according to a pre-defined merit function in the solution space. It reduces the number of design cycles and allows the designers to evaluate more configurations in a given time. The real-time graphical representation of the numerical solution also provides great benefits to the decision maker.

(5) Database Management System (DMS): The desired data management system not only stores and manipulates numerical data belonging to physical design parameters, but it also controls the utilization of the design methods library. Additionally, it is a communication platform for the inter-discipline modules. The availability of a robust DMS facilitates data transfer, reduces data transcription errors, and allows the designer to use different computing environments and widely distributed teams.

3. Design Knowledge, Primary Design Disciplines and Methods Library

It has been shown that the final success of any aerospace product is directly related to how much the design team has learned during the design process.¹⁹ We have observed that how much the design team will learn is a strong function of how much the design space is being explored. In addition to the availability of an efficient design synthesis capability and proficiency, flight vehicle design evolution is otherwise primarily dependent on the design information and knowledge available to the design team. The importance of internalizing the anatomy of design successes and failures to a design engineer emphasizes the task of systematically organizing relevant design information and knowledge and making it available to him ‘at the fingertips’. SAV design information and knowledge are critical to the development of a HTHL SAV design synthesis methodology.

3.1 Design Knowledge Base - *KBS^{DESIGN}*

Reference 19 presents an approach developed at the AVD laboratory at The University of Oklahoma and now adopted at the AVD Laboratory at The University of Texas at Arlington towards the development of this dedicated KBS which places strong emphasis on a systematic and thorough knowledge utilization process. Ideally, a combination of a *Data-Base System* containing information on existing designs, and a *Knowledge-Based System* with knowledge about the design process, coupled to CAD and analysis packages (Methods Library), should provide the designer with a great amount of

assistance at all stages. However, the elements usually missing in conceptual design methodologies are, in particular, an up-to-date DBS and KBS for making data, information, and knowledge readily available for design-decision making.

As a consequence, a dedicated SAV design knowledge-based system KBS^{DESIGN} (*Data Domain, Engineering Domain, and Process Domain*) is being developed, making relevant space access vehicle design knowledge effortlessly available to the design team. The workplace for the SAV designer needs to be organized to enable him here to learn from the past. Clearly, a synthesis work station (see Figure 20) has to consist of three separate computer screens next to each other organizing the (a) *Data Domain* (references, pictures, Jane's information, etc.), (b) *Engineering Domain* (design experience, design knowledge, interpretations, etc.), and (c) *Process Domain* (synthesis system, design processes, method libraries, etc.).

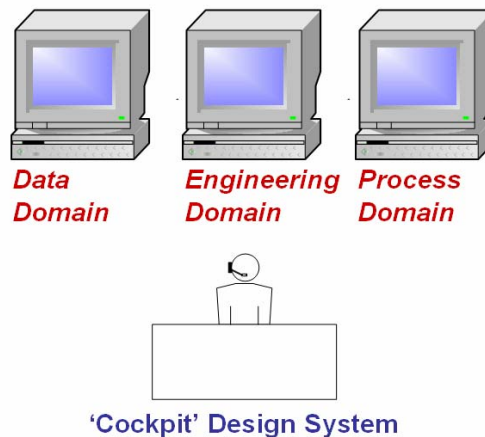


Figure 20: A 'cockpit' product development framework environment.⁷

The three primary elements of KBS^{DESIGN} are the DBS (data-base system – residing in the *Data Domain*), the information-base system (IBS – residing in the *Engineering Domain*), and the methods library (ML – residing in the *Process Domain*). A detailed

As discussed before, because of the comprehensive mission profile of HTHL, the HTHL SAV is considered as an underlying model for the development of a generic SAV design synthesis system. As a consequence, relevant HTHL SAV design concepts and information are assembled for the development of a HTHL SAV design synthesis methodology. Table 3 presents representative space access vehicle concepts selected from concepts in the SAV *KBS^{DESIGN}* for this research.^{59, 60, 61, 62}

Table 3: Selected SAV concepts for the development of SAV HTHL design methodology

SAVs	Flight Mission	Concept	Engine	Operation	Stages
HOTOL	Orbital launch vehicle	Winged	Airbreathing Rocket	HTHL	SSTO
NASP	Manned orbital vehicle	Winged	Scramjet rocket	HTHL	SSTO
Sänger/Horus	Air-breathing hypersonic first stage and delta wing second stage, low Earth orbit	Delta wing	Ramjet Rocket	HTHL	TSTO
SpaceShipOne	Suborbital tourism	Winged	Rocket	Air launch and horizontal landing	TSTO
Dyna-Soar	Single-pilot manned reusable orbit vehicle	Delta wing	Rocket	VTHL	MSTO
HL-10	Concept of safely maneuvering and landing a low L/D vehicle designed for reentry from space	Lifting body	Rocket	Air launch and horizontal landing	
X-24A	Titan III-launched manned orbital ferry vehicle	Lifting body	Rocket	Air launch and horizontal landing	MSTO
X-24B	Explore the supersonic and subsonic handling characteristics of the hypersonic configurations	Lifting body	Rocket	Air launch and horizontal landing	
Space shuttle	Low earth orbit	Delta wing	Rocket	VTHL	TSTO
DC-X	Suborbital vehicle	Circular Cone	Rocket	VTHL	SSTO
X-33	Suborbital vehicle	Lifting body	Rocket	VTHL	SSTO
X-15	Experimental rocket plane	Winged	Rocket	Air launch and horizontal landing	
X-43	Hypersonic research plane	Winged	Scramjet	Air launch and horizontal landing	

As can be seen in Table 3, the selected SAV concepts include various (a) mission profiles: suborbital tourism (SpaceShipOne), low earth orbit (Space Shuttle, HOTOL), and hypersonic cruiser (X-15, NASP). (b) operational modes: horizontal takeoff and horizontal landing (HOTOL, NASP, Sänger/Horus), vertical takeoff and horizontal

landing (Dyna-Soar, Space shuttle), air launch and vertical landing (SpaceShipOne, X-15, HL-10, X-24A/B,) and vertical takeoff and vertical landing (DC-X). (c) number of stages: single stage to orbit (HOTOL, NASP, DC-X), two stages to orbit (Space Shuttle, SpaceShipOne, Sänger/Horus), and multiple stages to orbit (Dyna-Soar, X-24A). (d) propulsion modes: ramjet (Sänger/Horus), scramjet (NASP, X-43), and rockets (SpaceShipOne, DC-X, X-15, Dyna-Soar, HL-10, X-24A/B, Space Shuttle). (e) configurations: winged (HOTOL, NASP, Sänger/Horus, X-15), lifting body (HL-10, X-24A/B), and circular cone (DC-X). The survey shows that the SSTD design is the most complicated, and until today, no SSTD launch vehicles have ever been successfully constructed and flown. The main challenge is how to size the weight of the SSTD vehicle which can carry enough propellant and deliver payload to orbit. Recall that the development of a HTHL SAV design synthesis methodology should provide a generic design tool applicable to the conceptual design of all of the above SAV concepts. Therefore, the HTHL SAV design methodology will be initially developed based on a SSTD suborbital tourism vehicle (Rocketplane), and then extended to other applications (such as a TSTD vehicle - Sänger/Horus) in a follow-on step. The specifications, design related data, and information on all of these relevant SAV concepts will be used as key design points for the development and validation of the HTHL design synthesis methodology.

2. The Aerospace Flight Vehicle Conceptual Design *Information-Base System* (IBS):

The primary objective of developing the dedicated SAV conceptual design IBS has been to make relevant normal and radical design knowledge effortlessly available. The

particular strength of the system results from enabling the user to advance his/her understanding with respect to the variety of flight vehicle configuration concepts by identifying product configuration commonalties and peculiarities. A snap-shot of the dynamic IBS is presented in Figure 22. Currently, the SAV conceptual design IBS is being continuously updated and will be added to the existing aerospace conceptual design IBS system.

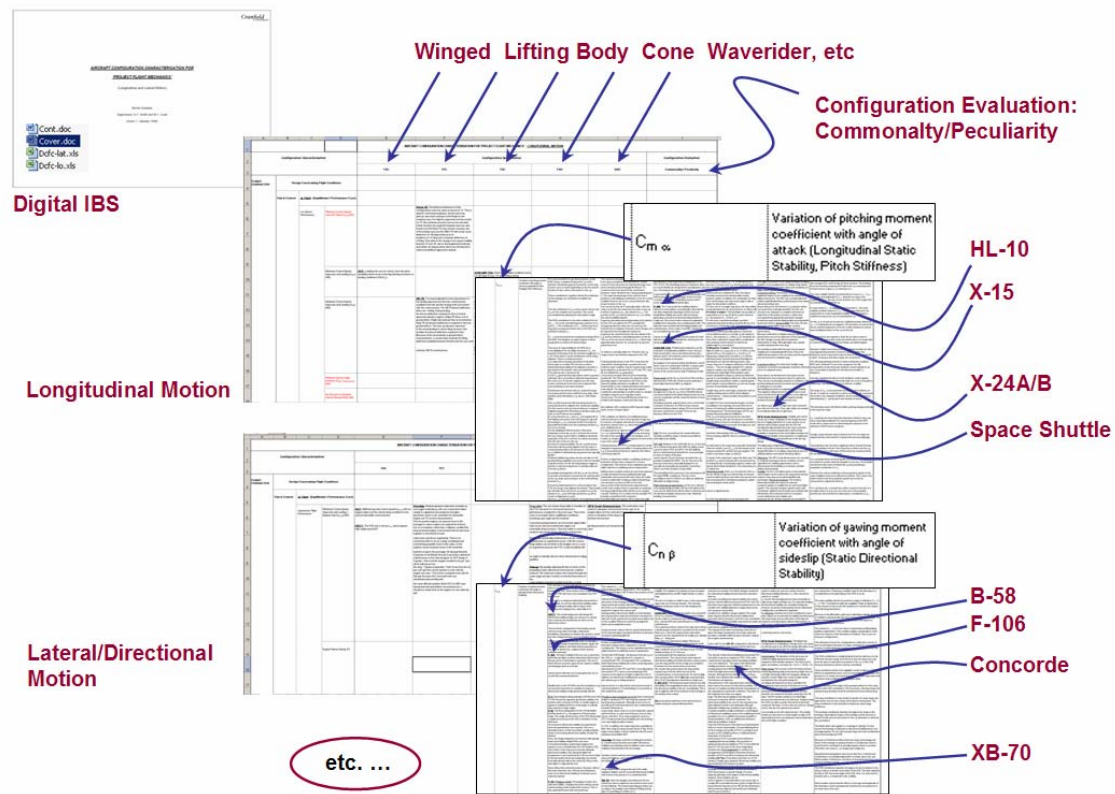


Figure 22: IBS – a dedicated aerospace conceptual design dynamic information-base system.¹⁹

3. The Aerospace Flight Vehicle Conceptual Design Methods Library (ML): Various discipline design methods are available during the conceptual design of space access vehicles. These engineering design and analysis techniques are usually based on three different approaches: experiment, theory, and computation. Therefore, all existing

engineering methods can be categorized into the following distinct classes: (1) analytical methods, (2) semi-empirical methods, (3) numerical methods.

(1) Analytical Methods: Classical analytical methods are based on physical modeling. Their predictable accuracy is determined by the theoretical analysis model. These methods can be used to make a first order estimation of design parameters during the conceptual design. Some methods are restricted in practice to specific geometries and operational applications.⁶

(2) Semi-empirical and Empirical Methods: The empirical (database) method depends on historical data and practical experience to estimate design parameters. The semi-empirical methods (engineering) empirically correct the first estimation of the analytical methods. However, both approaches are not sufficient to predict the design parameters involving new concepts and technologies.

(3) Numerical Methods: Industry computational legacy codes were developed based on industrial best practice and knowledge. They have been developed and validated over the years. Therefore, they usually have high accuracy, and this type of code is the ‘backbone’ of the industry design process.⁴² Therefore, these methods will be integrated into our generic design methodology in the best way possible. However, because of old architectures and user interfaces, some methods might not be well suited for today’s computer design environment.

Analysis modules (methods) have been documented thoroughly during the course of this research. These documentations describe the legitimacy of the underlying methods. In general, only validated stand-alone methods and tools are implemented in the development of the HTHL SAV synthesis methodology. Figure 23 shows an example of methods integration into the AVDS-PrADO synthesis system.

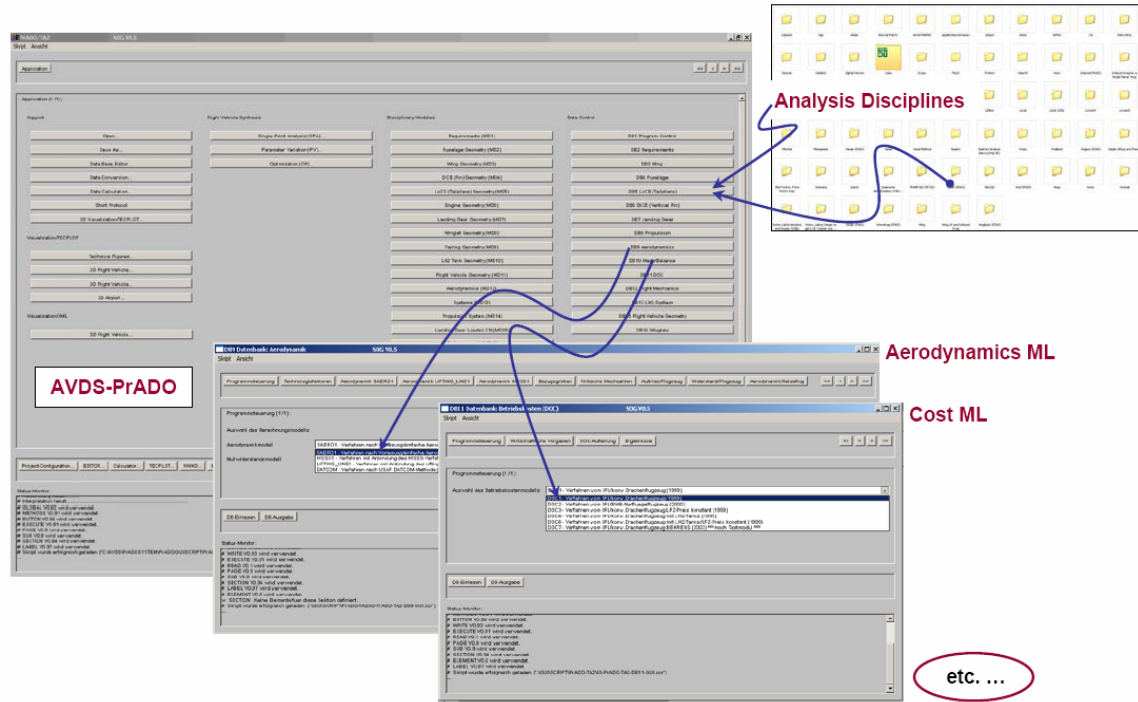


Figure 23: ML – a dedicated aerospace methods library integrated into AVDS-PrADO.¹⁹

It is a challenging task to develop a generic multi-disciplinary SAV design system. The development of a dedicated SAV conceptual design knowledge-based system is beyond the scope of the present research. As a consequence, the current research approach focuses on correctness in the context of ‘how to get started’ compared to the often seen focus on accuracy where preliminary/detail design tools are often embedded into conceptual design-level methodologies. The design data, information, and

knowledge of selected SAV concepts presented in Table 3 will be used below to identify key design disciplines and design parameters for the development of a HTHL SAV design methodology.

3.2 Primary Design Disciplines

As shown in Chapter 2, a typical design synthesis program consists of a synthesis module and several disciplinary sub-modules which perform the various dependent multidisciplinary studies required in the conceptual design of flight vehicles. Having passed the multidisciplinary analysis, these sub-modules pass primary design variable information to a system level module, the synthesis module for the further system level assessment. Overall, the integrity, consistency, and precision of data derived from these sub-modules is very important. In order to assemble the discipline modules for the development of the HTHL SAV design methodology, the present study will identify the gross design parameters followed by assembling a disciplinary methods library.

Clearly, only key disciplines and methods related to the conceptual design level and relevant to the development of the prototype SAV design system are investigated and documented. This is made possible by consequently and systematically appreciating and integrating the lessons learned from previous project failures and successes, expert advice, and overall design experience. A summary of major disciplines involved in selected SAV design synthesis systems is presented in Table 4.

Table 4: Key disciplines involved in SAV design synthesis systems

Disciplines	SSSP	PrADO-Hy	K.D. Wood	P.A. Czysz	J.L. Hunt	W.E. Hammond
Geometry		■			■	■
Aerodynamics	■	■	■	■	■	■
Propulsion	■	■	■	■	■	■
Performance	■	■	■	■	■	■
Thermal Analysis	■				■	■
Weights	■	■	■	■	■	■
Stability and Control		■				
Structures		■		■	■	■
Cost						■
Noise						
KBS		■				

The two existing and available computerized design synthesis systems SSSP (used for Space Shuttle Design) and PrADO-Hy (used for the Sanger project) are selected to visualize the multidisciplinary design characteristics driving the conceptual design of SAV configuration concepts of the HTHL and VTHL types. The Space Shuttle Synthesis Program (SSSP^{63, 64, 65}) was developed by General Dynamics Corporation in the 1970s and implemented in the conceptual design of the Space Shuttle. It is a highly useful tool in conceptual design studies, where the effects of various trajectory configurations and shuttle subsystem parameters can be evaluated relatively rapidly and economically. The space shuttle synthesis program automates the estimation of trajectories, weights, and performance computations essential to the predesign of the space shuttle system for earth-to-orbit operations. The design synthesis process in PrADO-Hy⁶⁶ simulates the sequential interdisciplinary design process with interactions between the involved disciplines, e.g., aerodynamics, flight performance, propulsion, structure mass, and thermal protection system (TPS) analysis as well as stability and control.

As seen in Table 4, the key conceptual design disciplines integrated in the design synthesis systems are weight/sizing, propulsion, aerodynamics, stability/control, aerothermodynamics, trajectory/performance, and cost. In the present study, only the key disciplines and methods related to the SAV conceptual design level and the development of the prototype design synthesis system are investigated and documented. The description of the primary design parameters, associated analysis disciplines, and the methods library are presented in the following sub-sections.

3.2.1 Weight and Sizing

With this discipline, the initial weight and volume of a baseline SAV is estimated to provide a necessary vehicle input for the continuous design analysis. The vehicle weights estimations are obtained from the statistical equations for the body, wing, tail, equipment, payload, propellant, and propulsion system. The sizing analysis determines SAV geometry (length and volume) which are consistent with the weight estimation of body, fuel, structures, and payload, etc. Initial size and weight of a SAV are important to ensure the success of the whole design process. Weight and size of the Space Shuttle were well predicted by SSSP.⁶³ In contrast, the HOTOL⁶⁷ airframe was initially sized from conventional vertical takeoff rockets with the engines mounted at the rear of a blunt based fuselage. However, the initial configuration suffered from a severe problem due to the movement of the aerodynamic center with respect to the center of gravity during the air breathing ascent. Various design changes were made to address these problems, all of which significantly reduced the payload margin.

A variety of weight and sizing methods have been used in SAV conceptual design and are summarized in Table 5.

Table 5: Weight and sizing analysis modules for SAV conceptual design

Analysis modules	Developer	Application	Availability	Description
WTVOL ⁶³ (SSSP)	General Dynamics	Space Shuttle	Y	Empirical
SMART ¹²	NASA	Hypersonic Vehicle	N	Numerical
WATTS ⁶⁸	NASA	Subsonic and supersonic vehicle	N	Empirical
VDK ⁴	Jean Vandekerckhove, Czysz	Hypersonic, orbital vehicles	Y	Analytical
HASA ⁶⁹	Sverdrup Technology	SSTO, TSTO, hypersonic vehicle, SST, fighter,	Y	Empirical

Several weight prediction methods have been developed based on the statistical data of specific vehicles. The weight module (WTVOL) of SSSP⁶³ was developed explicitly for the Space Shuttle and is difficult to extend to other applications. WAATS only can predict the weight but not the size of subsonic and supersonic vehicles.⁶⁸ Other weight prediction programs^{4, 68} developed by industry and NASA require specific vehicle parameters and are usually integrated into vehicle synthesis programs. The unavailability and difficulty of decoupling weight/sizing modules from these synthesis programs exclude these weight prediction programs from the current study. In addition, because of the lack of historical statistical data about new vehicles and technologies as well as different geometries, these programs are not sufficient for the weight and volume estimation of SAV vehicles in a generic context. A review of the SAV weight/sizing methods indicated that the Hypersonic Aerospace Sizing Analysis (HASA)⁶⁹ is a general weight/sizing analysis tool which is capable of predicting the weight and size of hypersonic single-stage and two-stage-to-orbit vehicles and transports, and is also relevant for supersonic transports. Improvements in the technology of materials and

propulsion systems are also accounted for in the HASA program. Therefore, HASA is the best available weight/sizing tool for the development of the HTHL SAV design methodology.

The WTVOL⁶³ program uses existing weight data of the thermal protection system, propulsion, and other subsystems and inputs weight ratios (the ratio of the initial vehicle weight to the final weight) and other mission requirements derived from the trajectory subprogram. It can determine the stage gross weight and volume for a specified payload weight. The SMART¹² program calculates the area, volume, c.g., and moments of inertia for any arbitrarily shaped component or group of components. PrADO-Hy⁶⁶ uses a combination of analytical models for the main components, e.g., structure, tanks, and landing gear, and semi-empirical methods for components evolving from previous designs, e.g., systems. In the VDK⁴ code (see Appendix E), the dry weight is determined by solving the weight and volume equations simultaneously. HASA predicts the weight of each component (body, wing, tail, TPS, and engines, etc.) and the total vehicle volume which includes empty body volume, fuel volume, payload volume, and air factory volume.⁶⁹ Therefore, based on all the analysis methods above, the key design parameters involved in the conceptual design vehicle weight and sizing disciplines can be defined as: (1) weight and volume of each component; (2) dry operating weight; (3) moment of inertia; (4) center of gravity location; (5) weight ratio.

3.2.2 Propulsion

There are different types of engines which derive their power from the combustion of fuel with oxidizer, which can be utilized for a SAV, such as rockets and airbreathing engines which can only be used in the first stage. The rocket is a self-contained engine, where the vehicle carries its own oxidizer; it functions independent of the atmosphere. The rocket engine has been extensively used in previous SAV concepts (Dyna-Soar, HL-10, X-24A/B, Space Shuttle, X-15, etc), and especially for SSTO concepts (SpaceShipOne, DC-X, X-33). In contrast, airbreathing engine requires atmospheric oxygen in order to work. Examples are: the Sanger/Horus concept, which is a ramjet hypersonic first stage and a delta wing second stage, in a low earth orbit SAV. The NASP (X-30) is an air-breathing scramjet manned vehicle. The scramjet technology was successfully demonstrated by a small experimental research aircraft (X-43) in 2004.⁷⁰

Various propulsion analysis methods have been used in SAV conceptual design as shown in Table 6 and summarized below:

Table 6: Propulsion analysis modules for SAV conceptual design

Analysis modules	Developer	Application	Availability	Description
SIMPO ⁶³	General Dynamics	Rocket	Y	Analytical
SRGULL ⁴⁰	NASA	air-breathing	N	Numerical
DASA ⁶⁶	Daimler Benz Aerospace	turbojet/ramjet	Y	Empirical
Handbook Methods ^{4, 71,72,73,74}	Anderson, Czysz, etc	Turbojet/ramjet scramjet/rocket	Y	Analytical

(1) The SIMPO model of SSSP⁶³ is a propulsion model defined by three propulsion parameters from which the current propulsive thrust, propellant flow rate, and specific impulse can be obtained. There are 11 basic procedures by which thrust, propellant flow

rate, and engine specific impulse can be defined. For instance, given the vacuum thrust, the sea level thrust, and the propellant flow rate, the current thrust and specific impulse can be obtained by assuming that thrust and specific impulse are uniquely defined according to a linear dependence on atmospheric pressure.

(2) For the group of air-breathing engines, cycle analysis (SRGULL) in J.L. Hunt's methodology⁴⁰ can accurately resolve the net propulsive thrust of an air-breathing vehicle as a small difference between the combustor/nozzle thrust and the forebody/inlet drag.

(3) A complete database of a turbojet/ramjet engine is available from the German aerospace company Daimler Benz Aerospace (DASA), Munich. This accurate model contains thrust, specific fuel consumption, as well as aerodynamic forces and moments for inlet and nozzles as a function of Mach number, altitude, and angle of attack, see PrADO-Hy.⁶⁶

(4) Handbook methods in the form of simplified first-order approximate estimations of a propulsion model can be derived with vacuum and sea-level-specific impulse as inputs, along with vacuum thrust. Altitude performance of the engine is computed using ambient pressure corrections to specific impulse and thrust. Anderson shows the basic relation in this approach as ^{71,72} $T = T_{SL}(\sigma)$. P.A. Czysz is using a more precise approach⁴,

$$T = T_{SL}(\sigma)^{0.6}$$

$$\text{where } \delta = p/p_{sl} \quad \theta = T/T_{sl} \quad \sigma = \rho/\rho_{sl}$$

As can be seen in Table 6, only the analytical handbook methods are generic tools applicable to the design analysis of all types of engines (turbojet, ramjet, scramjet, and rocket). They are especially useful for the purpose of estimating SAV propulsion performance at the conceptual design level. They should not be taken too literally for any detailed analyses where more precise engine data are needed. Handbook methods have been successfully used for the conceptual design of the Space Shuttle (SSSP) and the Rockeplane OU XP project and, therefore, will be utilized in the development of the SAV design methodology.

After careful investigation of the propulsion modules^{40,63,66} and engine design handbooks^{4,71,72,73,74} available, it is concluded that, in the propulsion analysis, propulsive thrust, propellant flow rate, and specific impulse are the key design parameters for the design analysis of all different types of engines and sufficient for the conceptual design level. The specific impulse (thrust per pound of total engine airflow) is a measure of propulsive efficiency and also a useful parameter in determining engine noise.

3.2.3 Aerodynamics

The conceptual design of a SAV requires the capability to analyze the aerodynamic behavior of flight vehicle across the subsonic, transonic, supersonic, and hypersonic speed regimes, e.g., Mach 20 for the Space Shuttle, Mach 6.7 for the hypersonic research vehicle X-15, and Mach 3.26 for the suborbital tourism vehicle - SpaceShipOne. Subsonic flow is normally characterized by steady streamlines. Transonic flow is defined between Mach 0.8 and Mach 1.2, where unsteady and weak shock waves create difficult-

to-predict flow patterns. Supersonic flow always has shock waves across the surfaces of the vehicle. In this regime, Mach number increases, and the shock layer is reduced in thickness leading to an interaction between the shock wave and the viscous boundary layer on the surface. X-15 testing discovered^{75,76,77} that, in hypersonic flight, if the shock layer temperature grows high enough, chemical reactions start in the air and produce aerodynamic heating which can cause buckling of the wing skin. Therefore, viscous interaction, chemically reacting effects, and aerodynamic heating are important characteristics of hypersonic flow.

Various engineering analytical, empirical, and numerical methods have been developed to determine the conceptual level aerodynamic characteristics of SAV vehicles, see Table 7.

Table 7: Aerodynamic analysis modules for SAV conceptual design

Analysis modules	Developer	Application	Availability	Description
DATCOM ⁷⁸	USAF	Subsonic, transonic, supersonic, hypersonic	Y	Semi-empirical
PANAIR ⁷⁹	Douglas Corporation	Subsonic, supersonic	Y	Numerical
S/HABP ⁸⁰	NASA	Supersonic, hypersonic	Y	Numerical
ASAP ^{81,82}	Rockwell	Subsonic, supersonic, transonic, hypersonic	N	Numerical
GTSM ⁶³	General Dynamics	Subsonic, supersonic, hypersonic	Y	Numerical
VLM ⁶⁶	Technical University of Braunschweig	Subsonic, supersonic, hypersonic	Y	Numerical
Handbook Methods ^{83,84,85,86}	Prandtl-Meyer, Schlichting, Newton, Kucheman, etc	Subsonic, supersonic, hypersonic	Y	Analytical
Experimental data ^{87,88}	Horner, NASA, McDonnell Douglas	Subsonic, transonic, supersonic, hypersonic	Y	Empirical

(1) DATCOM⁷⁸ is a semi-empirical code that can determine the forces and moments on a cylindrical or nearly cylindrical body, with small protuberances and axisymmetric fin sets over a wide range of Mach numbers. Some errors will occur in using Missile

DATCOM to analyze hypersonic vehicle shapes. A simple, analytical aerodynamic model ⁸⁹ has been developed at NASA Langley and is suitable for a winged-cone aerospace plane concept. It is based on DATCOM methods and supplemented by the current theoretical methods (see Appendix C).

(2) PANAIR⁷⁹ is a general-purpose aerodynamic code that uses a linear panel method. PANAIR is capable of determining the pressures on bodies and surfaces of arbitrary shape at subsonic and supersonic speeds. It calculates pressures, forces, and moments using a variety of pressure formulas (such as isentropic, linear, etc.), including the forces and moments due to flow through the surface.

(3) S/HABP⁸⁰ (Supersonic/Hypersonic Arbitrary Body Program) uses first order methods to calculate the pressures on arbitrarily shaped bodies and lifting surfaces at supersonic and hypersonic speeds. HABP can calculate surface pressure and skin-friction coefficients, radiation equilibrium wall temperatures or heat fluxes for a given wall temperature, for each surface element of an analysis model. HABP can also compute aerodynamic stability derivatives and predict pressure.

(4) ASAP^{81,82} has been developed by Rockwell for NASA Langley. It calculates pressure distributions as well as force and moment coefficients laterally and longitudinally for the configuration in the total speed range from subsonic to hypersonic speeds. ASAP is used for engineering analysis and is suited for the conceptual design phase. It is an interactive code that features the United Distributed Panel (UDP) Method

for subsonic, transonic, and low supersonic analysis, and the Hypersonic Arbitrary Body Program (HABP) for hypersonic analysis.

(5) The aerodynamic module in SSSP⁶³, GTSM, has a three-dimensional aerodynamic modeling capability which can be used to define the aerodynamic forces along the standard pitch axis, roll axis, and yaw axis. Each of these models is specified by defining the appropriate aerodynamic coefficients as a function of Mach number and the pitch angle of attack. This is accomplished by means of three-dimensional tables for each aerodynamic coefficient to be modeled.

(6) For the determination of the aerodynamic load distribution on the aircraft surface, necessary for structural analysis, PrADO-Hy⁶⁶ includes a vortex lattice method for subsonic design cases and a first-order shock expansion method for hypersonic design cases. The latter method also provides the radiation-adiabatic surface temperatures in hypersonic flight used for the TPS layout.

(7) Analytical handbooks methods show that the subsonic and transonic aerodynamic characteristics are a function of flight Mach number, angle of attack, and gross geometric parameters of the flight vehicle geometry. In the supersonic/hypersonic speed range, the fuselage pressure and aerodynamic forces (lift and pressure drag) can be obtained by using real-gas tangent-wedge/tangent cone, independent-panel methods. In the higher hypersonic Mach number regime, Newtonian methods are used to estimate surface

pressure coefficients. Table 8 presents some basic methods and theories which are applied in NASA's hypersonic aerospace vehicle design.⁹⁰

Table 8: Aerodynamic analysis methods for hypersonic aerospace vehicle design.⁹⁰

Parameters	Subsonic	Transonic	Supersonic and Hypersonic
Lift			
Body	Empirical function (AR, Mach)		Tangent wedge/Tangent cone Newtonian Mach >18
Wing	Low AR Theory		Linearized supersonic
Drag			
Induced	Empirical function (AR)		Tangent wedge/Tangent cone Newtonian Mach >18
Skin friction	Schlichting		Reference enthalpy Eckert, Van Driest, Schlichting Re/M (transition criteria)
Body wave	No	Empirical function (mean sweep, FR, Mach)	Tangent wedge/Tangent cone Newtonian Mach >18
Wing wave	No	Empirical function (sweep, t/c)	Prandtl-Meyer Shock expansion
Bluntness	No	No	Leading –edge radius/Sweep and Newtonian
Engine Base	No	Empirical function (Mach)	70% Vacuum

As can be seen in Table 7, the handbook analytical methods, wind tunnel testing data, and the ASAP code show a capability for aerodynamic analysis in all the subsonic, transonic, supersonic, and hypersonic speed regimes. However, ASAP is not a public domain software and not available for the current study. Some subsonic and transonic handbook analytical methods shown in Table 8 are based on empirical functions (wind tunnel test result). As of today, various SAV concepts (winged vehicle, lifting body, circular cone, etc.) have been tested in low and high speed wind tunnels; these wind tunnel data are especially useful for estimating SAV aerodynamic characteristics at the conceptual design level.^{91,92} USAF DATCOM⁷⁸ has been applied and validated for a long time in the conceptual design of subsonic, supersonic, and hypersonic vehicles. Therefore, experimental data (Horner, NASA, MDC, etc.) will be mainly used in the

development of the SAV design methodology, and the semi-empirical method DATCOM will be used as a supplementary tool.

Based on the survey of all above aerodynamic analysis modules in Tables 7 and 8, it is concluded that, in aerodynamic disciplinary analysis, key design parameters are lift coefficient, drag coefficient, and moment coefficient which are required to be estimated for all subsonic, transonic, supersonic, and hypersonic regimes under a range of angles of attack.

3.2.4 Stability and Control

The stability and control design analysis of a SAV is highly challenging and complicated because it flies across broad altitude and speed ranges. Generally, SAVs (Space Shuttle, X-15, Dyna-soar, etc) use conventional aerodynamic control surfaces for pitch, yaw, and roll control in the dense atmosphere and reaction control systems (for example, hydrogen peroxide thruster systems in the X-15 and Dyna-soar) for flight outside the Earth's atmosphere. Supersonic and hypersonic flows have great effects on the stability and control characteristics of a SAV: (1) movement of aerodynamic center: In order to counteract the resulting nose-down pitching moment, the XB-70, Concorde, and SR-71 all use the fuel pump system to move the CG aft.⁹³ (2) reduction of fin effectiveness at high Mach number: X-15 uses thick wedge-shaped tail fins to provide directional stability at high speeds where conventionally shaped airfoils were not efficient.⁷⁷ In the Mod II configuration of the lifting body vehicle HL-10, the leading edge of the tip fins was modified due to problems involving a loss of roll effectiveness.⁹⁴

(3) decrease in directional stability: Like many high-speed craft, SpaceShipOne loses its directional stability at high Mach numbers, and this effect is especially greater at low or negative angles of attack (AOA).^{95,96}

Therefore, in conceptual design, rapid and economical estimation of stability and control characteristics is important. The estimation results can provide a good measure to check whether enough stability and control power is available for maintaining static and dynamic stability and for maneuvering. Various engineering analytical, empirical, and numerical methods have been developed to determine the stability and control characteristics of SAV vehicles, see Table 9.

Table 9: Stability and control analysis modules for SAV conceptual design

Analysis modules	Developer	Application	Availability	Description
DATCOM ⁷⁸	USAF	Subsonic, transonic, supersonic, hypersonic	Y	Semi-empirical
VORSTAB ⁹⁷	University of Kansas	Subsonic, supersonic, hypersonic	Y	Numerical
PrADO-Hy ⁶⁶	Technical University of Braunschweig	Subsonic, supersonic, hypersonic	Y	Numerical
Wind tunnel data Flight testing data ^{94,98,99}	NASA	HL-10, X-15, Space Shuttle, X-24A/B	Y	Empirical

(1) The fundamental purpose of the USAF Stability and Control DATCOM⁷⁸ is to provide a systematic summary of methods for estimating stability and control characteristics in preliminary design applications. Consistent with this philosophy, the development of the Digital DATCOM computer program is an approach to provide rapid and economical estimation of aerodynamic stability and control characteristics. Digital DATCOM requires Mach number and Reynolds number to define a flight condition. This requirement can be satisfied by defining combinations of Mach number, velocity,

Reynolds number, altitude, and pressure and temperature. Aerodynamic stability methods are defined in Datcom as a function of vehicle configuration and Mach regime.

(2) VORSTAB⁹⁷ is a computer program developed at the University of Kansas for aircraft aerodynamic coefficient and stability derivative prediction for any aircraft configuration. The code behind the program is based on the vortex method which can predict derivatives at high angles of attack. VORSTAB is capable of calculating lift, drag, side force, pitching moment, rolling moment, yawing moment, hinge moment, torsional moment, bending moment, longitudinal stability derivatives, and lateral-directional stability derivatives.

As seen in the design synthesis methodologies of Table 4, only PrADO-Hy⁶⁶ analyzes the tailplane and rudder sizes and checks stability and control aspects. There are no stability and control analyse in other SAV design methodologies such as SSSP.⁶³ VORSTAB⁹⁷ requires a detailed geometry input of the airplane configuration (at least 6 pages of input file for one SAV configuration) and is a tool desired for preliminary/detailed analysis. In contrast, the USAF DATCOM⁷⁸ only requires a few geometry data as input (one page input for one SAV configuration) and provides a good estimation of aerodynamic stability and control characteristics. As a consequence, the USAF DATCOM is selected for the development of the current SAV design methodology, and flight test data/wind tunnel data will be used to provide additional design points for the study.

The stability and control characteristics of each component and the built-up configuration can be obtained from the DATCOM output file as: (1) longitudinal coefficients and lateral-directional stability characteristics: C_D , C_L , C_m , C_n , and C_A , and the derivatives C_{L_α} , C_{m_α} , C_{Y_β} , C_{n_β} , and C_{l_β} . (2) dynamic derivative characteristics: pitch, acceleration, roll, and yaw derivatives of C_{L_q} , C_{m_q} , $C_{L_{\dot{\alpha}}}$, $C_{m_{\dot{\alpha}}}$, C_{l_p} , C_{n_r} , C_{Y_p} , C_{n_r} and C_{l_r} . Based on the stability and control analysis modules in Table 9 and in design books,^{100,101} the derivatives C_{L_α} (lift-curve slope), C_{m_α} (the longitudinal stability criterion), C_{n_β} (the direction stability criterion), C_{l_β} (the dihedral effect), C_{m_q} (damping in pitch), C_{l_p} (the resistance in roll), and C_{n_r} (damping in yaw) are considered important design parameters and provide sufficient information for the stability and control analysis at the conceptual design level.

3.2.5 Aerothermodynamics

In subsonic flight, the heat produced from friction is very low and presents no problem. However, for supersonic/hypersonic flight, the heat produced at high Mach numbers is prominent and transferred from the flow to the space plane surface by convection through the boundary layer. The temperature of the SR-71 leading edges is approximately 800°F at Mach 3.¹⁰² For the X-15, the temperature of the wing leading edge is nearly 2400°F and the forward fuselage temperature is around 1600° to 1800°F at the 8000 ft/s, 100,000 ft altitude flight condition.⁷⁷ Besides high temperature being caused by air-surface friction, there is even higher temperature produced at the stagnation point on a body where the air is brought to rest and all of the kinetic energy contained in the air

is converted to heat. When the Space Shuttle reenters at 400,000 ft altitude with approximately 25,000 ft/s velocity, the surface temperatures of the Space Shuttle may range from 3000°F at the stagnation points on the nose and leading edges of the wing and tail down to about 600°F on leeward surfaces.¹⁰³ The maximum re-entry temperatures of Dyna-Soar could reach 3650°F at the nose-cap, 2822°F on the wing leading edge, and 2400°F on the lower wing surface.¹⁰⁴ It is obvious that the estimation of thermal conditions of a SAV is vital in conceptual design.

A variety of engineering codes can be used to calculate the aeroheating of SAV vehicles as shown in Table 10.

Table 10: Aerothermodynamics analysis modules for SAV conceptual design

Analysis modules	Developer	Application	Availability	Description
MINIVER ¹²	NASA	Hypersonic	N	Numerical
S/HABP ⁸⁰	NASA	Supersonic, hypersonic	N	Numerical
PrADO-Hy ⁶⁶	Technical University of Braunschweig	Subsonic, Supersonic, Hypersonic	Y	Numerical
SSSP ⁶³	General Dynamics		Y	Analytical
Handbook Methods ^{4,105}	Bertin, Czysz	Supersonic, hypersonic	Y	Analytical

(1) MINIVER¹² is a simple engineering code that employs a number of user selectable methods to compute post shock and local flow properties as well as heating rate values based on either a perfect gas or equilibrium air chemistry.

(2) S/HABP⁸⁰ can calculate radiation-equilibrium wall temperatures or heat fluxes for a given wall temperature, for each surface element of an analysis model.

(3) PrADO-Hy⁶⁶ includes a first-order shock expansion method for hypersonic design cases. The last method also provides the radiation-adiabatic surface temperatures in hypersonic flight used for the TPS layout.

(4) SSSP⁶³ has a General Trajectory Simulation Module (GTSM) program to define the time rate of change of the three-degree-of-freedom vehicle motion, the vehicle mass, the ideal velocity and velocity losses, and a heating parameter. The heating parameter equation is the product of the relative velocity and the dynamic pressure.

The first two aerothermodynamics analysis modules (MINIVER, S/HABP) in Table 10 are not available for the current study, and the VLM method used in PrADO-Hy usually requires detailed geometry data inputs. SSSP uses the same basic heating parameter equations as the handbook methods. Therefore, basic analytical handbook methods (heat equations) will be used for the development of the SAV design methodology.

The thermal conditions are required to be considered in the early design phase to define the TPS system and the airframe materials. The study shows that the thermal conditions of a SAV depend on flight Mach number, altitude, and the leading-edge geometry.¹⁰⁵ The magnitude and duration of the heat flux imposed on the space vehicle are key design parameters in the aerothermodynamics design analysis of SAV conceptual design. Therefore, two key design parameters are stagnation temperature (the maximum heat rate) and heat flux. The approximate stagnation point temperature limitation of the

vehicle is estimated as a function of free stream temperature T_∞ and flight Mach number M . The stagnation-point convective heat transfer is roughly proportional to $(\rho_\infty)^{0.5}(U_\infty)^3/(R_N)^{0.5}$ ¹⁰⁵ Thus, the blunter the body, the lower the convective heat-transfer rate of the stagnation point. The Blunt Body Theory was published by Allen and Eggers¹⁰⁶ in 1958 and has been applied to the heat shield designs in the Mercury, Gemini, and Apollo capsules.

3.2.6 Trajectory

The SAV mission is to deliver payloads to certain altitudes: suborbital tourism (100 km above the earth's surface), low earth orbit (LEO, typically 200-1200 km), medium earth orbit (altitude between LEO and GEO), and geostationary orbit (GEO at altitude of 36000 km). Table 3 shows that most SAV mission profiles are to an altitude of low earth orbit. The suborbital tourism vehicles (SpaceShipOne, DC-X) reach an altitude of 100 km. The service ceiling of Dyna-soar is 160 km.¹⁰⁴ Typical Space Shuttle flight altitudes range from 300 km to 600 km.¹⁰³ The mission and design requirements determine the different operational modes of SAV concepts and also various SAV trajectories. The HTHL SSTO vehicle (NASP)⁶⁰ is designed to take off horizontally from a runway, accelerate up to twenty-five times the speed of sound, and go into LEO or travel over intercontinental ranges at hypersonic speeds. The VTHL vehicles (Space Shuttle, X-33) take off vertically and land on a runway. The VTVL vehicles (DC-X, Michelle-B) take off vertically from earth, achieve sub-orbit and return with a vertical landing. The air launch vehicles (X-15, SpaceShipOne, Sanger/Horus) are dropped from the first stage vehicles and then climb to a certain altitude. The trajectories of all SAVs are required to

provide efficient energy transfer for the vehicle to fulfill its intended mission. The objective of trajectory analysis in the conceptual design of a SAV is to provide a decision support tool that can help the conceptual designer to size, evaluate, and analyze SAV concepts throughout the flight envelope.

Typical trajectory analysis is based on two analytical approaches. (1) A point mass approach: A three (or six) degree-of-freedom model can be built to compute a flight trajectory by using the equations of motion of a point mass aircraft moving relative to a rotating, spherical earth.¹⁰⁷ Solutions can be found by using these complicated boundary condition trajectory equations. (2) An Energy-State Approximate (ESA): The ESA technique was first introduced by Rutowski in 1953.¹⁰⁸ It uses total energy as a state variable, and optimal trajectories for a variety of performance objectives, such as minimum time and fuel-climb problems, can be defined. ESA techniques have been successfully applied to a wide variety of aircraft, providing a simple and fast graphical solution to the optimization problem.¹⁰⁹ For conceptual design, it is desired to have a trajectory analysis tool to quickly obtain information about design feasibility, sensitivities, boundaries, and constraints from this top-level simulation process as valuable feedback to the designer.

Currently, there are many well-developed numerical methods (such as POST, OTIS shown in Table 11) for trajectory optimization of point-mass vehicle models.

Table 11: Trajectory analysis modules for SAV conceptual design

Analysis modules	Developer	Application	Availability	Description
POST ²⁷	NASA	launch, on-orbit, and reentry trajectories subject to a number of constraints, such as maximum acceleration, heating boundaries, and cross range requirements.	N	Numerical
OTIS ¹¹⁰	Boeing	simulating and optimizing point mass trajectories of a wide variety of aerospace vehicles	N	Numerical
PrADO-Hy ⁶⁶	Technical University of Braunschweig	a flight path simulation to estimate the necessary thrust and fuel mass of the aircraft. For every point of time during the flight simulation, Mach number and altitude are given.	Y	Numerical
GTSM (SSSP) ⁶³	General Dynamics	a general purpose high speed, precision flight program which simulates the flight for an aerospace vehicle in the gravitational field of a central body.	Y	Numerical
Handbook Methods ^{4,101,107,108}	Rutowski,	Energy-State Approximate (ESA)	Y	Analytical

Both the POST²⁷ and OTIS¹¹⁰ programs were developed for simulating and optimizing point mass trajectories of a wide variety of aerospace vehicles and solving very complicated and highly constrained problems. However, these two programs are not available for the current study. Also, these higher-fidelity trajectory analysis programs (POST, OTIS, GTSM, and PrADO-Hy) are too expensive computationally and not robust enough to use at the conceptual design stage, in which many hundreds of vehicles must be evaluated and compared on a consistent basis. Thus, there is a clear demand for a CD-level trajectory analysis approach, capable of bridging the gap between the high fidelity trajectory analyst and the conceptual designer. It is required to provide the SAV designer with a CD-level tool capable of synthesizing relevant launch vehicle design disciplines for top-level sensitivity and trade studies to be visualized throughout the trajectory. As a consequence, a trajectory synthesis simulation program (SAV_TSSP)¹¹¹ has been

developed as a design decision support tool for the development of the HTHL SAV design methodology. Its synthesis capability provides quick design feedback to the conceptual designer.

The POST²⁷, and General Trajectory Simulation Module (GTSM) of SSSP⁶³ can define the time rate of change of the three-degree-of-freedom vehicle motion, the vehicle mass, the ideal velocity and velocity losses, and a heating parameter. In PrADO-Hy,⁶⁶ Mach number and altitude for every point in time are given during the flight simulation. Therefore, primary design parameters like thrust, weight, velocity, altitude, dynamic pressure, and time at each flight interval are necessary to be estimated at the conceptual design level. As a consequence, the trajectory analysis supports the configuration concept selection process by quantifying design sensitivities of key design parameters as early as possible in the design process.

3.2.7 Life-Cycle Cost

During the past decades, launch vehicle design has switched from maximum performance and minimum weight to minimum cost design, especially for commercial launch vehicles. Clearly, cost issues play a decisive role today in designing commercially feasible space-access vehicles. The current launch cost to low earth orbit is approximately \$10,000/lb for the Space Shuttle, \$6,000/lb for the Pegasus (Orbital Sciences), \$4,000/lb for the Delta and Atlas, and \$2,500/lb for the Proton (Russian).¹¹² The main goal of NASA's research development of next generation launch vehicles and technologies is to reduce launch cost.¹¹³

Cost estimation for a new SAV must be based on past experience. Cost models depend on the statistical cost data of realized projects, where SAV reusability, proven and existing technologies coupled with flight rate are all evaluated. The larger the number of reference projects, the better and more credible is the cost estimation. Many cost models have been developed by NASA, USAF, universities, and commercial entities. These cost models evolve and take into account lessons learned of early cost models. The key parameter for cost estimation is life cycle cost (LCC), based on airframe and engine development, vehicle acquisition, and operational costs. Generally, LLC includes the following key cost areas:

- Development cost
- Production cost
- Direct and indirect operating cost

The selection of the appropriate cost model to use for a SAV cost analysis is very important. It is a key consideration in the SAV conceptual design process. In order to provide a status of existing cost models, a literature review is performed to show the capability and limitations of these models.¹¹⁴ A list of these system level cost models is presented in Table 12.

Table 12: Comparison of cost models^{115,116,117,118}

Cost Model Name	Developer	Availability	Applicability
Advance Missions Cost Model	NASA JSC	N/A	Launch vehicles, spacecraft Human explorations missions
Aerospace Small Satellite Cost Model	The Aerospace Corp.	N/A	N/A
ALS/ADP Cost Model	USAF Phillips Lab	N/A	N/A
EHF/SHF Communications Cost Model	USAF SMC/FMC	N/A	N/A
Hypercost	NASA JPL	N/A	N/A
Launch Vehicle Cost Model	TECOLOTE	N/A	Launch vehicle
MicroFASTE	Mainstay Software Corporation	N/A	N/A
NAFCOM	NASA MARSHALL	Documentation	launch vehicles, upper stages, engines, and spacecraft
Non Nuclear Power	NASA LeRC	N/A	N/A
Nuclear Space Power	NASA LeRC	N/A	N/A
Parametric Cost Model	Parametric Consultants/England	N/A	N/A
ParaModel	Mainstay Software Corporation	N/A	N/A
PRIZE	LLC	N/A	Components, Boxes
SCEEDOS	USAF SMC	N/A	N/A
SEER	Galorath Inc.	N/A	Components, subsystems, and systems
Sensat	Owl Wise Laboratory	N/A	N/A
Solid Rocket Motor Cost Model	TECOLOTE	N/A	N/A
SUBORB-TRANSCOST	Dr.-Ing Robert A. Goehlich	Documentation, Software	Suborbital launch vehicle
TRANSCOST	Deutsche Aerospace, KOELLE	Documentation	Launch vehicle
Unmanned Spacecraft Cost Model	USAF SMC	N/A	N/A

All cost models listed can be used as the primary cost estimation for space vehicles. However, among these, NAFCOM, Launch Vehicle Cost Model (LVCM) and other USAF and NASA cost models are partially or fully classified. The commercial PRICE-H Model and SEER cost models have confidential databases. Therefore, it is difficult to complete a full review of these cost models. Also, most of these models, such as NAFCOM, LVCM, are subsystem-based estimation. This means that a detailed design of the vehicle is required with definition of subsystems. In contrast, the TRANSCOST model¹¹⁹ is a system-based model (subsystem data not required, except the engine data),

and the reference projects for each cost estimation relationship are well documented. The literature review¹¹⁴ of all cost models clearly shows the extraordinary capability of the TRANSCOST model for estimation of SAV system cost.

The TRANSCOST Model and its modified model, SUBORB-TRANSCOST¹²⁰ are described in more detail in Appendix D. The advantages of the TRANSCOST model compared to the other described cost models are summarized as follows:

- It is based on a comprehensive and continuously updated vehicle and engine cost data collection from a period of over 43 years (1960 to 2002).
- The cost model structure is associated with the development, manufacturing, and operation of SAVs (both ELVs and RLVs). The advantage of this model structure is the possibility of making a cost assessment in all of these areas separately and/or combining them as well, depending on the specific case of application. It is conceived such that it allows for cost-optimized vehicle designs.
- It can estimate cost at the very beginning of a vehicle design process, and NOT after a detailed design has been established. It may lead to cost results which are not acceptable – and the complete design process must start again.
- It has been validated with real cost data from existing launch vehicles, such as the Space Shuttle, Ssturn, ARIANE, etc.
- A modified SUBORBIT-TRANSCOST¹²⁰ has been developed by Goehlich and is available for the cost estimation of suborbital vehicles (SpaceShipOne, DC-X, RocketPlane).

4. A Generic Space Access Vehicle Design Methodology

In Chapter 3, the input and output parameters and the methods library of each primary design discipline have been defined and assembled. With this information, key design disciplinary modules will be developed and integrated into the generic (configuration independent) SAV design methodology.

When comparing the design of transonic transport aircraft with the design of SAVs, especially reusable launch vehicles (RLV), we quickly realize that the design of a SAV is far more complicated for two reasons:

First, in comparison to aircraft design, the design of SAVs promises many more ‘known-unknowns’ but in particular ‘unknown-unknowns’ due to the lack of a statistical data base and the lack or even absence of adequate SAV design tools. Until today, it is not yet known which RLV configuration concept promises a feasible launch system complying with the metrics of cost effectiveness and reliability. As a consequence, we observe the exploration of radically different configuration concepts today, an exploration between the design extremes HTHL and VTVL.

Secondly, the highly integrated nature of SAVs results in a much smaller payload margin compared to aircraft. To be precise, no truly reusable SAV has yet demonstrated a positive payload margin. As a consequence, the traditional handbook-method approach routinely used for the design of aircraft has to fail when applied to SAVs. Also, the development of future efficient SAVs requires dedicated systematically developed and

consistently applied design tools for the evaluation and comparison of competing SAV design alternatives, leading to a well explored design space. As discussed in Chapter 2, a generic Class V design synthesis system promises such potential.

The generic methodology concept ultimately produces consistent, more accurate, and efficient SAV simulation model representations. In 2000, Diaz-Calderon, *et. al.*, have shown that generic models can facilitate the simulation analysis process, reduce the monetary investment, and provide more accurate, reusable modules.¹²¹ In 2002, Steele, *et. al.*, generate a generic simulation environment for modeling future launch operations (GEMFLO) to analyze the operations performance of several RLV architectures. It allows one model to be applied to multiple systems and provides feedback to system designers.¹²² In the design of the orbital space plane (OSP), Cope, *et. al.*, in 2004 presented a methodology of parametric estimation with generic modeling. This design assessment model provides a fast estimation capability of system performance for the designer.¹²³ All of these studies clearly show that the generic model systematically organizes the design process and provides fast-paced design platforms for multiple systems like SAVs. However, the development of a generic model usually requires more time.

A generic SAV design synthesis system is a design system capable of analyzing and comparing different SAV alternatives of either the reusable launch vehicle (RLV) or expendable launch vehicle (ELV) category. It is a stringent requirement that the generic design synthesis methodology has to be capable of evaluating the range of potential SAV

design alternatives at the conceptual design level with emphasis on correctness rather than accuracy. Clearly, a generic design capability implies greater complexity of the underlying model. Thus, it is required to find the level of model abstraction appropriate for a specific design application, but still have sufficient abstraction to be generic, thus, applicable to different design applications.

4.1 Generic Methodology Development

Generally, there are two principal alternatives leading to the development of a generic SAV design system: (1) Directly develop a generic model applicable to all SAV configuration concepts. This is similar to finding a universal formulation like Newton's laws (e.g., $F = m \cdot a$), which can be applied to physical motions in general. (2) Starting a configuration-specific model and, subsequently, extending the model to cope with additional SAV configuration concepts (gradually developing the model into a generic formulation). Overall, it is a truly challenging task to develop a generic design synthesis system for future SAVs due to the limited statistical data base available, a fact especially valid for the class of reusable launch vehicles (RLV). Rather than waiting for the 'lucky moment to find the formula for everything' (option 1), the present research adopts the rather incremental approach (option 2) in order to arrive at a feasible generic design methodology in due time.

Figure 24 outlines the second approach for developing a generic SAV design synthesis methodology. First, the investigation of physical SAV characteristics and available design methodologies leads to the definition of a generic SAV design system. A

baseline design system architecture is then selected capable of representing the basic characteristics of all SAVs. It includes a relatively complete operations process and design requirements involved. At some level of abstraction, this model has the potential to be generic and easily extended to other applications (VTHL, VTVL, and ELV, etc.). Therefore, based on the framework and on reusable modules (e.g., disciplinary analysis methods) of the representative design system, a generic model can be developed and applied to alternative SAVs.

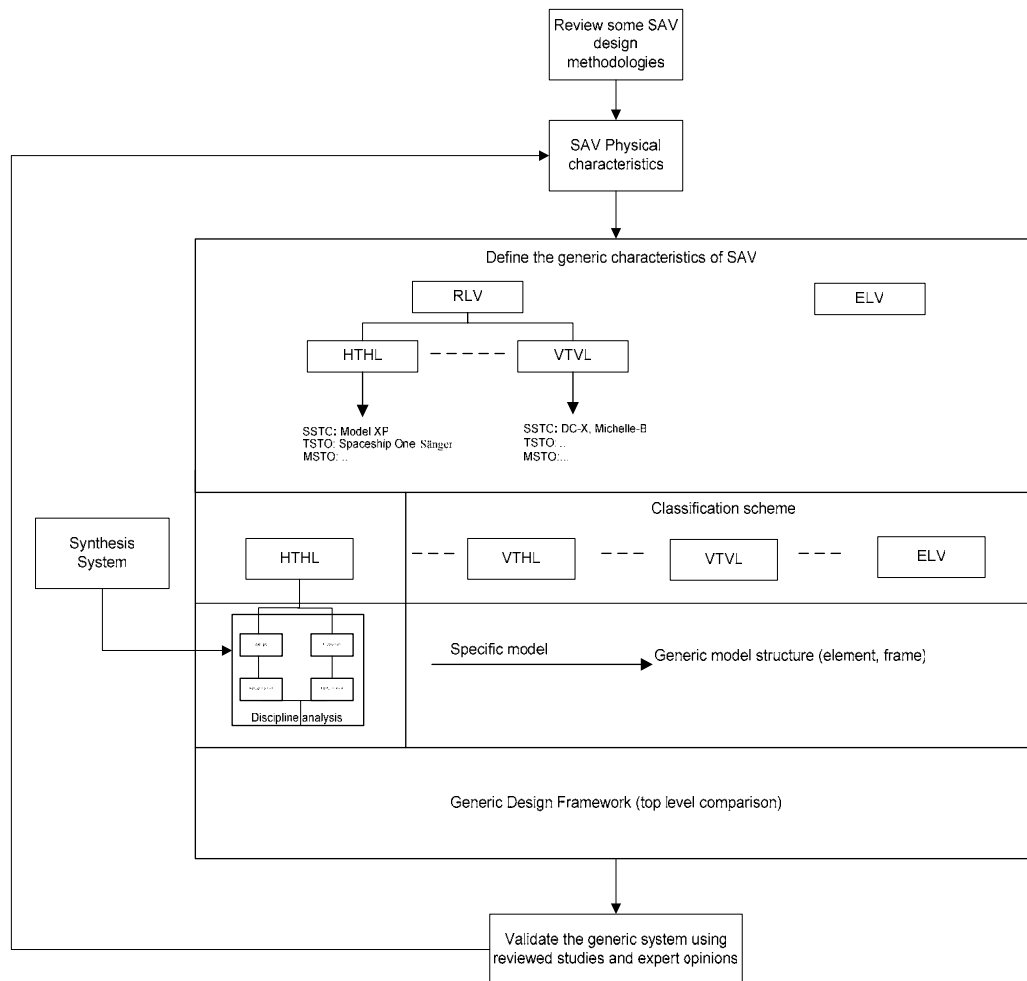


Figure 24: Methodology for developing a generic SAV design synthesis system

The development of a generic design synthesis methodology consists of four distinct stages:

- 1) Identify physical characteristics of possible SAVs and methodology concepts leading to a generic SAV design system
- 2) Develop and validate a generic SAV synthesis methodology starting with HTHL vehicles
- 3) Extend the HTHL methodology and apply it to VTVL vehicles
- 4) Integrate the algorithm of the baseline design system architecture into a computerized design synthesis environment – AVDS-PrADO.

4.2 Alternative Methodology Concepts Towards a Generic SAV Synthesis System

The process of evaluating existing space access vehicle design methodologies is essential to appreciating existing design approaches with associated trains of thoughts. Overall, it provides the developer the possibility to adopt already existing elements for the generic methodology since time is too short to reinvent the wheel. The synthesis review in Chapter 2 indicates that each particular design study and associated methodology are inclined to be applied to specific vehicle types. Hunt's design methodology focused on hypersonic airbreathing vehicles (NASP, X-43, etc.) with emphasis on engine and airframe integration. Wood's design methodology is applicable to launch vehicles (Atlas, Delta, etc.) using rocket propulsion. Heinze's PrADO-Hy was developed to analyze waverider type TSTO vehicles (e.g., with air-breathing hypersonic first stage and winged second stage - Sanger/Horus). However, this *application specific*

approach contradicts the main research objective to develop a configuration independent (generic) design methodology.

Currently, there are several manual SAV design methodologies in existence, where the task of converging (see definition in Chapter 4.3.5) the product is in the hand of the capable project manager. For example, Hammond's methodology manually integrates existing higher-order analysis codes, such as ASAP, POST, SMART, etc., to arrive at a solution. However, the execution sequence of the manual approach very much depends on the project lead and team, thus, it includes an element of randomness. In contrast, a computer-integrated synthesis approach as seen in Heinze's methodology shows an efficient multi-disciplinary process, an organized analysis, design and optimization capability leading to a converged SAV design, a design sequence which can easily be reproduced. Clearly, the *discipline type approach*, as seen in the manual design methodology, is faced with the challenge of synthesizing individual analysis disciplines into a coherent context. Overall, it is difficult to develop a generic methodology concept based on the *discipline type approach* since most available disciplinary tools are of non-generic in character.

For a given mission specification, there are many different SAV design alternatives. For each potential SAV candidate, the mission profile usually consists of combinations of the following flight phases: take-off, ascent, orbital operation, reentry, approach, and landing. In the present research investigation, the abstract mission profile shown in Figure 25 has been selected as the starting point for building the generic SAV

methodology. This *mission type approach* has shown to be very useful for the definition of a generic simulation tool for RLVs.¹²² It can be constructed through several iterations but requires some additional abstraction compared to a single system model. Based on the mission profile, it is possible to logically expand the methodology to a generic model applicable for any space access vehicle. The generic model is not derived from a single formula but rather implies an approach utilizing a methods library. If the underlying methodology architecture is expandable in its structure, then it is possible to derive any specific system model in case such system information is available. Such an approach will ultimately lead to the generic methodology concept.

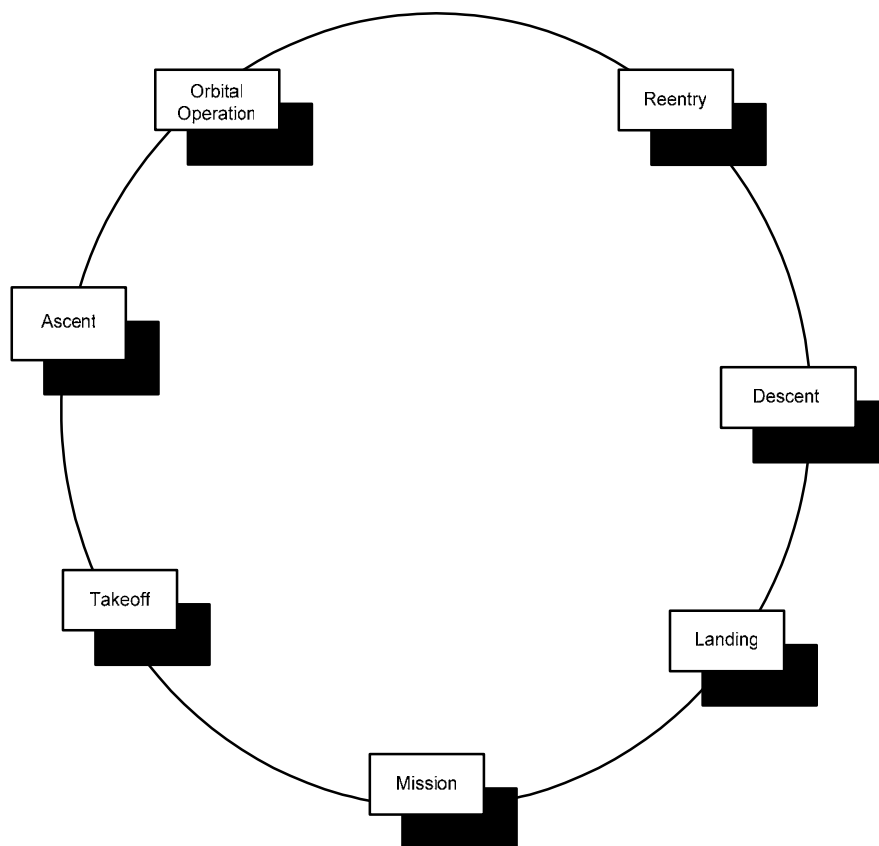


Figure 25: Generic SAV mission profile.

The design process of ELVs and RLVs can be included in this approach using a consistent level of abstraction. Taking the *Ariane* ELV as an example, its mission ends after the orbital operation. So, the mission segments reentry, decent, and landing provided with the generic methodology architecture are ignored, but they have to be activated for *DC-X* SSTO types. Overall, the *mission type approach* shows potential to extend either the manual or the computer integrated methodology to a generic system. For each potential SAV candidate, the mission profile always consists of either the complete set or a selection of the flight phases take-off, ascent, orbital operation, reentry, approach, and landing.

4.3 Design Synthesis Methodology for Baseline Vehicle – HTHL

The development of the generic SAV synthesis methodology is initiated by addressing first the HTHL type (e.g., *Sänger* TSTO) as the baseline concept because of its comprehensive mission profile. For this type of SAV, every flight phase in the abstract mission profile, see Figure 25, has to be modeled in the methodology concept.

For each mission segment, see Figure 25, the synthesis system is employed to assess the feasibility of the SAV design configuration concept under investigation. Throughout each flight phase (e.g., ascent) it is required to consider the primary design disciplines: geometry, weight and balance, aerodynamics, stability and control, aerothermodynamics, propulsion, performance, cost, and others. For each mission segment, the results of the multidisciplinary design analysis are imported into the sub-synthesis module which determines and visualizes design constraints for this mission segment only. Clearly, sub-

design spaces are defined for each individual mission segment (see Chapter 4.3.1 - 4.3.4). Then, the sub-synthesis constraints for each mission segment are input to the master synthesis level, which discusses the resulting design space for the entire mission profile by superposition of the sub-synthesis results. Vehicle design convergence (see hands-on convergence in Chapter 4.3.5) leading to a SAV design proposal is sought based on sub-synthesis and master-synthesis design spaces. It should be noted that designing the SAV through distinct flight phases generates sub-synthesis level design space information which allows the design team to work on the configuration concept concurrently. Finally, at the master-synthesis level, each distinct flight phase is balanced and converged into a feasible SAV design which complies with the entire mission profile.

However, like other methodologies pictured in the literature, the flow-chart shown in Figure 5 represents a top level process only and is not sufficient to describe the design process with sufficient detail. As described in Chapter 2, a traditional design synthesis program consists of a synthesis module and disciplinary sub-modules, which perform dependent multi-disciplinary studies required during the conceptual design (CD) phase of the flight vehicle. After the disciplinary analysis level, information related to primary design variables are passed by the sub modules to the system level module for further system level assessment. The integrity, consistency, and trend-accuracy of data derived from these sub modules is considered very important.

In order to improve the overall transparency of our design synthesis methodology, we have developed a logical sequence of process visualizations. Figure 26 shows a detailed

level of the design methodology, which identifies key design parameters, disciplines, and interactions amongst relevant disciplines.

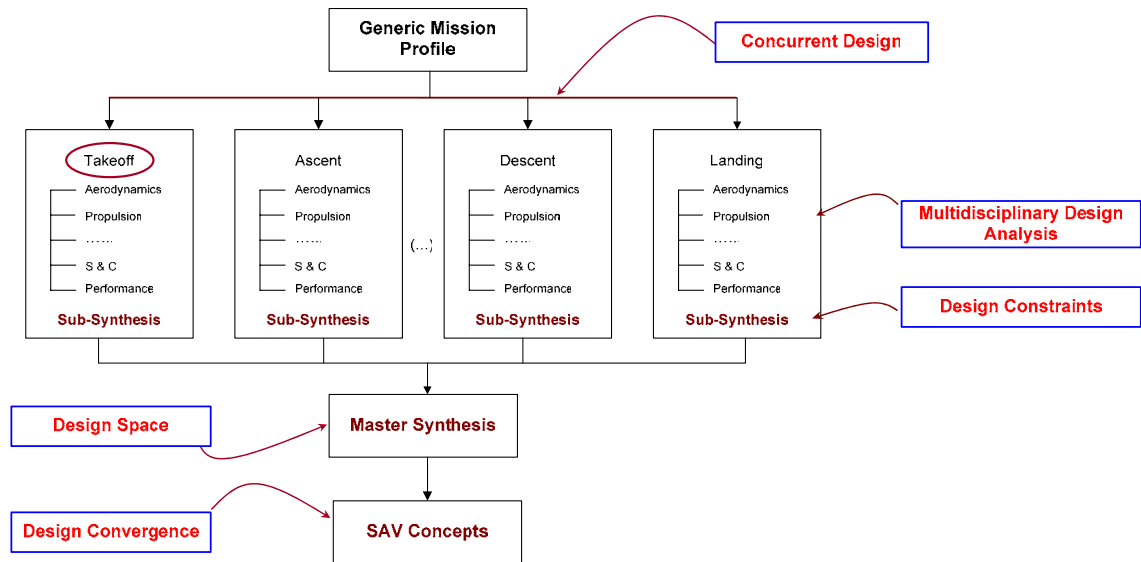


Figure 26: Top level mission type approach design methodology for a HTHL SAV.

The next level is shown in Figure 27, where the *Take-Off* mission phase is selected as an example. In this figure, the *Take-Off* input-analysis-output structure is detailed. The geometry parameters of interest (e.g., sweep of wing leading edge) are predefined. The input data (design variables) have been quantified in detail. Recommended design parameter variations are indicated, where the number of iterations involved has been quantified. The notes written in red usually refer to our DBS and KBS, where key references and selected design case studies support the decision making of the design engineer. Clearly, having historic design information available ‘at the fingertips’ helps to identify ‘design short-cuts’.

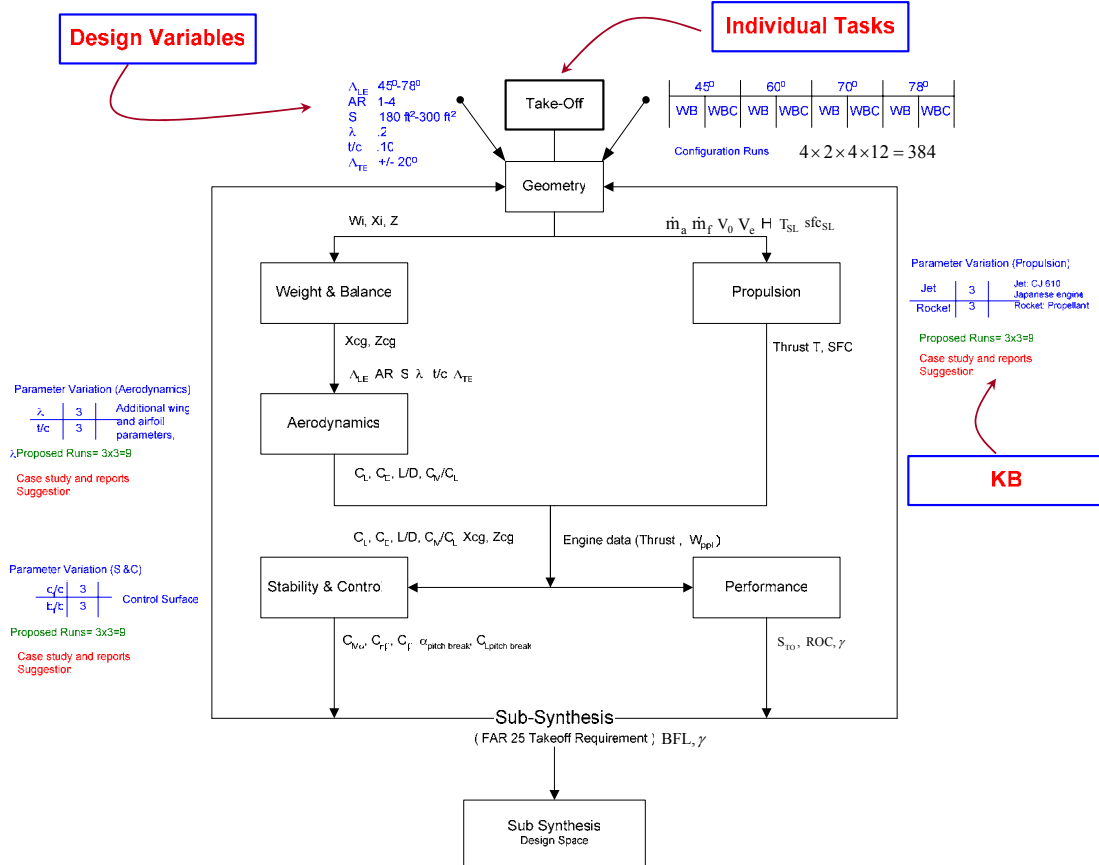


Figure 27: Detailed design methodology for each mission segment: take-off methodology.

The implementation of knowledge-based techniques provides a dynamic and intelligent design information source supporting decision making. We have experienced that the availability of a dedicated DBS and KBS truly accelerates the conceptual design (CD) process by not ‘reinventing the wheel’. The disciplinary boxes in Figure 27 (e.g., *Weight & Balance*, *Aerodynamics*) refer to the analysis tools utilized in the input-analysis-output sequence. Still, Figure 27 does not provide sufficient detail regarding the analysis methods actually utilized for a particular design study. In general, those boxes refer to a methods library, from which the design engineer selects one or a sequence of appropriate methods based on the design analysis requirements imposed. This remaining

Input - Analysis - Output

Take-Off

Configuration

Input

Analysis

Output

Weight and Balance

Propulsion

Method Library

Aerodynamics

Stability and Control

Performance

Figure 28: Detailed break-down of analysis methods utilized for the take-off mission segment example.

98

a SAV or any other flight vehicle. Ultimately, this allows, for the first time, for the reproduction of results if desired. Our approach is in analogy to structured programming, where the logic of the software is developed in a structogram¹²⁴ ahead of the actual programming task, using a programming language like *Fortran*, *Matlab*, or an *Excel* spreadsheet.

Overall, the development of the SAV ‘hands-on’ methodology has two distinct advantages. First, the methodology helps the engineer to design flight vehicles using a highly structured and organized process without the need for a computer-integration framework. Second, with the AVD Lab’s intention to implement this ‘hands-on’ design methodology into a computer-based synthesis environment (AVDS-PrADO), it is now possible, before the actual integration, to test and iteratively refine the design logic, methods, and algorithms in a highly organized fashion.

Before initiating the development of the SAV HTHL design methodology, various supersonic and hypersonic flight vehicles were been investigated in Chapter 3 and were selected as case studies to appropriately validate the design methods and tools. The SAV *KBS^{DESIGN}* presented in Chapter 3 shows a survey of hypersonic research programs by NACA and NASA from the late 1950’s to the early 1990’s as documented in References 59, 60, and 61. The actual vehicles developed from the X-15 through ASSET, and PRIME, along with the M2, HL-10, X-24A/B, and the Space Shuttle, provide an extensive technology knowledgebase for the design and development of future space access vehicles. The vehicle concepts developed can be categorized into three basic

types: ballistic capsule, lifting body, and winged body, as shown in Figure 29. The lifting body and winged body SAVs are both attractive configuration concepts for the launch vehicle designer because of their crossrange and downrange operational capability and their low-speed handling qualities. Also, because of the very low L/D ratio of ballistic capsules, only lifting-bodies and winged-bodies are capable of offering aircraft-type horizontal takeoff and horizontal landing capabilities. Examples for these two different trains of thought include the HL-10, X-24A, X-24B, X-15, Space Shuttle, and the X-prize winner SpaceShipOne. However, as shown in Reference 59, most of the above vehicles are either air-launched or vertical-launched like the Space Shuttle. Clearly, although there are some research SAV concepts (HOTOL, Sänger/Horus, NASP) for horizontal takeoff studies, there is a lack of available real flight test cases.

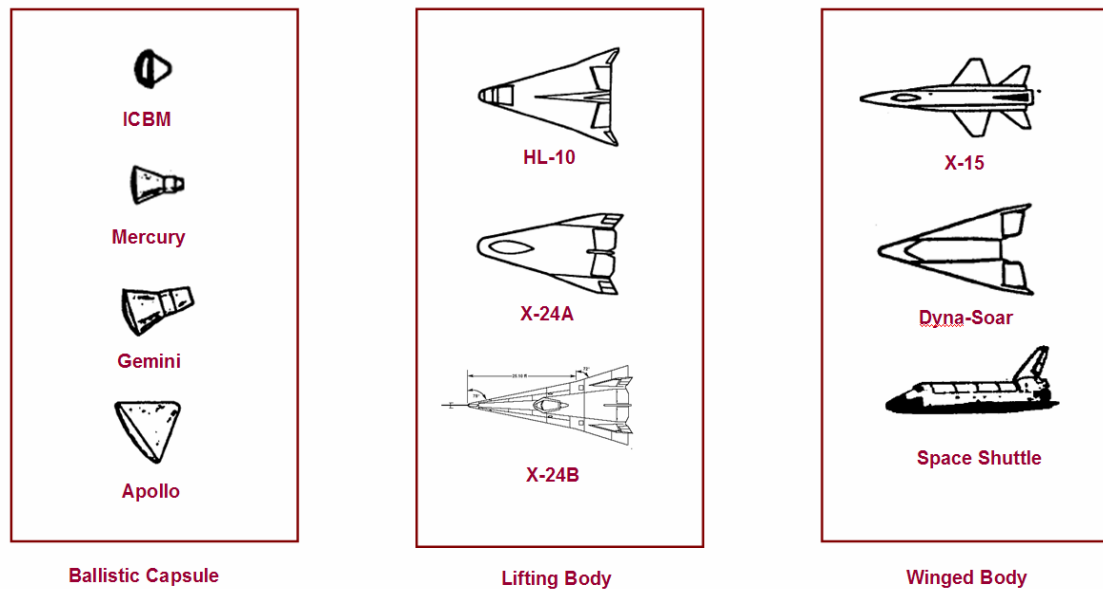


Figure 29: SAV concepts from NASA hypersonic research programs.




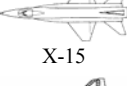


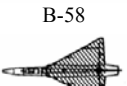
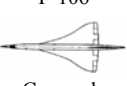
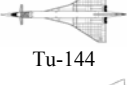
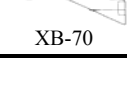
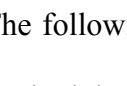
Because of the current research interest in developing a generic HTHL design methodology, the existing design case studies for the horizontal takeoff phase are critical.

As a consequence, several supersonic vehicles (B-58, F-106, Concorde, Tu-144, and XB-70) of widely varying size and configuration have been selected to complete the case studies for the whole flight loop, especially for the takeoff and landing phase. Each of these vehicles represents a key step in supersonic research and development. Concorde and Tu-144 are the only two supersonic commercial jets, illustrating the metrics of high-speed commercial operation. The Convair B-58 was the first supersonic bomber built in the West. The XB-70 Valkyrie was designed to fly at Mach 3 at altitudes in excess of 70,000 feet. This research aircraft has a delta-wing with a movable canard. The F-106 supersonic interceptor was developed from the F-102 “Delta Dagger”. The XB-70, F-106, and the B-58 have highly swept wings and a blended Sears-Haack fuselage. Two bomber aircraft (the XB-70 and B-58 planes) show higher L/D ratios than the fighter aircraft F-106.⁹⁹

In total, eleven high speed flight vehicles have been chosen for the current study. They consist of hypersonic vehicles (HL-10, X-24A, X-24B, X-15, Space Shuttle, and SpaceShipOne) and supersonic vehicles (B-58, F-106, Concorde, Tu-144, XB-70) as shown in Table 13. All of these vehicles not only have lifting shapes, but they were also all piloted and can perform either routine powered and unpowered horizontal takeoffs or landings. In terms of aerodynamic design, all of the vehicles have low aspect ratio wings varying from 0.6 to 2.5. The L/D ratio varies between 1 and 7. Most importantly, these vehicles are reasonably well documented, including available flight test data, wind tunnel data, and design data. In the present research context, emphasis has been placed on physically understanding those representative high speed vehicle designs, and also on

validating/calibrating the methods and tools that have been selected and integrated for the development of the HTHL design methodology. In addition, the conceptual design study of a HTHL tourist SAV vehicle, the Rocketplane Ltd. OU XP, made a solid contribution to arrive at a generic HTHL design methodology. References 125 to 129 provide more detailed information about this industry-funded conceptual design study towards a commercial tourist SAV, performed by the AVD Laboratory, at the University of Oklahoma. The OU XP study was initiated and funded by Oklahoma-based Rocketplane Ltd., which is a company at the forefront of the emerging tourist SAV industry.

Table 13: Selected supersonic, hypersonic and SAV vehicles.^{94,98,99}

SAVs	Flight Mission	Concept	Max L/D	AR	Max Mach	Weight (lb)
 HL-10	Concept of safely maneuvering and landing a low L/D vehicle designed for reentry from space	Lifting body	3.60	1.156	1.86	9,000
 X-24A	Titan III-launched manned orbital ferry vehicle	Lifting body	4.25	0.0617	1.62	11,450
 X-24B	Explore the supersonic and subsonic handling characteristics of hypersonic configurations	Lifting body	4.5	1.108	1.752	13,800
 X-15	Experimental rocket plane	Winged	4.2	2.5	6.7	31,000
 Space Shuttle	Low earth orbit	Delta wing	4.7	2.265	26	4,520,235
 SpaceShipOne	Suborbital tourism	Winged	7	1.67	3.26	6,800
 B-58	First supersonic bomber	Delta wing	4.84	2.09	2.1	160,000
 F-106	Supersonic interceptor	Delta wing	4.17	2.08	2.31	35,300
 Concorde	Supersonic commercial jet	Delta wing	7.7 (Mach 2.2)	1.85	2.17	385,000
 Tu-144	Supersonic commercial jet	Delta wing	8.8 (March 2.2)	1.89	2.4	396,830
 XB-70	Supersonic bomber	Canard delta wing	6.015	1.04	3	550,000

The following sections summarize the development of the hands-on HTHL SAV design methodology throughout the flight loop. For each mission segment (take-off, ascent, orbital operation, reentry, approach, landing, etc.), a series of methodology flow charts has been prepared in analogy to Figures 27 and 28, detailing the step-by-step hands-on design processes.

4.3.1 Takeoff

The horizontal takeoff procedure of a HTHL space access vehicle is similar to subsonic and supersonic aircraft. It includes the ground run, rotation, transition, and climb. Figure 30 shows the definition of takeoff field length. The takeoff field length is the total distance from rest to the point of clearance of a specified obstacle height (e.g., 35 feet or 50 feet for FAR 25).¹³⁰ A typical takeoff procedure of space vehicles includes ground roll to rotation velocity, rotation to liftoff attitude, liftoff, and climb to a specified obstacle height. There are two types of takeoff conditions: all engines operating (AEO) and one engine inoperative (OEI). At the all-engines-operating condition, the aircraft accelerates from a stop or taxi speed to the velocity of rotation (V_R), rotates to the liftoff attitude with corresponding liftoff velocity (V_{LOF}), and then climbs over a specified obstacle height. The velocity at the end of the specified obstacle height is usually called the takeoff safety speed (V_2). At the one-engine-inoperative condition, the aircraft speed at engine failure is called critical engine failure speed. There is a slightly higher speed called the decision speed (V_1) at which the pilot must decide to either continue takeoff or abort. The acceleration to stop distance is the distance from aircraft acceleration to V_1 and stop. This distance has to be balanced with the distance which the vehicle attains if it continues to accelerate with one failed engine and climbs to a specified height. The velocities (V_R , V_{LOF} , V_1 , V_2) mentioned above are defined as important design velocities for the aircraft during takeoff.

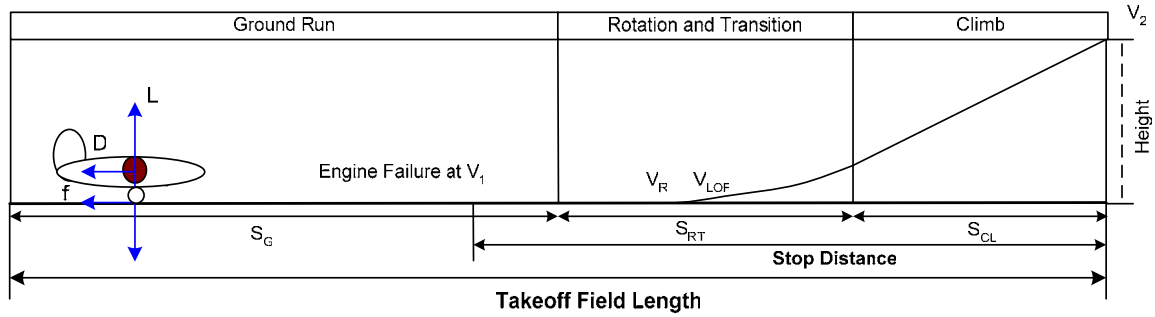


Figure 30: Definition of takeoff field length.

As can be seen in Table 13, a highly swept wing, low lift to drag ratio, low lift coefficient, and slender long fuselage are typical characteristics of high speed vehicles. The inherently poor low-speed performance of SAVs requires early consideration during the conceptual design phase. The takeoff field length is one of the key design requirements for the development of horizontal takeoff and horizontal landing (HTHL) space vehicle, which intend to use existing runways. The statistic data in Table 13 show that a HTHL SAV usually weights more than 12,500 lb. Therefore, if a SAV is required to be certified as a commercial vehicle (e.g., a space tourism vehicle - SpaceShipOne), it belongs to a category under FAR 25 certification requirements.

A. Design Parameters and Design Constraints

(1) Design Parameters: There are several design analysis methods for the horizontal takeoff analysis. The comparisons of these typical methods, relevant design parameters, and applications are summarized in Table 14. As shown in the *Applications* column of Table 14, most methods can be applied as well to subsonic vehicles, supersonic cruiser vehicles, and fighters. Therefore, the methods presented in Table 14 such as Roskam, Torenbeek, Shevell, and MDC are considered applicable for the takeoff analysis of

SAVs. Especially, the Roskam and Shevell methods are based on extensive previous aircraft design experience and have been validated by real flight test data.

Table 14: Design analysis methods for takeoff study.

Methods	Description	Design Parameters	Applications
Loftin ¹³¹	Approximate empirical method. It is a quick, simple, physical interpretable method for roughly estimating the aircraft design parameters. It is evolved from extensive study of existing aircrafts with well-known design parameters.	FAR Takeoff Filed Length Density Ratio Takeoff Weight Average Ground Acceleration Lift off Speed, Thrust to Weight Ratio Wing Loading, Lift off Lift Coefficient Climb Life Coefficient Aspect Ratio Flight Path Angle, Lift to Drag Ratio, Engine Number	Subsonic aircraft: jet-powered cruising aircraft propeller-driven aircraft
Roskam ¹³²	Approximate empirical method. It is based on an extensive aircraft design database in 10 years effort. It allows the rapid estimation of airplane design parameters which have influence on the takeoff performance. The methods can determine a range of values of wing loading, thrust loading, and maximum lift coefficient to meet certain performance requirements.	Airport Condition Gross Takeoff Weight Takeoff Thrust Wing Area Wing Aspect Ratio Wing Loading Maximum Takeoff Lift Coefficient FAR Takeoff filed length Takeoff Speed Aerodynamic drag coefficient Ground friction coefficient Stall Speed Engine number	Propeller Driven Airplane Agricultural Airplanes Business Jet Transport Jet Military Trainers Fighters Military Patrol/Bomb/Transpo rt supersonic cruise aircraft
Torenbeek ¹⁸	Simple analytical approach. The takeoff distance is comprised of two segments: a takeoff run and an airborne phase. The equations of motion for the landing are derived from basic physics. The approximations of some coefficients are provided.	Airport Condition Gross Takeoff Weight Engine Thrust Drag coefficient Lift Coefficient Wing Area Climb gradient Stall Speed Mean Acceleration Engine out deceleration FAR Takeoff filed length Wing loading Thrust to Weight Ratio	Propeller and Jet Aircraft
Shevell ¹³³ , MDC ¹³⁴	Simple analytical approach. Equations of motion are derived from simple physics. Empirical charts are provided to reasonably estimate takeoff performance.	FAR Takeoff Filed Length Density Ratio Takeoff Weight Wing Area Maximum Lift Coefficient Thrust Engine Number Drag Braking coefficient of friction Decision Speed Rotation Speed Takeoff Safety Speed Minimum Control Speed	Propeller and Jet Aircraft

Nguyen ¹³⁵ Mair and Birdsall ¹³⁶	Complex analytical equations with reasonable assumptions to simplify. The takeoff performance can be evaluated with good accuracy.	Airport Condition Gross Takeoff Weight Braking coefficient of friction Wing loading, Engine thrust, Lift coefficient Drag coefficient Angle of Attack Stall Speed Runway Slope Rotation Speed, Lift off Speed, Climb angle Thrust to Weight Ratio, Lift-drag ratio, Load factor, Wing Area FAR Takeoff field length	All types
Miele ¹⁰⁷	Complex analytical equations. Solves detailed integration process, great accuracy, however the physical relationships of various parameters may sometimes tend to be obscured in the complex analysis process, also some design parameters input are not available at the conceptual design level.	Airport Condition Gross Takeoff Weight Thrust Drag Lift Braking coefficient of friction Angle of Attack Lift off Speed Stall Speed Stall Lift Coefficient Climb angle PDF Boundary Conditions FAR Takeoff field length	All types

As can be seen in Table 14, there are two main categories used in the current takeoff analysis. One is based on empirical methods (Loftin, Roskam, etc) based on an extensive conventional aircraft database, the other on analytical methods (Torenbeek, Shevell, Nguyen, Miele, etc.), which analyze takeoff performance based on physical characteristics. The rather complex analytical equations of motion for this case are highly accurate and applicable to different types of aerospace vehicles including SAVs. However, complex equations require more input data (such as the detailed variation of engine thrust), which are usually not available at the conceptual design level. One has to recall that the knowledge database for space access vehicles is limited, making the use of complex formulations more difficult. Therefore, it is desirable to utilize reduced order models leading to approximate solutions. This provides physical transparency for the

major interacting design disciplines during the conceptual design phase. Thus, the available modeling techniques above have been reviewed critically in order to arrive at a balance between the data available and key design parameters.

First, key design parameters for the development of a generic takeoff design methodology have been investigated. The takeoff design methodology has to find a balance between takeoff distance requirements and the takeoff capability of the vehicle for the purpose of sizing engine thrust and the wing. For this purpose, the takeoff airport conditions (altitude, takeoff balanced field length) are needed before any takeoff analysis can be performed. The takeoff field length is determined primarily by the thrust to weight (T/W) ratio, wing loading (W/S), which, in turn, is governed by various parameters, the wing area, gross takeoff weight, and maximum takeoff lift coefficient. Also, an increase in the lift to drag ratio (L/D) improves climb performance and increases the minimum thrust requirement. All of these key parameters are closely coupled with the aerodynamic characteristics, weight, and thrust available of the vehicle. Therefore, the aerodynamic estimation (lift coefficient and drag coefficient) and thrust range of SAV are required as input for the takeoff design study.

Table 15 summarizes the key design parameters needed for the takeoff design analysis. Based on these parameters, the aim of the takeoff design methodology is to determine the thrust and wing loading necessary to meet required takeoff field length and one-engine-out performance for a given takeoff lift coefficient. These parameters, presented in Table 15, are the design drivers for the takeoff performance analysis.

Table 15: Design parameters required for reduced order model of takeoff design methodology.

Parameters	Notation	Normal Value
Airport Condition: Altitude	H	0
Airport Condition: Density	ρ	0.002377 slugs/ft ³
Takeoff Field Length	S_L	5000 – 8000 ft
Takeoff Lift Coefficient	C_{LO}	0.4 – 0.8
Ground Drag Coefficient	C_{DG}	
Lift to Drag ratio	L/D	4 – 8
Braking Coefficient	μ	0.4 – 0.6 (Dry concrete)
Stall Speed	V_s	
Wing Area	S	
Thrust	T	
Gross Takeoff Weight	W_{GL}	
Thrust to Weight	T/W_{GL}	
Wing Loading	W_{GL}/S	

(2) Design Constraints: Constraints placed on the vehicle design throughout the flight trajectory have to be addressed early during the conceptual design phase. The SAV takeoff is usually defined by to the takeoff-distance requirement for both, experimental and FAR 25 certified vehicles. For the present study, key CD design constraints defined by FAR 25 are summarized in Table 16.

Table 16: Design constraints imposed on vehicle takeoff requirements by FAR Part 25.

	Constraint Parameters	Notation	Constraint Value
Velocity	Decision Speed	V_I	$V_I < V_R$
	Rotation Speed	V_R	$\approx (1.1 - 1.15) V_s$
	Lift off Speed	V_{LOF}	$\approx (1.1 - 1.2) V_s$
	Nose Wheel Rotation Speed	V_{NWLO}	$V_R > V_{NWLO}$
	Takeoff Safety Speed	V_2	$> \approx 1.2 V_s \ (1.3 V_s)$
Takeoff Field Length Definition	Distance over 50 ft obstacle	S_L	5000 – 8000 ft or determined by the airport condition
Initial Climb Segment Gradients for One Engine Out	Two-engine aircraft	γ	1.2
	Three-engine aircraft	γ	1.5
	Four-engine aircraft	γ	1.7
Second Climb Segment Gradients for One Engine Out	Two-engine aircraft	γ	2.4
	Three-engine aircraft	γ	2.7
	Four-engine aircraft	γ	3.0

B. Equations of Motion

In order to arrive at a reduced order model or approximate solution for the takeoff sub-synthesis design methodology, the different takeoff analysis methods presented in Table 14 have been surveyed to select the most appropriate one for development. The reduced order models are based on classical complex analytical equations (e.g., Nguyen¹³⁵, Mair and Birdsall¹³⁶) with simplifying assumptions, such as steady climb, circular rotation and transition, etc. As a consequence, the equations of motion for the three separate takeoff phases (ground run, rotation, and transition/climb) of space vehicles are obtained as follows:

(1) Ground Run: Figure 31 shows the forces acting on an a/c during the takeoff ground run. During the takeoff, the thrust line can be used as a reference line to measure the

angle of attack. T is the thrust, W the vehicle takeoff weight, D the drag, L the lift, f the friction force, α the angle of attack which is the angle between the thrust line and the velocity, ϕ the runway slope angle. X is defined as the distance along the runway.

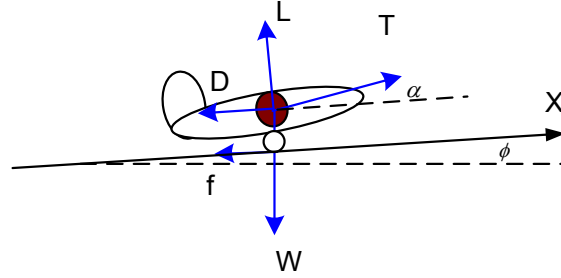


Figure 31: Ground run of aircraft takeoff phase.

As shown in Figure 31, the equilibrium equation parallel to the flight path is,

$$T \cos \alpha - D - f - W \sin \phi = m \frac{dV}{dt} \quad (4-1)$$

and the forces perpendicular to the flight path are

$$L + T \sin \alpha - W \cos \phi = 0 \quad (4-2)$$

In Eq. (4-1), the friction force f is $f = \mu R = \mu(W \cos \phi - L - T \sin \alpha)$

The lift L and drag (D) forces are defined as

$$L = \frac{1}{2} \rho S V^2 C_L \text{ and } D = \frac{1}{2} \rho S V^2 C_D$$

where ρ is the density, S is the wing area, C_D is the drag coefficient, C_L is the lift coefficient, and V is the velocity.

Let X_g be defined as the ground run distance from rest to the point of lift-off. It can be written as an integral function of velocity (V) and acceleration (a). V_{LOF} is the liftoff velocity.

$$X_g = \int_0^{V_{LOF}} \frac{V}{a} dV \quad (4-3)$$

As can be seen from Eq. (4-3) and Eq. (4-1), the ground distance is a function of takeoff weight (W) and C_L , dynamic pressure, atmospheric density, airport altitude, thrust, rolling friction coefficient, and runway slope angle. The runway slope angle is usually very small and is negligible for the current study. The integral terms in Eq. (4-3) are very difficult to estimate since both the velocity and acceleration are continuously changing throughout the takeoff flight phase. Therefore, a more practical method needs to be applied for the takeoff performance calculation.

The equations of motion for different aircraft takeoff phases have been derived by Dwight Taylor, a former aerodynamicist at McDonnell Douglas Company (MDC) and validated against detailed performance analysis and flight test results.¹³⁴ Most importantly, typical values of some coefficients inside the equations have been validated and provided in Reference 134.

The ground run distance X_g is given by¹³⁴,

$$X_g = K_1 \cdot \frac{\frac{1}{g \cdot \sigma \cdot \rho_{sl}} \cdot \frac{W}{S} \cdot \frac{1 - (T/W) \cdot \sin \alpha}{C_{L_{TO}}}}{\frac{T}{W} - K_2 \cdot \frac{C_{D_G}}{C_{L_{TO}}} - \mu_{eff}} \quad (4-4)$$

Reference 134 shows typical values of the above coefficients for high speed vehicles. K_1 is the correction factor for non-linear acceleration (≈ 1.04), K_2 is the correction factor

for average drag during ground roll, (≈ 0.3 to 0.5), σ is the ratio of atmospheric density at altitude to the density at sea level, ρ_{sl} is the atmospheric density at sea level, g is the sea level acceleration of gravity, $C_{L_{TO}}$ is the lift coefficient at V_R on the ground in ground effect, C_{D_G} is the drag coefficient at V_R on the ground in ground effect, and μ_{eff} is the effective rolling coefficient. Nominal values of the friction coefficients (μ_{eff}) are: 0.025 for rolling without brakes, 0.68 for braking on a dry concrete surface, 0.46 for braking in light rain on a concrete surface, 0.32 for braking in the heavy rain on a concrete surface, and 0.20 for braking on a smooth surface with clear ice.

(2) Rotation and Transition: Figure 32 presents the geometry of the takeoff rotation and transition period.

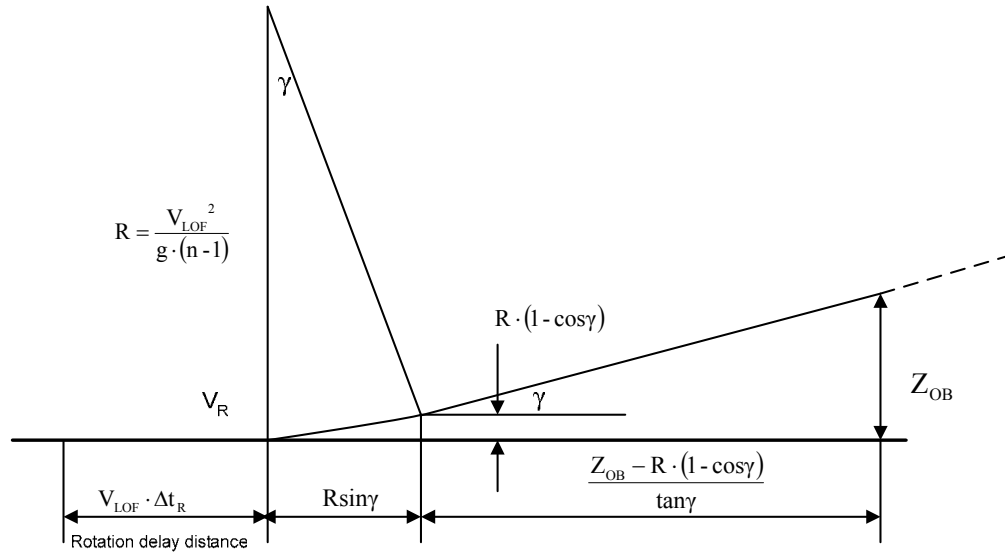


Figure 32: Takeoff rotation and transition.¹³⁴

As the geometric relationship shows in Figure 32, the horizontal and vertical distance of the takeoff rotation and the transition can be obtained. The horizontal distance X_{RT} parallel to the takeoff flight path is

$$X_{RT} = V_{LOF} \cdot \Delta t_R \quad (4-5)$$

where Δt_R is the time to rotate the aircraft (usually 3 second for commercial aircraft) and V_{LOF} is the liftoff speed, and given by¹³⁴

$$V_{LOF} = \sqrt{\frac{2 \cdot W \cdot [1 - (T/W) \cdot \sin \alpha]}{\sigma \cdot \rho_{sl} \cdot S \cdot C_{L_{TO}}}} \quad (4-6)$$

The liftoff speed can also be estimated from FAR 25 requirements. It is approximated as 1.15 to 1.2 V_{stall} .

$$V_{Stall} = \sqrt{\frac{2 \cdot W}{\sigma \cdot \rho_{sl} \cdot S \cdot C_{L_{max}}}} \quad (4-7)$$

In Eq. (4-5), R is the rotation radius and is defined as

$$R = \frac{V_{LOF}^2}{g \cdot (n - 1)} \quad (4-8)$$

where n is the load factor and defined as $n = L/W$.

(3) Nose Wheel Lift-off Speed: The decision velocity (V_1), rotation speed (V_R), and liftoff speed (V_{LOF}) are usually determined by a takeoff performance analysis. A highly swept wing vehicle with a relative slender fuselage especially requires sufficient control power to rotate the aircraft. This fact can become a critical design issue for a SAV; the

addition of an extra mechanical nose strut extensions or a canard can augment rotation of the nose. Therefore, it is necessary to check the aerodynamic authority of the control surfaces to determine whether the nose can actually be rotated through the aerodynamic pitching moment at V_R . Under certain conditions (nose wheel lift off speed $V_{NWLO} <$ rotation speed V_R), the rotation speed (V_R) can provide sufficient aerodynamic power to lift the nose wheel off the runway. Figure 33 shows takeoff geometry at vehicle rotation velocity.

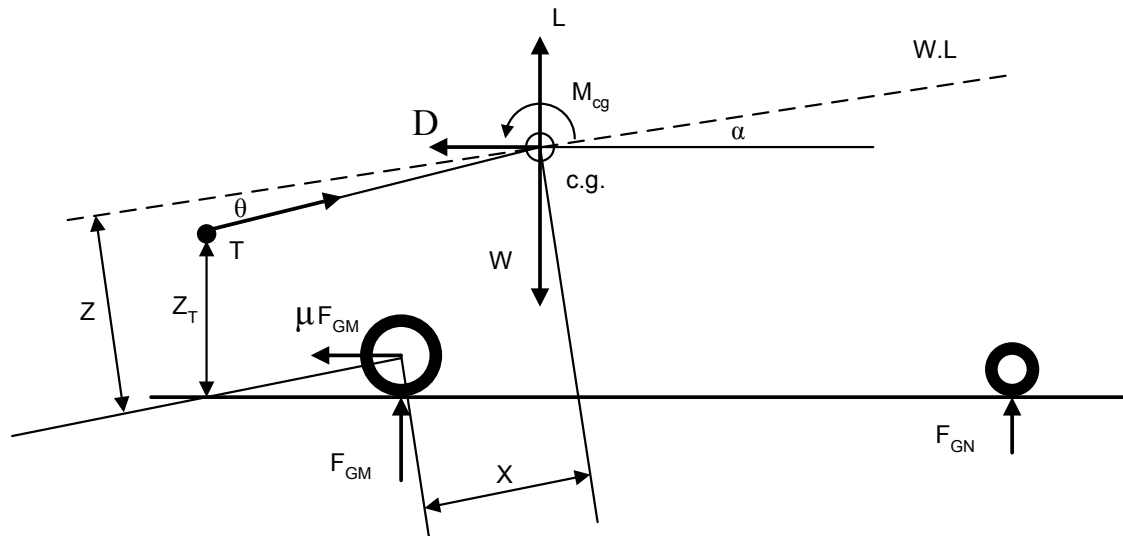


Figure 33: Takeoff geometry at vehicle rotation velocity. ¹³⁴

X is the distance from main wheel to c.g. parallel to aircraft water line. Z is the distance of the c.g. from the main wheel axle. Z_T is the distance of the thrust position from the ground. T is the thrust, D is the drag, and μ is the rolling friction coefficient. The nose lift off speed is, ¹³⁴

$$V_{NWLO} = \left[295 \cdot \left(\frac{W}{S} \right) \cdot \frac{\left\{ \left(\xi + \mu \cdot n \right) - \left(\frac{T}{W} \right) \cdot \left[n \cdot (\cos\beta + \mu \sin\beta - Z_T \cos\theta) \right] \right\}}{\left[\bar{c} \cdot C_{m_{cg}} + C_L (\xi + \mu \cdot n) \right]} \right]^{0.5} \quad (4-9)$$

\bar{c} is mean aerodynamic chord in ft, $C_{m_{cg}}$ is the pitching moment about the c.g from the pitch control surfaces, C_L is the lift coefficient at V_R , T/W is the thrust to weight ratio at V_R , and W/S is the wing loading. Geometry relationships are $\beta = \alpha + \theta$, $\xi = X \cos \alpha - Z \sin \alpha$, and $n = Z \cos \alpha + X \sin \alpha$.

(4) Initial Climb: After the rotation and transition period, the vehicle continues to steadily climb at a small flight path angle. During this steady climb, both speed and the flight path angle vary slowly. The equations of motion for a steady climb can be written as^{107,135}

$$\frac{dX}{dt} = V \cos \gamma \quad (4-10)$$

$$\frac{dH}{dt} = V \sin \gamma \quad (4-11)$$

$$m \frac{dV}{dt} = T \cos \alpha - D - W \sin \gamma \quad (4-12)$$

$$mV \frac{d\gamma}{dt} = T \sin \alpha + L - W \cos \gamma \quad (4-13)$$

Eq. (4-11) divided by Eq. (4-10) given

$$\frac{dH}{dX} = \tan \gamma$$

From the takeoff geometry shown in Figure 32, the air distance X_{OB} from nose liftoff to takeoff obstacle height Z_{OB} is given with

$$X_{OB} = \left[R \cdot \sin\gamma + \frac{Z_{OB} - R \cdot (1 - \cos\gamma)}{\tan\gamma} \right] \quad (4-14)$$

Therefore, the total takeoff distance is the sum of ground run distance, rotation/transition distance, and air distance.

$$X_{TO} = X_g + X_{RT} + X_{OB}.$$

(5) Second Segment Climb: The FAR second-segment climb gradient requirement also needs to be considered in relation to the take-off maneuver. The second-segment climb is the flight path after takeoff safety speed (V_2), which starts from an altitude of 50 ft to 400 ft. Under the Federal Air Regulations, sufficient thrust is required to maintain climb in the event of an engine failure. The requirements of the second-segment climb gradients are: 3 percent for four-engine aircraft, 2.7 percent for three-engine aircraft, and 2.4 percent for two-engine aircraft.^{130,131} During the second segment climb, the aircraft operates with flaps in the take-off position and the landing gear retracted. The climb angle depends on the installed thrust, drag, and takeoff weight at liftoff in the one-engine-out condition. A minimum specified engine out rate of climb can be obtained as

$$\sin\gamma = \frac{T - D}{W} = \frac{T}{W} - \frac{1}{L/D} \quad (4-15)$$

C. Design Synthesis Process

Figure 34 shows the design synthesis process for the conceptual design of a SAV during the takeoff phase. The aim of this process is to deliver proof of convergence, estimate design sensitivities, and optimize the configuration in order to reach the design targets specified.

The design synthesis process starts with a baseline vehicle and SAV mission requirements (e.g., suborbital/orbital, payload, operational modes, etc). The mission profile provides the payload information for the mass properties module and airport information required by the performance module to define the takeoff mission. After obtaining geometry data from the baseline vehicle, the mass properties module inputs the takeoff weight obtained from initial weight estimation. Meanwhile, the design constraints are identified at the early design process and called into the optimization module. During the activity to synthesize the flight vehicle, the performance module communicates with the atmosphere module, aerodynamics module, propulsion modules, and optimization module to determine feasible takeoff performance under the specified design constraints. Finally, all the design requirements for the SAV mission are checked and, if necessary, the configuration can be iterated on to arrive at efficient aerodynamic characteristics, wing loading, thrust to weight ratio, and vehicle weight. At this point, the vehicle design space for the takeoff phase can be defined. It will provide design data for further studies.

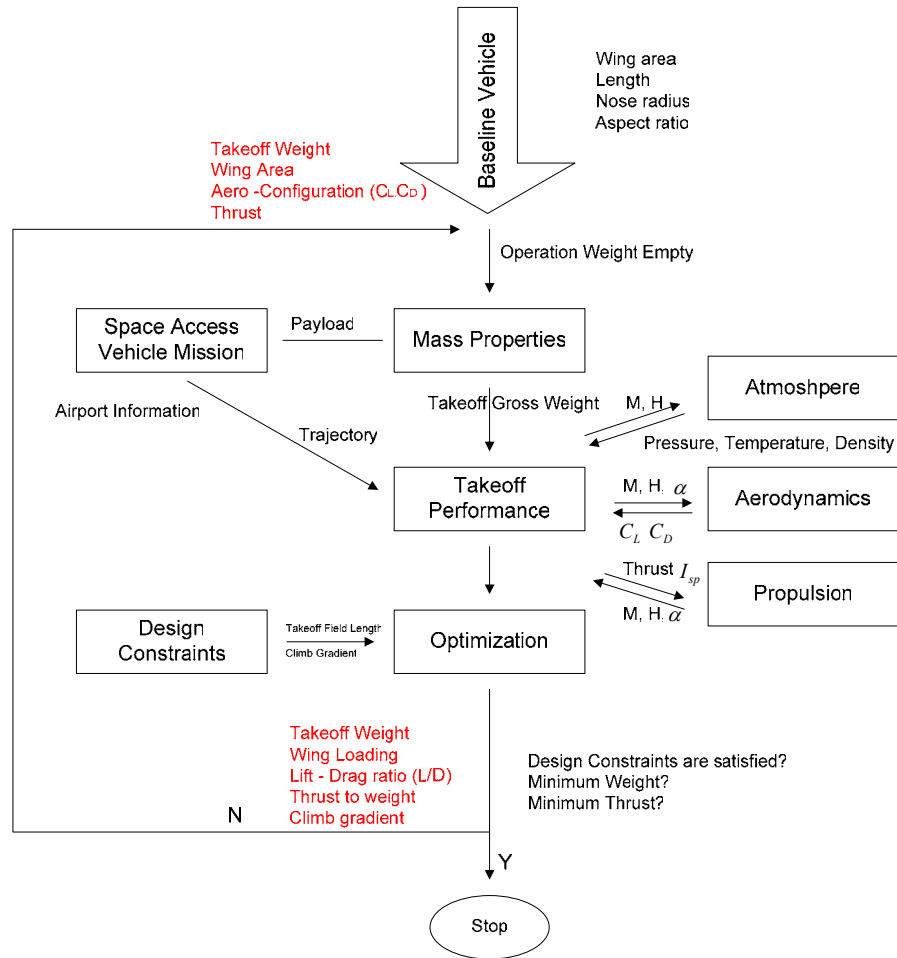


Figure 34: Design synthesis process for takeoff phase of a HTHL SAV vehicle.

(1) Program Organization: Two programs (**SAV_BFL**, **SAV_CLM**) have been developed, based on both empirical and analytical methods to implement the above synthesis takeoff design methodology, in an MS Excel PC environment (see Appendix G). These simple, integrated computer programs are capable of demonstrating the vehicle's flight readiness through takeoff and initial climb. This allows for visualization of the coupling of the main design parameters (takeoff field length, T/W , W/S , L/D , maximum takeoff lift coefficient). In accordance with the particular characteristics of the CD phase, emphasis has been placed on overall simplicity and minimum data input

requirements. All basic equations used to mathematically model the atmosphere, aerodynamics, performance, and propulsion are kept as simple as possible to ensure that the key design parameters involved are evaluated quickly, offering physical transparency.

(2) Takeoff Sub-Synthesis Design Study: Based on the sub-synthesis takeoff design methodology and computer programs, a conceptual design takeoff study of a suborbital HTHL vehicle, *OU XP*, has been performed to identify the design space of this vehicle. The geometric characteristics of the *OU XP* configuration are presented in Appendix A. In this study, four wings were selected with varying leading edge sweep angles: 78°, 70°, 60°, and 45°. A comparative study of these four wings was performed to assess their aerodynamic and performance characteristics during the takeoff phase. At the design point, all four wings were sized to have the same induced drag. Thus, these wings were comparable at the same drag level. The aerodynamic characteristics of the four wings were determined using the MDC (McDonnell Douglas) method¹³⁷, which has been applied in the aircraft design industry for 40 years. Apart from these MDC methods, DATCOM⁷⁸ was used to serve as a validity check and for interpretation of the analytical results (see Reference 128 stems from a collaboration work with Gary Coleman). Figure 35 shows the drag polars of four different wings with a NACA 64-206 airfoil section derived from MDC methods. With the results from the aerodynamic analysis, performance, thrust, and wing loading calculations were performed.

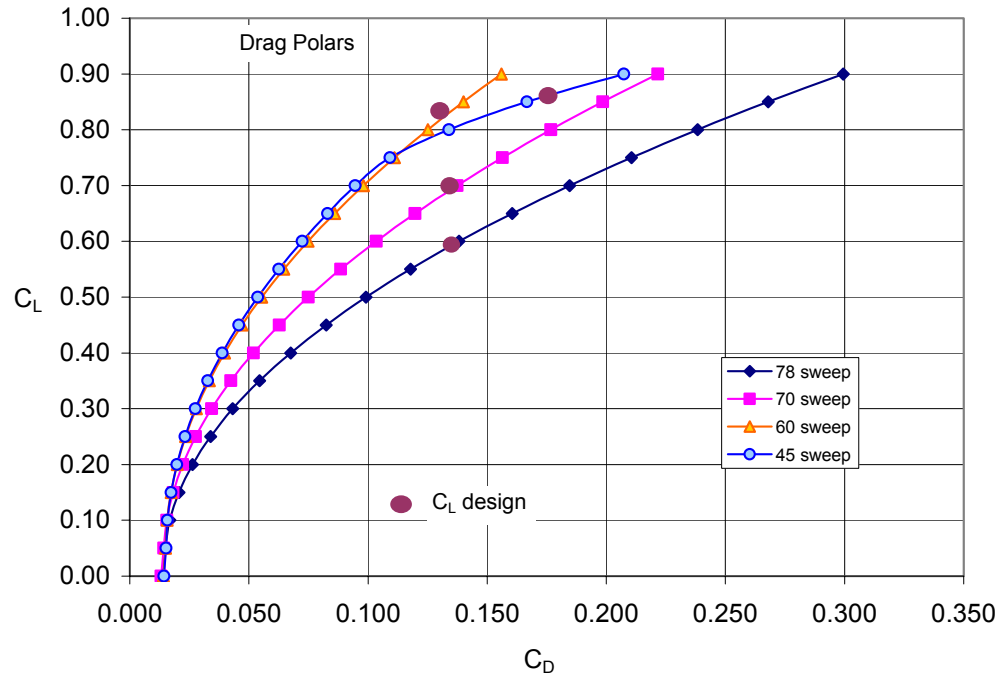


Figure 35: Drag polars of four wings from MDC methods.

In order to demonstrate that the design methodology has generic design capability for various high speed vehicle configurations, the takeoff design methodology has also been applied to several selected supersonic vehicles. Table 17 presents a comparison of the takeoff performance of some selected high speed vehicles.^{138 – 153}

Table 17: Takeoff performance data of some supersonic vehicles.

Parameters	Vehicle	Concorde	Tu -144	B-58	F-106	XB-70
Takeoff Field Length (ft)		10,950	9,842	7850		8,000
Takeoff Weight (lb)		385,000	396,830	160,000	35,300	550,000
Lift to Drag ratio		4.35 (approach)		4.84 (max)	4.17 (max)	6.015 (max)
Wing Area (ft ²)		3856	4716	1542	698	6297.8
Takeoff Wing Loading (lb/ft ²)		100	84.17	103.8	50.57	80
Aspect Ratio		1.85	1.89	2.09	2.08	1.04
Wing Swept (deg)		55	70	60	55	51.77
W_{GT}/W_E		2.73	2.52	2.375	1.524	1.934
Thrust		152000	176368	60000	24500	0.29 -0.38
Thrust to Weight		0.395	0.44	0.375	0.694	0.29 -0.38
V_1 (ft/s)		280 ³³	374 ²⁹			
V_r (ft/s)		307	491			329
V_{LOF} (ft/s)		332.5	521			354
V_2 (ft/s)		335.8	550			
Rate of Climb at Sea Level (ft/min)		5,000	13,780	17,830	13,054	

(a) Balanced Field Length:

The determination of the takeoff balanced field length constraint is, at this point, independent of the particular aircraft type. The required takeoff field length with critical engine failure (OEI) is given as function of the generalized parameter $W^2/\sigma SC_{LTO}$ in Figure 36 for two jet engine aircraft, see Shevell¹³³. It has been shown that this presentation applies well when correlating the required runway length results for several aircraft. There is a clear correlation between the required takeoff field length for certified aircraft and the generalized parameter $W^2/\sigma SC_{LTO}$. As can be seen in Figure 36, if the OEI aircraft aims to take off from a 11,000 ft runway, it requires a takeoff field length of 8,900 ft with both jet engines operating.

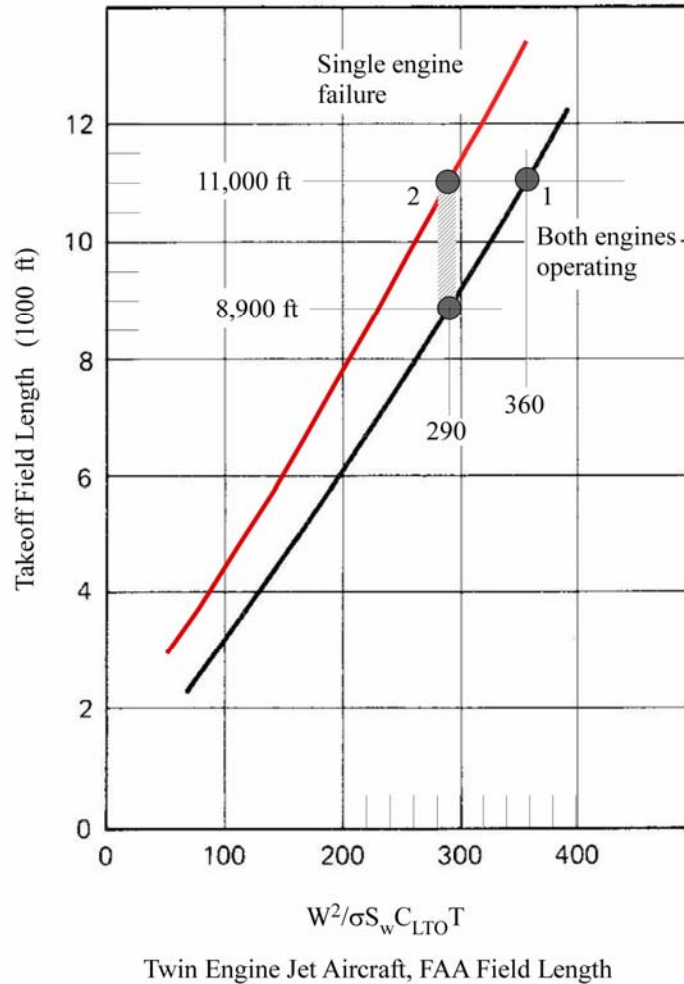


Figure 36: Two engine jet aircraft FAR25 takeoff field length with engine failure.¹³³

Figure 37 shows that the design for the single-engine-out (OEI) operation reduces the twin engine takeoff distance from 11,000 ft to 8,900 ft. Under this condition, Figure 38 compares the thrust requirements with two trim mechanisms, canard and horizontal tail. It is obvious that the canard reduces the required thrust, while a horizontal tail increases the thrust requirement. In summary, the canard aircraft represents a lower-drag configuration requiring less thrust for the same runway length.

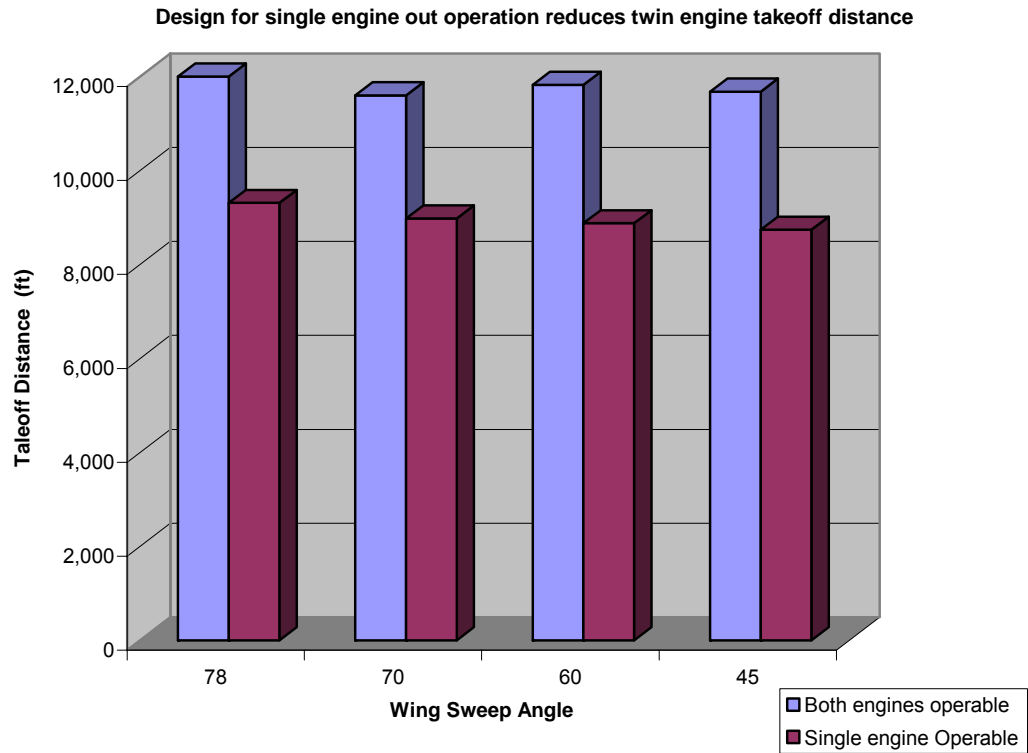


Figure 37: Variation of takeoff distance requirement with different wings.

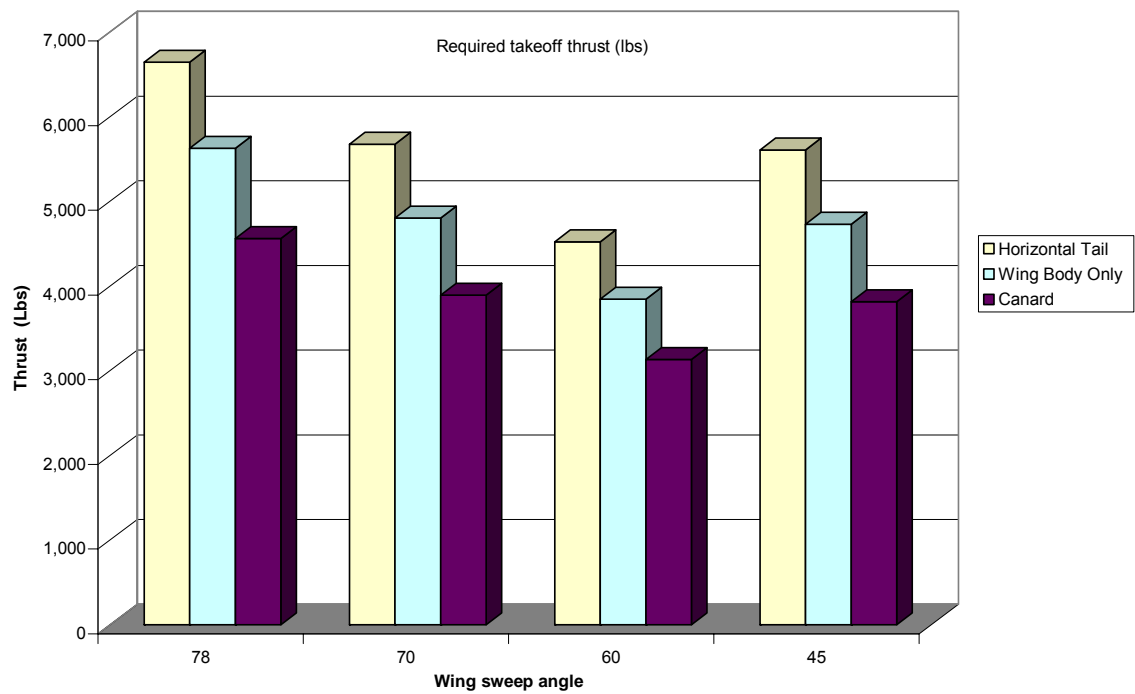


Figure 38: Required takeoff thrust for different trim mechanisms.

A comparison study of the takeoff length requirement was performed. The result from Roskam's AAA methodology is presented in Figure 39. Four maximum takeoff lift coefficients (0.4, 0.6, 0.8, 1.2) was selected to illustrate the FAA field performance requirements. The real design points of different high speed vehicles are also presented in the figure. As can be seen, the T/W requirements for different takeoff lift coefficients were:

1. At $C_{LTOmax} = 0.6$, the thrust to weight ratio needs to be longer than 0.3.
2. At $C_{LTOmax} = 0.8$, the thrust to weight ratio needs to be longer than 0.24.
3. At $C_{LTOmax} = 1.2$, the thrust to weight ratio needs to be longer than 0.12.

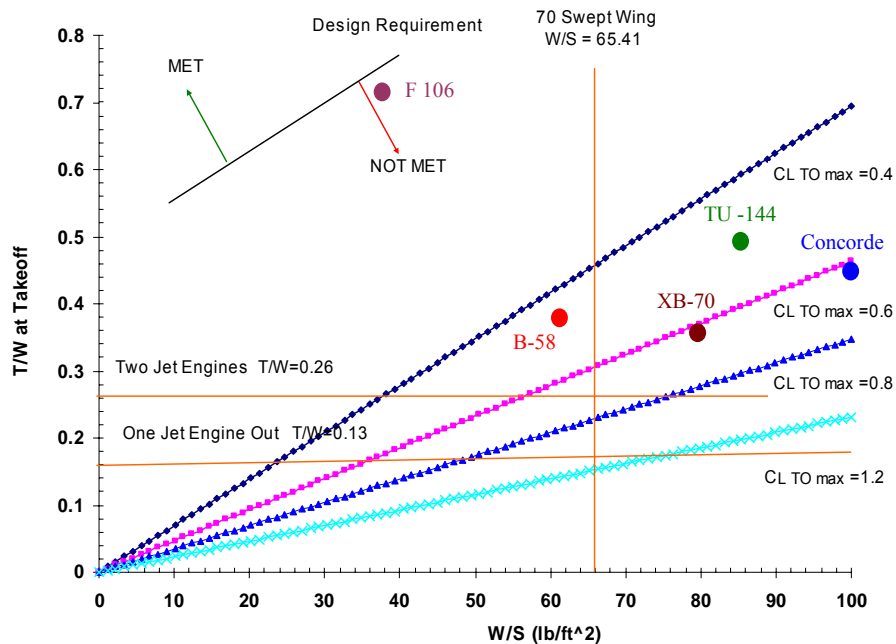


Figure 39: Takeoff length sizing of Supersonic Vehicles.

(b) Takeoff Field Length:

Figure 40 shows the analytical calculations (based on the equations of motion derived in Chapter 4.3.1-B) of the total takeoff distance for different wing planforms. The total

takeoff distance includes ground run distance, rotation distance, and air distance over 50 feet.

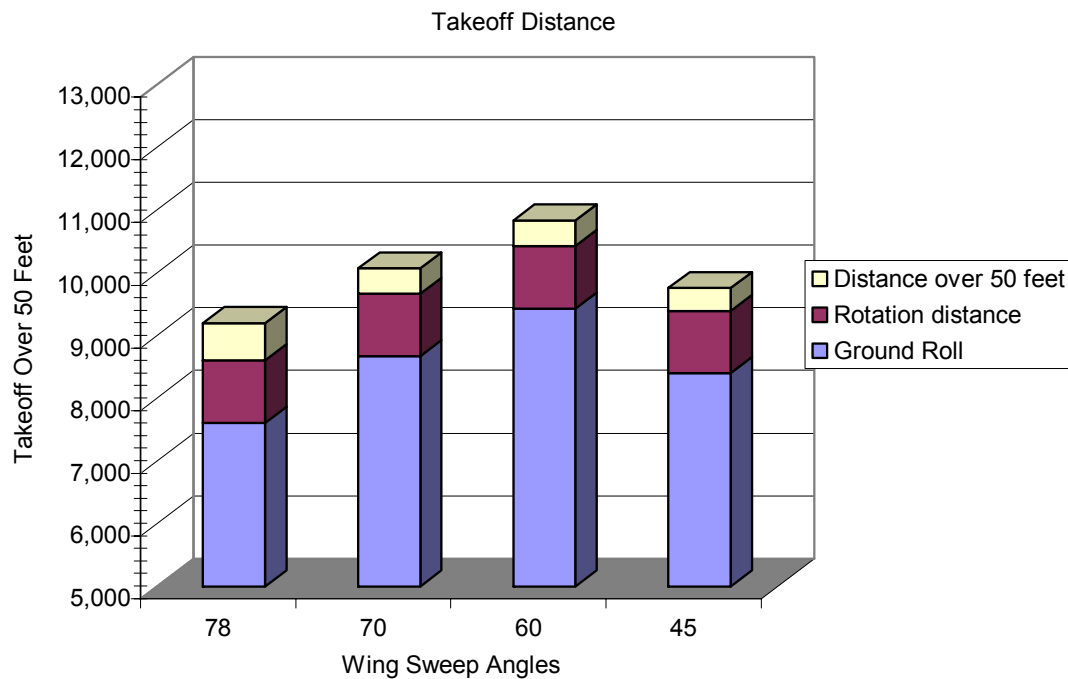


Figure 40: Variation of takeoff field length with wing sweep angle.

(c) Wing Loading:

As mentioned before, four wings were sized to have the same induced drag instead of the same wing area. If the same wing area would be used instead, the wings would operate at a different lift coefficient, hence, the results would not be comparable. Figure 41 shows the variation of wing loading with varying sweep angles. It can be seen that the wing loading is increasing from 78° sweep angle to 45° sweep angle.

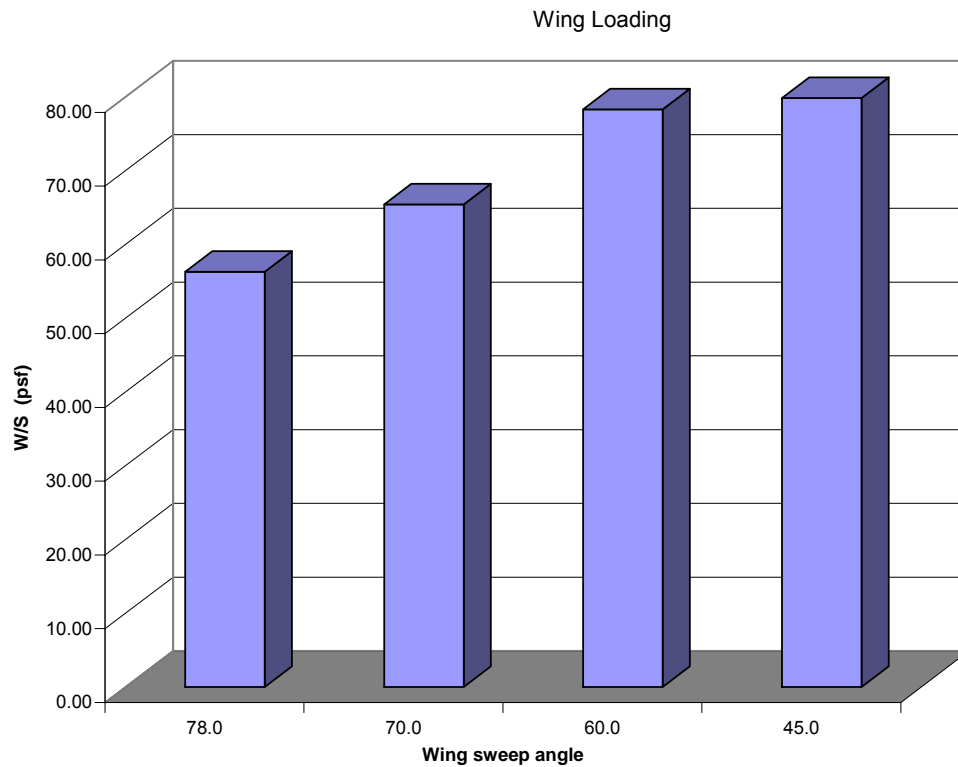


Figure 41: Variation of wing loading with sweep angles.

(d) Takeoff Speed and Nose Wheel Lift off Speed:

The center of gravity locations of four wing configurations were assumed to be the same for the comparison of longitudinal stability characteristics. Figure 42 shows the variation of the *OU XP* takeoff speed and nose wheel lift-off speed for different wing sweep angles. The nose wheel lift-off speed is the speed when the aircraft lifts its nose wheel off the ground. For lower swept wings, there is a problem to lift the nose wheel because the nose lift-off speed is higher than the takeoff speed. This requires additional control power to rotate the nose. For the 78° and 70° swept wings, the aircraft is able to lift the nose wheel at takeoff speed.

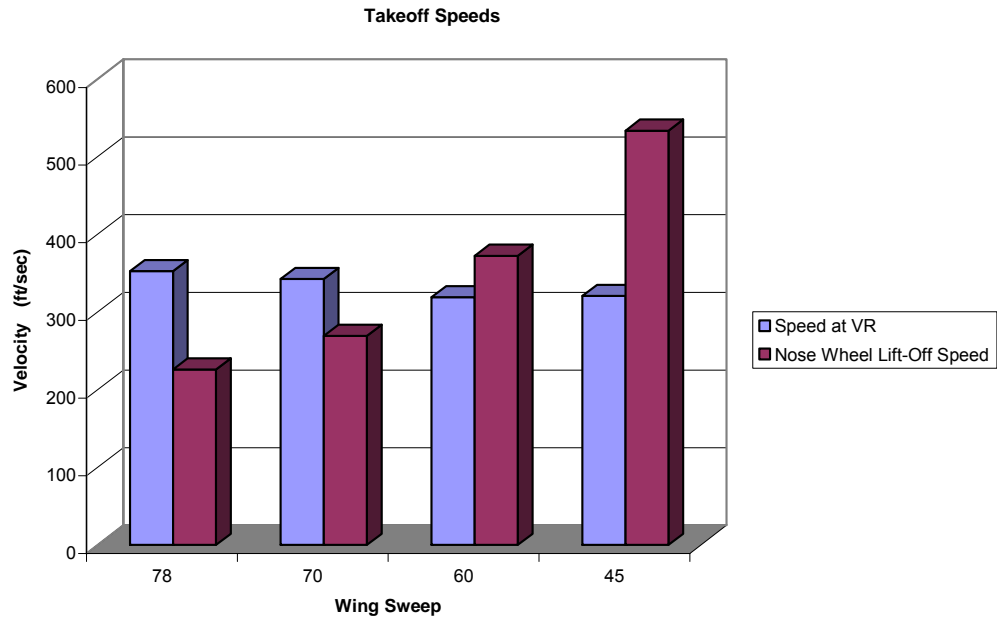


Figure 42: Takeoff speed and nose wheel lift-off speed for different swept wings.

(e) Initial Climb gradient (Takeoff with One Engine out Study):

Figure 43 shows the general takeoff climb gradient requirement applied to both the winged body and the lifting body configurations. Lifting body configurations require a larger T/W due to their lower L/D and takeoff lift coefficients.

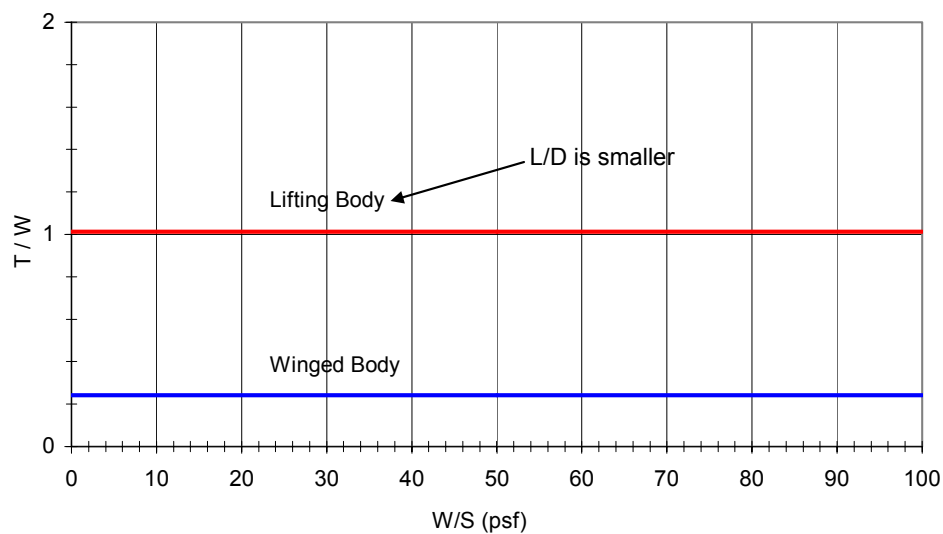


Figure 43: Takeoff climb gradient requirement.

(f) Second Segment Climb gradient (Takeoff with One Engine out Study):

For safety reasons, the FFA demands that commercial aircraft can take off with one engine out. The following study discusses the takeoff performance of the *OU XP* with the selected engines under the one-engine-inoperative (OEI) condition. The variation of the angle of climb γ with altitude for a Learjet engine (GE CJ-610) is shown in Figure 44. Figure 45 shows the variation of rate of climb with altitude. As can be seen from these two figures, with one GE CJ-610 engine out, angle of climb and rate of climb are both negative during takeoff.

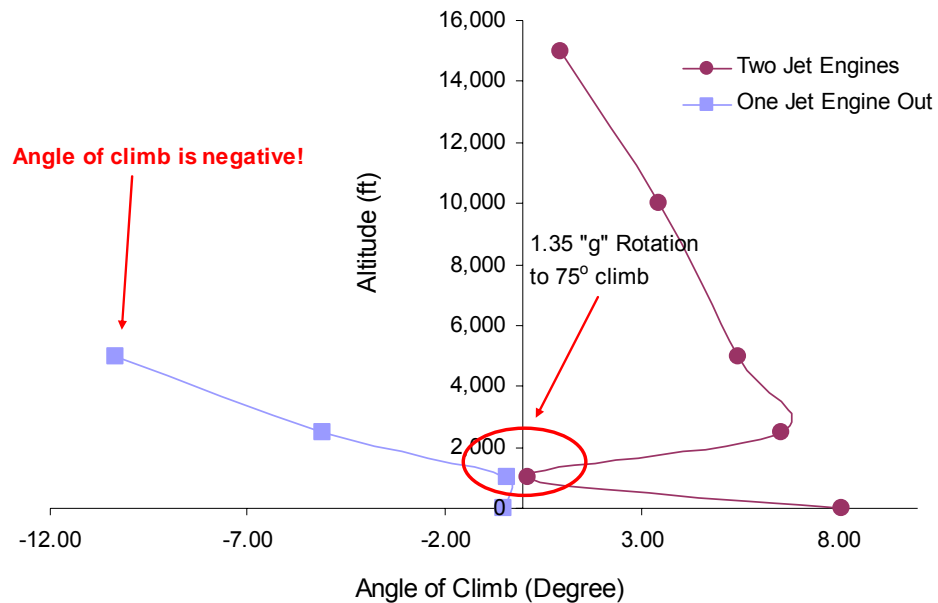


Figure 44: Angle of climb with altitude for OU XP Jet and Rocket Engines (GE engine).

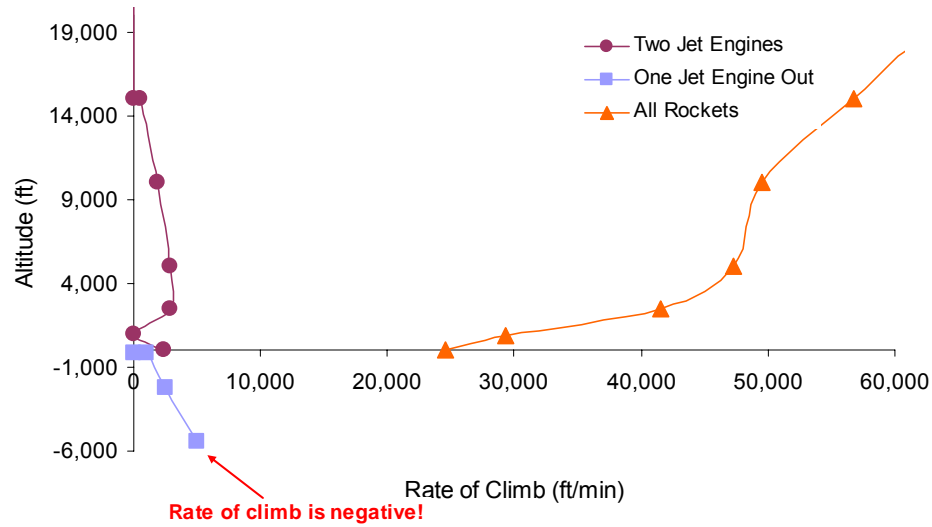


Figure 45: Rate of climb with altitude for OU XP Jet and Rocket Engines (GE engine).

4.3.2 Ascent

A space access mission requires the selection of an ascent trajectory that efficiently delivers a given payload mass or volume to orbit. Usually, the ascent trajectory of a SAV into suborbital/orbital space is confined to a restrictive ascent corridor determined by thermal, structural, aerodynamic, and acceleration constraints. Any multi-disciplinary design synthesis methodology for the design of a SAV requires a trajectory analysis tool capable of sizing fuel weight and also visualizing mission performance throughout the ascent profile. During the conceptual design level, the designer is challenged to explore the maximum mission performance for a baseline vehicle configuration. This performance maximum can be obtained by defining a minimum-fuel trajectory, which ultimately leads to the maximum orbital mass fraction.

A. Design Parameters and Design Constraints

(1) Design Parameters:

A multitude of higher-fidelity trajectory analysis software^{27,110} is available for the detail design phase. Table 18 summarizes trajectory analysis tools for some key design methodologies and multiple versions of equations of motion developed to described the ascent trajectory.^{155,156,157}

Table 18: Design analysis methods for ascent study.

Methods	Description	Design Parameters	Applications
Czysz ³⁹	It is assumed that data sets have been generated, based on past experience and extensions as well as on predictions from sizing programs, on capabilities in propulsion, fuels, materials, and industrial manufacturing. A series of design spaces are constructed with respect to various parameters. A vehicle design convergence is sought based on the influence of various parameters on the vehicle performance as depicted by the design spaces. The design spaces are generated starting with data on various aspects of vehicle design. The construction of design spaces this becomes the most significant part of realizing vehicle convergence. Visibility, comprehensiveness, clarify, rationality and ease of interpretation are the main desired characteristics of design spaces.	Propulsion Fuel Mass Material Index Industry Index	Empirical method Rocket equation Not applicable for the reentry analysis
Hammond ^{12,27}	Once the aerodynamic characteristic have been determined and weights for the vehicle components are assumed for the initially trajectory analysis (POST). POST is a generalized point mass, discrete parameter targeting and optimization program capable of analyzing trajectories for powered or unpowered vehicles operating near a rotating oblate planet. In launch vehicle design POST is used to analyze launch, on-orbit, and reentry trajectories subject to a number of constraints, such as maximum acceleration, heating boundaries, and cross range requirements. The principal results from the performance analysis include propellant requirements for input to weights and sizing calculations and in-flight conditions used by aeroheating analysts.	Maximum Acceleration Heating Propellant Mass Weight Geometry	Launch, on-orbit, and reentry trajectories analysis
Hunt ⁴⁰	Performance/Trajectory: the performance routine is a trajectory code, whether a simple energy-state integration approach or a three-degree of freedom dynamic version. Aerodynamic and propulsion performance are the required inputs. Aerodynamic matrix (lift and drag coefficient, C_L and C_D as a function of Mach number, angle of attack and altitude) is calculated for an assumed trajectory bandwidth on dynamic pressure. (1) The net engine performance matrix (thrust	Lift Coefficient Drag Coefficient Mach Number Angle of Attack Altitude Dynamic Pressure Thrust Specific Impulse Fuel Fraction Ratio Weight Geometry	Ascent, orbital and insertion and deorbit trajectory analysis

	<p>coefficient and specific impulse as a function of Mach number, angle of attack and fuel equivalence ratio) is then assembled, with the thrust coefficients vectored along the vehicle wind axis and referenced to free stream static in the same manner as the aero coefficients. With this aero/propulsion performance set, the fuel fraction required to perform the ascent (98 percent of fuel requirement), orbital insertion/circularization, and deorbit is determined from the trajectory analysis.</p> <p>(2) Iterations are now required in the synthesis process to adjust the structures/insulation for the optimum (off-nominal) ascent and descent trajectory and vice versa and to perform an iteration on size/weight in the performance routine.</p>		
SSSP ⁶³	<p>The General Trajectory Simulation Module (GTSM) program is a general purpose high speed, precision flight program which simulates the flight for an aerospace vehicle in the gravitational field of a central body. It utilizes the efficient Kutta-Merson variable stepsize numerical integration technique to integrate with respect to time the twelve state equations. These equation define the time rate of change of the three degree of freedom vehicle motion, the vehicle mass, the ideal velocity and velocity losses, and a heating parameter. The vehicle motion equations consist of three kinematic and three kinetic equations and are expressed in a natural applied force coordinate system which minimizes the extend of matrix coordinate transformations common to other simulations.</p>	<p>Velocity Vehicle Mass Velocity Loss (ΔV) Time</p>	Ascent Analysis
PrADO ⁶⁶	<p>The flight performance module includes a flight path simulation to estimate the necessary thrust and fuel mass of the aircraft. For every point of time during the flight simulation, Mach number and altitude are given. From this information the time-dependent derivatives result from a numerical differentiation. It is now possible to fulfill the flight-mechanic differential equations in the flight direction and normal to it by an iteration over the angle of attack. The use of a fixed flight path provides the advantage of saving time during the iteration.</p>	<p>Thrust Fuel Mass Mach Number Altitude Time Angle of Attack Flight Path Angle</p>	Two Stage to Orbit
Allen, Eggers, Chapman, and Woods ^{155,156,157,38}	<p>The nonlinear equations of motion are derived for entry into an exponential planetary atmosphere. By disregarding some relatively small terms such as gravity force, the centrifugal acceleration and lift force, a single, ordinary, nonlinear differential equation of second order is reduced to be a linear differential equation of Allen and Eggers applicable to ballistic entry vehicle. If the vertical acceleration and vertical component of drag force are negligible, the resulting truncated differential equations are applicable for the equilibrium glide vehicle (Space Shuttle).</p>	<p>Velocity Deceleration Gravity Force Aerodynamic Drag Density Altitude Vehicle Mass, Size Flight Path Angle Aerodynamic Heating Total Heat Transfer Maximum Heat Lift to Drag Ratio Maximum Range</p>	Ballistic, Skip and Glide Vehicles with High Entry Speed
Aachen ¹⁵⁸	<p>Performance requirements, mission constraints, vehicle design and trajectory selection of typical reentry vehicles are briefly described. Some semi-empirical estimations of the lift-to-drag ratio and ballistic parameter of a reentry vehicle with cross range and heating constraints are presented.</p>	<p>Load Factor Dynamic Pressure Heat Flux Integral Heat Load Surface Temperature Atmosphere (density, temperature) Flight State Condition</p>	Atmosphere Reentry of Capsules and Winged Vehicle

		(velocity, angle of attack) Vehicle Properties (geometry, weight and aerodynamics) Wing Loading Ballistic Coefficient Lift-to-Drag Ratio	
Rutowski ¹⁰⁸	Energy-State Approximation (ESA) technology, The key idea of the ESA technique is, to introduce the total mechanical energy as a state variable and then to neglect all other dynamics. By using ESA techniques, optimal trajectories for a variety of performance objectives, such as minimum time and fuel-climb problems, can be obtained.	potential energy kinetic energy Velocity Thrust Weight Drag Engine Impulse	Subsonic, supersonic and hypersonic vehicles

In this context, it should be emphasized that it is of utmost importance to use CD tools during the CD phase. An unfortunate trend can be observed in many aerospace design environments that PD tools or even DD tools are utilized during the CD phase due to a lack of appropriate CD tools. In the context of trajectory analysis, utilization of a higher-fidelity trajectory program (POST,²⁷ OTIS,¹¹⁰ GTSM⁶³) or of complex analysis equations (Allen,¹⁵⁵ Eggers,¹⁵⁶ Chapman,¹⁵⁷ Aachen,¹⁵⁸ etc) during the CD phase usually requests input data not available or even relevant during this phase. Also, these high-fidelity disciplinary analysis programs usually lack the most important design capability: being able to identify the convergence design space for the integrated flight vehicle. Therefore, although there are a multitude of higher-fidelity trajectory analysis programs available, there is a clear demand for a CD level trajectory analysis approach, capable of bridging the gap between the high fidelity trajectory analyst and the conceptual designer.

As a consequence, a CD level trajectory program (**SAV_TSSP**) was developed based on the ESA technique¹⁰⁸. The aim was to preserve the physical transparency of the major design disciplines interacting during the ascent phase. The program does not intend to compute the detailed ascent trajectory in three DOFs as traditional higher-fidelity

trajectory tools do. Instead, this method aims to identify and define the feasible design space for the vehicle ascent phase while respecting and visualizing key design constraints. It provides a decision support tool that can help the conceptual designer size, evaluate, and analyze HTHL SAVs, ultimately supporting the configuration concept selection process by quantifying design sensitivities of key design parameters.

Key design parameters for the development of a generic ascent design methodology were investigated. The ascent design methodology aims to create a balance between ascent mission requirements and the design of the vehicle performance capability. The methodology should couple key design disciplines such as trajectory, propulsion, aerodynamics, weight, thermal, and performance. The interrelations between the primary design parameters thrust, weight, velocity, altitude, dynamic pressure, and others at each flight interval were estimated. For this purpose, the ascent atmospheric conditions (altitude, density and temperature) were required for the ascent analysis. The acceleration of a SAV is usually determined by thrust, vehicle weight, aerodynamic characteristics (lift and drag), and flight path angle. The aerothermodynamics analysis depends on vehicle velocity and geometry of the vehicle such as nose radius. The flight velocity, in turn, is governed by various key design parameters, vehicle weight, aerodynamic characteristics, engine thrust, and impulse. All of these parameters are interrelated; thus, the estimation of these key parameters was required for the ascent reduced-model performance study.

Table 19 summarizes these key design parameters, which allow the ascent design methodology to trade vehicle geometry characteristics (nose radius, wing loading), weight, and propulsion (engine thrust and impulse) in order to meet mission constraints (acceleration and heat loads). The key design parameters also allow the designer to understand the design drivers during the ascent performance analysis.

Table 19: Design parameters required for reduced order model of ascent design methodology.

Parameters	Notation
Atmospheric Environment	Density (ρ), Temperature (T_∞)
Velocity	V
Flight Path Angle	γ
Load Factor	n_d
Dynamic Pressure	q
Acceleration	a
Stagnation Temperature	T_0
Heat Flux	\dot{Q}
Vehicle Weight	W_0
Geometry	R_N (nose radius), S (wing area)
Drag	D
Lift	L
Engine Impulse	I_{sp}
Engine Thrust	T
Fuel Weight	W_{fuel}

(2) Design Constraints:

In the present study, only key design constraints relevant for the CD phase were considered. Generally, the ascent of an orbital/suborbital vehicle is primarily constrained by maximum dynamic pressure (q), maximum deceleration (dV/dt), and stagnation temperature and heat flux limitations (\dot{Q}). Each constraint along with its design limitations is presented as follows.

(1) The dynamic pressure limitation is defined as

$$q = \frac{1}{2} \rho V^2 \leq q_{\max} \quad (4-16)$$

(2) For the safety of the passengers of a manned ascent vehicle, the maximum acceleration should not exceed the forbearances of commercial passengers. The typical maximum acceleration rates¹⁵⁹ for manned flight are presented in Figure 44. The current recommended acceleration levels for aerospace vehicles by FAA-CAMI¹⁶⁰ are:

$$\begin{aligned} g_z: +4 \text{ to } -2 & \quad (\text{positive direction is from head to toe}) \\ g_x: \pm 4 & \quad (\text{positive direction is from front to back}) \\ g_y: \pm 1 & \quad (\text{positive direction is from left to right}) \end{aligned}$$

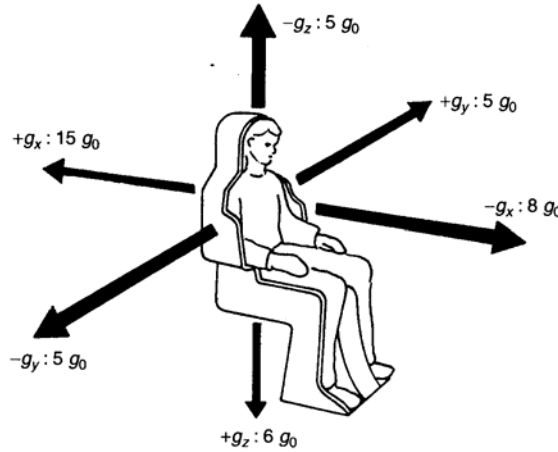


Figure 46: Typical human tolerance to directions of acceleration¹⁵⁹

Therefore, for the current design case study of a suborbital tourism passenger vehicle, the load factor limit was selected not larger than 4g. The load factor limitation constrains the acceleration of the vehicle in flight direction:

$$n_a = \left. \frac{dV}{dt} \right|_{\max} \leq 4g \quad (4-17)$$

(3) During orbital/suborbital flight, the space vehicle endures high temperatures T and convective heat rates \dot{Q} due to its high level of kinetic energy. The magnitude and duration of the heat flux imposed on the space vehicle determine the limitations of the thermal protection system (TPS) and airframe materials. These thermal constraints have to be considered in the early design phase. The approximate stagnation point temperature limitation of the vehicle is estimated as a function of free stream temperature T_∞ and flight Mach number M as

$$T_0 = T_\infty + \frac{\gamma - 1}{2} \cdot T_\infty \cdot M^2 \leq T_{\max} \quad (4-18)$$

The heat transfer rate at the stagnation region is approximately estimated^{161,162} by

$$\dot{Q} = 865 R_n^{-1/2} \left(\frac{V}{10^4} \right)^{k_1} \left(\frac{\rho}{\rho_0} \right)^{k_2} \leq \dot{Q}_{\max} \quad (4-19)$$

where R_n is a function of the vehicle's fineness ratio. For winged vehicles, empirical estimations of coefficients k_1 and k_2 are taken to be 2.65 and 0.5, respectively. The heating rates at other locations of the vehicle are proportional to the heating rate at the stagnation point. Figure 47 shows structural materials for high speed aircraft with their temperature constraints. As can be seen in Figure 47, if the stagnation temperature is over 500° F, composite materials such as metal matrix and carbon fiber are required.

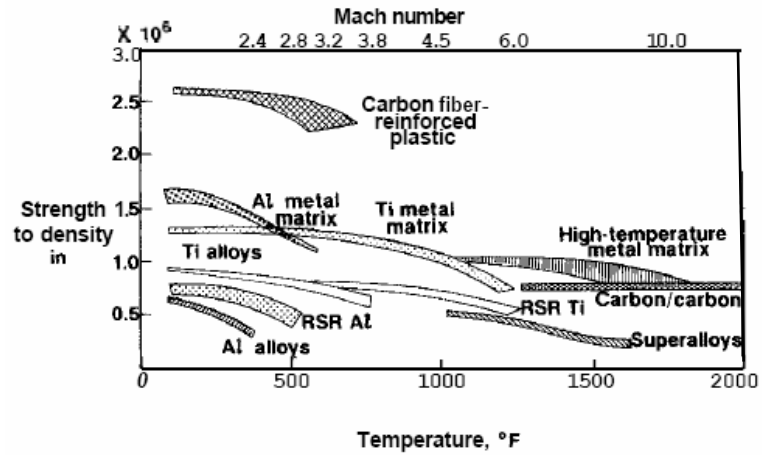


Figure 47: Structural materials for high speed aircraft ¹⁶³

The aim of the trajectory analysis in the sub-ascent design methodology is to determine a trajectory that minimizes the fuel mass required to achieve orbital/suborbital altitude while, at the same time, not violating vehicle dynamic pressure, acceleration, and heating constraints. A summary of conceptual design level design constraints applicable to a HTHL suborbital tourism vehicle is presented in Table 20. These design values will be used for the design case study in the following sections.

Table 20: Design constraints imposed on suborbital tourism vehicle ascent flight.

	Constraint Parameters	Notation	Constraint Value
Suborbital Mission	Final Altitude	H_f	100 km
	Final Speed	V_f	0 m/s
Weight and Sizing	Payload	W_{pay}	2- 3 passengers
Structure	Dynamic Pressure	q	500 psf
Aerothermodynamics	Stagnation Temperature	T_{stag}	600 F - 1500 F
	Heat Rate	\dot{Q}	< 400 BTU/ft ² /sec
Performance	Acceleration	n_d	5g

Figure 48 shows all of the above design constraints, which were accounted for in the ascent trajectory analysis of **SAV_TSSP**. As can be seen, the red lines represent the dynamic pressure constraints, 500 psf, 1000 psf, and 2000 psf, respectively. The stagnation temperature constraints (600° F, 700° F, and 1000° F) are indicated with green lines. The convective heat rates, 50 Btu/ft²/s and 100 Btu/ft²/s, are shown in the lower right hand corner.

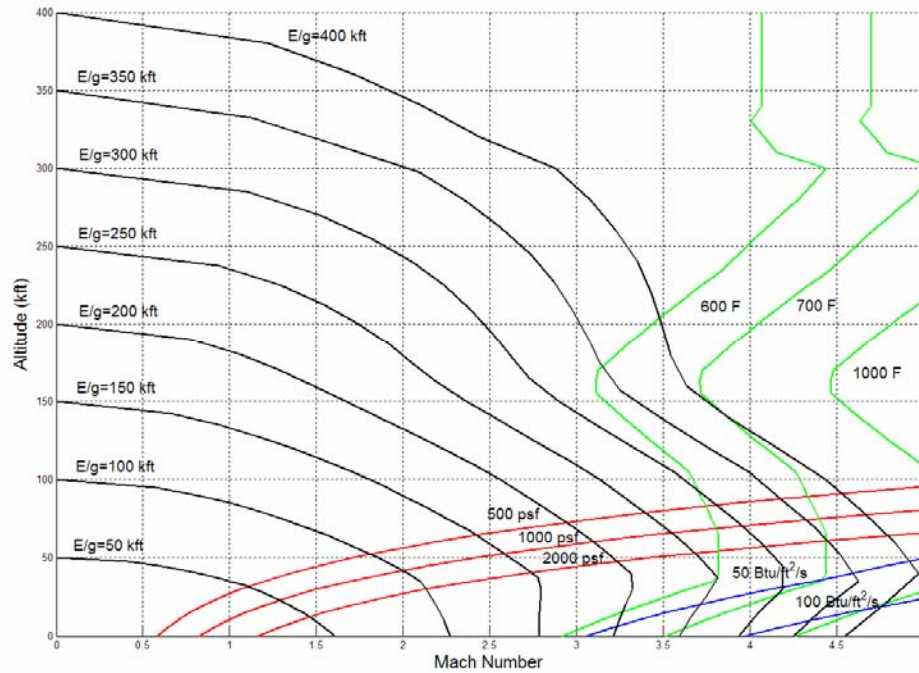


Figure 48: Energy height contour and design constraints

B. Equations of Motion

The SAV mission is to carry a passenger payload to a specified altitude (for example 100 kilometers for the suborbital tourism mission). For the low earth orbit mission, the equations of motion for a generic space access vehicle are governed by the dynamic equations for flight over a spherical, homogeneous non-rotating earth¹⁰⁷:

$$m\dot{V} = T \cos \alpha - D - mg \sin \gamma \quad (4-20)$$

$$mV\dot{\gamma} = T \sin \alpha + L - mg \cos \gamma \quad (4-21)$$

$$\dot{h} = V \sin \gamma \quad (4-22)$$

$$\dot{m} = -f = -\frac{T}{gI_{sp}} \quad (4-23)$$

where $T = T(V, h)$ is the thrust, $D = D(V, h, \alpha)$ is the drag, $L = L(V, h, \alpha)$ is the lift, g is the acceleration of gravity, $f = f(V, h)$ is the fuel flow rate, and α is the angle of attack.

The initial and final conditions of a suborbital tourism mission are

$$h(t_0) = 0 \quad h(t_f) = 35,000 \text{ ft}$$

$$M(t_0) = 0 \quad M(t_f) = 0$$

Although there are well-developed numerical methods for trajectory optimization of point-mass vehicle models, these methods are computationally too expensive and often lack robustness to be used during the CD stage where many vehicles must be evaluated and compared to a consistent basis. The approach selected in this dissertation was to avoid solving the complicated boundary condition trajectory equations. As a substitute, an Energy-State Approximation (ESA) technology was adopted to find the minimum-fuel trajectory.

The ESA technique was first introduced by Rutowski in 1953¹⁰⁸. By using ESA techniques, optimal trajectories for a variety of performance objectives, such as minimum time and fuel-climb problems can be obtained. ESA techniques have been successfully applied for a wide variety of aircraft¹⁰⁹, providing a simple and fast graphical solution to the optimization problem. Recently (References 164 and 165), it has been shown that the

ESA technique is also valid for the suborbital and orbital class of vehicles and missions. The application of ESA techniques compares well with more accurate and computationally expensive numerical solutions.^{108,109} This qualifies the approach particularly for the CD context, enabling rapid turn-around design sensitivity studies ultimately supporting the identification process of the correct convergence design space. In the current study, the ESA technique was implemented to determine minimum-fuel trajectories. The key idea of the ESA technique is to introduce the total mechanical energy as a state variable and, then, to neglect all other dynamics. The total mechanical energy of a suborbital vehicle is the sum of potential energy and kinetic energy. The ESA approach formulates the total energy E per unit weight of the vehicle as follows:

$$E = \frac{hR_e}{R_e + h} + \frac{1}{2g}V^2 \quad (4-24)$$

The time rate of change of E is given by

$$\frac{dE}{dt} = \frac{V(T - D)}{W} \quad (4-25)$$

The ESA approach defines the optimal trajectory as the flight path, which requires minimum fuel to ascend from an initial energy height to a final energy height (at least 100 km for the suborbital tourism mission). Therefore, the total vehicle weight W is defined as

$$W = \int_{t_0}^{t_f} \dot{W} dt = \int_{E_0}^{E_f} \dot{W} \frac{W}{V(T - D)} dE = \int_{E_0}^{E_f} \frac{T}{I_{sp}} \frac{W}{V(T - D)} dE \quad (4-26)$$

Clearly, we need to minimize the integrand in order to achieve minimum fuel consumption at each energy level. The key result from the energy-state analysis is that

the minimum-fuel trajectory can be obtained if the vehicle is operated at each energy level E such that $\frac{I_{sp}}{T} \frac{V(T-D)}{W}$ is maximized. Therefore, locally maximizing this term leads to the most efficient trajectory for the suborbital tourism vehicle mission.

Here, an energy height was defined as E/g . Figure 49 shows an example of the energy height contours for a suborbital space tourism vehicle mission. The vehicle transfers from its initial energy level (ground takeoff or air launch like SpaceShipOne) to an altitude of at least 100 km (328,083 ft). In Figure 49, two red points at the lower left corner represent two different initial energy positions related to the ground launch and air launch methods. The energy height at least 100km required for suborbital space tourism is shown by the red graph in Figure 49. During the rocket burn, the energy height is constantly increasing until the E/g level for suborbital flight (red line) is achieved.

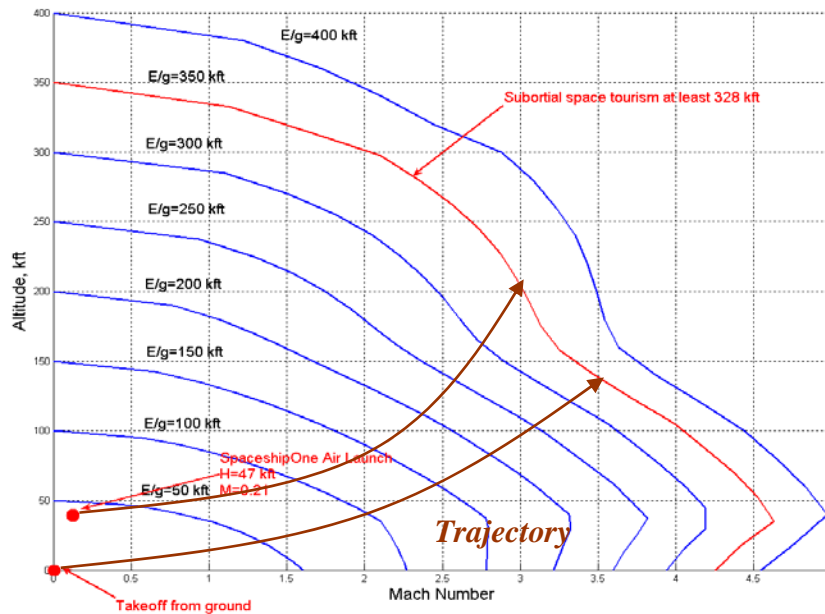


Figure 49: Energy height contour for suborbital space tourism mission.

C. Design Synthesis Process

Figure 50 shows the sub-synthesis conceptual design process for a HTHL SAV during the ascent phase. The design synthesis process starts with a baseline vehicle and the orbital/suborbital space mission requirement. The mission profile provides the payload information for the mass properties module and the altitude information required by the performance module in order to calculate the overall fuel requirement. After obtaining the geometry data from the baseline vehicle, the mass properties module estimates initial vehicle takeoff gross weight for the performance module. Meanwhile, the design constraints are identified early in the design process and forwarded to the optimization module. During the activity to synthesize the flight vehicle, the performance module communicates with the atmosphere module, aerodynamics module, propulsion module, and optimization module to define a minimum fuel weight trajectory under the specified design constraints. Finally, the fuel weight requirement and fuel volume available are compared. If the fuel volume available does not satisfy the fuel weight requirement for the space tourism mission, the configuration concept iterates until fuel volume available and fuel weight requirements converge. At this point, the initial baseline vehicle concept is closed and provides performance data for further design studies. As can be seen in Figure 50, the performance module (trajectory analysis) is the center of the overall design synthesis process.

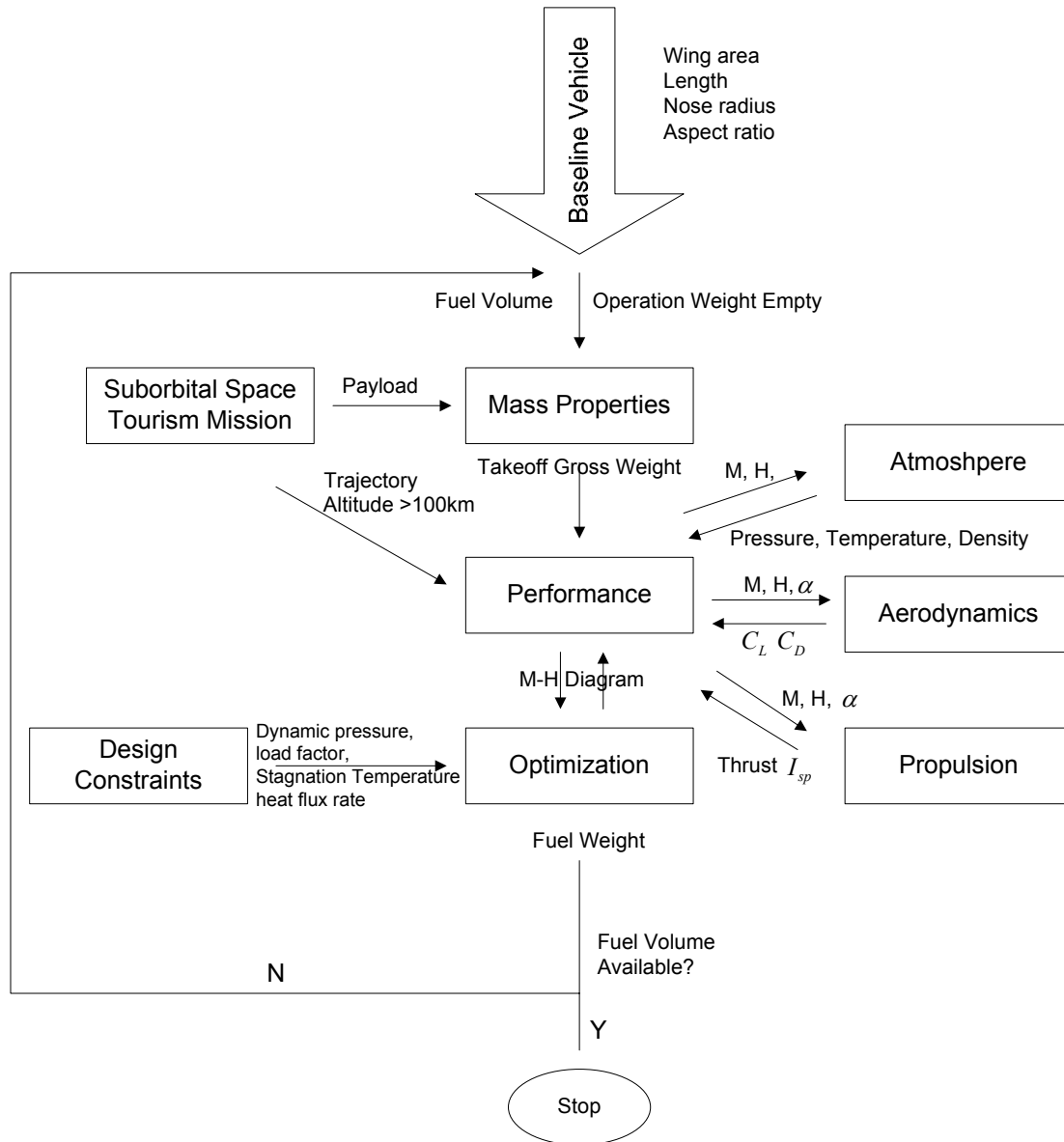


Figure 50: CD design synthesis process for sizing of suborbital space tourism vehicle

(1) Program Organization:

A trajectory synthesis simulation program (**SAV_TSSP**)¹¹¹ was developed to implement the above described design synthesis methodology. This simple, integrated, and modular computer program for the design of HTHL-class vehicles is capable of demonstrating the vehicle's flight potential through suborbital trajectory simulation. The

variation of the main design parameters throughout the trajectory flight path is visualized. The synthesis simulation program has both decomposition and integration capabilities. It reduces the complex engineering problem to the individual pertinent objects. The program is decomposed into a hierarchical network of systems and attributes. It has one synthesis main program with several sub-modules including propulsion, aerodynamics, performance, and thermal analysis, etc. Also, the framework of this program enables rapid modeling and the integration of modular analysis tools so it can be easily extended due to the software's modular structure. The concept of objects in this approach has shown the potential to provide a robust modeling and simulation environment.

The source code was written in Matlab¹⁶⁶, utilizing the powerful Matlab graphic functions to visualize the design space and find a graphic solution for the minimum fuel trajectories. The program was developed in the MS Windows PC environment. In accordance with the particular characteristics of the CD phase, emphasis was placed on overall simplicity and minimum data input requirements. All basic equations used to mathematically model the atmosphere, aerodynamics, propulsion, and performance, were kept as simple as possible to ensure that the key design parameters are evaluated quickly and efficiently. For detailed information about program organization and modules, please refer to Reference 111. Some analysis results of this software implementation are presented in the following.

(2) Ascent Sub-Synthesis Design Study:

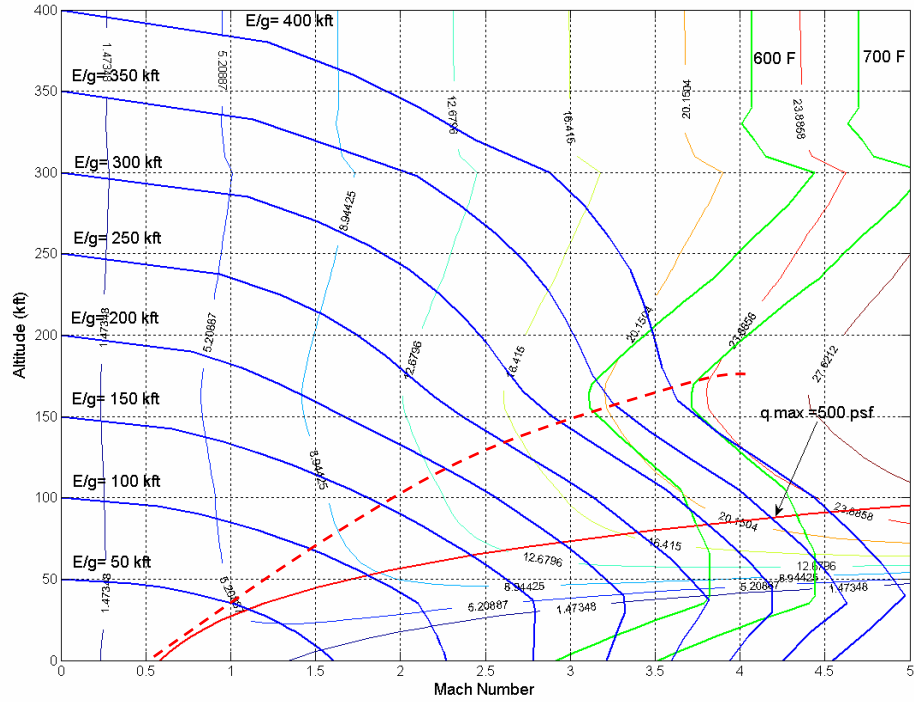
The main synthesis logic was integrated into the performance module and the optimization module. Its primary task is to communicate with the other modules, thereby deriving the variations of vehicle performance with key design parameters, such as gross weight and vehicle geometry. As a consequence, a minimum fuel ascent trajectory can be iterated on, using this multi-disciplinary process. The following describes how the synthesis process arrives at a minimum fuel trajectory.

(a) Minimum Fuel Ascent Trajectory:

As can be seen from the ESA trajectory analysis presented in Section B, in order to find a minimum fuel trajectory for a suborbital tourism mission, the expression

$$\frac{I_{SP} \cdot V \cdot (T - D)}{T \cdot W}$$

needs to be maximized at every energy level. Contours of constant energy increase per pound of fuel consumption for the above parameter are shown in Figures 51 and 52. Figure 51 shows the energy contours for the OU XP using rocket power only. Figure 52 shows the energy contours for the OU XP using jet power only. Based on these energy contours from the ESA technique, the minimum fuel trajectory path can be determined and illustrated by the red dotted lines in Figure 51 and Figure 52, respectively.



A comparative study was conducted where in a maximum dynamic pressure ascent trajectory was selected. Figure 53 shows the two different trajectories: (a) optimal minimum fuel trajectory and (b) maximum dynamic pressure trajectory. Clearly, for the maximum dynamic pressure trajectory, the vehicle ascent path is constrained by the maximum permissible dynamic pressure. This is illustrated in Figure 54 where the vehicle climbs shortly after takeoff at its maximum dynamic pressure (500 psf) until it reaches the cutoff point. In comparison, the minimum fuel trajectory estimated using the ESA technique led to smaller accelerations avoiding the maximum dynamic pressure peak (see Figure 54). Figure 55 shows the variation of flight speed with altitude for the minimum fuel trajectory and the maximum q trajectory. To compare both cases, the rocket only *OU XP* propulsion mode was selected for the baseline vehicle.

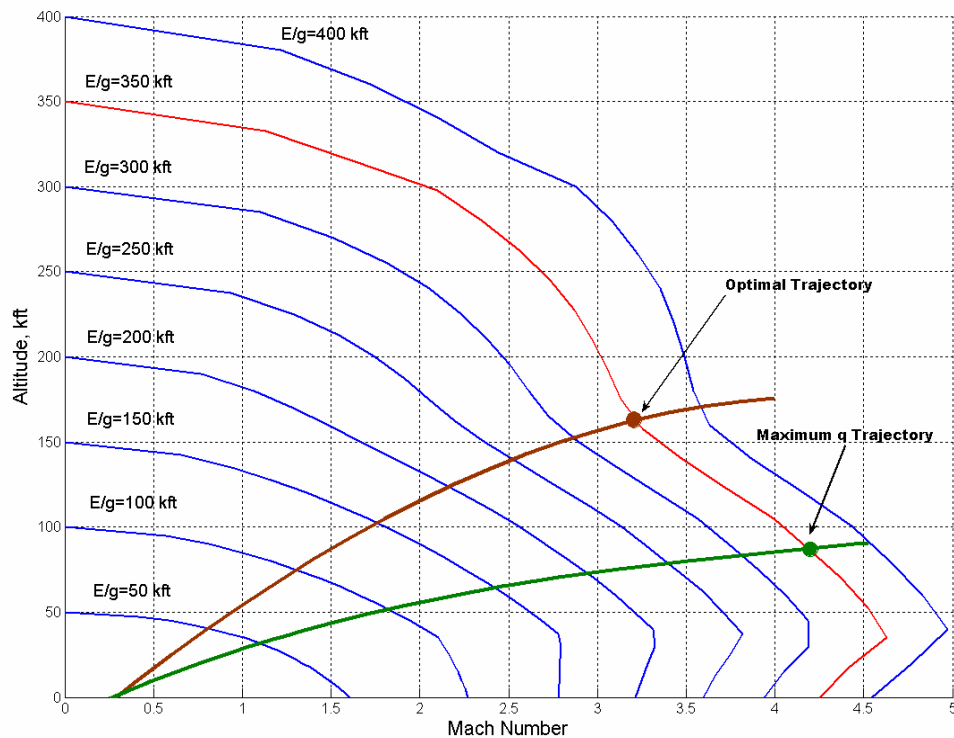


Figure 53: Comparison of minimum fuel trajectory and maximum q trajectory.

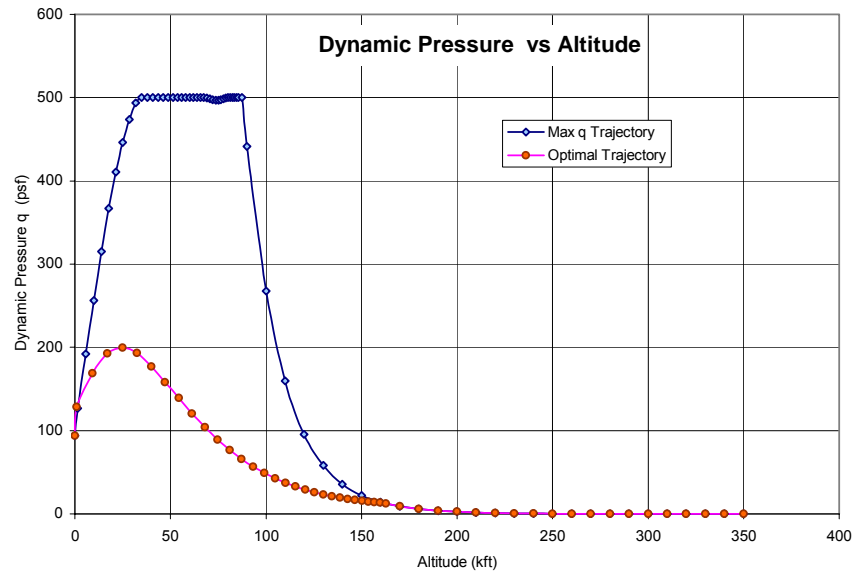


Figure 54: Variation of dynamic pressure with altitude for minimum fuel trajectory and maximum q trajectory.

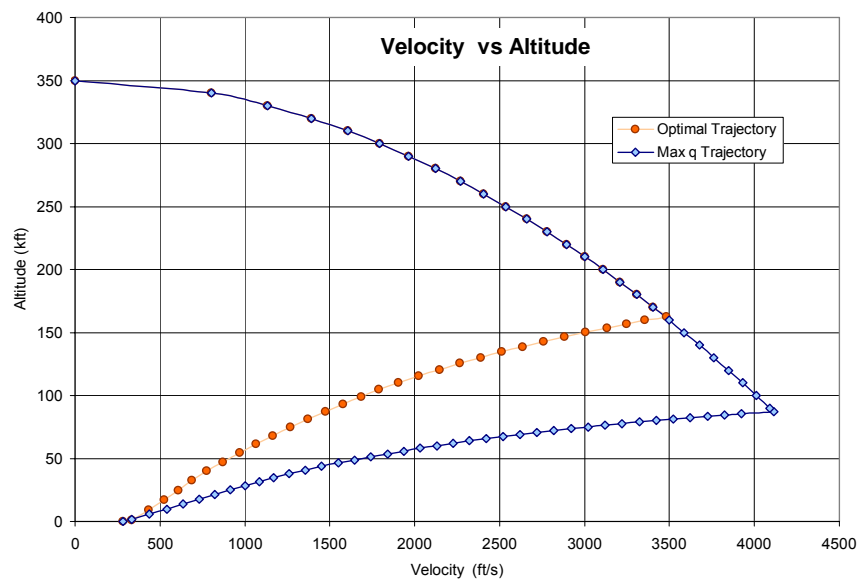


Figure 55: Variation of flight speed with altitude for minimum fuel trajectory and maximum q trajectory.

(b) Fuel Weight Convergence:

The design synthesis process, see Figure 50, indicates that, after having determined the initial trajectory (Mach number vs. altitude diagram), the total fuel weight can be estimated utilizing the synthesis iteration process. It can be seen in Figure 56 that the trajectory synthesis simulation program took 30 to 40 iterations to converge to the propellant weight required for the suborbital mission. The propellant weight of the maximum q trajectory was around 15,000 lb. This was 3,000 lb more than the minimum fuel trajectory determined using the ESA technique.

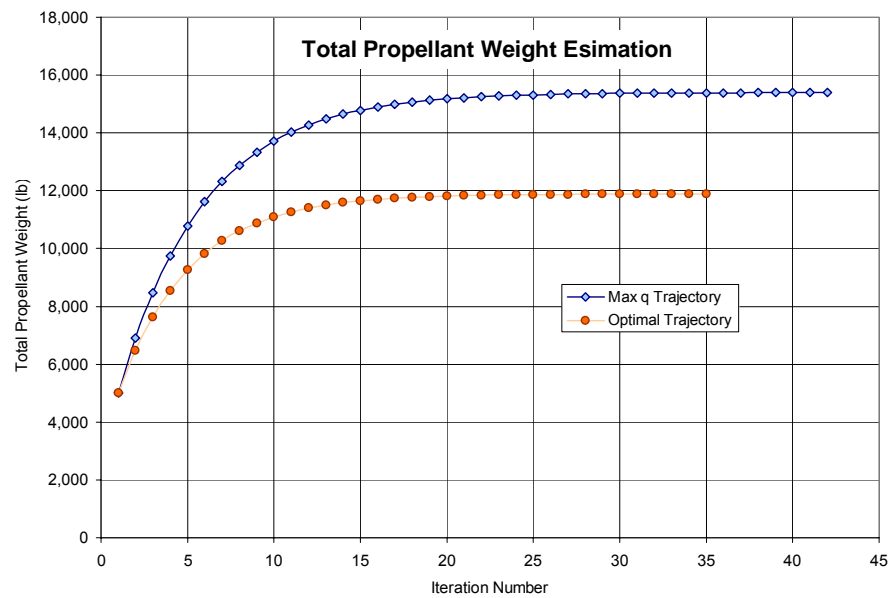


Figure 56: Iterations of propellant weight.

Figure 57 compares the variation of weight and flight speed for both trajectories.

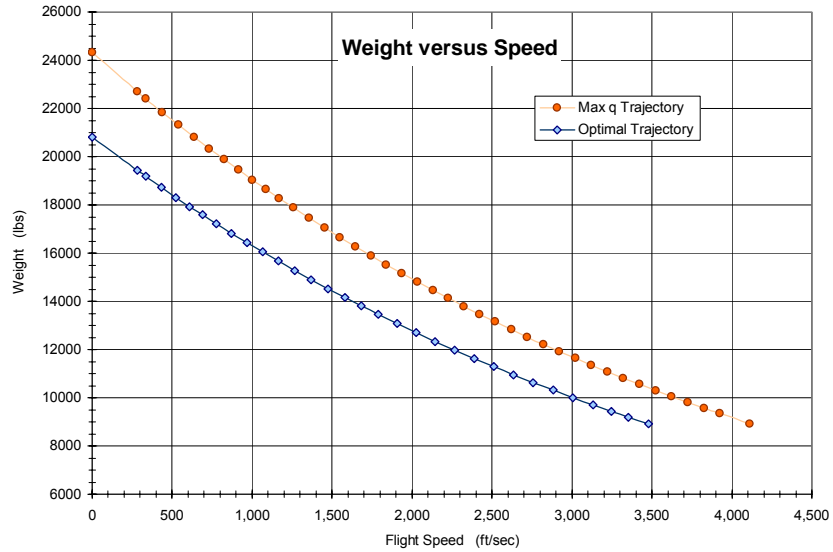


Figure 57: Variation of weight with flight speed for minimum fuel trajectory and maximum q trajectory.

The variation of fuel consumption and altitude is shown in Figure 58. The advantage of the minimum fuel trajectory with respect to fuel weight and fuel volume is obvious.

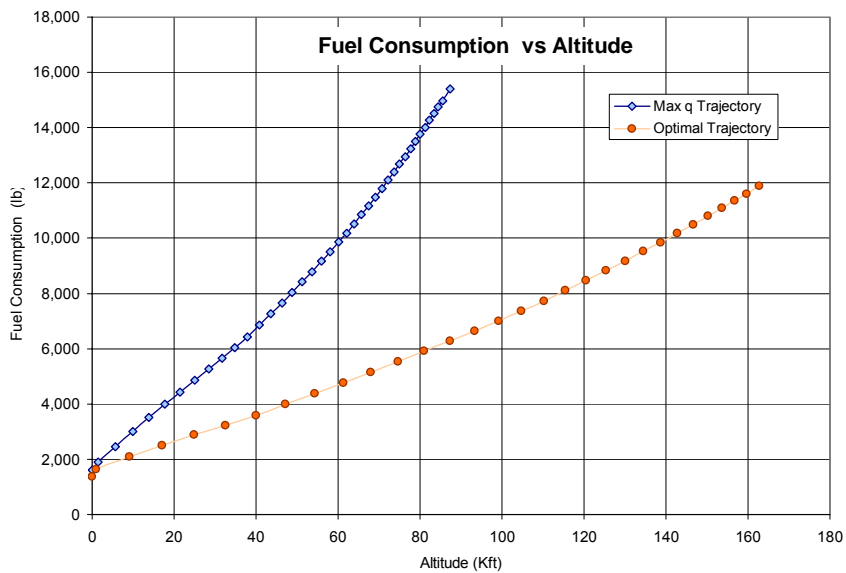


Figure 58: Variation of fuel consumption with altitude for minimum fuel trajectory and maximum q trajectory.

(c) Performance Results:

The systematic and consistent modeling approach underlying this trajectory synthesis simulation program (**SAV_TSSP**) finally results in a variety of performance maps (dynamic pressure vs. altitude; speed vs. time; thrust vs. speed; altitude vs. time; drag/weight vs. altitude; weight vs. speed; specific impulse vs. speed; etc.) for a first order converged vehicle. As a demonstration, Figure 59, 60 and 61 are assembled below to illustrate the variation of several key design parameters (flight speed, acceleration, altitude, and time) throughout the flight trajectory. This information helps the flight vehicle designer to understand the sensitivities of key design parameters.

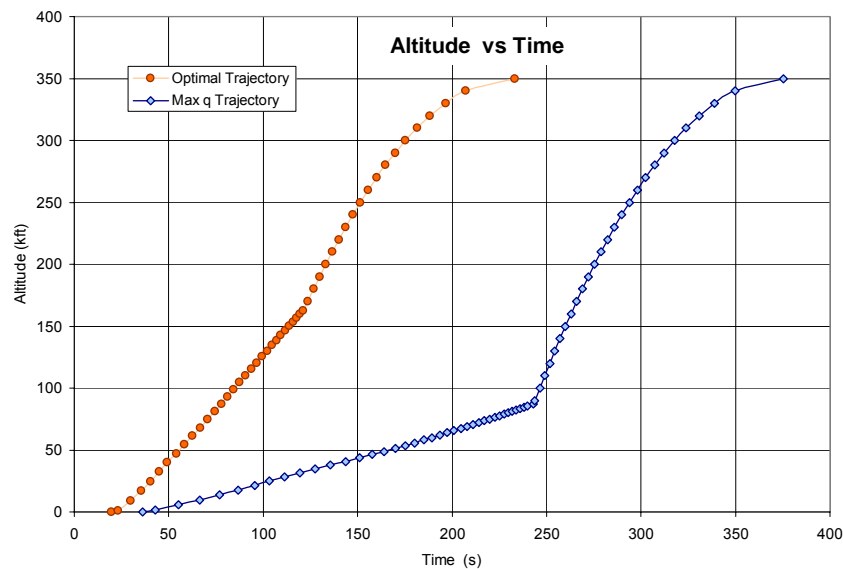


Figure 59: Variation of altitude with time for minimum fuel trajectory and maximum q trajectory.

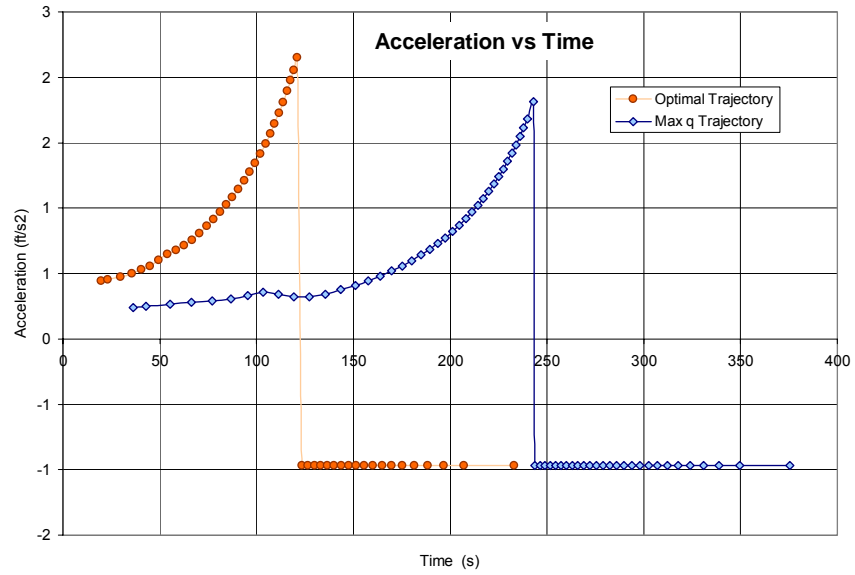


Figure 60: Variation of axial acceleration with time for minimum fuel trajectory and maximum q trajectory.

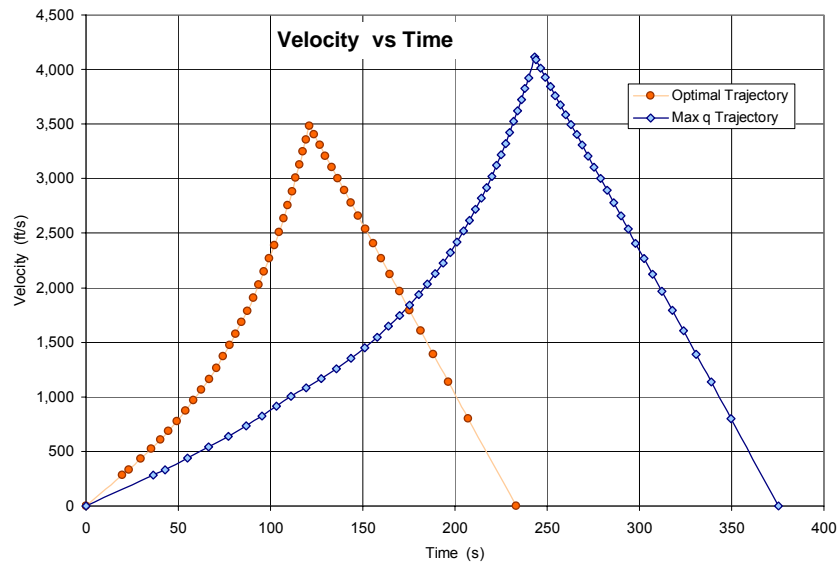


Figure 61: Variation of flight speed with time for minimum fuel trajectory and maximum q trajectory.

4.3.3 Reentry

After the orbital/suborbital space vehicle completes its missions in low-Earth orbit, the vehicle will carry the passengers or cargo back into the atmosphere and land at the designated terminal area. As the suborbital tourism vehicle enters the atmosphere, it is subjected to some extreme operational variables like high deceleration rate, aerodynamic heating, rapidly changing stability and control characteristics, etc. Figure 62 shows that a typical return trajectory of the suborbital tourism vehicle (SpaceShipOne) starts with ballistic reentry and continuous with a glide back to the terminal area.

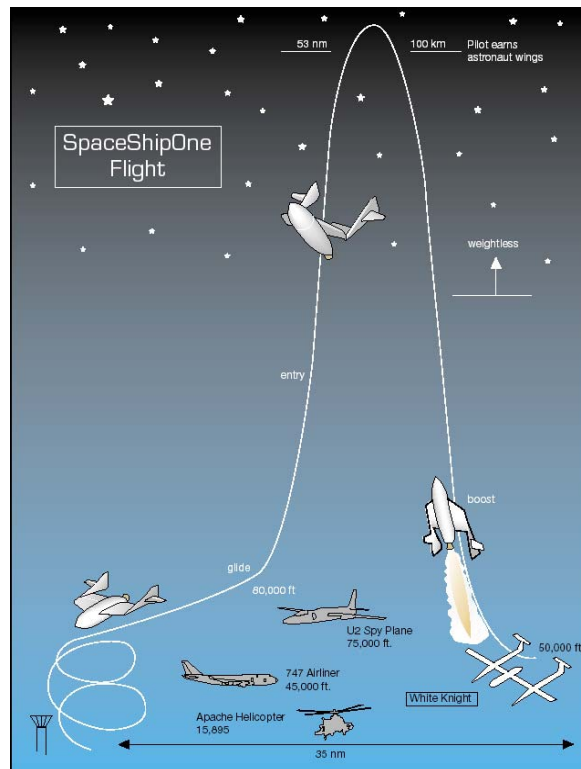


Figure 62: SpaceShipOne flight trajectory.¹⁶⁷

This return is quite different from the ballistic reentry of capsules (Apollo, Gemini) and the equilibrium reentry of the Space Shuttle. The reentry of these capsules and the Space Shuttle involves very high entry speeds. In contrast, the reentry speed of a space tourism vehicle is comparable low since it is falling from only 100 km altitude at an initial zero velocity. Also, throughout the equilibrium glide trajectory of the Space Shuttle, the lift and centrifugal forces balance the mass force (weight). Therefore, the equilibrium glide trajectory has adequate lift to provide low decelerations and is desirably implemented for manned vehicles that are returning with high entry speed from near earth orbit. During the reentry, a combination of bank angle and angle-of-attack can be chosen as the primary trajectory control parameters to achieve the required down range while the vehicle is still able to satisfy limitations such as aerodynamic heating, heat rate, deceleration rate, and dynamic pressure.

A. Design Parameters and Design Constraints

(1) Design Parameters:

There is a multitude of higher-fidelity trajectory analysis software^{27,110} available for the detailed design analysis of the reentry phase. Table 21 summarizes some trajectory modules of key design methodologies and multiple versions of equations of motion developed for high speed reentry.^{155,156,157, 168,169,170}

Table 21: Design analysis methods for reentry study.

Methods	Description	Design Parameters	Applications
Czysz ³⁹	It is assumed that data sets have been generated, based on past experience and extensions as well as on predictions from sizing programs, on capabilities in propulsion, fuels, materials, and industrial manufacturing. A series of design spaces are constructed with respect to various parameters. A vehicle design convergence is sought based on the influence of various parameters on the vehicle performance as depicted by the design spaces. The design spaces are generated starting with data on various aspects of vehicle design. The construction of design spaces this becomes the most significant part of realizing vehicle convergence. Visibility, comprehensiveness, clarity, rationality and ease of interpretation are the main desired characteristics of design spaces.	Propulsion Fuel Mass Material Index Industry Index	Empirical method Not applicable for the reentry analysis
Hammond ^{12,27}	Once the aerodynamic characteristic have been determined and weights for the vehicle components are assumed for the initially trajectory analysis (POST). POST is a generalized point mass, discrete parameter targeting and optimization program capable of analyzing trajectories for powered or unpowered vehicles operating near a rotating oblate planet. In launch vehicle design POST is used to analyze launch, on-orbit, and reentry trajectories subject to a number of constraints, such as maximum acceleration, heating boundaries, and cross range requirements. The principal results from the performance analysis include propellant requirements for input to weights and sizing calculations and in-flight conditions used by aeroheating analysts.	Maximum Acceleration Heating Propellant Mass Weight Geometry	Launch, on-orbit, and reentry trajectories analysis
Hunt ⁴⁰	Performance/Trajectory: the performance routine is a trajectory code, whether a simple energy-state integration approach or a three-degree of freedom dynamic version. Aerodynamic and propulsion performance are the required inputs. (1) Aerodynamic matrix (lift and drag coefficient, C_L and C_D as a function of Mach number, angle of attack and altitude) is calculated for an assumed trajectory bandwidth on dynamic pressure. (2) The net engine performance matrix (thrust coefficient and specific impulse as a function of Mach number, angle of attack and fuel equivalence ratio) is then assembled, with the thrust coefficients vectored along the vehicle wind axis and referenced to free stream static in the same manner as the aero coefficients. With this aero/propulsion performance set, the fuel fraction required to perform the ascent (98 percent of fuel requirement), orbital insertion/circularization, and deorbit is determined from the trajectory analysis. (3) Iterations are now required in the synthesis process to adjust the structures/insulation for the optimum (off-nominal) ascent and descent	Lift Coefficient Drag Coefficient Mach Number Angle of Attack Altitude Dynamic Pressure Thrust Specific Impulse Fuel Fraction Ratio Weight Geometry	Ascent, orbital insertion and deorbit trajectory analysis

	trajectory and vice versa and to perform an iteration on size/weight in the performance routine.		
SSSP ⁶³	The General Trajectory Simulation Module (GTSM) program is a general purpose high speed, precision flight program which simulates the flight for an aerospace vehicle in the gravitational field of a central body. It utilizes the efficient Kutta-Merson variable stepsize numerical integration technique to integrate with respect to time the twelve state equations. These equation define the time rate of change of the three degree of freedom vehicle motion, the vehicle mass, the ideal velocity and velocity losses, and a heating parameter. The vehicle motion equations consist of three kinematic and three kinetic equations and are expressed in a natural applied force coordinate system which minimizes the extend of matrix coordinate transformations common to other simulations.	Velocity Vehicle Mass Velocity Loss (ΔV) Time	Ascent Analysis
PrADO ⁶⁶	The flight performance module includes a flight path simulation to estimate the necessary thrust and fuel mass of the aircraft. For every point of time during the flight simulation, Mach number and altitude are given. From this information the time-dependent derivatives result from a numerical differentiation. It is now possible to fulfill the flight-mechanic differential equations in the flight direction and normal to it by an iteration over the angle of attack. The use of a fixed flight path provides the advantage of saving time during the iteration.	Thrust Fuel Mass Mach Number Altitude Time Angle of Attack Flight Path Angle	Two Stage to Orbit
Allen, Eggers, Chapman, and Woods ^{155,156,157,38}	The nonlinear equations of motion are derived for entry into an exponential planetary atmosphere. By disregarding some relatively small terms such as gravity force, the centrifugal acceleration and lift force, a single, ordinary, nonlinear differential equation of second order is reduced to be a linear differential equation of Allen and Eggers applicable to ballistic entry vehicle. If the vertical acceleration and vertical component of drag force are negligible, the resulting truncated differential equations are applicable for the equilibrium glide vehicle (Space Shuttle).	Velocity Deceleration Gravity Force Aerodynamic Drag Density Altitude Vehicle Mass, Size Flight Path Angle Aerodynamic Heating Total Heat Transfer Maximum Heat Lift to Drag Ratio Maximum Range	Ballistic, Skip and Glide Vehicles with High Entry Speed
Aachen ¹⁵⁸	Performance requirements, mission constraints, vehicle design and trajectory selection of typical reentry vehicles are briefly described. Some semi-empirical estimations of the lift-to-drag ratio and ballistic parameter of a reentry vehicle with cross range and heating constraints are presented.	Load Factor Dynamic Pressure Heat Flux Integral Heat Load Surface Temperature Atmosphere (density, temperature) Flight State Condition (velocity, angle of attack) Vehicle Properties (geometry, weight and aerodynamics) Wing Loading Ballistic Coefficient Lift-to-Drag Ratio	Atmosphere Reentry of Capsules and Winged Vehicle

Although some higher-fidelity trajectory programs (POST,²⁷ OTIS,¹¹⁰ GTSM⁶³) or complex analytical equations (Allen,¹⁵⁵ Eggers,¹⁵⁶ Chapman,¹⁵⁷ Aachen,¹⁵⁸ etc) are available, there is no efficient design methodology available for the conceptual design (CD) of the entry phase of either high speed entry vehicles or the suborbital tourism vehicle class. For instance, current conceptual design studies of TSTO vehicles^{171,172} do not compute the return trajectory of different entry vehicle configurations, but only approximate it by assuming the same reentry profile used in the detailed reentry analysis of the Space Shuttle Orbiter¹⁷³. As a result, there is a clear demand for a reentry design synthesis module capable of supporting the configuration concept selection process by quantifying design sensitivities of key design parameters.

It is desirable to have reduced order models or approximate solutions to show physical transparency of major disciplines interacting with each other during the reentry phase. Such reduced order models are generally derived based on complex analytical equations with reasonable simplifying assumptions. Therefore, the modeling techniques above (Allen,¹⁵⁵ Eggers,¹⁵⁶ Chapman,¹⁵⁷ Aachen,¹⁵⁸ etc) were reviewed in Section B to locate a balance among physical characteristics, data available, and key design parameters.

In the following, the key design parameters for use in the generic reentry design methodology are investigated. This methodology has to find a balance between reentry mission requirements and overall design performance capabilities of the vehicle. For this purpose, the atmospheric reentry conditions (altitude, density, and temperature) are

required for the analysis. The equations of motion derived by Allen¹⁵⁵, Eggers,¹⁵⁶ Chapman,¹⁵⁷ Aachen,¹⁵⁸ show that the maximum deceleration of the reentry vehicle is determined by vehicle velocity and flight path angle, down range is determined by lift-to-drag ratio, and stagnation temperature depends on vehicle velocity and vehicle geometry such as nose radius. The flight velocity, in turn, is governed by various key design parameters, the ballistic parameter, wing area, aerodynamic characteristics, and weight of the vehicle. All of these parameters are closely coupled, and estimations of these parameters are required for the reentry reduced-order model performance design study.

Table 22 summarizes these parameters. They allow the reentry design methodology to determine how the vehicle characteristics (wing loading, lift-to-drag ratio, and ballistic parameter) meet the mission constraints (deceleration and heat loads). Also, they allow the designer to understand the design drivers for the reentry performance analysis.

Table 22: Design parameters required for reduced order model of reentry design methodology

Parameters	Notation
Atmospheric Environment	Density (ρ), Temperature (T_∞)
Velocity	V
Flight Path Angle	γ
Load Factor	n_d
Dynamic Pressure	q
Deceleration	a
Stagnation Temperature	T_0
Heat Flux	\dot{Q}
Vehicle Weight	W_0
Geometry	R_N (nose radius), S (wing area)
Drag	D
Lift	L
Wing Loading	W/S
Ballistic Coefficient	$m/(C_D * S)$
Lift to Drag ratio	L/D

(2) Design Constraints:

In the present study, only key design constraints relevant to the CD phase were considered. Generally, the reentry of SAVs is constrained by maximum dynamic pressure (q), maximum deceleration (dV/dt), and stagnation temperature and heat flux limitations (\dot{Q}). Each constraint along with its design limitations is presented as follows:

(1) The dynamic pressure limitation is defined as

$$q = \frac{1}{2} \rho V^2 \leq q_{\max} \quad (4-16)$$

(2) For the safety of the passengers of a manned descent vehicle, the maximum deceleration should not exceed the forbearances of commercial passengers. The typical maximum deceleration rates¹⁵⁹ for manned flight are presented in Figure 63. The current recommended deceleration levels for aerospace vehicles by FAA-CAMI¹⁶⁰ are

$g_z: +4 \text{ to } -2$	(positive direction is from head to toe)
$g_x: \pm 4$	(positive direction is from front to back)
$g_y: \pm 1$	(positive direction is from left to right)

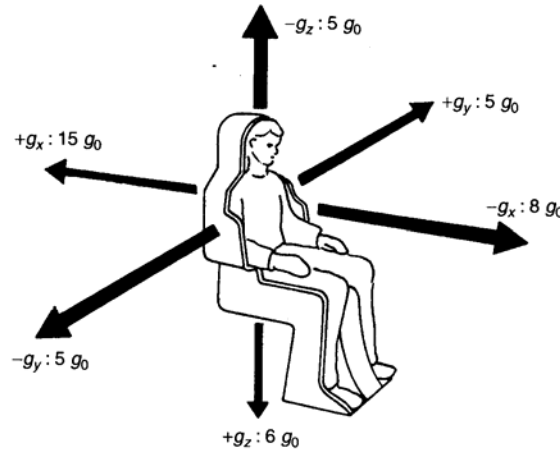


Figure 63: Typical human tolerance to directions of accelerations¹⁵⁹

Therefore, for the current design study of a suborbital tourism passenger vehicle, the load factor limit was selected to be no more than 4g. It constrains the deceleration of the vehicle in flight direction:

$$n_d = \left. \frac{dV}{dt} \right|_{Max} \leq 4g \quad (4-17)$$

(3) During suborbital flight, the space tourism vehicle endures high temperatures T and convective heat rates \dot{Q} due to its high level of kinetic energy. The magnitude and duration of the heat flux imposed on the space vehicle determines the limitations of the thermal protection system (TPS) and airframe materials. These thermal constraints have to be considered in the early design phase. The approximate stagnation point temperature limitation of the vehicle is estimated as a function of free stream temperature T_∞ and flight Mach number M

$$T_0 = T_\infty + \frac{\gamma-1}{2} \cdot T_\infty \cdot M^2 \leq T_{max} \quad (4-18)$$

and the heat transfer rate at the stagnation region is approximately estimated^{161,162} by

$$\dot{Q} = 865 R_n^{-1/2} \left(\frac{V}{10^4} \right)^{k1} \left(\frac{\rho}{\rho_0} \right)^{k2} \leq \dot{Q}_{max} \quad (4-19)$$

where R_N is a function of the vehicle's fineness ratio. For winged high-speed vehicles, empirical estimates of the coefficients $k1$ and $k2$ are 2.65 and 0.5, respectively. The heating rates at the other locations of the vehicle are proportional to the heating rate at the stagnation point.

(4) Downrange requirement: The suborbital tourism vehicle should have the capability to fly back to the designated terminal area. Thus, a down range constraint also has to be addressed in the early conceptual design. For the first flight of SpaceShipOne, the down range requirement was set to around 25 miles.^{95,96}

A summary of conceptual design (CD) level design constraints applicable to HTHL suborbital tourism vehicles is presented in Table 23. These design values will be used for the design case study in the following sections.

Table 23: Design constraints imposed on suborbital tourism vehicle reentry flight

	Constraint Parameters	Notation	Constraint Value
Suborbital Mission	Final Altitude	H_f	100 km
	Final Speed	V_f	0 m/s
Weight and Sizing	Payload	W_{pay}	2- 3 passengers
Structure	Dynamic Pressure	q	500 psf
Aerothermodynamics	Stagnation Temperature	T_{stag}	600 F - 1500 F
	Heat Rate	\dot{Q}	< 400 BTU/ft ² /sec
Performance	Deceleration	n_d	5g
	Down range		25 miles - 40 miles
	Angle of attack	α	-4 < α < 12 deg

B. Equations of Motion

The classical equations of motion for capsule (ballistic flight) and Space Shuttle (equilibrium flight) reentry have been derived by Allen¹⁵⁵, Eggers¹⁵⁶, and Chapman.¹⁵⁷ However, no general equations of motion have ever been derived for the suborbital tourism SAV class like SpaceShipOne or *OU XP*. A suborbital tourism SAV (*OU XP*) was selected as a design case study here. Therefore, the current study was focused on the derivation of reentry equations for this type of SAV. The reduced order models for

capsule (ballistic flight) and Space Shuttle (equilibrium flight) reentry will be considered in the process.

As mentioned before, the return of a suborbital tourism vehicle includes two distinct flight phases: ballistic entry and glide back. The equations of motion for both cases were derived to show the basic physical phenomena the vehicle experiences during the reentry flight phase. Emphasis was placed on obtaining a relatively simple analytic framework and solutions. This approach reduced computing time and permitted the methodology to be applied to tasks like parametric studies during the CD phase. The derivation of the equations of motion for the ballistic entry and glide back are presented as follows.

(1) Ballistic Entry: Figure 64 shows aerodynamic forces and thrust components in an inertial coordinate system. Oxyz is the planet-fixed system. M is the vehicle position, x' , y' , and z' are the axes from the position M of the vehicle, parallel to the axes x , y , and z . Let x_1 , y_1 , and z_1 be the axes from point M along the directions of lift component ($L \sin \sigma$), V , and drag (D). L is the lift, T is the thrust, m is the vehicle mass, V is the velocity, σ is the bank angle, γ is the flight path angle, ψ is the heading angle, ϕ is the rotation angle about the y axis, and r is the distance between the vehicle position and the origin of the inertial system. F_T is the component of the aerodynamic and propulsive forces along the velocity vector, F_N is the component orthogonal to it in the lift-drag plane, ε is the angle between the velocity and the thrust, g is the gravitational force, and ω is the angular velocity. The general equations of motion of a vehicle flying over a spherical planet can then be written as^{135,168}

$$\frac{dV}{dt} = \frac{1}{m} F_T - g \sin \gamma + \omega^2 r \cos \phi (\sin \gamma \cos \phi - \cos \gamma \sin \phi \sin \psi)$$

$$V \frac{d\gamma}{dt} = \frac{1}{m} F_N \cos \sigma - g \cos \gamma + \frac{V^2}{r} \cos \gamma + 2\omega V \cos \phi \cos \psi + \omega^2 r \cos \phi (\cos \gamma \cos \phi + \sin \gamma \sin \phi \sin \psi)$$

$$V \frac{d\psi}{dt} = \frac{1}{m} \frac{F_N \sin \sigma}{\cos \gamma} - \frac{V^2}{r} \cos \gamma \cos \psi \tan \phi + 2\omega V (\tan \gamma \cos \phi \sin \psi - \sin \phi) - \frac{\omega^2 r}{\cos \gamma} \sin \phi \cos \phi \cos \psi$$

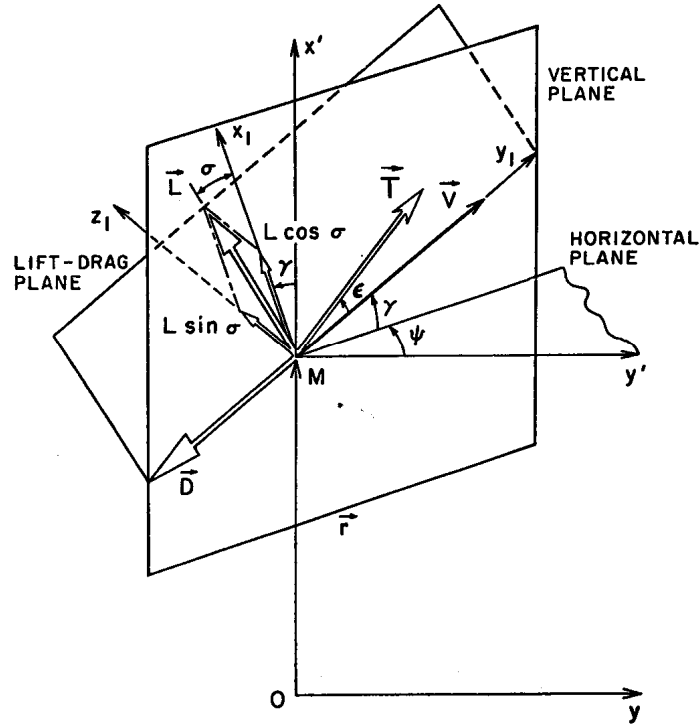


Figure 64: Aerodynamic forces and thrust in inertial frame. ¹⁶⁸

The term ω stems from the rotation of the planet. In general, the atmosphere has the same rotation as the planet. Hence, ω is small, and $\omega^2 r$ is considered to be negligible. In the case of a non-power ballistic reentry, thrust $T = 0$, $F_T = -D$, and $F_N = L$. The above equations then are reduced to

$$\frac{dV}{dt} = -\frac{D}{m} + g \sin \gamma \quad (4-27)$$

$$V \frac{d\gamma}{dt} = \frac{L}{m} \cos \sigma - g \cos \gamma + \frac{V^2}{r} \cos \gamma \quad (4-28)$$

$$V \frac{d\psi}{dt} = \frac{L \sin \sigma}{m \cos \gamma} - \frac{V^2}{r} \cos \gamma \cos \psi \tan \phi \quad (4-29)$$

Considering that the altitude range for a space tourism vehicle is 100 km, less than 2% of Earth's radius, and the altitude which aerodynamic force starts to affect is less than 1% of earth radius, the flat Earth assumption can be used in this analysis. In addition, during the reentry of the space tourism vehicle, the deceleration forces and heating constraints are dominating. Thus, the motion may be considered planar without rolling moment. Therefore, the bank angle σ can be considered small, leading to $\cos \sigma \approx 1$. The ballistic entry of a suborbital tourism vehicle in a two dimensional coordinate system is shown in Figure 65. The equations of motion in the directions perpendicular and parallel to the flight path are^{169,170}

$$\frac{dV}{dt} = -\frac{D}{m} + g \sin \gamma \quad (4-30)$$

$$V \frac{d\gamma}{dt} = \frac{L}{m} - g \cos \gamma + \frac{V^2}{r} \cos \gamma \quad (4-31)$$

For approximate solutions for a suborbital vehicle, the following assumptions can be made to simplify Eq. (4-30) and Eq. (4-31):

- The vehicle descends vertically. By definition, if the descent phase of the suborbital vehicle is purely ballistic, lift L is zero. This is called steep reentry without lift.¹⁷⁰ Under these circumstances, the ballistic flight path γ is close to 90 degrees, with axes X perpendicular to the flight path.

- The acceleration of gravity is constant, and decreases by only 1 percent for every 100,000-foot increase in altitude.

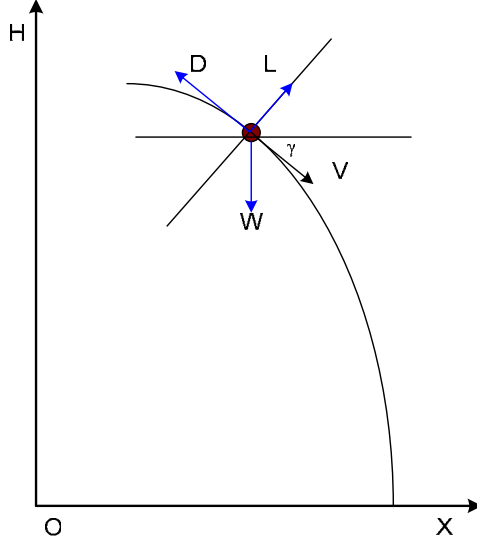


Figure 65: Ballistic entry of space tourism vehicle

As can be seen from Eq. (4-31), the centrifugal force is always less than the vehicle weight since the lift force is close to zero during ballistic entry. Therefore, a_n is smaller than 1 g during the ballistic descent, satisfying the normal direction satisfies the manned flight vehicle limitation (smaller than 4g). In contrast, the deceleration in the direction parallel to the flight path is considered as follows:

Substitute $D = \frac{\rho V^2 C_D S}{2}$ into Eq. (4-30),

$$m \frac{dV}{dt} = -\frac{\rho V^2 C_D S}{2} + mg \sin \gamma$$

$$\frac{dV}{dt} = -\frac{\rho V^2 C_D S}{2m} + g \sin \gamma \quad (4-32)$$

$$\frac{d^2V}{dt^2} = -\frac{C_D S}{2m} \left(2\rho V \frac{dV}{dt} + V^2 \frac{d\rho}{dt} \right) \quad (4-33)$$

Substitute $\frac{dV}{dt} = -\frac{\rho V^2 C_D S}{2m} + g \sin \gamma$ into Eq. (4-33), then

$$\frac{d^2V}{dt^2} = -\frac{C_D S}{2m} \left(2\rho V \left(-\frac{\rho V^2 C_D S}{2m} + g \sin \gamma \right) + V^2 \frac{d\rho}{dt} \right) \quad (4-34)$$

Setting Eq. (4-34) equal to zero to find the flight condition at maximum deceleration dV/dt :

$$\begin{aligned} -\frac{C_D S}{2m} \left(2\rho V \left(-\frac{\rho V^2 C_D S}{2m} + g \sin \gamma \right) + V^2 \frac{d\rho}{dt} \right) &= 0 \\ 2\rho V \left(-\frac{\rho V^2 C_D S}{2m} + g \sin \gamma \right) + V^2 \frac{d\rho}{dt} &= 0 \end{aligned} \quad (4-35)$$

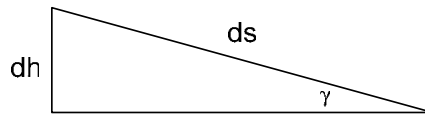
Recall that the exponential model atmosphere equation^{38,86,174} is

$$\frac{\rho}{\rho_0} = e^{-g_0 h / RT} = e^{-Zh} \quad (4-36)$$

where $z = g_0 / RT$. This atmosphere model is reasonably accurate compared to the actual atmosphere data and was used in early NASA studies of reentry vehicles^{155,160}. The time rate change of density is

$$\frac{d\rho}{dt} = \rho_0 e^{-Zh} \left(-Z \frac{dh}{dt} \right) = -Z\rho \frac{dh}{dt} \quad (4-37)$$

From the geometric diagram shown in the Figure below, we obtain



$$\frac{dh}{dt} = -\frac{ds}{dt} \sin \gamma = -V \sin \gamma$$

Therefore, we have $\frac{d\rho}{dt} = Z\rho V \sin \gamma$ and substituting into Eq. (4-35):

$$2\rho V \left(-\frac{\rho V^2 C_D S}{2m} + g \sin \gamma \right) + V^2 (Z \rho V \sin \gamma) = 0$$

$$\rho = \frac{m}{C_D S} \left(\frac{2g \sin \gamma}{V^2} + Z \sin \gamma \right) \quad (4-38)$$

The above equation shows the value of the atmospheric density at the point of maximum deceleration. Substituting into Eq. (4-34):

$$\left. \frac{dV}{dt} \right|_{Max} = -\frac{V^2 C_D S}{2m} \frac{m}{C_D S} \left(\frac{2g \sin \gamma}{V^2} + Z \sin \gamma \right) + g \sin \gamma$$

$$\left. \frac{dV}{dt} \right|_{Max} = -\frac{1}{2} V^2 Z \sin \gamma \quad (4-39)$$

(2) Gliding Back:

Based on several entry performance studies in References 175, 176, 177, and 178, a typical ground path of the entry vehicle' flight profile can be drawn, see Figure 66. Two design parameters (cross range and down range) of the space access vehicle can be obtained in this ground plane coordinate. Three orthogonal axes (X, Y, H) were chosen along the vehicle body axes at the designed maneuver point. The origin was at the mass center of the vehicle.

- X is the down range in the ground plane along the vehicle flight direction
- Y is the cross range in the ground plane and it is normal to the vehicle flight direction
- H is the vertical axis normal to the ground plane.

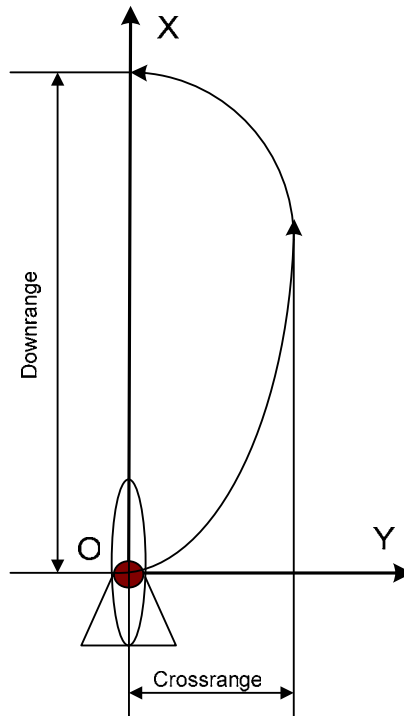


Figure 66: Ground flight path of space tourism vehicle

Figure 67 shows a suborbital tourism vehicle steadily gliding at a small flight path angle in the vertical plane. X is the down range and H is the altitude.

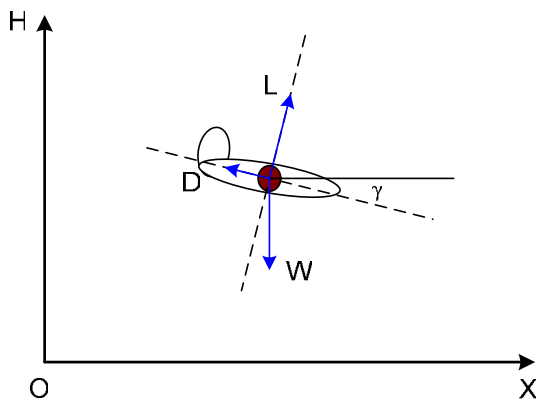


Figure 67: Gliding of space tourism vehicle.

The general equations of motion for the glide are:

$$\frac{dx}{dt} = V \cos \gamma$$

$$\frac{dH}{dt} = V \sin \gamma$$

$$m \frac{dV}{dt} = -D + W \sin \gamma$$

$$mV \frac{d\gamma}{dt} = L - W \cos \gamma$$

In the steady glide back phase, the flight path angle is small, so that

$$\cos \gamma = 1.0 \text{ and } \sin \gamma = \gamma$$

Also, during the steady glide flight, both speed and flight path angle vary slowly. The vehicle glides at low angle of attack. Hence, the inertial terms dV/dt and $d\gamma/dt$ are negligible. Therefore, the general equations are reduced to:

$$\frac{dx}{dt} = V \quad (4-40)$$

$$\frac{dH}{dt} = V\gamma \quad (4-41)$$

$$D = -W\gamma \quad (4-42)$$

$$L = W \quad (4-43)$$

Dividing Eq. (4-42) by Eq. (4-43), we have

$$-\gamma = \frac{D}{L}$$

Dividing Eq. (4-40) by Eq. (4-41), we have

$$\frac{dx}{dH} = \frac{1}{\gamma} = -\frac{L}{D} \quad (4-44)$$

As can be seen in Eq. (4-44), the down range of the suborbital vehicle is determined by the glide ratio (L/D). As shown in References 105 and 161, the generic winged orbital vehicle L/D is approximately 4 to 7 during the glide phase. In order to obtain the same down range (40 miles), the vehicle is required to glide from an altitude of at least 10 miles above the ground. There is usually a distance between the vehicle launch point and the return terminal (e.g., SpaceShipOne's was around 25 nm), and this constraint needs to be considered in defining the vehicle's design space. Up to this point, the major equations of motion have been derived and will be used for the development of the reentry sub-synthesis design methodology and computer programs.

C. Design Synthesis Process

Figure 68 shows the sub-synthesis design process for the conceptual design of suborbital space tourism vehicles during the reentry phase. The process starts with a baseline vehicle and suborbital space tourism mission requirements. The mission profile provides the payload information for the mass properties module, the altitude, and down range information required by the performance module. After obtaining the geometry data from the baseline vehicle, the mass properties module inputs the vehicle takeoff gross weight obtained from the sub-synthesis design analysis in the ascent phase. Meanwhile, design constraints are identified at the early design process and entered into the optimization module. During the activity to synthesize the flight vehicle, the performance module communicates with the atmosphere module, aerodynamics module, and optimization module to locate a feasible descent path under the specified design constraints. Finally, all the design requirements for the space tourism mission are checked

and, if necessary, iterated to arrive at efficient aerodynamic characteristics and a minimum vehicle weight. At this point, the vehicle design space for the reentry phase can be defined. It provides performance data for further design studies.

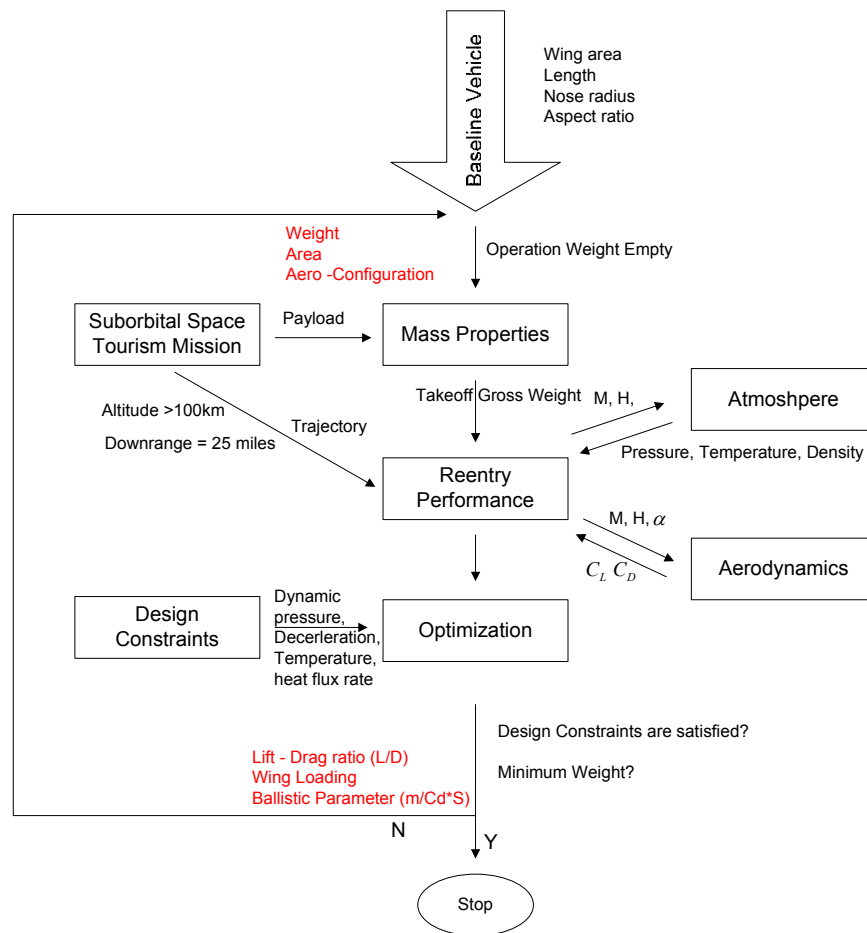


Figure 68: Design synthesis process for re-entry phase of suborbital space tourism vehicle

(1) Program Organization: A program **SAV_REENTRY** (see appendix G) was developed to implement the above design synthesis methodology. The program was developed in the MS Excel PC environment. This simple, integrated computer program is capable of demonstrating the vehicle's flight readiness through suborbital reentry. The

variation of the main design parameters throughout the trajectory flight path was visualized. In accordance with the particular characteristics of the CD phase, emphasis was placed on overall simplicity and minimum data input requirements. All basic equations used to mathematically model the atmosphere, aerodynamics, and performance, were kept as simple as possible to ensure that the key design parameters involved are evaluated quickly and efficiently.

(2) Reentry Sub-Synthesis Design Study:

Based on the sub-synthesis design methodology and computer program, a conceptual design study for typical ballistic entry of a suborbital HTHL vehicle was been performed to identify the design space of the vehicle. The variation of vehicle deceleration with altitude is shown in Figure 69. In the early portion of ballistic reentry, the atmospheric density is very low and the vehicle is constantly accelerated by gravity g . The speed increases. As the density increases rapidly, drag becomes significant, and the vehicle starts to decelerate. Although, the velocity decreases, at this stage, from Eq. (4-32), the increase in density is much larger than the decrease in velocity. The vehicle continues to decelerate until it achieves its maximum deceleration value. Then, the decrease of velocity overcomes the increase in density. As a consequence, the deceleration decreases in magnitude. Figure 70 shows the variation of velocity with altitude for ballistic entry.

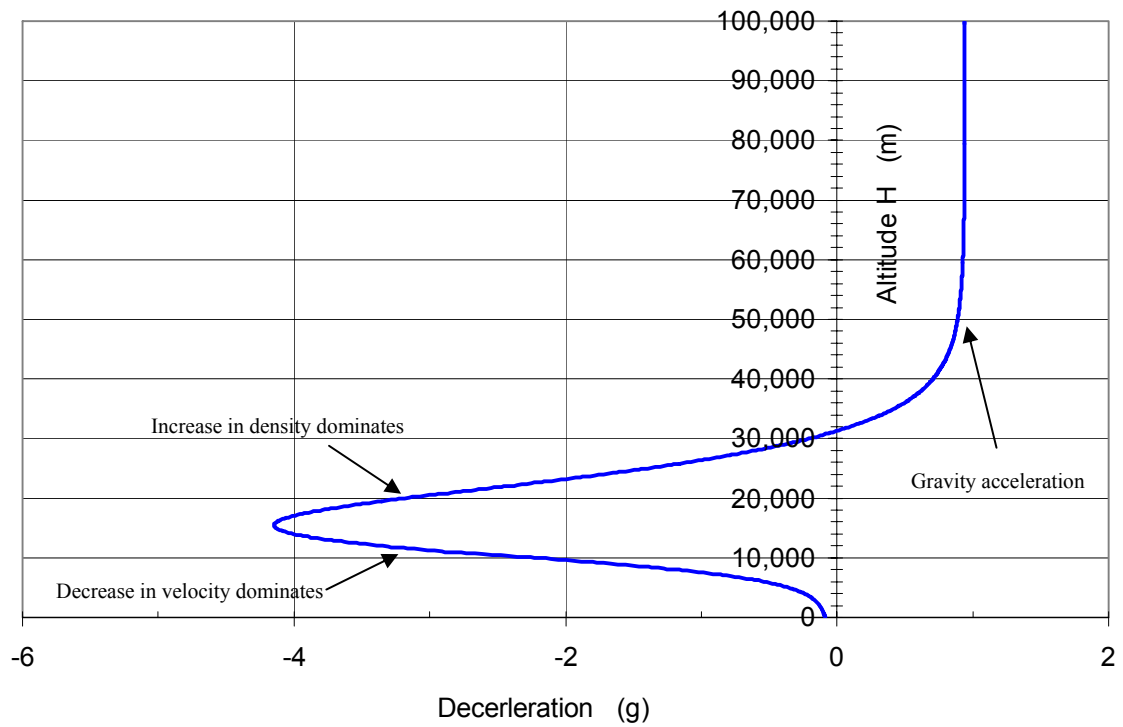


Figure 69: Variation of deceleration with altitude for ballistic entry of suborbital vehicle

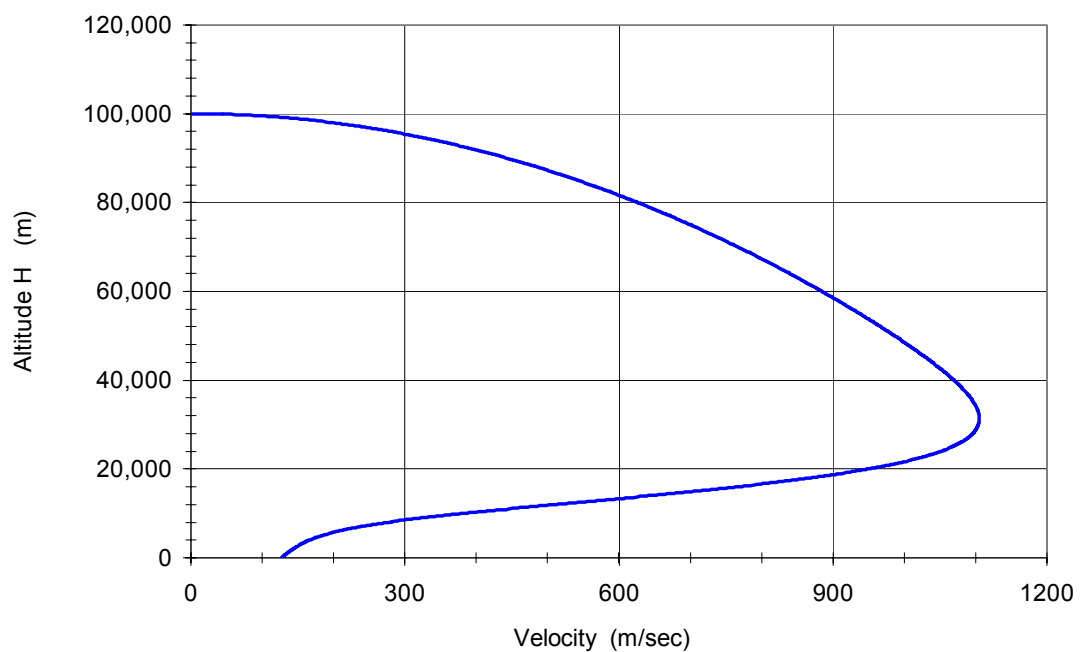


Figure 70: Variation of velocity with altitude for ballistic entry of suborbital vehicle

As can be seen in Eq. (4-32), the vehicle deceleration rate is determined by the flight path, dynamic pressure, altitude and a term $m/(C_D*S)$, called ballistic parameter. Among these, the ballistic parameter shows several important design aspects for the suborbital entry vehicle. It includes the conceptual design information related to vehicle weight, cross sectional area, and aerodynamic characteristics. Figure 71 presents a typical L/D and ballistic parameter for a range of generic configurations. As can be seen in this figure, a winged glider configuration (like SpaceShipOne) has a higher L/D ratio and a higher ballistic coefficient based on cross sectional area. Note that the angle of attack during suborbital vehicle reentry also changes the value of C_D*S in the ballistic coefficient.

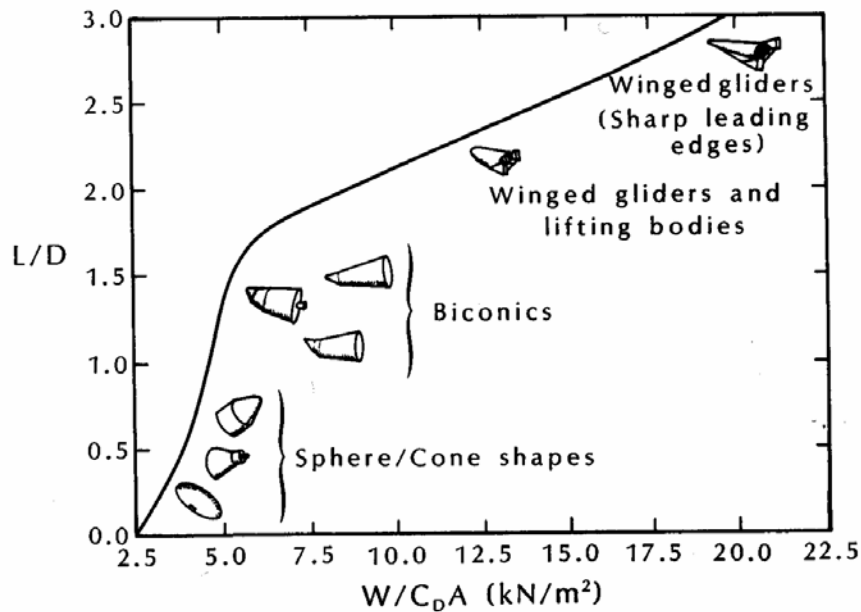


Figure 71: Lift/drag ratios and ballistic coefficient values for typical lifting vehicles ¹⁷⁹

Figure 72 shows the variation of deceleration with altitude for different flight path angles. As can be seen, the magnitude of maximum deceleration increases as the flight

path angle increases. Note that the effect of the angle of attack is difficult to quantify individually; in our study its effect was considered and included in the generic ballistic parameter. Therefore, the maximum deceleration of the suborbital vehicle can be adjusted by the flight path angle.

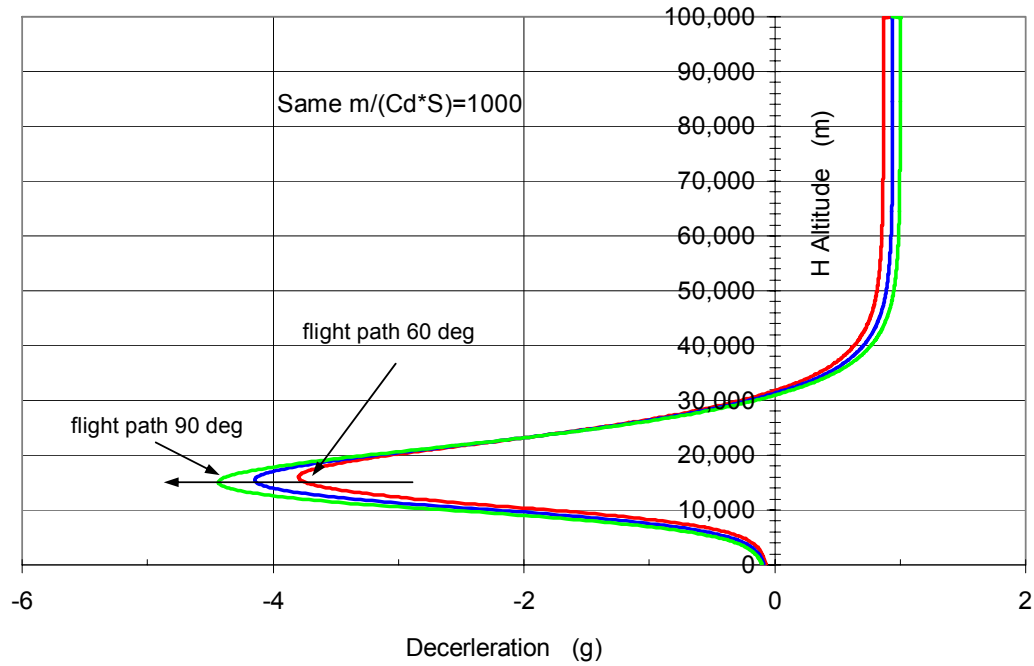


Figure 72: Variation of deceleration with altitude for different flight paths

In Figure 73, the variation of deceleration with altitude for different values of the ballistic parameter $m/(C_D \cdot S)$ is presented. As can be seen, the lower the ballistic parameter, the higher the altitude where the vehicle obtains its maximum deceleration. The maximum deceleration of SAVs with lower ballistic parameter is less than that of SAVs with higher ballistic parameter. Figure 74 shows the variation of velocity with altitude for different values of the ballistic parameters $m/(C_D \cdot S)$.

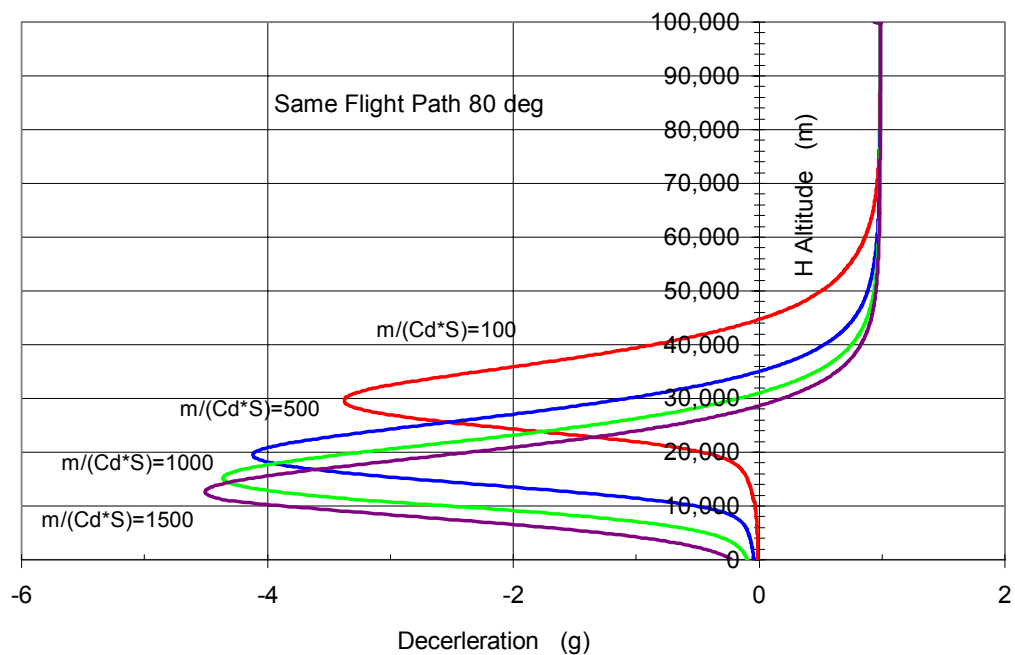


Figure 73: Variation of deceleration with altitude for different ballistic parameter $m/(C_D \cdot S)$

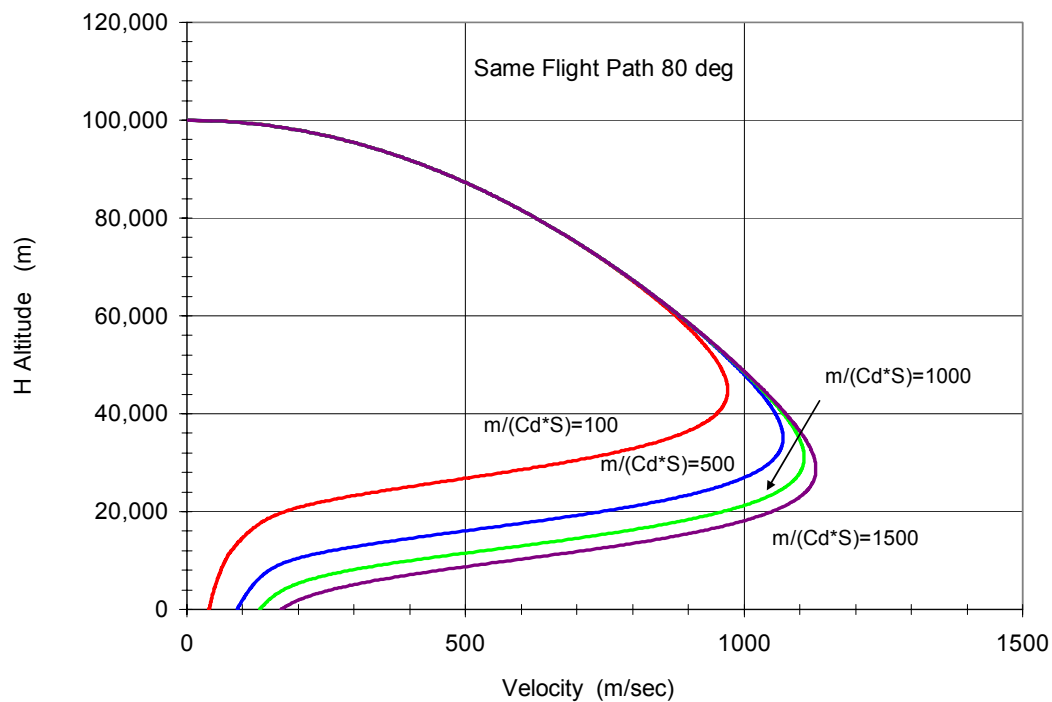


Figure 74: Variation of velocity with altitude for different ballistic parameter $m/(C_D \cdot S)$

The design constraints described in Chapter 4.3.3.A were accounted for in the sub-synthesis computer program and are shown in Figure 75. As can be seen, the brown lines represent the dynamic pressure constraints, 500 psf, 1000 psf, and 2000 psf, respectively. The stagnation temperature constraints (600° F and 800° F) are indicated with orange lines. The convective heat rates, 50 Btu/ft²/s and 100 Btu/ft²/s, are shown in the lower right hand corner.

Based on the information provided in Figure 75, the design analysis of the reentry path of a suborbital vehicle can be performed. As shown in Appendix F, the ballistic parameter for SpaceShipOne is estimated around 1040 kg/m². The value of $m/(C_D * S)$ for the Shuttle Orbiter is around 700 kg/m² at high speeds.¹⁸⁰ Based on Figure 75, an entry flight path can be determined with the consideration of related design constraints. The suborbital vehicle initially enters the atmosphere at relatively high angle of attack with relatively high ballistic coefficient until it reaches a design constraint (for example, stagnation temperature is 600° F). Then, it starts to rotate its nose down to decrease the angle of attack and glides back to the terminal area. It can be seen that this transition altitude for a SpaceShipOne type vehicle is around 10 miles. Data from the first flight of SpaceShipOne show that the altitude at which SpaceShipOne started to glide was around 57,000 ft (10 miles).^{95,96} Also, since the glide ratio (L/D) of SpaceShipOne is around 7, from Eq. (4-44), the cross range (25 miles in its first flight) can easily be achieved from an altitude of above 4 miles. This design analysis matched well with the flight data of SpaceShipOne.

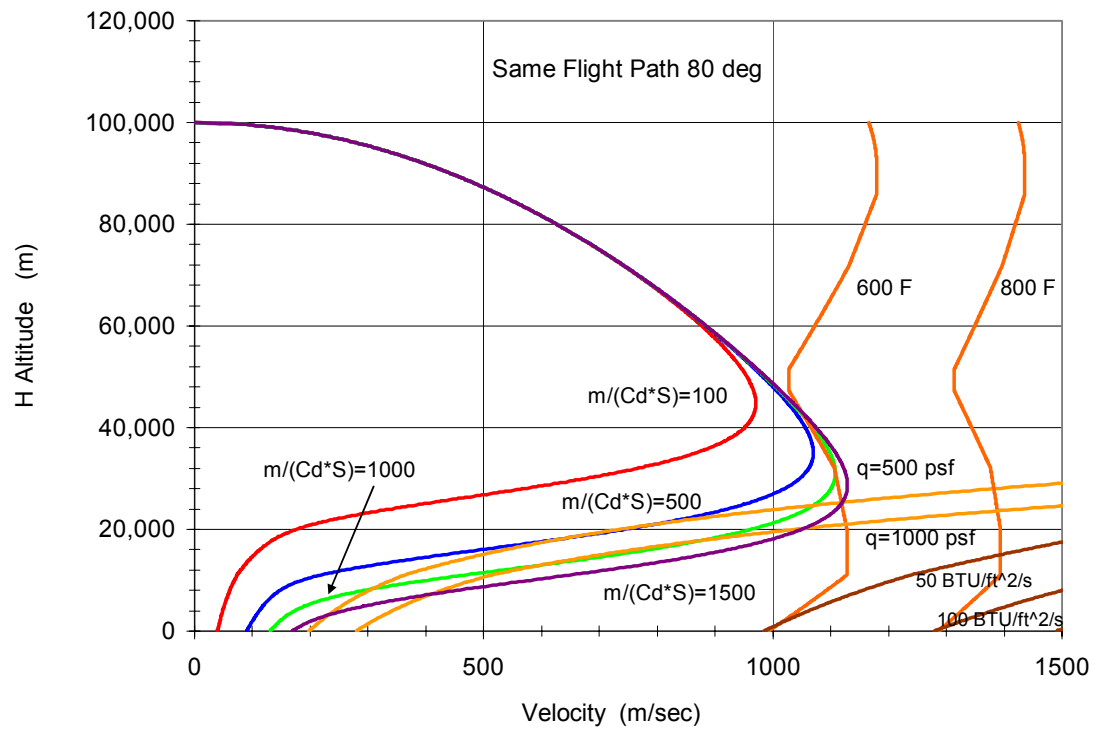


Figure 75: Design space for ballistic entry of suborbital vehicle

4.3.4 Approach and Landing

The SAV can return to the terminal area via various approach and landing alternatives: horizontal landing, vertical landing, and parachute landing at different designed landing sites. Recall that the horizontal takeoff and horizontal landing (HTHL) space access vehicle (SAV) has the most comprehensive mission profile, thus, it has been selected as the baseline model for the current HTHL design methodology. Also, since the operational mode of future SAVs requires to take off and landing at existing conventional airports, the development of a sub-synthesis approach and landing design module should focus on the horizontal landing.

During the approach and landing phase, the SAV initially glides at a certain flight path angle straight toward the landing site. For example, the Space Shuttle Orbiter¹⁵⁴ starts to glide at 10,000-ft altitude with a 17 degree flight path angle. Usually, at this moment, the space vehicle has a relative high sink rate (166 ft/s for the Shuttle Orbiter). If the vehicle carries this high sink rate all the way to the landing site, the impact force will be unacceptable to the vehicle's landing gear and structure. Therefore, the flight path needs to curve upward, "flare", to reduce the vertical component of velocity to a reasonable level. Generally, it is desirable for commercial aircraft to have a vertical component of velocity less than 0.5 m/s when the main landing gear wheels touch the ground.¹³¹ The final phase of the landing is the ground deceleration run of the vehicle from touch down to a complete stop. The ground run distance is constrained by the runway length.

In general, space vehicles are typified by high approach and landing speeds, low lift-to-drag ratios, and highly swept wings. All of these characteristics depreciate their approach and landing qualities. There are factors which determine the landing performance of space vehicle, such as ^{18,131,132,133}

- Landing weight
- Approach speed, touchdown speed
- Deceleration method (brakes, thrust reversers, drag chutes, wheel brakes, arresting system, crash barriers, etc.)
- Flying qualities of aircraft (lift to drag ratio, etc.)
- Pilot technique
- Ground conditions.

Since the landing speed of a space vehicle is usually much higher than that of commercial aircraft (e.g., the landing speed of the Space Shuttle Orbiter is around 23.7% higher compared to the supersonic commercial aircraft Concorde), a longer runway is required or other deceleration devices are required (drag chutes). Here, two categories of landing performance were investigated to show the different landing requirements during the conceptual design phase of space vehicles. One landing performance analysis was based on experimental space vehicles, the other was for FAR certified space vehicles.

(1) Experimental Vehicle Landing: Most SAVs are currently and have been designed and operated under the category of experimental vehicles, such as the Space Shuttle, X-15, X-24, etc. The landing distance requirement of experimental vehicles is that the vehicle has

to land (from touch down to stop) within the available runway length. Figure 76 shows a typical landing of the Space Shuttle Orbiter.¹⁵⁴

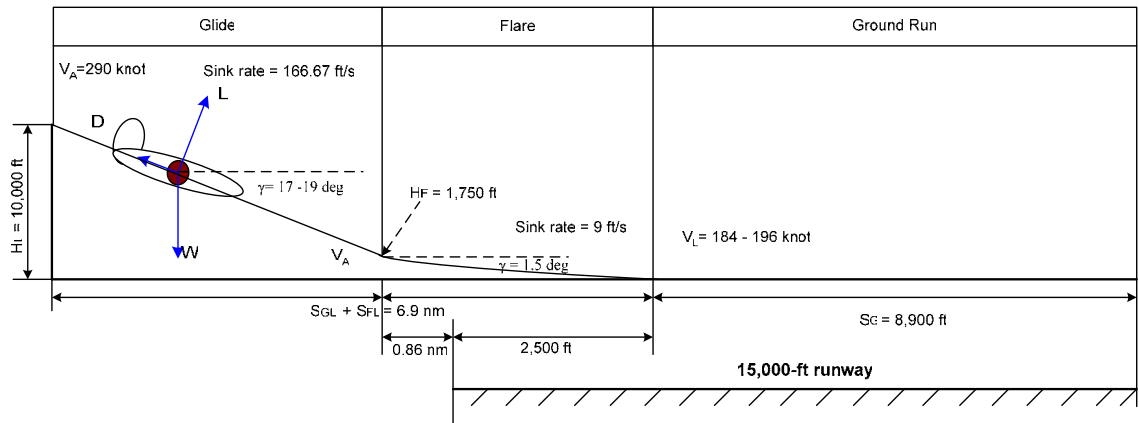


Figure 76: Approach and landing of the Space Shuttle.

(2) FAR Certified Vehicle Landing: Most space vehicles usually weight more than 12,500 lb; thus, they are categorized according to FAR rules as large transports. Therefore, future space commercial tourism SAVs may have to comply with airworthiness certification regulations like FAR 25 or to the reference landing distance specified by the Joint Airworthiness Authority in JAR (BB)-25.125. Figure 77 shows the FAR landing requirement, which is comprised of two segments: (a) the air-run from a height of 50 ft to the surface, and (b) the ground deceleration from touchdown speed to a stop. The FAR landing field length is defined as *the actual distance of vehicle approaching from a 50-ft height to a full stop increased by the factor 67%*.¹³³ This safety factor is included to account for variations in pilot technique and other conditions beyond the control of the FAA.^{130,132} Also, according to FAR Part 25, the velocity at a height of 50 ft (V_{50}) must be at least 1.3 times the stall speed (V_s). V_L is the landing or touchdown speed and is usually about 1.25 times V_s or 1.15 times V_s .¹³³

If the space vehicle performs a powered landing, the FAR ‘missed approach’ requirement was to be considered. The missed approach is a special circumstance for an aircraft landing. At this stage, the aircraft is on its final approach but can’t land for whatever reasons. Instead, engine thrust is increased, and the aircraft climbs to prepare for the next landing approach. Federal Air Regulations for transport-category aircraft require that the aircraft has sufficient thrust to climb under this missed approach condition. The specified climb gradients are 2.7 percent for four-engine aircraft, 2.4 percent for three-engine aircraft, and 2.1 percent for two-engine aircraft.¹³⁰

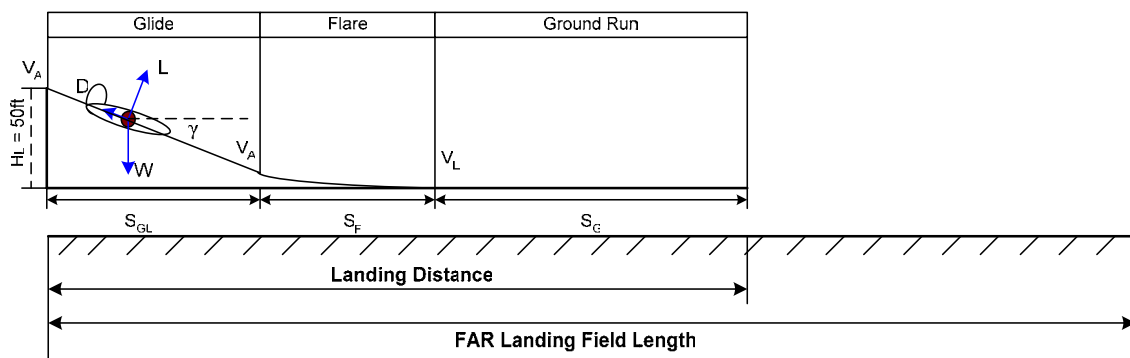


Figure 77: FAR landing field length requirements

A. Design Parameters and Design Constraints

(1) Design Parameters: There are several design methods for the landing performance analysis. Comparisons of typical methods and related design parameters are summarized in Table 24. As shown in the “*Applications*” column of Table 24, most methods can be applied to subsonic vehicles, supersonic cruiser vehicles and fighters.

Table 24: Design analysis methods for landing performance study

Methods	Description	Design Parameters	Applications
Loftin ¹³¹	Approximate Empirical method. It is a quick, simple, physical interpretable method for roughly estimating the aircraft design parameters. It is evolved from extensive study of existing aircrafts with well-known design parameters.	Approach speed wing loading density ratio approach lift coefficient engine thrust aircraft drag aircraft landing weight flight path angle lift-drag ratio FAR landing filed length	Subsonic aircraft: jet-powered cruising aircraft propeller-driven aircraft
Roskam ¹³²	Approximate Empirical method. It is based on an extensive aircraft design database in 10 years effort. It allows the rapid estimation of airplane design parameters which have influence on the landing performance. The methods can determine a range of values of wing loading, thrust loading, and maximum lift coefficient to meet certain performance requirements.	Landing Weight Thrust loading Approach Speed Wing Area Wing Aspect Ratio Wing Loading Stall Speed Maximum Required Lift Coefficient FAR landing filed length	Propeller Driven Airplane Agricultural Airplanes Business Jet Transport Jet Military Trainers Fighters Military Patrol/Bomb/Transport supersonic cruise aircraft
Torenbeek ¹⁸	Simply Analytical Approach. The landing distance is comprised of three segments: glide, flare and ground run. The equations of motion for the landing are derived from basic physics. The approximations of some coefficients are provided.	Thrust Drag Mean Deceleration Wing Loading Density Maximum Lift Coefficient Landing Weight Approach Speed Stall Speed Touchdown Speed Load Factor FAR landing filed length	Low Altitude Approach FAR certified aircraft,
Shevell ¹³³	Simply Analytical Approach. Equations of motion are derived from simple physics. Empirical charts are provided to reasonably estimate landing performance.	Thrust Drag Braking coefficient of friction Approach Speed Landing Speed Lift to Drag Ratio Flight path angle Landing Weight FAR landing filed length	Low Altitude Approach FAR certified aircraft,
Nguyen ¹³⁵ Mair and Birdsall ¹³⁶	Complex analytical equations with reasonable assumptions to simplify. The landing performance can be evaluated with great accuracy.	Approach speed wing loading density ratio Braking coefficient of friction approach lift coefficient engine thrust aircraft drag aircraft landing weight flight path angle lift-drag ratio Wing Area FAR landing filed length	All types

Miele¹⁰⁷	Complex analytical equations, Solve with detail integration process, great accuracy, however the physical relationships of various parameters may sometimes tend to be obscured in the complex analysis process, also some design parameters input are not available at the conceptual design level.	Thrust Drag Landing Weight Braking coefficient of friction Angle of Attack Lift off Speed Landing Speed Deceleration Stall Lift Coefficient flight path angle Stall Speed Touchdown speed Touchdown Lift Coefficient Boundary condition FAR landing field length	All types
----------------------------	--	--	-----------

Table 24 shows that there are two main categories used in current landing performance analyses. One category consist of empirical methods (Loftin¹³¹, Roskam¹³², etc.) based on available extensive conventional aircraft databases. The other category includes analytical methods (Torenbeek¹⁸, Shevell¹³³, Nguyen¹³⁵, Miele¹⁰⁷, etc.) which analyze the landing performance via physically robust characterization. There is a trend that only complex analytical equations of motion are thought to be capable of addressing different types of vehicles including SAVs and aircraft. However, these complex formulations require input data, which are usually not available during the conceptual design (CD) phase.

Clearly, the existing limited knowledge database for SAVs makes it difficult to arrive at meaningful empirical estimations. Therefore, it is desirable to have reduced order analytical models to retain as much physical transparency of the major interacting disciplines as possible. The available modeling techniques (Torenbeek¹⁸, Shevell¹³³, Nguyen¹³⁵, Miele¹⁰⁷, etc.) have been reviewed to arrive at reduced order analytical formulations balancing between the available data and key design parameters. Overall,

the reduced order models for the approach and landing phase were based on complex analytical equations with simplifying assumptions, such as steady glide or a circular flare.

The following investigates the key design parameters for use in the generic landing design methodology. Any landing design methodology should strike a balance between landing distance requirements and landing capability of the vehicle. For this purpose, the landing airport conditions (altitude, landing field length) are required before any landing analysis can be performed. The analytical equations (Torenbeek¹⁸, Shevell¹³³, Nguyen¹³⁵, Miele¹⁰⁷, etc.) show that the landing field length is determined primarily by the approach velocity, which, in turn, is governed by various design parameters: wing area, landing weight, and maximum landing lift coefficient. All of these parameters are closely coupled with the aerodynamic characteristics and thrust available of the vehicle. Therefore, the aerodynamic characteristics (lift coefficient and drag coefficient) and thrust range of the SAV are required as input for the landing performance methodology. Table 25 summarizes the key design parameters needed for the reduced order model. Based on these key design parameters, the landing design methodology is capable of determining the output wing loading necessary to meet the required landing field length for a given approach lift coefficient. These key design parameters are presented in Table 25; they allow the designer to understand the key design drivers during the landing performance analysis.

Table 25: Design parameters required for reduced order model of landing design methodology

Parameters	Notation	Value	Input/Output
Airport Condition: Altitude	H	0	Input
Airport Condition: Density	ρ	0.002377 slugs/ft ³	Input
Landing Field Length	S_L	5000 – 8000 ft	Input
Landing Lift Coefficient	$C_{L,A}$	1.2 – 1.8	Input variable
Landing AOA	α	15 deg	Input variable
Lift to Drag ratio	L/D	4 – 8	Input variable
Drag	D		Input
Braking Coefficient	μ	0.4 – 0.6 (Dry concrete)	Input
Stall Speed	V_s		Output
Wing Area	S		Output
Thrust	T	0	Input
Landing Weight	W_L	8000 lb	Output
Thrust to Weight	T_0/W_L		Output
Wing Loading	W_L/S		Output

(2) Design Constraints: Operational constraints imposed onto the vehicle design throughout the flight trajectory have to be addressed early during the conceptual design phase. The landing of a suborbital space vehicle is usually confined to the landing distance requirement for both, experimental and FAR 25 vehicles, in case they require FAA certification. For experimental SAVs, the landing distance is the only relevant constraint. In the present study, key FAR25 design constraints relevant to the CD phase are summarized in Table 26.

Table 26: Design constraints imposed on vehicle landing requirements by FAR Part 25

Constraint Parameters		Notation	Constraint Value
Velocity	Approach Speed	V_A	$> 1.3 V_s$
	Touchdown Speed	V_{TD}	$> 1.15 V_s$
Field Length Definition	Landing Distance over 50 ft obstacle divided by 0.6	S_L	5000 – 8000 ft or defined by the airport condition
	Two-engine aircraft	γ	2.1
Climb gradients for Missed Approach	Three-engine aircraft	γ	2.4
	Four-engine aircraft	γ	2.7

B. Equations of Motion

A typical power-off approach and landing trajectory of a space vehicle is presented in Figure 78. It includes three flight phases: glide, flare, and ground run. The equations of motion for the SAV landing performance are derived in the following sections.

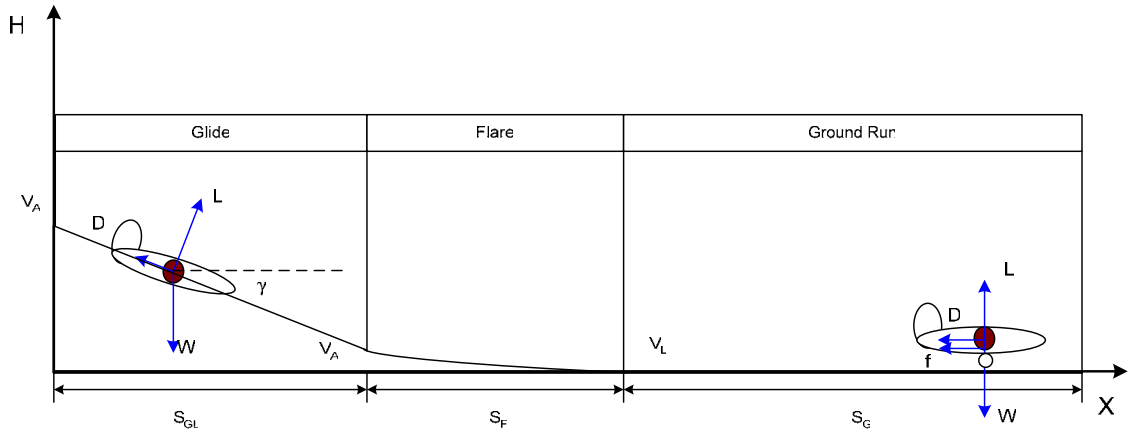


Figure 78: Typical landing trajectory of space vehicles.

(1) Glide: The general equations of motion of the gliding vehicle were derived in Reference 107 and 135. They are

$$\frac{dx}{dt} = V \cos \gamma \quad (4-45)$$

$$\frac{dH}{dt} = V \sin \gamma \quad (4-46)$$

$$m \frac{dV}{dt} = -D + W \sin \gamma \quad (4-47)$$

$$mV \frac{d\gamma}{dt} = L - W \cos \gamma \quad (4-48)$$

where X denotes the longitudinal distance, H the altitude, V the speed, γ the flight path angle, W the weight, D the drag, L the lift, and m the mass.

(2) Flare: In the flaring phase, the space vehicle is steadily gliding at a small flight path angle. As shown in Reference 154, the flaring path angle of the Space Shuttle Orbiter is 1.5 degrees, and commercial aircrafts glide at less than 3 degrees. Since the flight path angle is small.

$$\cos \gamma = 1.0$$

$$\sin \gamma = \gamma$$

and both speed and flight path angle vary slowly during the steady glide flight. Hence, the time derivative terms dV/dt and $d\gamma/dt$ are negligible. Therefore, the general equations for the glide phase are reduced to

$$\frac{dx}{dt} = V \quad (4-49)$$

$$\frac{dH}{dt} = V\gamma \quad (4-50)$$

$$D = -W\gamma \quad (4-51)$$

$$L = W \quad (4-52)$$

Dividing Eq. (4-51) by Eq. (4-52), we have

$$-\gamma = \frac{D}{L}$$

Dividing Eq. (4-49) by Eq. (4-50), we have

$$\frac{dx}{dH} = \frac{1}{\gamma} = -\frac{L}{D} \quad (4-53)$$

Therefore, the flare distance S_F is determined by the lift-to-drag ratio and the altitude where the flare starts.

$$S_F = H_F \cdot \left(\frac{L}{D} \right)_F \quad (4-54)$$

(3) Ground Run: The equations of motion parallel to the flight path direction are:

$$\begin{aligned} -f - D &= W_L/g \cdot a_G \\ -\mu(W_L - L) - D &= W_L/g \cdot a_G \end{aligned} \quad (4-55)$$

where f is the friction force on the runway, μ is the friction coefficient, W_L is the landing weight, D is the drag force, L is the lift force, m the mass, and a_G is the average deceleration. The ground deceleration distance is

$$\begin{aligned} S_G &= \frac{V_L^2}{2a_G} \\ a_G &= \frac{\mu(W_L - L) + D}{W_L/g} \end{aligned} \quad (4-56)$$

At this point, the generic equations of motion applicable for both experimental and FAR certified vehicle have been derived and ready for the development of the sub-synthesis design methodology for the approach and landing phase. As shown in Figure 77, the FAR landing field length considers the actual landing distance from a 50-ft height. It is reasonable to make some assumptions to simplify the approach and landing equations applicable to FAR-certified space vehicles. The glide from 50 ft can be approximate as a steady-state glide distance with small glide angle. The landing flare may be approximately as a circular arc as shown in Figure 79. The vehicle is flown with a constant incremental load factor Δn .

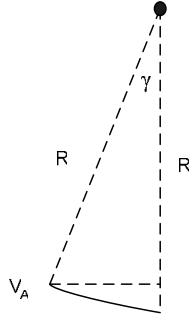


Figure 79: Landing flare approximation as circular arc

The first order approximation for the landing flare distance is derived as

$$L - W_L = \frac{W_L}{g} \frac{V_A^2}{R}$$

where V_A is the approach speed, usually about 1.3 times V_s .^{18,132}

Substituting $L = nW_L$,

$$nW_L - W_L = \frac{W_L}{g} \frac{V_A^2}{R}$$

$$R = \frac{V_A^2}{g(n-1)} = \frac{V_A^2}{g\Delta n}$$

Then, the landing flare distance is obtained as

$$S_F = R \sin \gamma = R \frac{D}{W_L} = \frac{V_A^2}{g\Delta n} \frac{D}{W_L} \quad (4-57)$$

Some coefficients presented in the above equations of motion have been estimated by

Torenbeek¹⁸ and Roskam.¹³² They are:

$$\left(\frac{D}{W_L} \right) = 0.05$$

$$\Delta n = 0.1$$

$$a_G = 0.4 - 0.5$$

(4) Missed Approach: An equation of motion is needed to estimate the thrust required to meet the FAR climb gradient requirement. This is a simple equation for the forces along the flight path:

$$T = D + W \sin \gamma$$

$$\frac{T}{W} = \frac{1}{L/D} + \gamma$$

C. Design Synthesis Process

Figure 80 shows the sub-synthesis design process for the conceptual design of a HTHL SAV during the landing phase. This process starts with a baseline vehicle and suborbital space tourism mission requirement. The mission profile provides the payload information for the mass properties module, the altitude, and airport landing information required by the performance module. After obtaining the geometry data from the baseline vehicle, the mass properties module inputs the landing weight obtained from the sub-synthesis design analysis for the reentry phase. Meanwhile, design constraints are identified early on in the design process and called into the optimization module. During the flight vehicle synthesis, the performance module communicates with the atmosphere module, aerodynamics module, propulsion (if landing with power) module, and optimization module to determine a feasible landing flight path under the specified design constraints. Finally, all the design requirements for the space tourism mission are checked and if necessary, the configuration concept can be iterated to arrive at efficient aerodynamic characteristics, wing loading, thrust to weight ratio, and a minimum vehicle weight. At this point, the vehicle design space for the landing phase can be defined. It will provide performance data for further design studies.

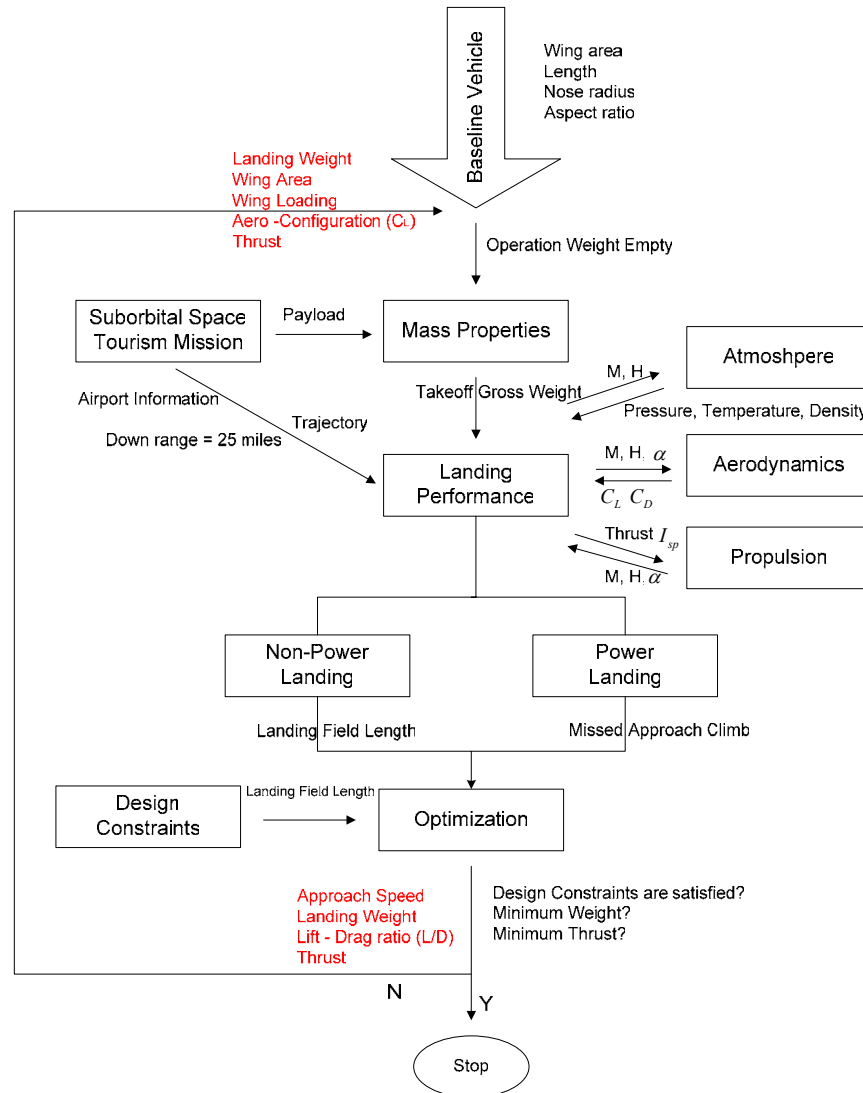


Figure 80: Design synthesis process for landing phase of a HTHL SAV.

(1) Program Organization: Two programs **SAV_LANDE** and **SAV_LANDA** (see Appendix G) were developed based on empirical and analytical methods to implement the above design synthesis methodology. The programs were developed in the MS Excel PC environment. These simple integrated computer programs are capable of demonstrating the vehicle's flight readiness throughout the approach and landing phases. The variation of the main design parameters throughout the landing flight path is

visualized. In accordance with the particular characteristics of the CD phase, emphasis were placed on overall simplicity and minimum data input requirements. All basic equations used to mathematically model the atmosphere, aerodynamics, performance, and propulsion, were kept as simple as possible to ensure that the key design parameters involved can be evaluated quickly and efficiently.

(2) Landing Sub-Synthesis Design Study: Based on the sub-synthesis design methodology and computer program, a conceptual design study representing the typical landing of a suborbital HTHL vehicle was been performed to identify the design space of the vehicle during this mission phase. Table 27 and Table 28 compare the landing performance of some selected supersonic and space access vehicles. Lifting body and winged vehicles were both included to show that the current design methodology has generic design capabilities for different SAV configurations.

Table 27: Landing performance data of some space access vehicles ^{181,182,183,184}

Parameters	Vehicle	Space shuttle Orbiter	Winged Vehicle (X-15)	Lifting body (HL-10)	Lifting body (X-24A)	Lifting body (X-24B)
Landing Field Length (ft)		10,000			Like SST	< 5000 ft
Landing Speed (knot)		171 (touchdown) 184 - 196	200 knots (Design) 200 mph – 160 mph			189.6
Landing Weight (lb)		187,000	14,600	6,000	6,360	8,500
Takeoff Weight (lb)		240,000	31,000		11,450	13,800
Landing Lift Coefficient		0.669				
Lift to Drag ratio		4.7	4.05	3.60	4.25	4.5
Wing Area (ft ²)		2690	200	160	162	330.5
Landing Wing Loading (lb/ft ²)		69.5	73	37.5	39.26	25.72
Wing Loading (lb/ft ²)			73 -170			
Lift Curve Slope (deg ⁻¹)		0.0446	0.0649	0.023	0.0239	0.0217
Aspect Ratio		2.265	2.5	1.156	0.617	1.108
Wing Swept (deg)		45 (36?)	25.6			
Landing AOA (deg)		15				

Table 28: Landing performance data of some supersonic vehicles ^{138 -153}

Parameters	Vehicle	Concorde	Tu -144	B-58	F-106	XB-70
Landing Field Length (ft)		8,800	8,530	4420 2615 (drag chute)		
Landing Speed (knot)		163	151			199 (Approach) 189 (Flare) 173 (Touchdown)
Landing Weight (lb)		245,000	250,000	63,100	26,250	290,000
Takeoff Weight (lb)		408,000	396,830	160,000	35,300	550,000
Lift to Drag ratio		4.35 (approach)		4.84 (max)	4.17 (max)	6.015 (max)
Wing Area (ft ²)		3856	4716	1364	698	6297.8
Landing Wing Loading (lb/ft ²)		63.57	53.01			
Wing Loading (lb/ft ²)		100 (max)	84.17 (max)	58.3	38.7	57.2
Approach Lift Coefficient		0.6				
Aspect Ratio		1.85	1.89	2.09	2.08	1.04
Wing Swept (deg)			76	60		51.77
W_{GT}/W_E		2.73	2.52	2.375	1.524	1.934
Landing AOA (deg)		14				7.5

The program **SAV_LANDE** (empirical method approach) was used to estimate the landing performance of different supersonic vehicles and the Space Shuttle Orbiter. The variation of wing loading (W/S) with maximum lift coefficient at different landing field length requirements is shown in Figure 81. The red points represent real data for the Space Shuttle Orbiter, Concorde, and Tu-144. It can be clearly seen that the Shuttle Orbiter requires a longer landing field length compared to both, Concorde and Tu-144 due to its high approach speed and low landing lift coefficient.

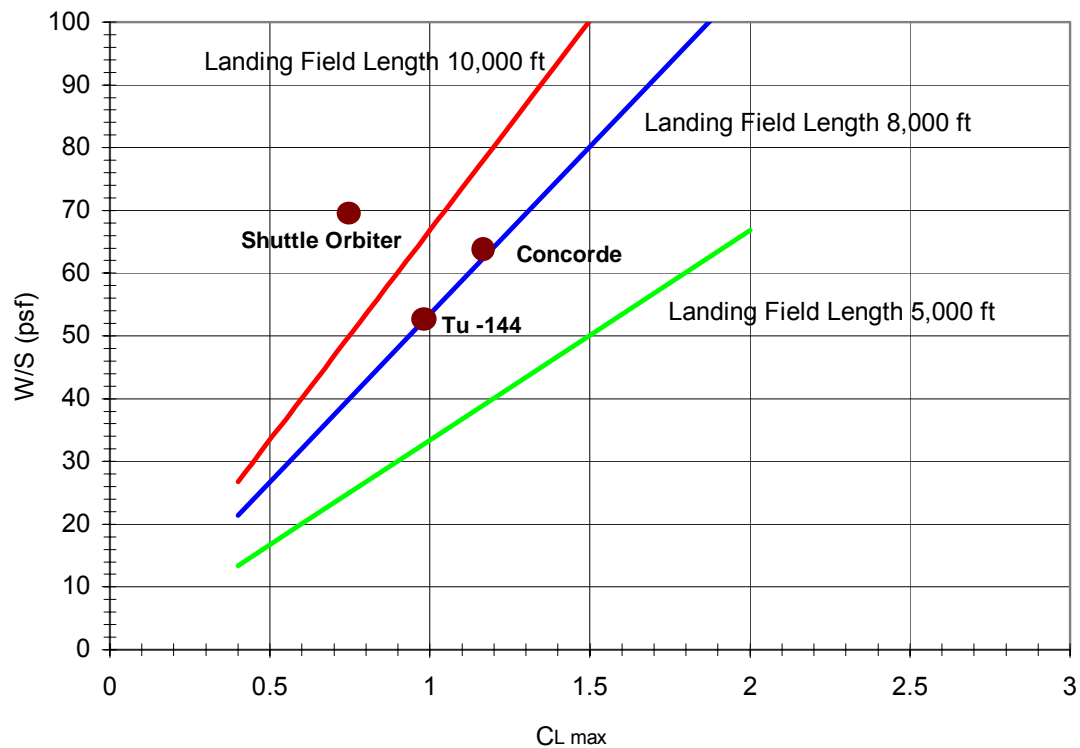


Figure 81: Wing loading vs. maximum lift coefficient

Figure 82 and Figure 83 present wing loading variation with aspect ratio based on two methods by Peckham at RAE and NASA without consideration of leading edge vortex lift. The Peckham method ⁹⁸ was developed by the Royal Aeronautical Establishment (RAE), where as the Krienes Method ⁹⁸ is applied at NASA. As seen in these two figures, without additional leading edge vortex lift, the Concorde and Tu-144 may not land at a 8000-ft runway. In comparison, Figure 84 shows the landing performance of Concorde and Tu-144 with the addition of leading edge vortex lift. It is clearly shown that vortex lift (as a high lift device) will greatly improve the landing performance of high speed vehicles.

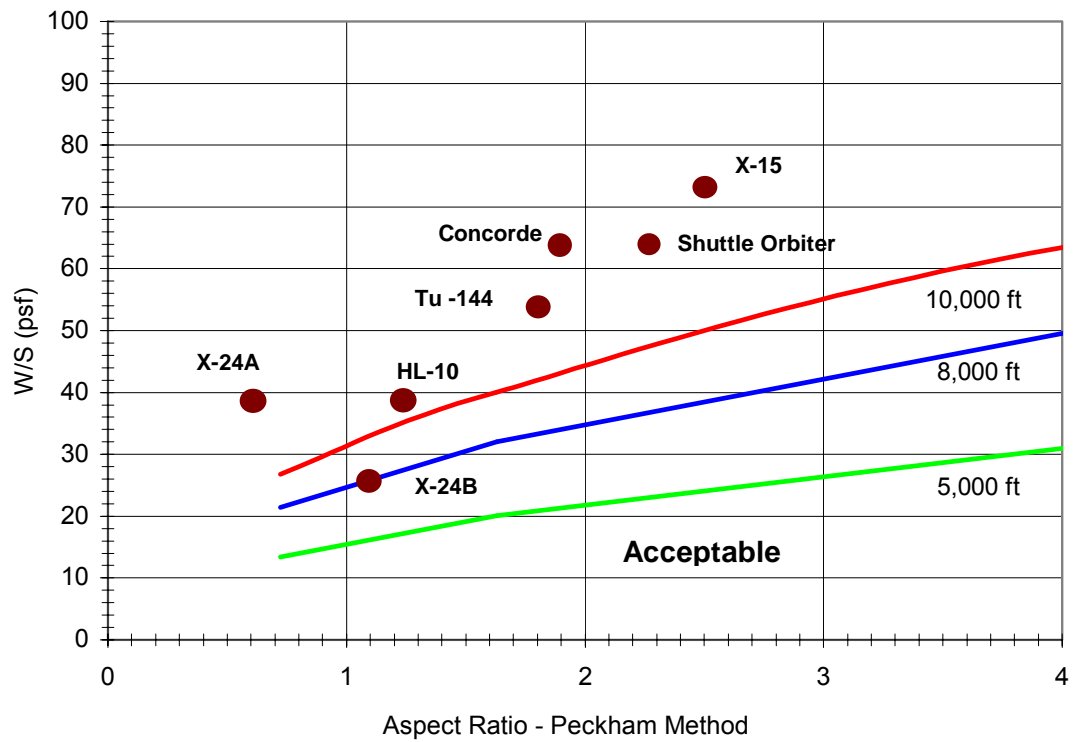


Figure 82: Wing loading vs. aspect ratio based on Peckham method

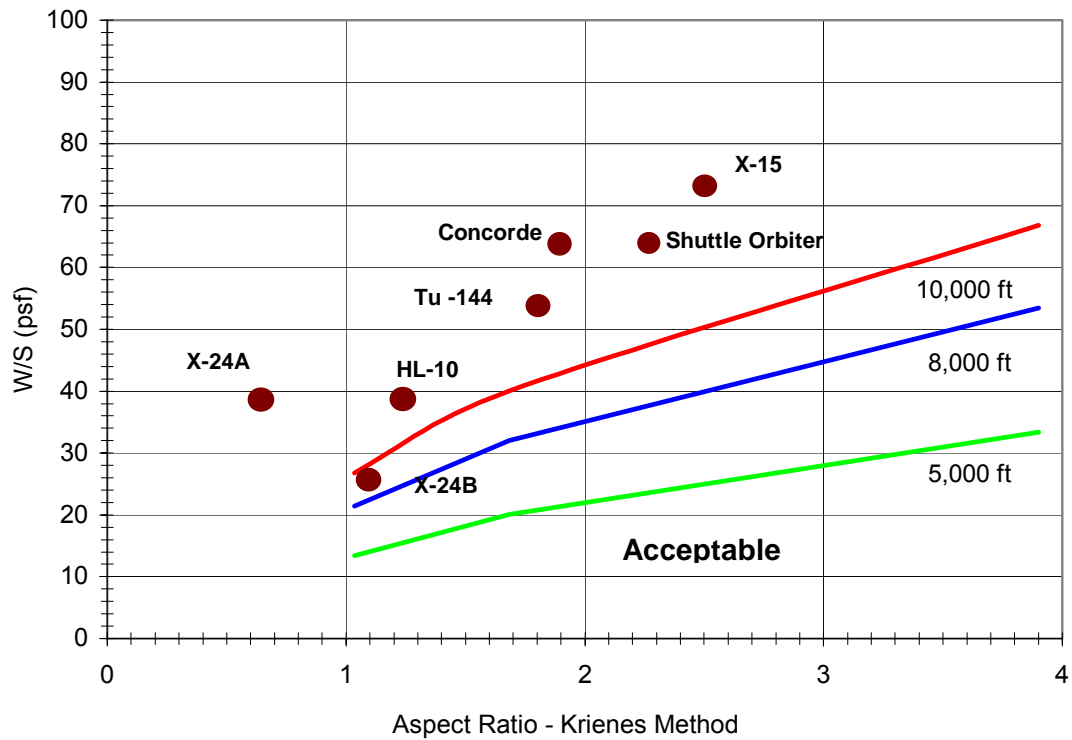


Figure 83: Wing loading vs. aspect ratio based on Krienes method

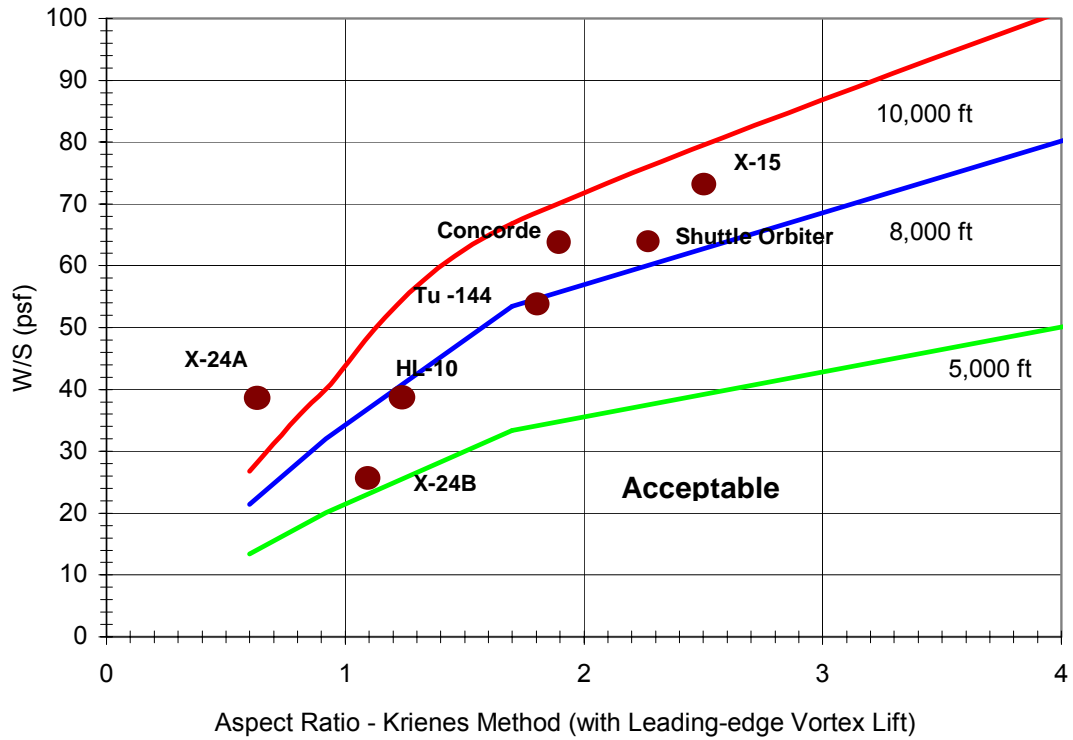


Figure 84: Wing loading vs. aspect ratio with consideration of leading edge vortex lift

Figure 85 shows the thrust to weight ratio of a SAV landing with power-on under the FAR missed approach climb gradient requirement. The lifting body requires a higher T/W due to its lower L/D .

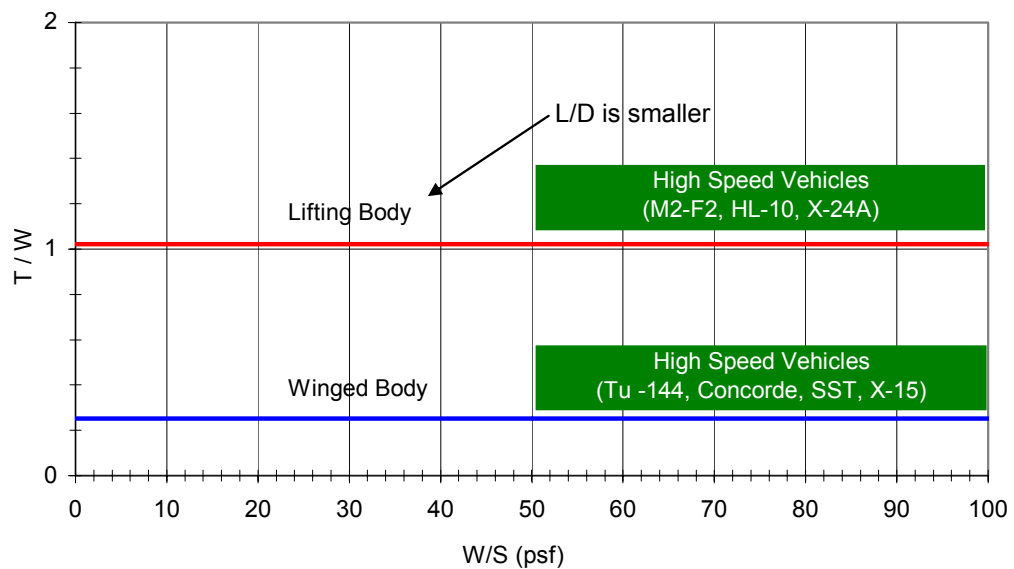


Figure 85: Thrust to weight ratio vs. wing loading

The program **SAV_LANDA** was developed based on reduced order analytical methods. It is capable of accurately estimating SAV landing performance at various flight conditions. Based on the geometry and aerodynamic data presented in Table 27, this program was applied to the design case study of the Space Shuttle Orbiter landing. Some reasonable assumptions were required for this particular case study. For example, the Space Shuttle is assumed to be initially steadily gliding at a large flight path angle back to the landing site. During the flare phase, the Space Shuttle glides at a very small flight path angle. Table 29 shows a comparison of the analytical results obtained from **SAV_LANDA** and Space Shuttle Orbiter real flight data.¹⁵⁴ The glide distance, flare distance, and ground run predicted by the program compare well with the flight test data for the Space Shuttle Orbiter. The percentage differences are -2.16% for the glide distance, 0.32% for the flare distance, and 7.07% for the ground run, respectively. For the ground run, the comparison is not as accurate due to the modeling of the ground deceleration used in this program based on empirical data for commercial aircraft. The ground deceleration coefficient can be refined if more detailed deceleration methods and experimental data for a specific vehicle are obtained.

Table 29: A comparison study of analysis results with flight data of the Space Shuttle

Parameters	Space Shuttle Data	Analytical Analysis	Flight Data	% Difference
Landing Speed	(knot)	190	190	Input
Landing Weight	(lb)	187,000	187,000	Input
Wing Area	(ft ²)	3856	3856	Input
Lift to Drag ratio		4.35 (approach)	4.35 (approach)	Input
Landing flight path angle	(deg)	17	17	Input
Program Output				
Gliding Distance	(ft)	34939	34199	-2.16
Flaring Distance	(ft)	7700	7725	0.32
Ground Run	(ft)	8271	8900	7.07
Landing Field Length from 10000 ft (ft)		50910	50825	-0.17

4.3.5 Design Space Screening and Design Convergence

As discussed in Chapter 1, flight vehicles are usually designed by bringing the respective disciplines together, each optimized to their own accord, and subsequently compromising individual disciplines as needed to ensure a converged vehicle. However, this does not ensure an optimized total vehicle—and, especially in the case of high-speed flight, many times not even a feasible vehicle.²⁰ Therefore, a system needs to be developed that brings these disciplines together and subsequently converges the entire vehicle according to its performance and overall design requirements. The lack of the ability to ensure convergence is the precise reason there are not many new design concepts carried to completion, as Torenbeek states: *“Design concepts are therefore being developed continuously, while only very few actually result in a preliminary design and subsequent development program.”*¹⁸ This section presents the development of the design convergence process capable of identifying the possible design solution space which will assure the design engineer that the final concept will meet the design requirements.

A. Design Convergence

The mathematical definition of convergence implies that the terminal value of a series approaches some limit as the number of terms increases.¹⁸⁵ In aircraft design, design convergence is a design process, which can define the needed boundaries within which a feasible design will reset in a multidisciplinary context for a given mission and flight regime. As a consequence, a converged vehicle configuration can be obtained in the conceptual design phase.

The famous aerodynamicist and aircraft designer, Dietrich Küchemann, considered design convergence as resulting in a final aircraft design solution to accomplish the mission within specified design constraints. Such design space contours for transonic, supersonic, and hypersonic configuration concepts are presented in Figure 86. He emphasizes that each specific parameter should not lead to an optimum at a single design point, but rather that all subsystems and systems should interact together to result in harmony, *“not in conflict for a set of design points and off-design conditions, and the final solution is sound and healthy.”*⁸³

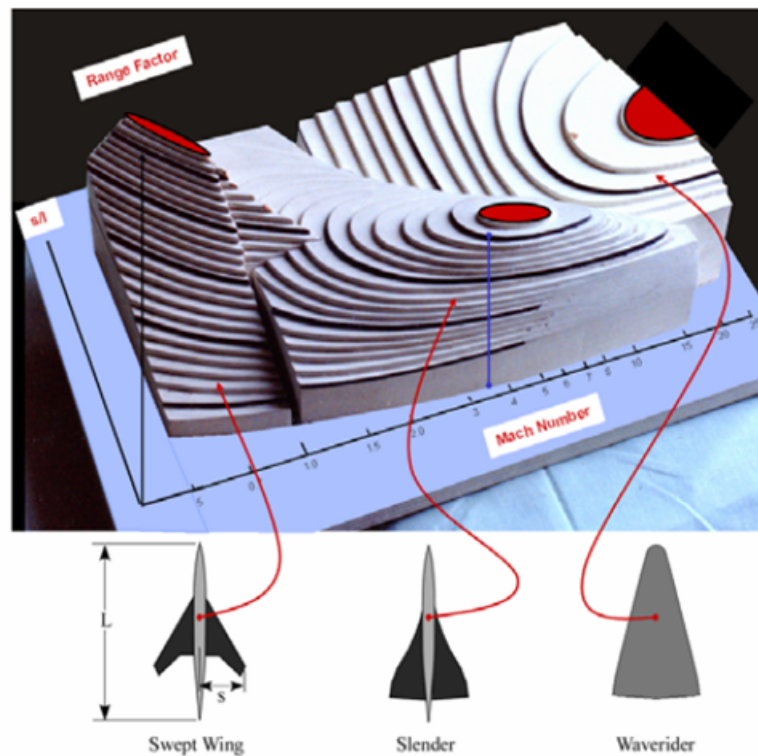


Figure 86: Design space contours of transonic, supersonic, and hypersonic configuration concepts by D Küchemann^{4,83}

In describing the design process as an iterative process, Torenbeek implies that convergence result in an aircraft that satisfies all of its design requirements

simultaneously. It is the most efficient design that could be obtained with the starting configuration selected. Torenbeek states that the iterative process of design “starts with a trial configuration which will then be analyzed and altered after comparison with the requirements. The entire cycle will then start afresh, until the result shows either that the design is not feasible or that it is reasonably well defined and may in fact be further developed with some confidence.”¹⁸ Figure 87 illustrates this design process devised by Torenbeek. Note the ‘convergence test’ built into the process, able to flag a scenario in which no improvements of the design will result in a converged vehicle, that is, one that cannot meet all the requirements simultaneously.¹⁸ This ‘convergence test’ works by indicating whether or not the improvements have moved the design closer to the required design constraints.¹⁸

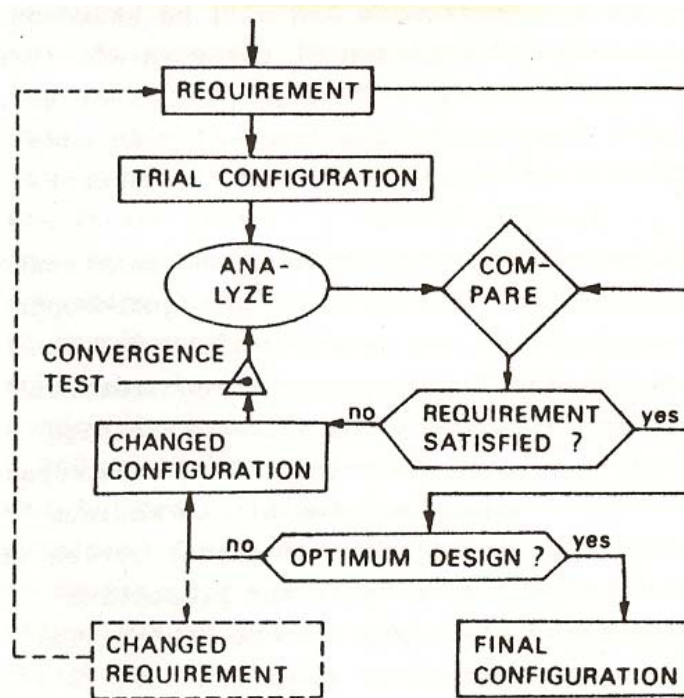


Figure 87: Torenbeek's general design procedure¹⁸

The definitions above show the true meaning of convergence: *to achieve union between all systems to ensure that a fully efficient and working vehicle will emerge as the final result.* Though there are various methods that seek to accomplish this, no clear procedures yet exist by which the design of a vehicle is guaranteed to converge.¹⁸ This is precisely the aim of developing a generic SAV design methodology: to provide a transparent design procedure that will ensure solution space convergence during the conceptual design phase. The ultimate aim is to arrive at a design standard in SAV design evolution.

B. Design Space Screening

The key in developing a generic SAV methodology that will guarantee convergence during the conceptual design phase lies in the ability to define the boundaries within which the vehicle will be able to converge. In other words, the conceptual designer must have the ability to identify the boundaries within which a vehicle can succeed. This can be accomplished by design space screening as shown in Reference 20, which forms the foundation for the three-tiered generic CD methodology. This process of screening the available design space results not only in a fully converged vehicle, but a range of vehicles which populate the solution space. The final step is to identify the particular converged design which complies with the pre-defined figure-of-merit most efficiently.

The process of design space screening incorporates the KBS^{DESIGN} system, historical and empirical information, and current technology limitations to narrow the design space.¹⁹ It narrows the design space by evaluating the past, but it also has the unique

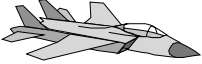
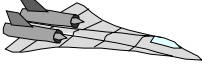




capability of evaluating the present state of the industry, an ability to ‘zone in’ on the design space that is possible for the given design requirements. This approach ultimately eliminates many design permutations, which possess no potential to converge at all, ultimately saving R&D time and cost.

A technique for identifying the solution design space, based on historical experience, key design parameters, and available industrial capability is presented in Reference 4. It is used to assess the realm of possible solutions for an initial input configuration. In this way, the design space for a particular configuration may be mapped, identifying the ‘ballpark’ design space.

One key result of the ‘*Hypersonic Convergence*’ work⁴ is the definition of a primary structure and propulsion interaction that controls the size and weight of the aircraft, an interrelation expressed with the Industrial Capability Index (*ICI*). Although *ICI* was the original emphasis for space launchers, the approach presented IS NOT limited to hypersonic aircraft only. The mass and volume relationships developed in *Hypersonic Convergence* have been successfully applied to aircraft that include the MD-80, DC-10, F-15, and to over thirty High Speed Civil Transports Phase I/II concepts. The design parameters of some configuration concepts of the HSCT Phase I/II work are presented in Table 30. *ICI* is a measure of the practicality of the vehicle under consideration, in terms of the industrial materials/fabrication/propulsion capability available. With the development of the Industrial Capability Index (*ICI*), overall technical maturity can be represented for a number of disciplines, starting with propulsion through aerodynamics, materials, manufacturing, and vehicle integration, as well as others. As a consequence,

the regions of possible design convergence will be identified prior to an extensive computational investigation. That is “*locating the possible oil field before a lot of expensive, random dry holes are drilled*”.⁴ The ability to locate the solution design space where convergence can occur is the essence of the SAV CD design methodology.

Table 30: Geometry, mass, and propulsion parameters of six reference aircraft configurations⁴

Configurations	Parameters	Concepts	τ	I_p	I_{str}	ICI	S_{plan}
		Tactical Fighter	0.080	100 lb/ft ³	3.56 lb/ft ²	22.5	825 ft ²
		Supersonic Cruise Fighter	0.070	75.0 lb/ft ³	3.50 lb/ft ²	18.8	1000 ft ²
		Supersonic Cruise Reconnaissance	0.044	56.0 lb/ft ³	3.53 lb/ft ²	15.5	2200 ft ²
		Mach 6 Interceptor	0.054	30.0 lb/ft ³	3.62 lb/ft ²	8.46	2200 ft ²
		Mach 12 Strike-Reconnaissance	0.091	11.0 lb/ft ³	3.65 lb/ft ²	3.16	2200 ft ²
		Boost-Glide Strike-Reconnaissance	0.195	4.00 lb/ft ³	3.70 lb/ft ²	1.27	2300 ft ²

The *Industry Capability Index (ICI)*, seen in Eq. (4-58), makes it possible to incorporate a specific industry standard and production capability into a new design⁴

$$ICI = \frac{I_p}{I_{str}} \quad (4-58)$$

As the availability of advanced propulsion and structural material technologies proves to be limiting in the design of space access vehicles, the *ICI* represents a ratio of the indexes of these two parameters. These indexes are based on current technology in each of these two disciplines, as seen in Eq. (4-59) and Eq. (4-60).⁴ Therefore, the higher the *ICI*—the ratio of the parameters for structural and propulsion technology—the higher the technical challenge associated.⁴

$$I_p = \frac{\rho_{ppl}}{(WR-1)} \quad (4-59)$$

$$I_{str} = \frac{W_{str}}{S_{wet}} \quad (4-60)$$

This, of course, implies that there exists a certain *ICI* for a certain point in time, based on the available technology available during this era. The higher the *ICI*, the longer it will take for technology to be readily available or economically feasible. This is clearly illustrated in Figure 88. Referring to this figure, the vertical line represents the *ICI* for a specific technology point. To the right of this line are vehicles which must wait on technology to catch up in order to be produced, whereas to the left of this line are vehicles which, could, technologically, be readily produced.⁴

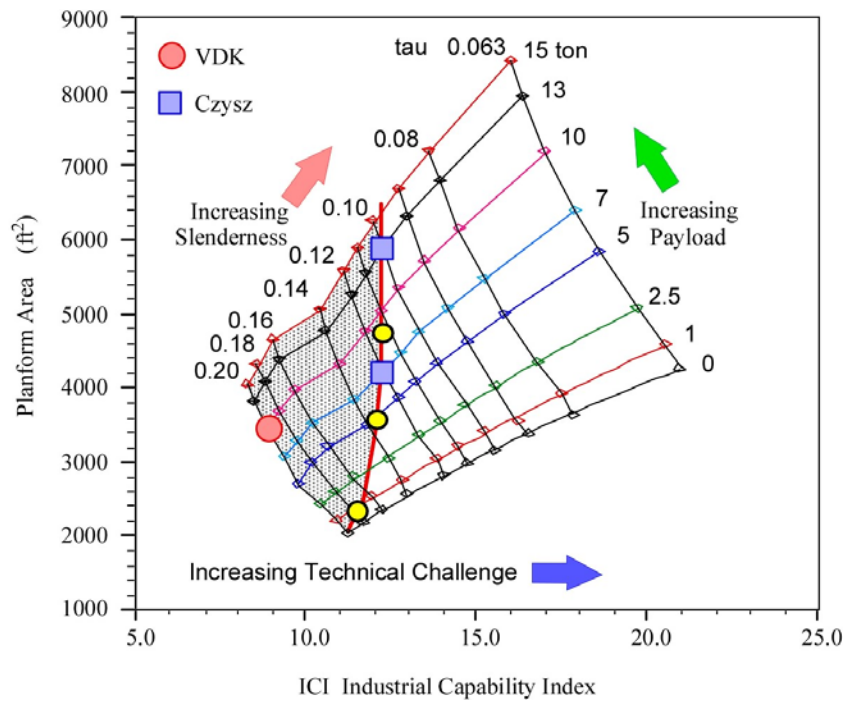


Figure 88: Feasible design space example.⁴

The volume characteristics of space access vehicle can be characterized by a non-dimensional volume index, Küchemann tau.

$$\tau = \frac{V_{total}}{S_{plan}^{1.5}} \quad (4-61)$$

where V_{total} is the vehicle total volume and S_{plan} is the planform area.

As the general design parameters are defined from flight loop analysis, various configurations are analyzed at the master synthesis level for their feasible design space with the given design requirements. This is illustrated in Figure 89, as it shows the corresponding design convergence space of various configurations that can be located by their technology indices (I_p and I_{str}). The shaded area above the horizontal is where available capability in propulsion, material, and fabrication exceeds the minimum required. It is clearly seen that the circular cone requires the least demanding technology, whereas the waverider requires the most advancement, as seen in current hypersonic vehicles.⁴

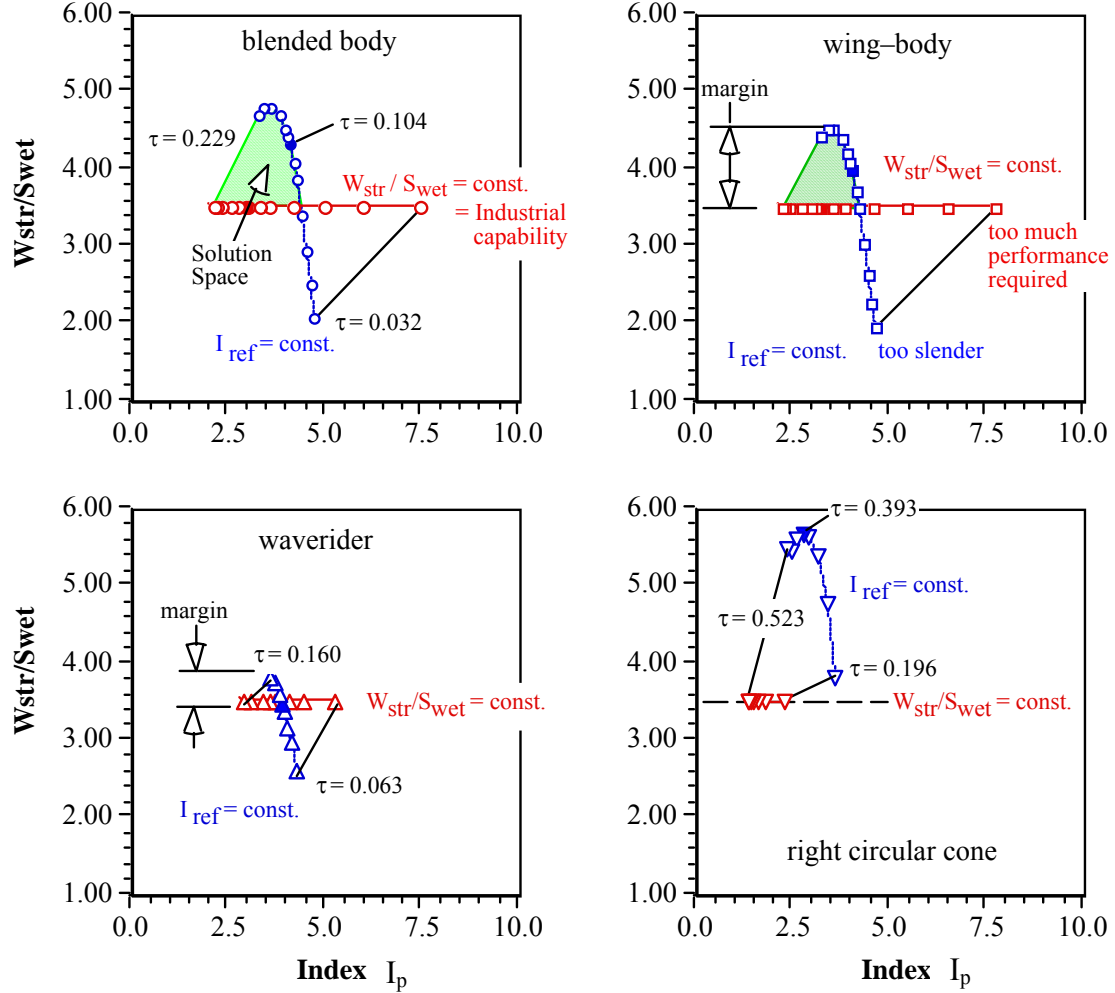


Figure 89: Overall design space possibilities of SAV concepts⁴

Figure 90 illustrates a design space plot for an individual configuration (blended wing body). The design convergence space, in Figure 90, is dictated by the design requirements and available technology (industrial capability to manufacture).⁴ The arched line of the upper left portion represents the reference value of the propulsion Index, I_p (4.2) compared with the maximum structural index, I_{str} , determined for which convergence is possible. The upper left portion of the graph represents an area where propulsion performance required is less than the judged Industrial Capability, and the specific structural weight (I_{str}) is greater than the minimum capability for manufacturing.

a structural specific weight greater than $3.9 \text{ lb}_m/\text{ft}^2$ and less than $4.2 \text{ lb}_m/\text{ft}^2$. The result is a larger vehicle, but one with greater margin for both payload and structural weight. Clearly, each configuration concept have its own unique margin representation.

4.4 Extension of the HTHL Methodology to VTVL Vehicles

Based on a given abstract mission profile, the HTHL SAV design methodology was derived in Chapter 4.3. The design methodology and design analyses at each mission segment are both based on generic key design parameters such as the ballistic parameter and L/D ratio during the reentry phase. As shown in Figure 71, the ballistic parameter and typical L/D can represent a range of generic configurations. For instance, the ballistic parameter for the Apollo reentry capsule is about 500 kg/m^2 , for a lifting body configuration it is about 1250 kg/m^2 , and for a winged glider with sharp leading edge it is about 2000 kg/m^2 . By varying these key design parameters, the design methodology and computers programs can be easily applied to different design concepts. Therefore, this design synthesis methodology has a generic character and can consistently compare all design alternatives of interest.

In order to further show the generic design character of the overall methodology concept, we investigated the possibility to extend the HTHL design methodology to any other extreme vehicle, the VTHL (vertical take-off and horizontal landing) Space Shuttle and X-33 launch vehicles, and especially to the VTVL (vertical take-off vertical landing) DC-X type launch vehicle¹⁸⁵, see Figure 91. The Delta Clipper family concept attempted to achieve a prototype reusable single-stage to orbit capability with the vertical

takeoff/vertical landing operational mode. The DC-X was first built as an experimental vehicle, 1/3 the size of a planned DC-Y vertical-takeoff/vertical-landing, single stage to orbit prototype. The flight tests of the DC-X and DC-XA demonstrated technology readiness for the vertical takeoff and vertical landing operation scheme.

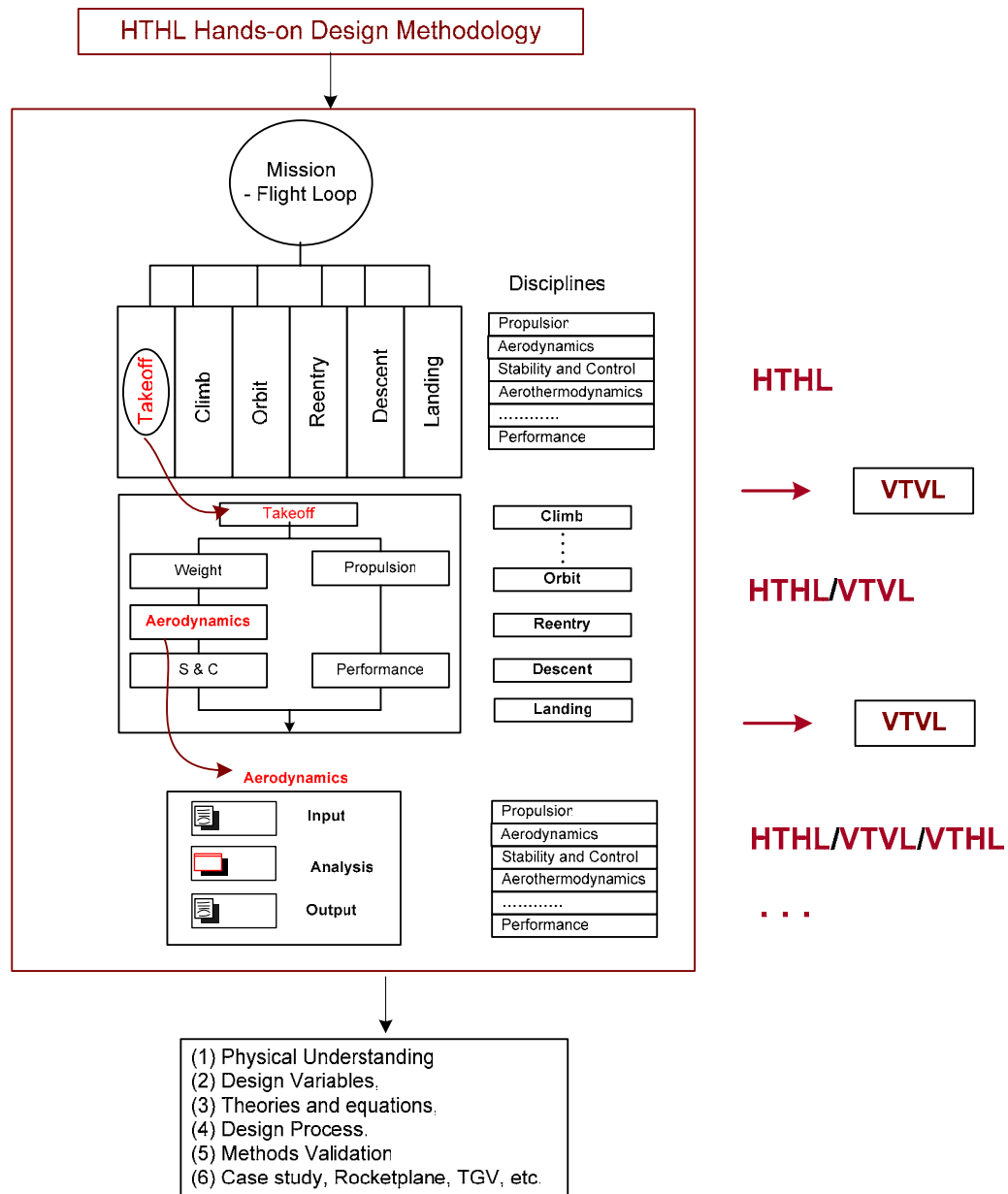


Figure 91: Capability extension of HTHL methodology to combined HTHL/VTVL and HTHL/VTVL/VTHL methodologies.

As indicated in Figure 92, the VTVL vehicle in particular has a similar mission profile to the HTHL vehicle. The VTVL vehicle takeoff phase is basically an initial ascent phase. When applying the generic design model applicable to HTHL designs to the VTVL vehicle, the takeoff segment is not required per se. During the ascent, the generic model and computer programs developed in Chapter 4.3.2 are still applicable. The minimum-fuel trajectory can be obtained to maximize $\frac{I_{sp}}{T} \frac{V(T-D)}{W}$ at each energy level E . Only the aerodynamic characteristics (drag and lift) and the propulsion module (T , I_{sp}) have to be adjusted for this new VTVL model. Then, the program can still be executed in the same way to estimate the propellant weight and the performance of the flight mission. As discussed before, the reentry segment of the generic HTHL design methodology is characterized by key design parameters (ballistic parameter and L/D) which can represent a range of SAV configurations varying from capsule, lifting body, to winged body. The same framework of design analysis is also applicable for VTVL vehicles. The only significant difference between VTVL and HTHL vehicles is their approach and landing phases. The approach and landing segment of the HTHL design methodology is not longer applicable for the VTVL vehicles. Instead of a glide approach, VTVL vehicles use rocket power with small moveable flaps to land. Therefore, a new approach and landing segment is required to be developed for the VTVL vehicle. This development is beyond the scope of the current study and can be considered for a follow-on study. As can be seen from above, the HTHL design methodology has the potential to be readily extended into a generic model by adding the logic and analysis modules for VTVL and others.

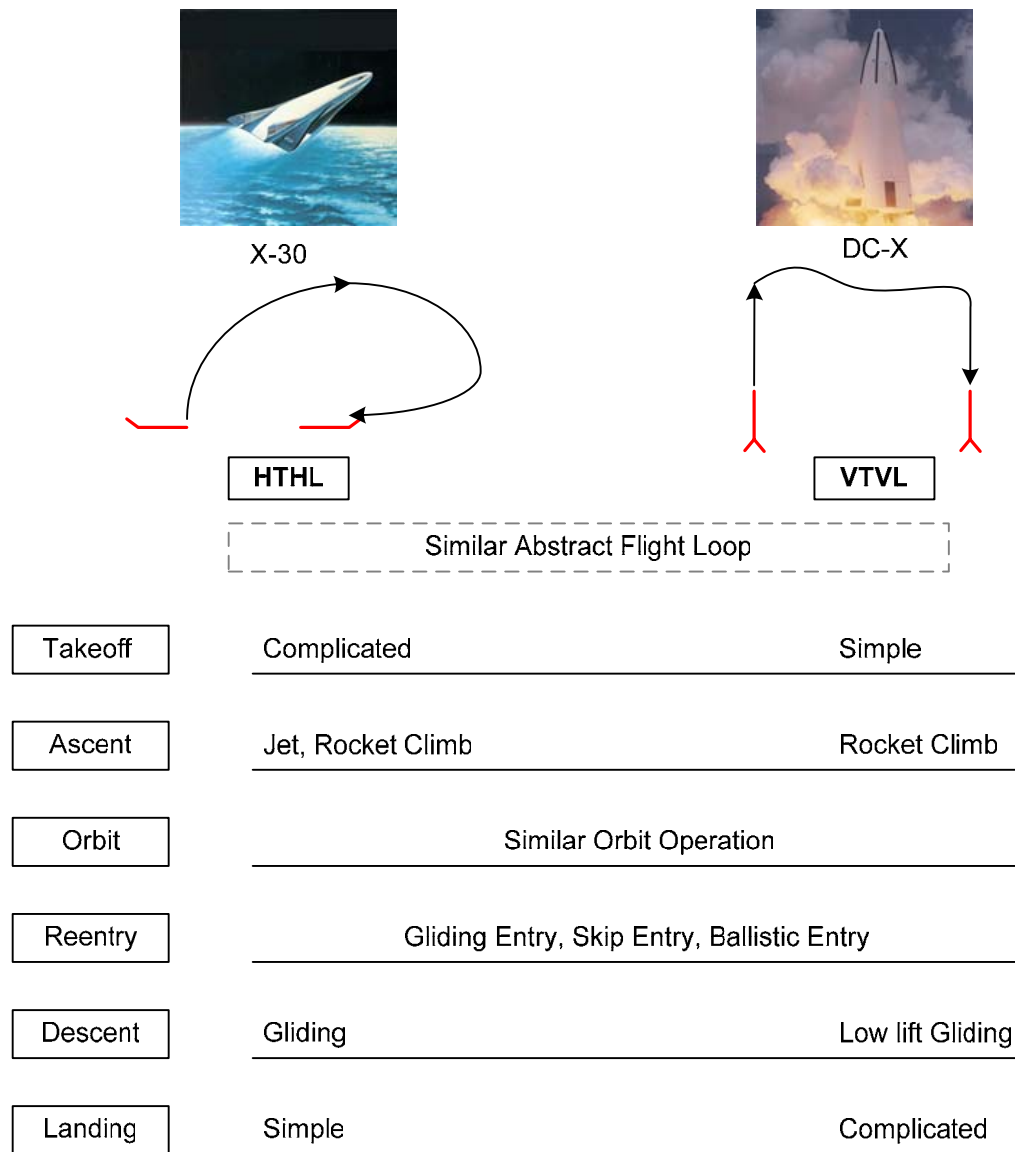


Figure 92: Comparison of analysis complexity throughout the abstract mission profile for HTHL and VTVL space access vehicle configuration concepts.

5. Application of HTHL Design Methodology

A HTHL suborbital space tourism vehicle was selected to be designed using the ‘hands-on’ methodology. This baseline vehicle concept was derived during a conceptual design study of a low-cost suborbital space tourist vehicle, which was based on an adaptation of a Learjet 24/25/35/45 series aircraft. References 125 to 129 summarize the conceptual design (CD) study of a tourist SAV, performed by the AVD Laboratory at The University of Oklahoma, funded by Oklahoma-based Rocketplane Ltd. Rocketplane Ltd. is one of the companies at the forefront of the emerging tourist SAV industry. In the AVD Laboratory, a family of feasible OU XP space tourism vehicles was derived. Here, the rocket OU XP HTHL concept is used as a design case study. Some geometric characteristics of the OU XP tourist SAV configuration concept are presented in Appendix A.

The following summarizes the general design guidelines for OU XP.¹⁸⁶ Program focus is that OU XP earns revenue transporting 3-4 paying participants to space. The XP aims for aircraft-like operations to support the space segment, see Figure 93.

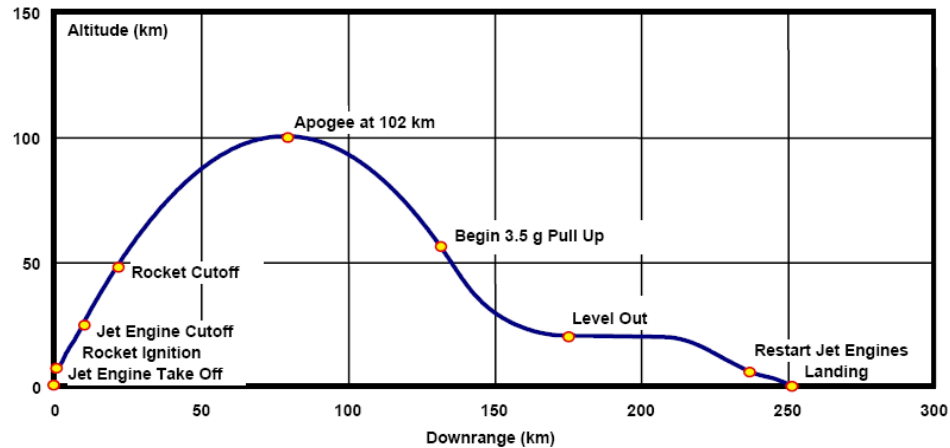


Figure 93: Nominal trajectory with 3 minutes micro-gravity at 100 km apogee¹⁸⁶

The operational mission starts with jet engine take-off from the runway.¹²⁹ The climb to the launch point takes place under jet power. The rocket powered suborbital trajectory requires a 3g aerodynamic pull up to ascent angle. The non-lifting ascent will be flown at around 70°. The thrust-to-weight ratio increases throughout the powered ascent. The rocket cuts off at approximately 48 km altitude, leading to a 3.2 minute coast to an 102 km altitude apogee while providing a space perspective of earth. During the parabolic fall back to atmospheric conditions the aircraft decelerates. Minding the maximum dynamic pressure, a pull-up maneuver is initiated, leading to leveling out. The aircraft decelerates while descending to approximately 6 km altitude for restarting the jet, followed by a powered approach and landing or alternatively a dead stick landing. It is planned to operate the XP from a single site, the certified launch site a Burns Flat, OK, having a 4.1 km (13,500 ft) long runway for takeoff and landing. Rocketplane plans to built and exclusively operate at most 3 vehicles since the available market limits fleet size and service. The initial XP vehicles will retire after a 3 to 5 year service, accumulating fewer than 1000 ops cycles or 750 hr for each vehicle.¹²⁵

Development aim is to use the Learjet 24 airframe and convert it into OU XP. This approach is thought to minimize cost and time to flight. The following modifications are considered necessary: add rocket engine, replace wing, add LOX and compressed air tanks, add aerodynamic and reaction flight control system, add crew systems for brief flight to space, select and integrate jet and rocket propulsion systems. The development effort targets to make Rocketplane OU XP a practical concept by utilizing the Learjet hull, integration of reusable rockets by ORBITEC, thermal protection from Space Shuttle and commercial sources, flight control concepts and systems using proven hardware and software. In short, a ‘minimum-change configuration’ is envisioned.

The following figure has been provided by Rocketplane (RLI); it shows the baseline OU XP which was the starting point for the AVD Lab conceptual design (CD) study.

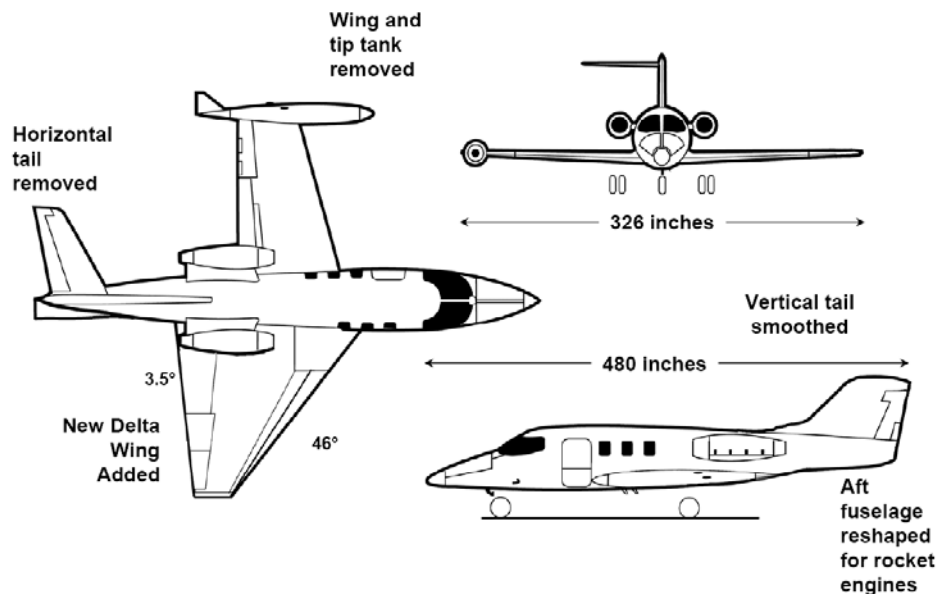


Figure 94: Baseline OU XP based on Learjet 24. Status: March 2004 ¹⁸⁶

Figure 95 shows the design process of the ‘hands-on’ methodology applied to the *OU XP* HTHL tourist SAV. At first, the mission and design requirements were defined for the suborbital tourism. The mission was to deliver at least 1200 lb payload to an altitude of 100 km. The baseline vehicle was derived based on the Learjet 24 aircraft. The design process started with the definition of the initial geometry and a first weight estimation. Based on these initial inputs, the disciplinary analyses were performed. For each mission segment, the results of the multidisciplinary design analysis were imported into the sub-synthesis module which determines and visualizes design constraints in a multidisciplinary context. The sub-synthesis constraints for each mission segment were then input into the master synthesis level, which discussed the resulting solution design space for the entire mission profile. Finally, at the master-synthesis level each distinct flight phase was converged (check physical feasibility in the design space) into a feasible SAV design, which complied with the entire mission profile.

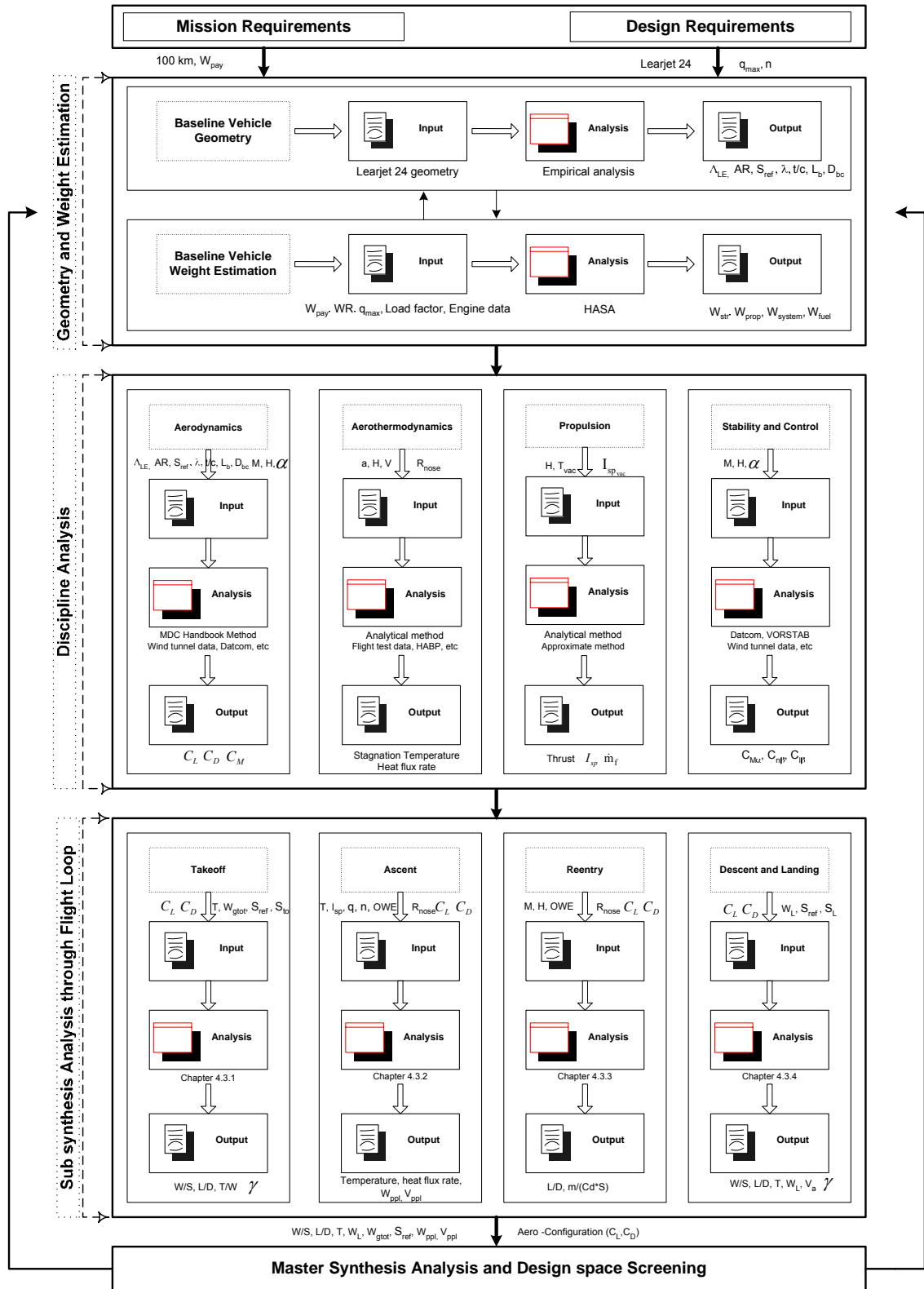


Figure 95: Design process of hands-on methodology.

5.1 HTHL Baseline Vehicle Description

Table 31 presents the mission and design requirements for this suborbital tourism vehicle concept.

Table 31: Mission requirements and design requirements.

Mission Requirements	Altitude > 100 km
	Payload: 3 passengers
Design Requirements	Use Learjet 24 as baseline vehicle
	Maximum dynamic pressure 500 psi
	g load is less than 4
	Certified by FAR Part 25

5.1.1 Geometry Estimation

Based on the mission requirements and baseline vehicle Learjet 24, the initial geometry of the *OU XP* concept was derived and documented in the main data sheet, see Table 32. Main features were the pointed nose, simple area-ruled fuselage, 70° dry delta wing with subsonic leading edge, delta wing leading-edge extension (LEX), 0° trailing edge, original pressurized fuselage section from Learjet 24, wing tip controls, elevons and wing-mounted verticals with side-area below the lifting surface, and finally utilization of the original Learjet 24 wing attachments. Note that this chapter only discusses one configuration concept of *OU XP* in order to illustrate the capability of the HTHL design methodology. The same principal design process would be applied to other HTHL configurations like Hotol, Sänger, X-15, SpaceShipOne, etc.

Table 32: Geometry characteristics of OUXP

GEOMETRY	
Vehicle Length, Forward Cone (ft)	9
Vehicle Length, Cylinder (ft)	32
Vehicle Length, Aft Cone (ft)	0
Total Vehicle Length (ft)	41
Fuselage diameter (ft)	5.25
Equivalent Body Diameter (ft)	3.8
Length/Diameter	15.94
Body Wetted Area (ft ²)	500
Wing Area, S_{ref} , (ft ²)	344
Wing Span, b (ft)	22
Wing taper ratio	0
Wing sweep angle	70°
Wing thickness ratio	0.06
Aspect Ratio, AR	1.44
Wing Loading (lb/ft ²)	80
Vertical Tail Area (ft ²)	30
Volume Required (ft ³)	600

5.1.2 Weight Estimation

To design a successful space access vehicle (SAV), the designer is required to clearly define the mission of the vehicle, which includes the definitions of payload, orbit, and operation. The payload is the most significant driver of SAV design. Its parameters, such as weight, size, etc, dominate the physical parameters of the vehicle. Therefore, the initial sizing of the vehicle aims to arrive at a configuration concept capable of meeting the mission requirements, especially the payload demand. In this study, the mission of the space tourism vehicle OU XP was to carry a payload of 1200 lb to an altitude of 100 km.

Based on the mission requirements, vertical trajectory equations were used to find the necessary velocity change ΔV to approach the altitude of 100 km. Then, the propulsion mass can be estimated using the rocket equation, which converts velocity change ΔV to propellant mass. Three vertical trajectory Equations (5-1, 5-2, 5-3) obtained from the 1954 Bell Aircraft Handbook, “Pocket Data for Engines”³⁸, are presented below and were applied to determine an important sizing parameter - weight ratio (WR). Weight ratio is the ratio of the initial vehicle weight to final weight (the difference is the fuel weight).

$$V_c = g \cdot I_{SPE} \cdot \ln\left(WR - \frac{WR-1}{a_i \cdot WR}\right) \quad (5-1)$$

$$Z_c = g \cdot I_{SPE}^2 \cdot \left(\frac{WR-1}{a_i \cdot WR}\right) \cdot \left(1 - \frac{\ln WR}{WR-1} - 0.5 \cdot \frac{WR-1}{a_i \cdot WR}\right) \quad (5-2)$$

$$Z_p = g \cdot I_{SPE}^2 \cdot \left[\frac{(\ln WR)^2}{2} - \frac{1}{a_i} \cdot \left(\ln WR - \frac{WR-1}{WR}\right)\right] \quad (5-3)$$

$$I_{SPE} = I_{SP} \cdot \left(\frac{T/D-1}{T/D}\right) \quad (5-4)$$

where a_i is the initial thrust to weight ratio, V_c is the cutoff velocity, Z_c is the cutoff altitude, Z_p is the peak altitude, g is the average earth acceleration, WR is the weight ratio (typical values: 2.0 - 2.4 for a suborbital mission), I_{SPE} is the effective I_{SP} (vacuum I_{SP}), and T/D is the thrust to drag ratio (usually taken to be 5 from the Bell Aircraft Handbook).⁴

These three equations were programmed in an Excel Spreadsheet as shown in Figure 96. The weight ratio and initial acceleration can be obtained by simultaneously solving these vertical trajectory equations. The results of the equations for each propellant

combination are presented in Table 33. The design data (I_{sp} , density, etc.) of each propellant combination were again obtained from the Bell Aircraft Handbook.⁴

Table 33: Weight ratio of different propellant combinations⁴

Propellant Combinations	WR	a_i	I_{SP}	I_{SPE}	Density (lbm/ft ³)
Hydrogen Peroxide Monopropellant	2.3735	1.5812	288	230.4	86.86
Hydrazine Monopropellant	3.0395	1.3327	236	188.8	63.02
Hydrogen Peroxide + Hydrazine	2.9639	1.3568	240	192.0	76.13
Nitrogen Tetroxide +Hydrazine	2.8140	1.4070	249	199.2	74.44
LOX + Kerosene	2.8140	1.4070	249	199.2	63.65
LOX + Ethanol	2.9280	1.3684	242	193.6	60.53
LOX + Ammonia	3.0103	1.3419	237.5	190.0	72.07
LOX + Methane	2.625	1.4763	263	210.4	46.61
LOX + Hydrogen (O/F = 2.98)	2.0183	1.7629	345	276.0	14.35
LOX + Hydrogen (O/F = 6.00)	1.7869	1.9115	410	328	23.00
White Fuming Nitric Acid + JP4	3.1901	1.2870	229	183.2	81.12
WFNA + Hydrazine	2.8609	1.3909	246	196.8	76.75
Fluorine + Hydrazine	2.2792	1.6251	300	240.0	66.77

As can be seen in Table 33, it is a challenging task to size the weight and geometry of a SAV because the weight ratio (WR) to orbital speed is directly related to the oxidizer carried on board. The propellant mass fraction of a space access vehicle can range from 50% to over 90%, whereas it is only 30% to 50% for an aircraft. The individual propellant densities vary from 14 lb/ft³ to 86 lb/ft³.⁴ Therefore, propellant volume becomes a dominant factor during the SAV sizing process. As a consequence, the estimation of geometry and weight requires an intensely iterative process in order to arrive at a preliminary geometry configuration, which satisfies mission and design requirements.

A preliminary sizing analysis tool, Hypersonic Aerospace Sizing Analysis (HASA) was used for the current study. The basic theory and mathematical formulas of HASA⁶⁹ have been derived by NASA from statistical data of four hypersonic transports, a Mach 6

fighter, a supersonic transport, a SSTO vehicle, a two-stage Space Shuttle with a booster and an orbiter, and two methane-fueled vehicles. HASA can be used to predict the size and weight of hypersonic single-stage-to-orbit (SSTO) and two-stage-to-orbit (TSTO) vehicles and transonic and supersonic transports. It determines vehicle length and volume consistent with the body, fuel, structure and payload weights. A MS Excel program was developed to implement the above methodology, and a screen shot of this program is shown in Figure 96. The **SAV_HASA** program includes three parts: mission and design requirements, geometry, and weight estimations. First, based on the mission requirement, the initial weight ratio (WR) is obtained as an input for the weight analysis. During the geometry estimation process, the sizes of payload and propellant are defined. The process of geometry and weight estimations is an iterative sizing process required to meet both mission and design requirements.

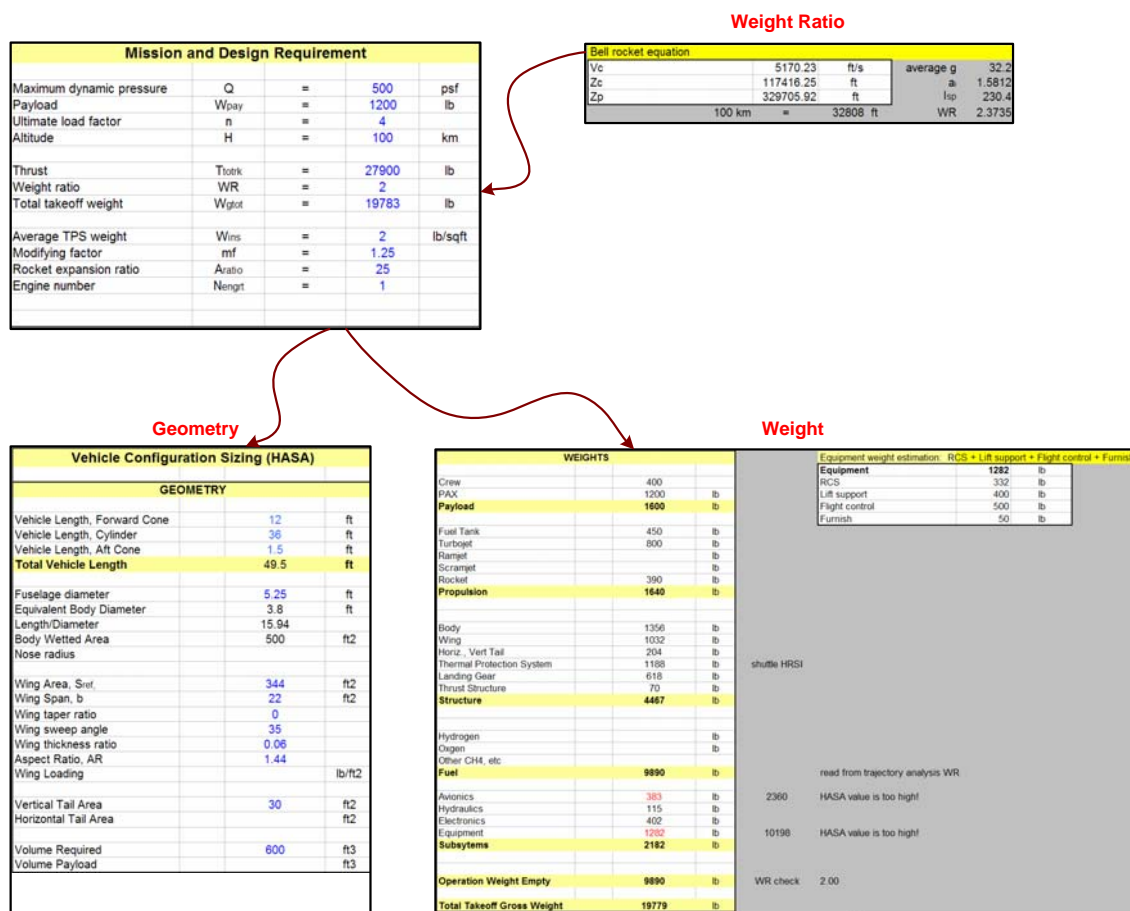


Figure 96: SAV_HASA Excel program for geometry and weight estimations

Table 34 shows the results of the weight estimation of *OU XP* for the different categories payload, propulsion, structure, fuel and subsystems. As soon as the geometry and weight of the vehicle are estimated, the center of gravity can be determined.

Table 34: Weight estimation of OUXP.

WEIGHTS (lb)	
Crew	400
PAX	1200
Payload	1600
Fuel Tank	450
Turbojet	800
Rocket	390
Propulsion	1640
Body	1356
Wing	1032
Horiz., Vert Tail	204
Thermal Protection System	1188
Landing Gear	618
Thrust Structure	70
Structure	4467
Fuel	9890
Avionics	383
Hydraulics	115
Electronics	402
Equipment	1282
Subsystems	2182
Operation Weight Empty	9890
Total Takeoff Gross Weight	19779

5.2 Disciplinary Analysis

An initial disciplinary analysis of this HTHL baseline vehicle, *OU XP*, was required to provide basic geometry (wing area, length, aspect ratio, etc.), weight, aerodynamics, and propulsion information as input for the design synthesis process. The processes and results of the disciplinary analysis sections are presented below.

5.2.1 Atmosphere

The atmosphere module used here¹⁸⁷ allows the determination of temperature, pressure, and density at any altitude. The statistical atmosphere data used are documented in the "U.S. Standard Atmosphere, 1976", published by the U.S. Government Printing Office, Washington, D.C.¹⁸⁸ The 1976 atmosphere tables cover the altitude band from 0 to 86 km. Steven Pietrobon in Reference 187 extended the table from 86 to 1000 km, using cubic spline curve fits instead of numerical integration and solution of differential equations. This atmosphere model has proven to be highly accurate, thus, it was selected for the current study. The reference sea level (*SL*) conditions are

$$g_{SL} = 31.1741 \frac{ft}{s^2}, P_{SL} = 2116.22 \frac{lbf}{ft^2} \quad (5-1)$$

$$T_{SL} = 518.67^\circ R, \rho_{SL} = 0.002377 \frac{slug}{ft^3} \quad (5-2)$$

The above parameters are presented in atmosphere tables by non-dimensional ratios as follows:

$$\delta = \frac{P}{P_{SL}}, \theta = \frac{T}{T_{SL}}, \sigma = \frac{\rho}{\rho_{SL}} \quad (5-3)$$

5.2.2 Aerodynamics

It is a challenging task to define the aerodynamic characteristics of the suborbital *OU XP* tourism vehicle since it operates across the subsonic, transonic, and supersonic boundaries. Several configuration aerodynamic tools were initially validated and calibrated using subsonic wind tunnel data from the Learjet 24.¹⁸⁹ The vortex-lattice methods LinAir Pro¹⁹⁰, VORSTAB⁹⁷, and the handbook method DATCOM⁷⁸ were used with success. For delta wing aerodynamics, references by Hoerner^{87,88}, Küchemann⁸³, and Schlichting and Truckenbrodt⁸⁴ were most helpful. The aerodynamic analysis module is capable of implementing numerical data derived from all the above methods and available wind tunnel data. Figure 97 shows an Excel program developed by using the MDC handbook methods.¹³⁴ Under different flight conditions (Mach number, altitude, and angle of attack), the lift and drag coefficients of the baseline vehicle can be derived for further design analysis.

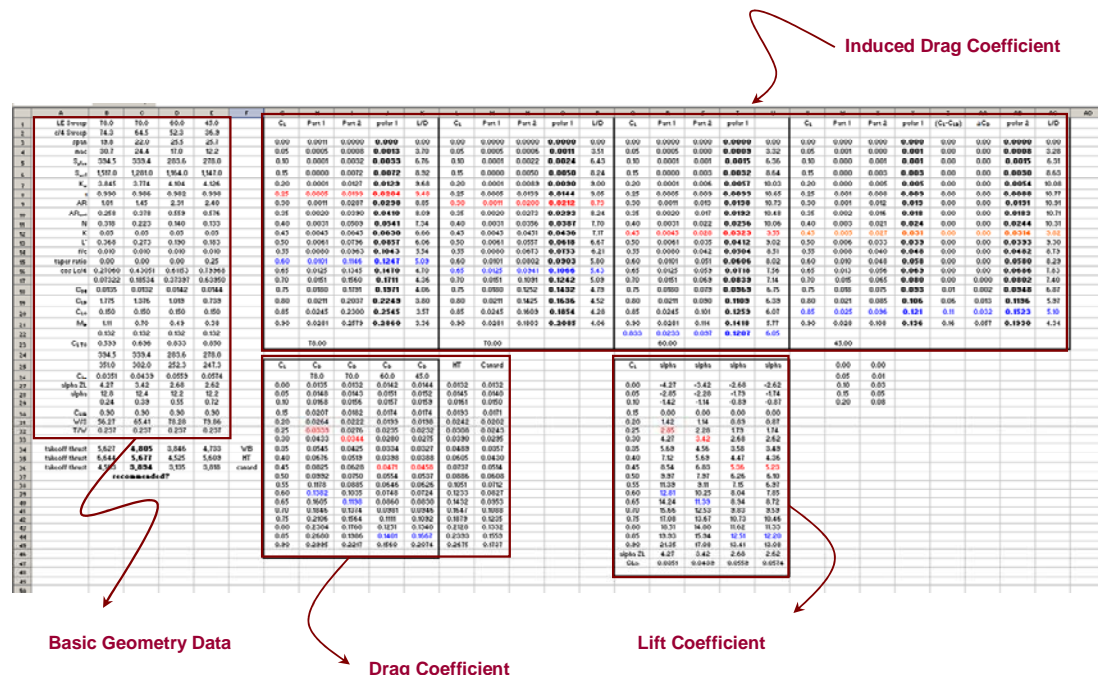


Figure 97: Aerodynamics analysis using MDC handbook methods¹³⁴

Figure 98 shows the drag polar of the *OU XP* with 70° LE sweep based on the MDC Handbook method. Figure 99 presents some wind tunnel results of two supersonic configurations related to the *OU XP* concept. The solid symbols show the induced drag factor from the AIAA engineers design handbook⁷² for the subsonic leading edge (round) and supersonic leading edge (sharp) compared to results generated by the McDonnell Advanced Design aero group.

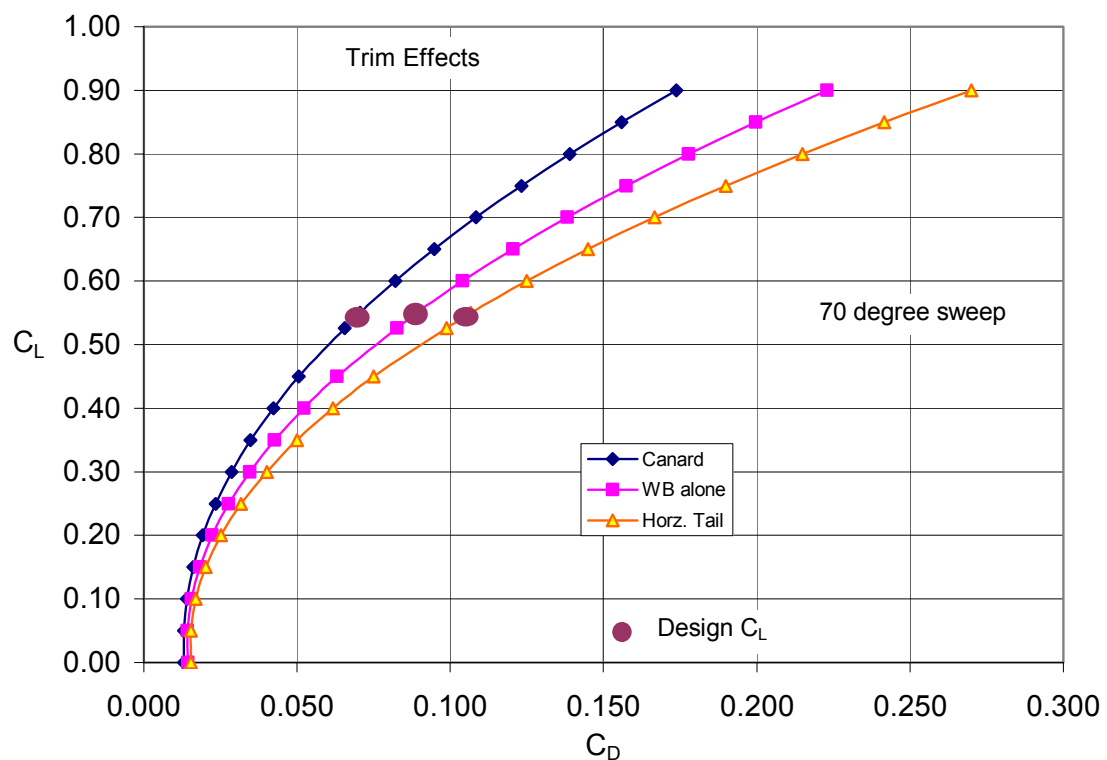


Figure 98: Drag polar of OU XP with 70° LE sweep

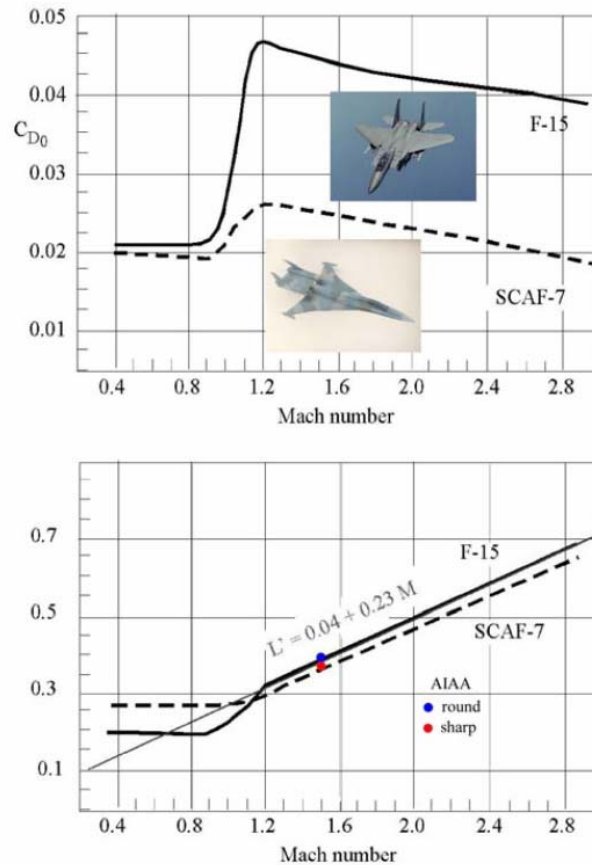


Figure 99: Wind tunnel results of two supersonic fighters
from McDonnell Douglas advanced design¹⁹¹

5.2.3 Stability and Control

As described in Aviation Week (October 11, page 31)⁹⁵, SpaceShipOne became unstable at Mach 1.4, and it used up all on-board reaction control gas in order to stop the roll motion. When SpaceShipOne hit the apogee, there was no reaction control capability left. This is a dangerous flight condition since any motion at this point can initiate inertia coupling, leading to tumbling. During the second flight, the pilot tried to hold a zero angle of attack as long as possible because any change from zero will easily lead the vehicle to roll because of an unbalance in lift on both sides. SpaceShipOne is also directionally unstable at Mach 1.25.^{95,96}

OU XP is structurally constrained by a maximum dynamic pressure of 500 psf up to an altitude of 110,000 ft. Assuming a 300 ft² wing area and $q*S_{plan}=150,000$ lb, even with a small lift coefficient of $C_L = 0.1$, the wing can still produce 15,000 lb lift. It was the original design driver to have a 70° or 78° swept wing, which has a flat lift-curve slope. The delta wing planform fortunately reduces the sensitivity to gust and small changes in angle of attack, minimizing the inertia-coupling tendency at high altitudes.

At the conceptual design level, it is desirable to have a tool available capable to quickly estimate the stability and control characteristics of the proposed configurations. Figure 100 shows the analysis process of the USAF Stability and Control Datcom. The longitudinal coefficients ($C_{m_\alpha}, C_{m_q}, C_{L_\alpha}$) and lateral-directional stability coefficients ($C_{n_\beta}, C_{l_p}, C_{l_\beta}, C_{n_r}$) can be obtained from the output file.

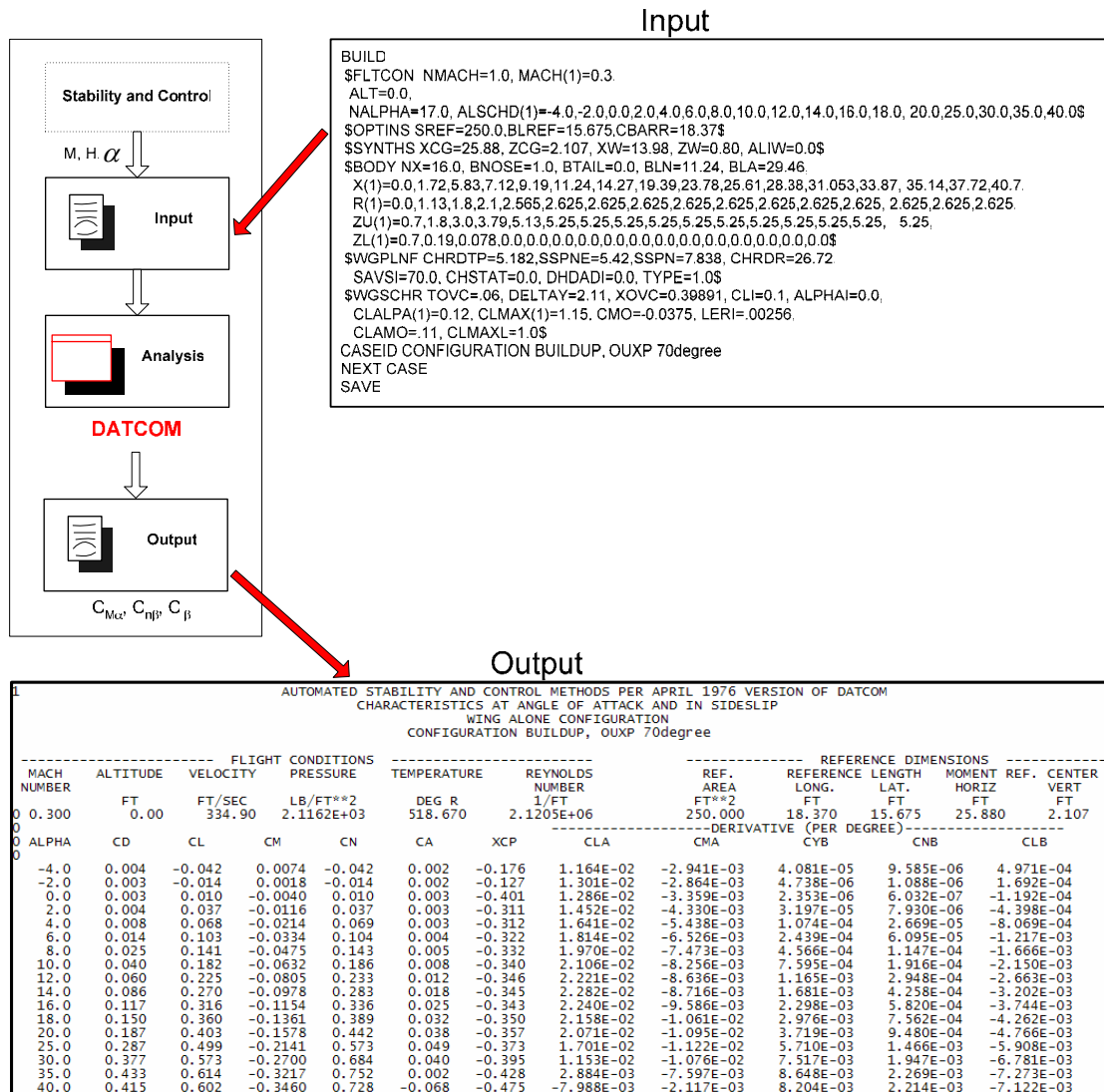


Figure 100: Analysis process of digital DATCOM

5.2.4 Propulsion

Only key engine design parameters such as specific impulse (I_{sp}), propellant flow rate (\dot{W}), and thrust (T) were considered. The propulsion analysis used first-order approximate equations as shown in Chapter 3.2, which are sufficient for conceptual design. It receives its input information (Mach number, altitude, and angle of attack) from each flight interval to determine the specific impulse (I_{sp}), propellant flow rate (\dot{W}), and

thrust (T). Table 35 shows the selected thrust and weight characteristics for the jet and rocket engines selected for the OU XP.

Table 35: OU XP jet and rocket engines characteristics

Parameters	OU XP Engines	GE CJ - 610	Rocket Engine
Thrust (lb)		2950	27900
Weight (lb)		411	2325

5.2.5 Aerothermodynamics

During suborbital flight, the space tourism vehicle endures high temperatures T and convective heat rates \dot{Q} due to its high level of kinetic energy. The approximate stagnation point temperature limitation of the vehicle was estimated as a function of free stream temperature T_∞ and flight Mach number M as

$$T_0 = T_\infty + \frac{\gamma - 1}{2} \cdot T_\infty \cdot M^2 \leq T_{\max} \quad (5-4)$$

and the heat transfer rate at the stagnation region was approximately estimated^{161,162} by

$$\dot{Q} = 865 R_n^{-1/2} \left(\frac{V}{10^4} \right)^{k1} \left(\frac{\rho}{\rho_0} \right)^{k2} \leq \dot{Q}_{\max} \quad (5-5)$$

where R_n is a function of the vehicle's fineness ratio. For a winged high speed vehicle such as the *OU XP*, empirical estimates of coefficients $k1$ and $k2$ were taken to be 2.65 and 0.5, respectively. The heating rates at the other locations of the vehicle were proportional to the heating rate at the stagnation point. For suborbital flight, the maximum flight Mach number was estimated at around 4. Therefore, the stagnation temperature for the suborbital mission ranged from 500 F to 700 F, and the heat flux was also within the temperature capability of aluminum alloy.

5.3 Design Synthesis Process

As shown in Figure 91, after the estimation of geometry and weight, disciplinary design analyses are performed for each mission segment (takeoff, ascent, reentry, approach, and landing). The results are imported into each sub-synthesis module, which determines and visualizes design constraints for the first time in the multi-disciplinary context. In a follow-on step, the sub-synthesis constraints for each mission segment are input to the master synthesis level, which determines the resulting design space for the entire mission profile. At the master-synthesis level, design parameters are converged into a feasible SAV design configuration, which satisfies with the entire mission profile. The processes of sub-synthesis and master-synthesis level design analysis for the *OU XP* are presented in the following.

5.3.1 Takeoff

Before proceeding towards the takeoff sub-synthesis design process (see Figure 101), the airport runway and FAR 25 design requirements for the space tourism mission had to be defined. Based on the geometry and estimated weights, the initial configuration concept was iterated to arrive at efficient aerodynamic characteristics, wing loading (W/S), thrust to weight (T/W) ratio. Then, the vehicle design space for the takeoff phase could be determined.

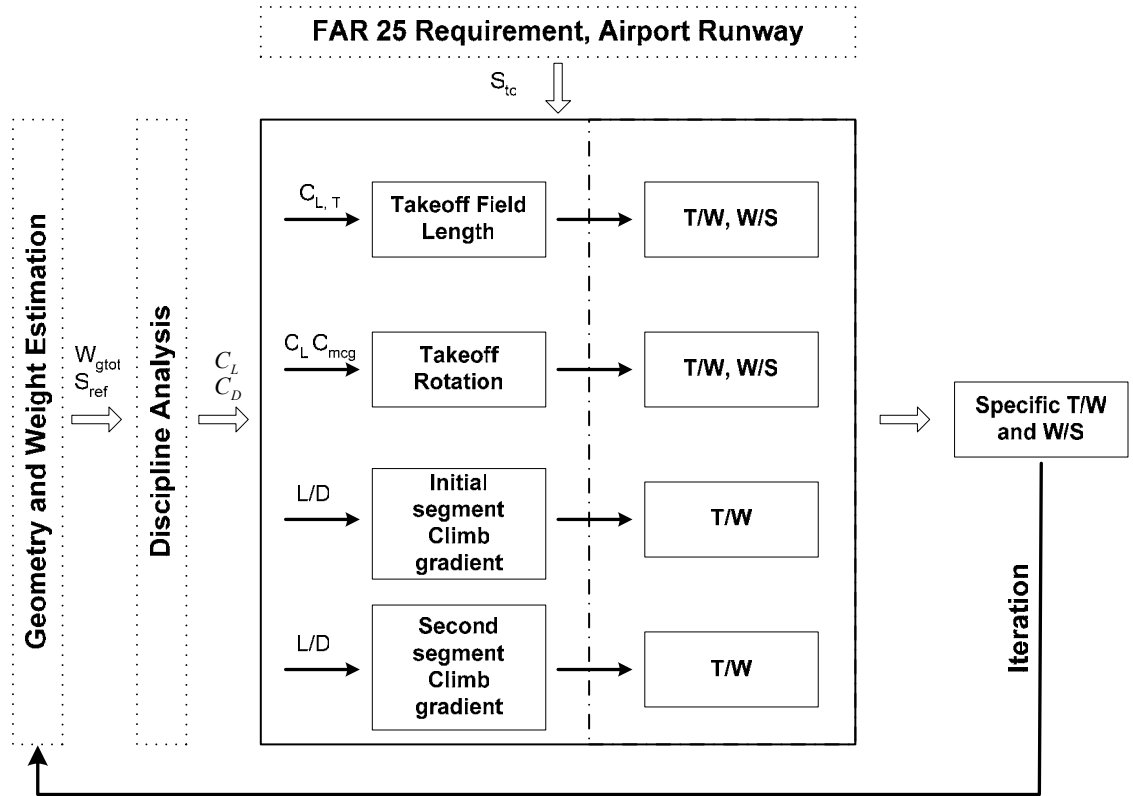


Figure 101: Multidisciplinary design analysis of takeoff segment

Two programs (**SAV_BFL**, **SAV_CLM**) were developed to determine the variations of the main design parameters throughout the takeoff phase. Figure 102 shows the Excel program to calculate the takeoff field length, takeoff speed, and nose liftoff speed. Figure 103 shows the Excel program to determine the T/W for different trim mechanics (horizontal tail and canard). Based on these Excel programs, the key design parameters involved (such as T/W and W/S) were evaluated quickly and efficiently.

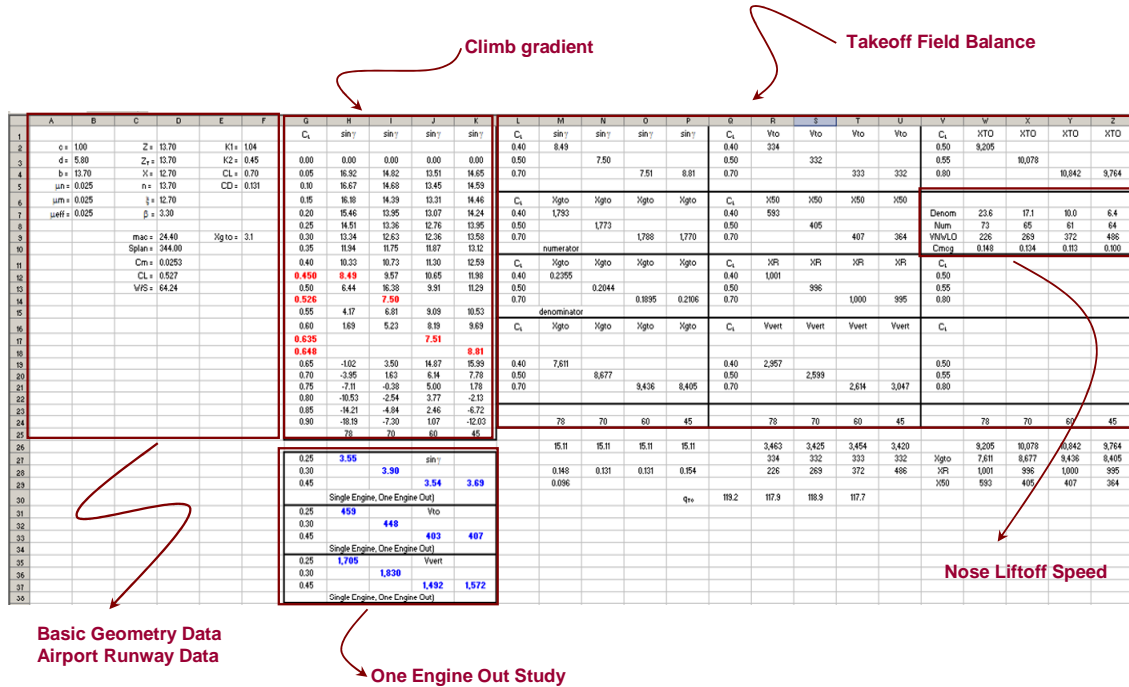


Figure 102: Calculation of takeoff field length and nose liftoff speed

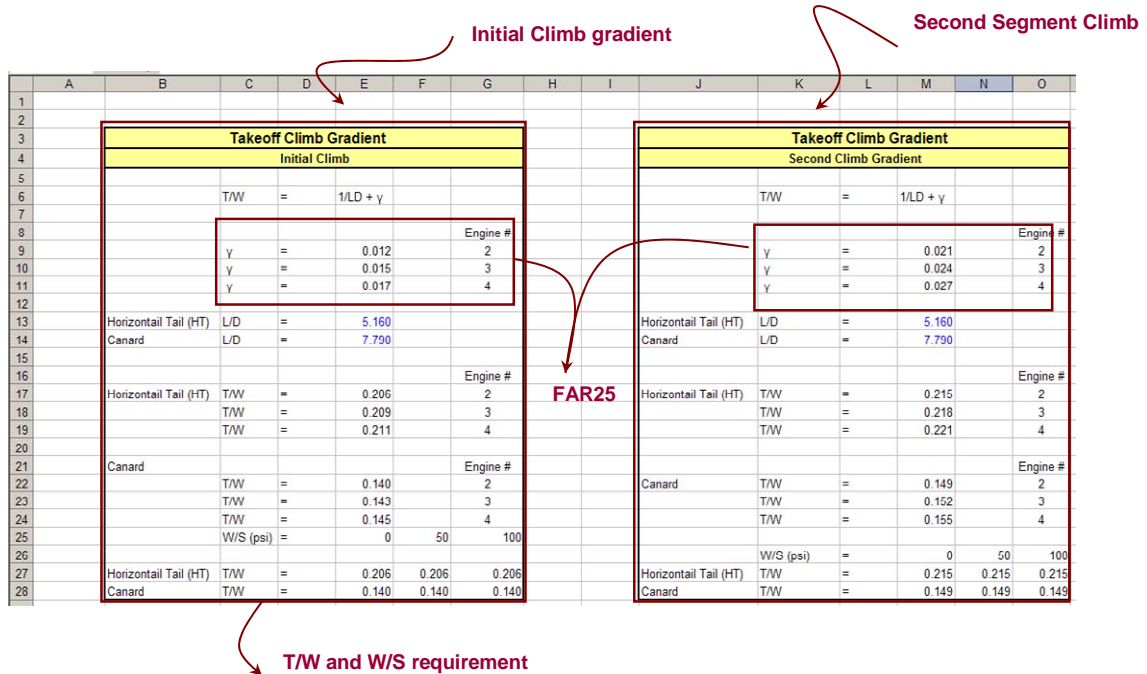


Figure 103: T/W requirement for initial climb and second segment climb

(a) Takeoff Field Length:

It was assumed that the *OU XP* would take off from a 11,000-ft runway (Oklahoma Burns Flat runway). As shown in Figure 36, the design for the single-engine-out operation reduced twin engine takeoff distance from 11,000 ft to 8,900 ft. Under this condition, the required thrust for takeoff is shown in Figure 104. The thrust requirements of two trim mechanisms, canard and horizontal tail, were compared. It is obvious that the canard configuration reduced the required thrust while the opposite trend was observed for the horizontal tail configuration. One reason is that, with a canard, the wing induced drag is significantly reduced, resulting in an overall reduced drag layout.

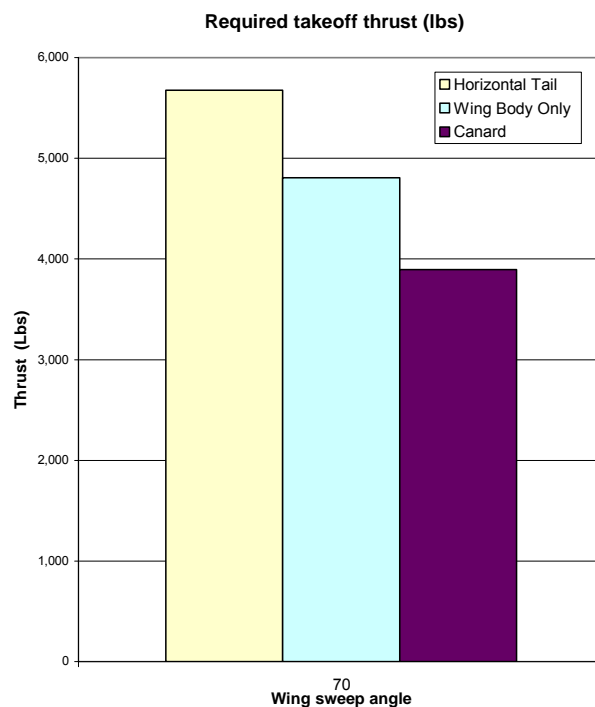


Figure 104: Required takeoff thrust for different trim mechanisms

Figure 105 shows the wing loading of the *OU XP* of a 70° LE sweep. Figure 106 shows the total takeoff distance required for the 70° leading edge (LE) sweep wing

configuration. The total takeoff distance includes ground run distance, rotation distance, and the air distance over a 50 feet obstacle.

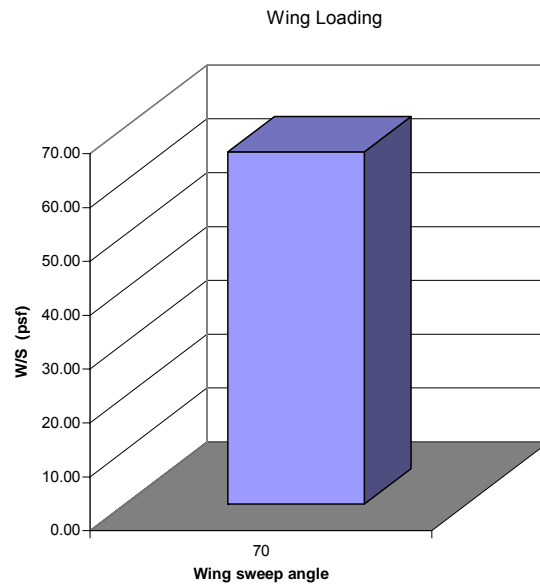


Figure 105: Wing loading

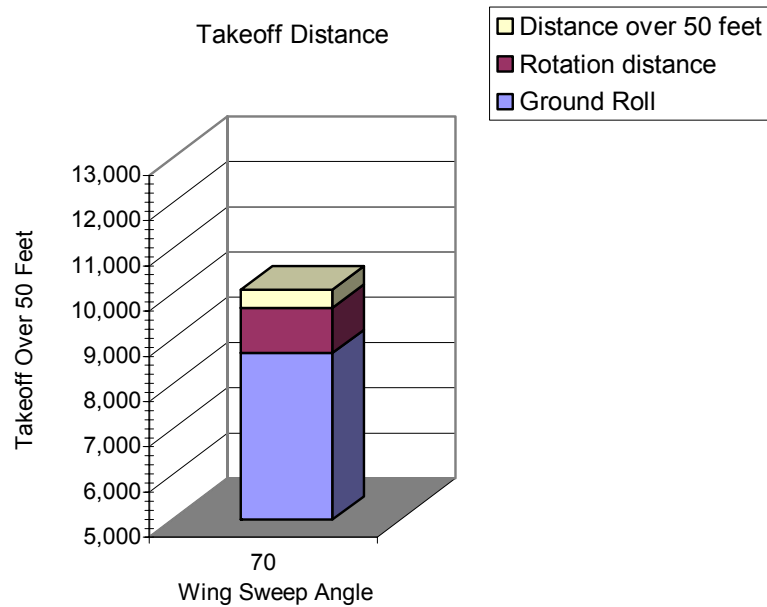


Figure 106: Takeoff field length

(b) Takeoff Speed and Nose Wheel Liftoff Speed:

Figure 107 shows the takeoff speed and nose wheel lift-off speed for 70° LE sweep. As discussed in Chapter 4, the takeoff speed has to be higher than the nose lift-off speed for the vehicle to have enough control power to rotate the nose. It can be seen from Figure 107, that for 70° LE sweep, the airplane is capable of lifting up the nose wheel slight below takeoff speed.

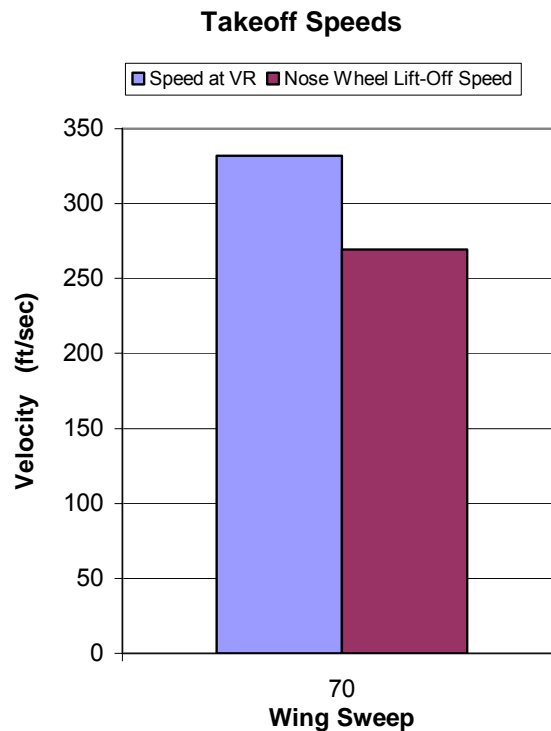


Figure 107: Takeoff speed and nose wheel liftoff speed

(c) Initial Climb Gradient and Second Segment Climb Gradient:

The lift to drag (L/D) ratio of the *OU XP* with different trim mechanisms was calculated based on the MDC handbook methods shown in Figure 97. The L/D ratio was 7.79 for the canard configuration and 5.16 for the horizontal tail configuration. Therefore, the thrust to weight (T/W) ratios for the takeoff initial and second climb gradient

requirements were obtained and are shown in Figure 108. The solid line refers to the thrust to weight (T/W) ratio for the initial climb gradient requirement, while the dashed line describes the second segment climb gradient requirement. As can be seen, the horizontal tail configuration requires a larger T/W due to its lower L/D .

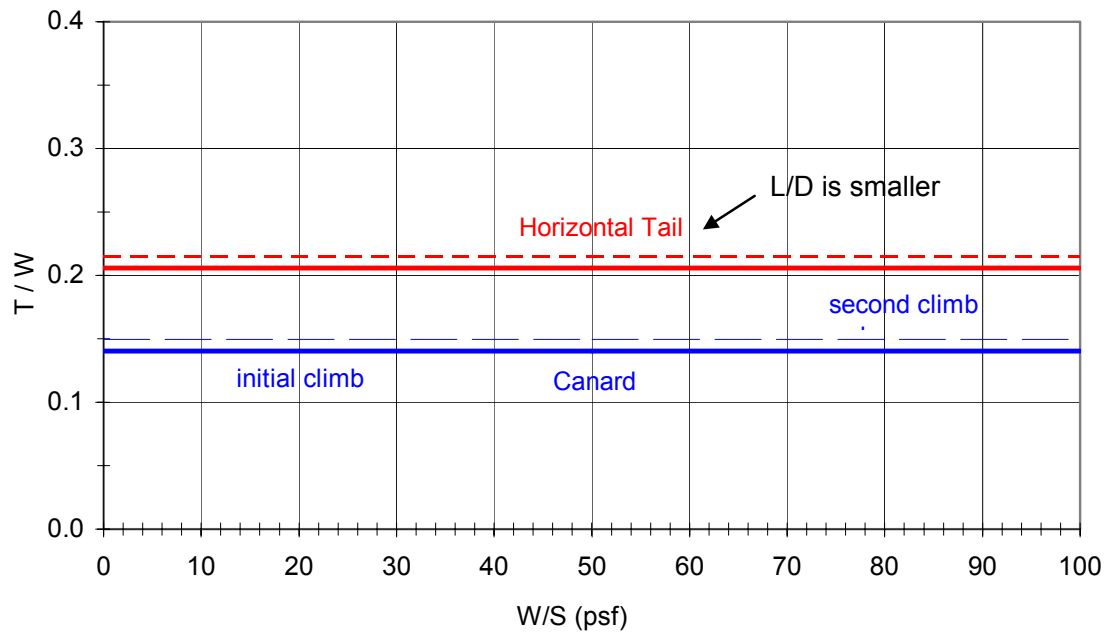


Figure 108: Takeoff climb gradient requirement

5.3.2 Ascent

Maximum mission performance of a baseline vehicle was explored at the ascent sub-synthesis design segment. This performance maximum was obtained when a minimum-fuel ascent trajectory was defined, which ultimately led to a maximum orbital mass fraction. Figure 109 presents the sub-synthesis design process for the ascent segment. The geometry, weight, aerodynamics, and propulsion characteristics of the baseline vehicle, *OU XP* with 70° LE sweep, were estimated and used as input for the trajectory program **SAV_TSSP** (see Appendix G). **SAV_TSSP**¹¹¹ uses ESA technology and was developed

by the author in a Matlab environment. It utilizes the powerful Matlab graphic functions to visualize the design space and find the graphic solution for a minimum fuel trajectory. **SAV_TSSP** couples key design disciplines such as trajectory, aerodynamics, weight, aerothermodynamics, and propulsion. The variation of the main design parameters throughout the ascent flight path can be visualized. As a consequence, valuable feedback discussing design feasibility, sensitivities, boundaries, and constraints can be obtained in short time from this top-level simulation process.

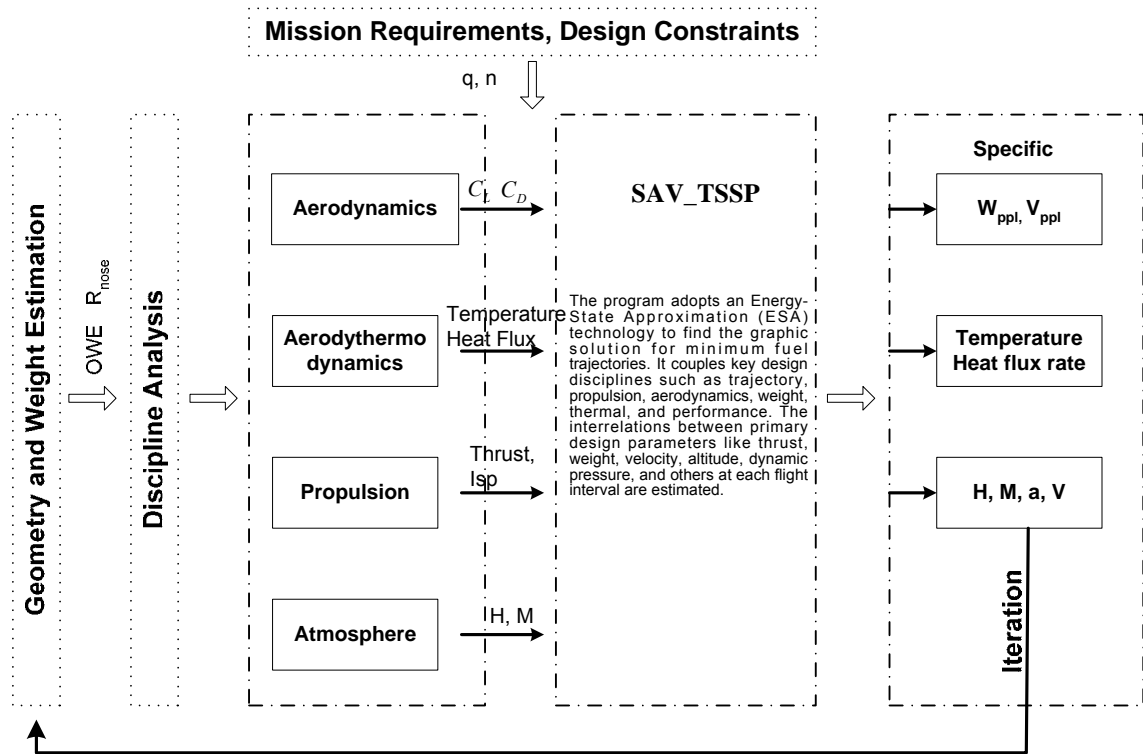


Figure 109: Multidisciplinary design analysis of ascent segment

(a) Minimum Fuel Ascent Trajectory:

The minimum fuel trajectory (dashed line) as determined using the ESA technique led to smaller accelerations avoiding the maximum dynamic pressure peak (see Figure 110).

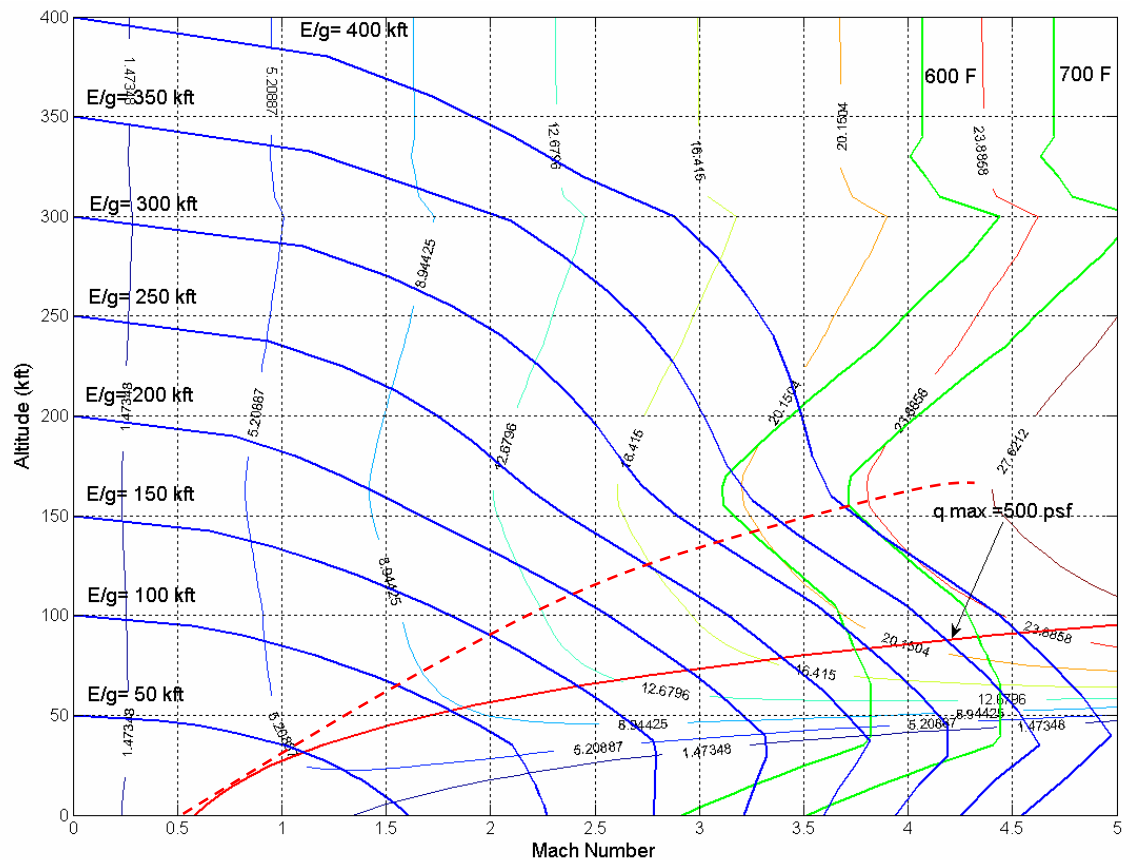


Figure 110: Minimum fuel trajectory and design constraints

After having determined the initial trajectory (Mach number vs. altitude diagram), the total fuel weight was estimated utilizing an iterative process. It can be seen in Figure 111 that the trajectory synthesis simulation program took 30 to 40 iterations to converge the propellant weight required for the suborbital mission. The propellant weight of the minimum fuel trajectory was around 12,000 lb.

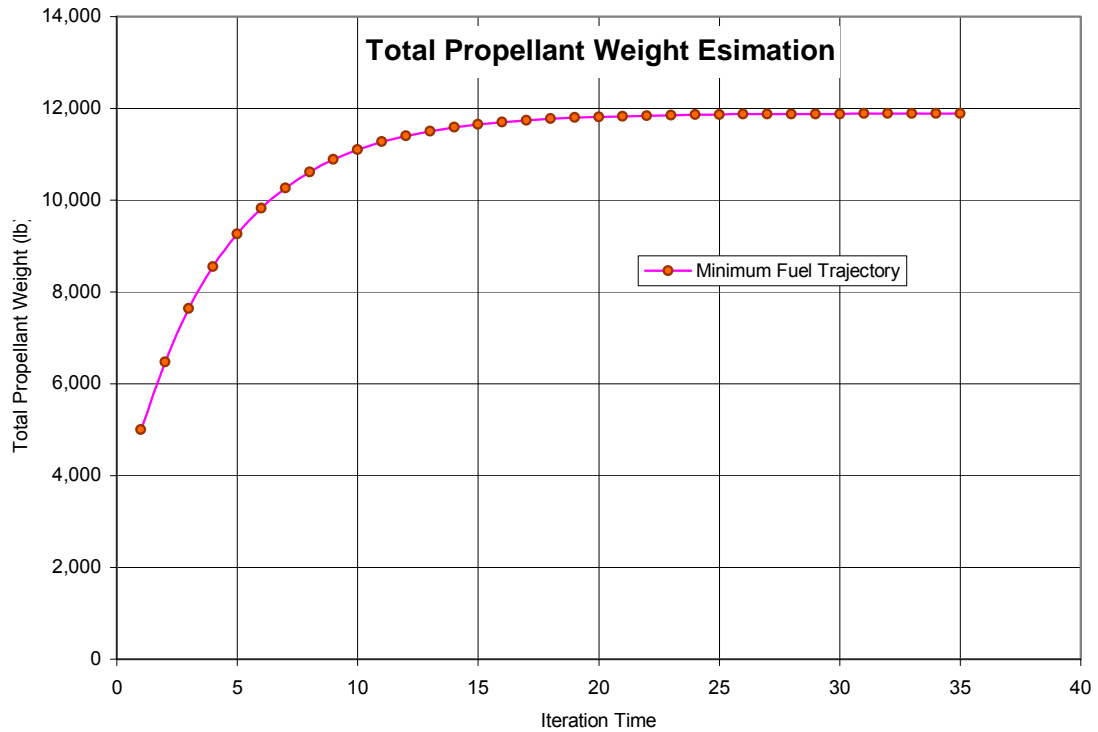


Figure 111: Iterations of propellant weight of OU XP

(b) Parameter Estimations:

The systematic and consistent modeling approach underlying the trajectory synthesis simulation program (**SAV_TSSP**) resulted in a variety of performance maps (dynamic pressure vs. altitude; speed vs. time; thrust vs. speed; altitude vs. time; drag/weight vs. altitude; weight vs. speed; specific impulse vs. speed; etc.). In order to demonstrate this, Figures 112, 113, and 114 were assembled to illustrate the variations of several key design parameters (flight speed, acceleration, dynamic pressure, and altitude) throughout the flight trajectory. This information helps the conceptual designer understand the sensitivities of key design parameters.

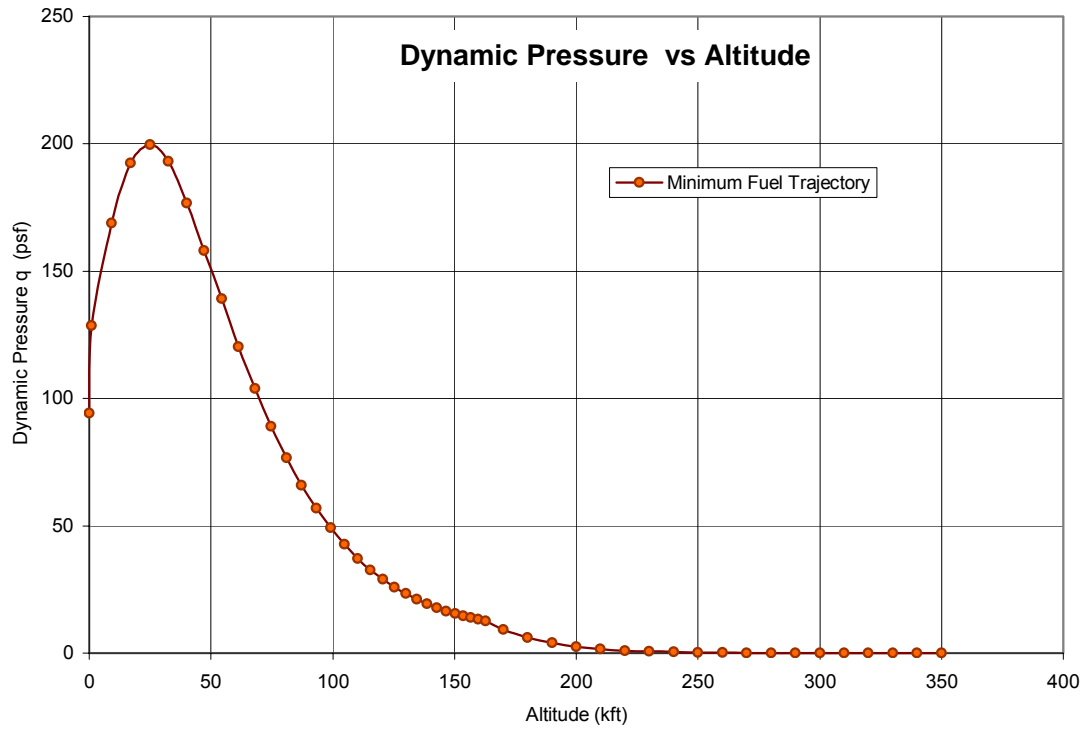


Figure 112: Variation of dynamic pressure with altitude for minimum fuel trajectory of OU XP

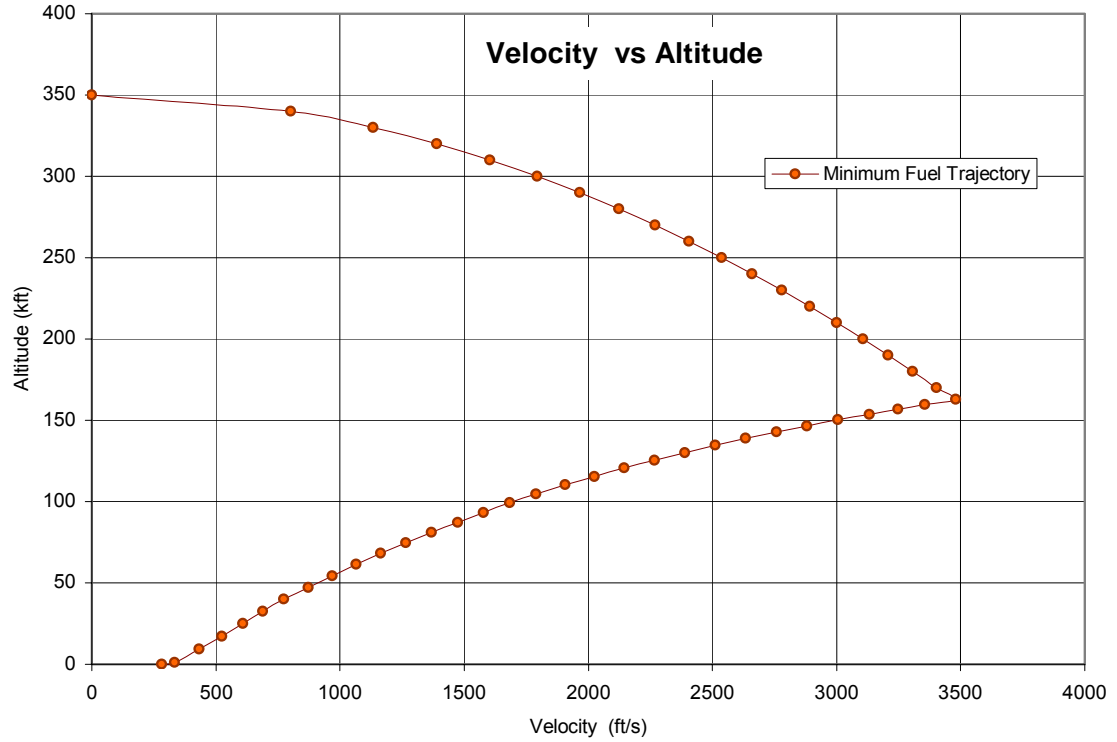


Figure 113: Variation of flight speed with altitude for minimum fuel trajectory of OU XP

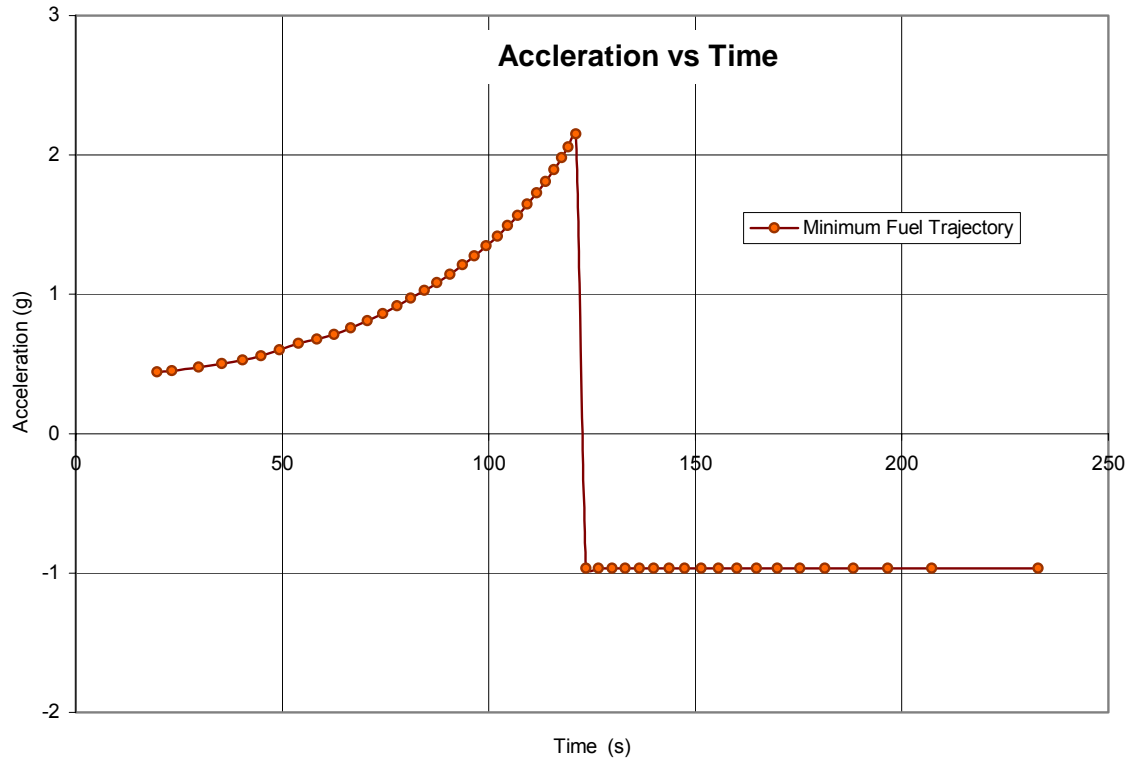


Figure 114: Variation of axial acceleration with time for minimum fuel trajectory of OU XP

5.3.3 Reentry

A typical return trajectory of a suborbital space vehicle starts with ballistic reentry and continues with a glide back to the terminal area. The primary design parameters of reentry trajectories were investigated to achieve the required down range, while the vehicle still satisfied limitations such as aerodynamic heating, heat flux rate, deceleration rate, and maximum dynamic pressure. Figure 115 shows the sub-synthesis design process of the reentry segment. After obtaining the geometry data from the baseline vehicle and the propellant weight from the ascent phase, the configuration concept was iterated to arrive at efficient aerodynamic characteristics and a ballistic parameter valid for the imposed mission and design requirements.

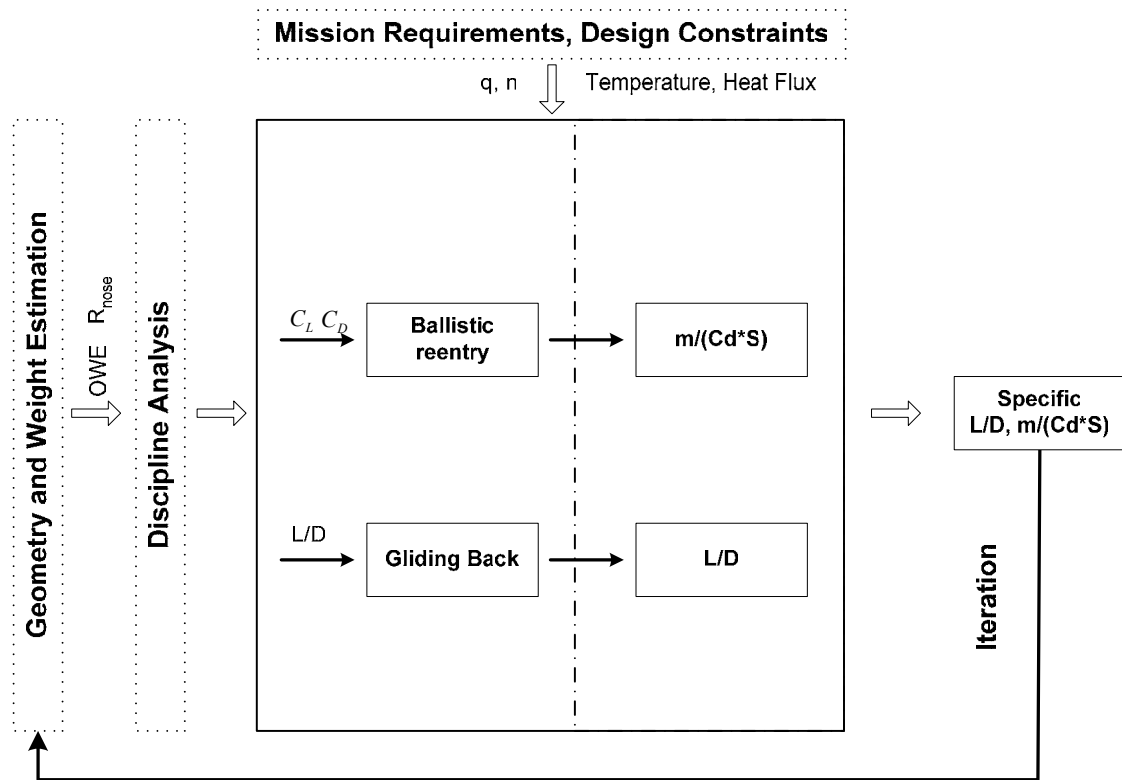


Figure 115: Multidisciplinary design analysis of reentry segment

A program (**SAV_REENTRY**) was developed based on the reentry equations derived in Chapter 4.3.3. It can determine the variation of the main design parameters throughout the reentry phase. Figure 116 shows a screen shot of this Excel program to estimate reentry speed and deceleration for different reentry conditions.

Design Parameters				Performance Analysis						
Design Parameters				Performance Data						
m	4050	kg		g	ΔH	s	V	a	"g"	an + at
Sw	245	ft ²		m	m					
γ	80	deg		9.8						
SIN	0.98			9.8	100	101.54				
COS	0.17			9.8	100	101.54				
m/Cd*A	1200	kg/m ²		9.8	100	101.54				
Cd*A	4.16666667			9.8	100	101.54				
an	0.17			9.8	100	101.54				
Z=g/RT	0.000118	m-1		9.8	100	101.54				
Design Constraints				9.8	100	101.54	0		0.94	
q	500	psf		9.8	100	101.54	44.2718872	9.65	0.98	1.00
	23939.48	pa	N/m ²	9.8	100	101.54	62.6099026	9.65	0.98	1.00
	1000	psf		9.8	100	101.54	76.6811561	9.65	0.98	1.00
	47878.96	pa	N/m ²	9.8	100	101.54	88.5437711	9.65	0.98	1.00
	500	psf		9.8	100	101.54	98.9949443	9.65	0.98	1.00
	23939.48	pa	N/m ²	9.8	100	101.54	108.443527	9.65	0.98	1.00
Temperature	500	F		9.8	100	101.54	117.132395	9.65	0.98	1.00
	959.67	R		9.8	100	101.54	125.219795	9.65	0.98	1.00
	533.15	K		9.8	100	101.54	132.815647	9.65	0.98	1.00
	800	F		9.8	100	101.54	139.999983	9.65	0.98	1.00
	1259.67	R		9.8	100	101.54	146.833219	9.65	0.98	1.00
	699.82	K		9.8	100	101.54	153.362293	9.65	0.98	1.00
	1000	F		9.8	100	101.54	159.624533	9.65	0.98	1.00
	1459.67	R		9.8	100	101.54	165.650203	9.65	0.98	1.00
	810.93	K		9.8	100	101.54	171.464247	9.65	0.98	1.00
				9.8	100	101.54	177.08751	9.65	0.98	1.00
				9.8	100	101.54	182.537624	9.65	0.98	1.00
				9.8	100	101.54	187.829662	9.65	0.98	1.00
				9.8	100	101.54	192.97663	9.65	0.98	1.00
				9.8	100	101.54	197.989841	9.65	0.98	1.00
				9.8	100	101.54	202.879211	9.65	0.98	1.00
				9.8	100	101.54	207.653489	9.65	0.98	1.00
				9.8	100	101.54	212.320438	9.65	0.98	1.00
				9.8	100	101.54	216.886987	9.65	0.98	1.00
				9.8	100	101.54	221.359349	9.65	0.98	1.00
				9.8	100	101.54	225.743124	9.65	0.98	1.00
				9.8	100	101.54	230.043374	9.65	0.98	1.00
				9.8	100	101.54	234.2647	9.65	0.98	1.00
				9.8	100	101.54	238.411294	9.65	0.98	1.00
				9.8	100	101.54	242.486991	9.65	0.98	1.00
				9.8	100	101.54	246.495306	9.65	0.98	1.00
				9.8	100	101.54	250.439475	9.65	0.98	1.00
				9.8	100	101.54	254.322482	9.65	0.98	1.00
				9.8	100	101.54	258.147089	9.65	0.98	1.00

Figure 116: SAV_REENTRY program for reentry analysis

Based on this Excel program, the design analysis of the vehicle reentry path was performed. The ballistic parameter $m/(C_D S)$ of OU XP was estimated at around 1000 kg/m². Figure 117 shows the design constraints for the vehicle. The light green lines represent the dynamic pressure constraints, 500 psf and 1000 psf, respectively. The stagnation temperature constraints (500°F and 800°F) are indicated with green lines. The

convective heat rates, 50 Btu/ft²/s and 100 Btu/ft²/s, are shown in the lower right hand corner.

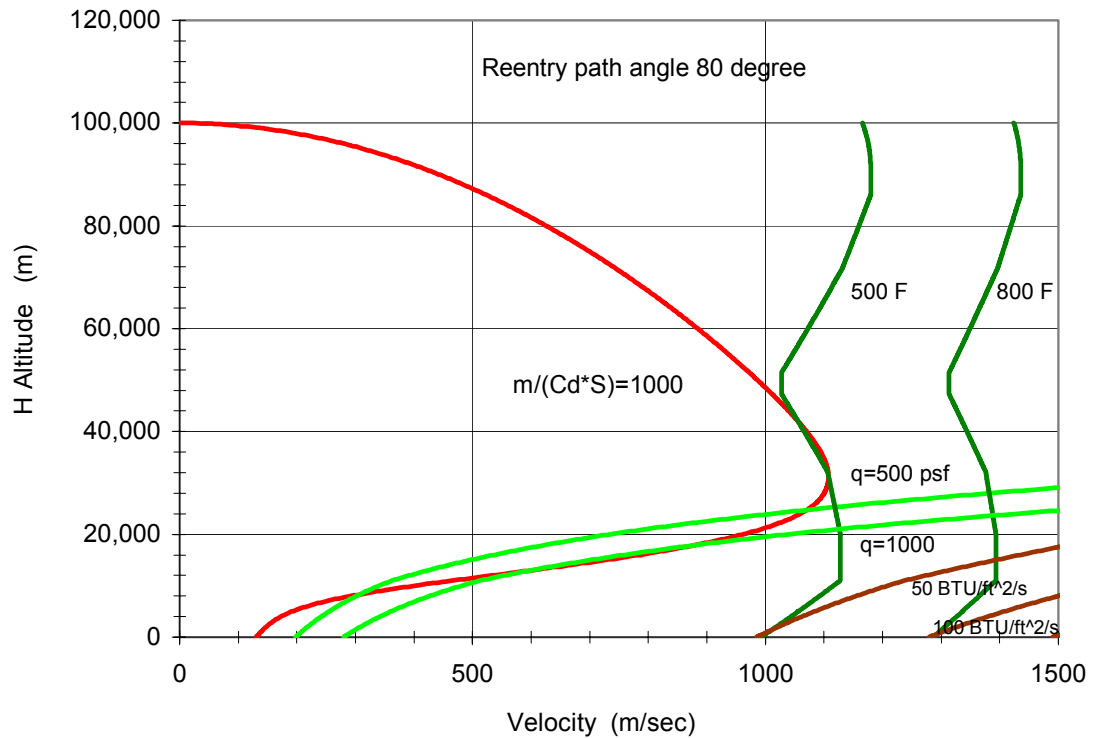


Figure 117: Design space for ballistic entry of OU XP

Based on Figure 117, an entry flight path was determined with the consideration of the related design constraints. The suborbital vehicle initially enters the atmosphere at higher angle-of-attack, thus, with a higher ballistic coefficient, until it reaches a design constraint (for example, a stagnation temperature of 500°F). Then, it starts to rotate its nose down (de-rotates) to decrease the angle-of-attack resulting in the final glide back to the terminal area. Also, since the aerodynamic efficiency (L/D) of the *OU XP* was between 5 and 7 at this flight phase, the cross range (assumed 25 miles from the launch

airport) was easily achieved by Eq. (4-44) for the vehicle starting to glide at an altitude of above 5 miles. Figure 118 shows the variation of deceleration rate with altitude.

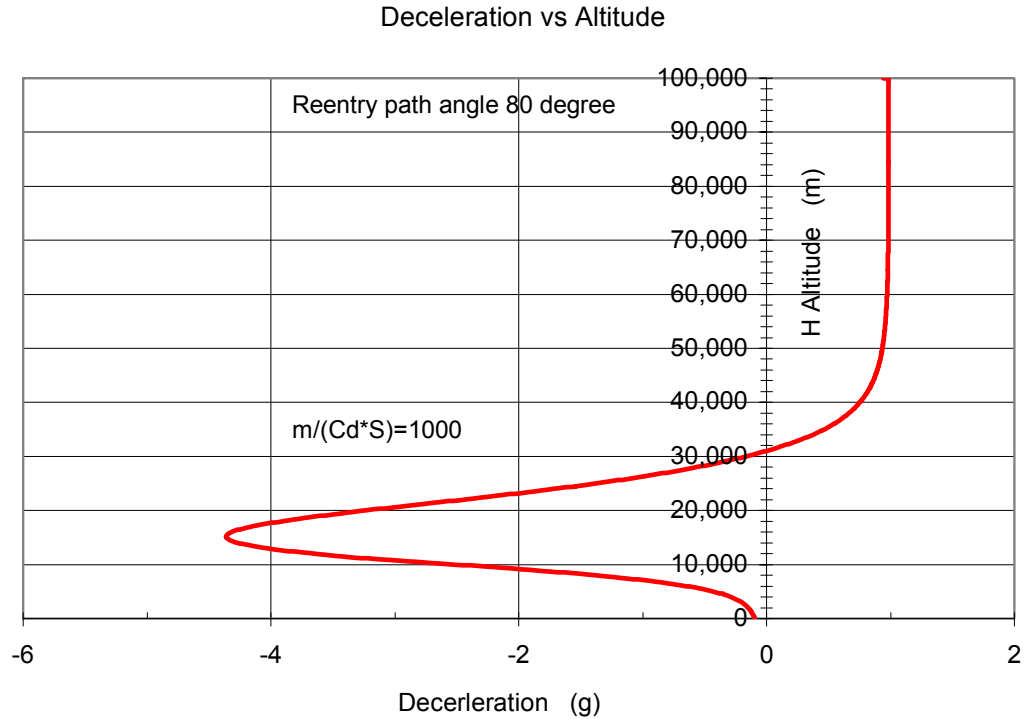


Figure 118: Variation of deceleration with altitude

5.3.4 Approach and Landing

Figure 119 shows the sub-synthesis design process of the landing segment. The design of the landing phase aims to provide a balance between landing distance requirements and the landing performance of the vehicle. For detailed information about the approach and landing design analysis, please refer to Chapter 4.3.4.

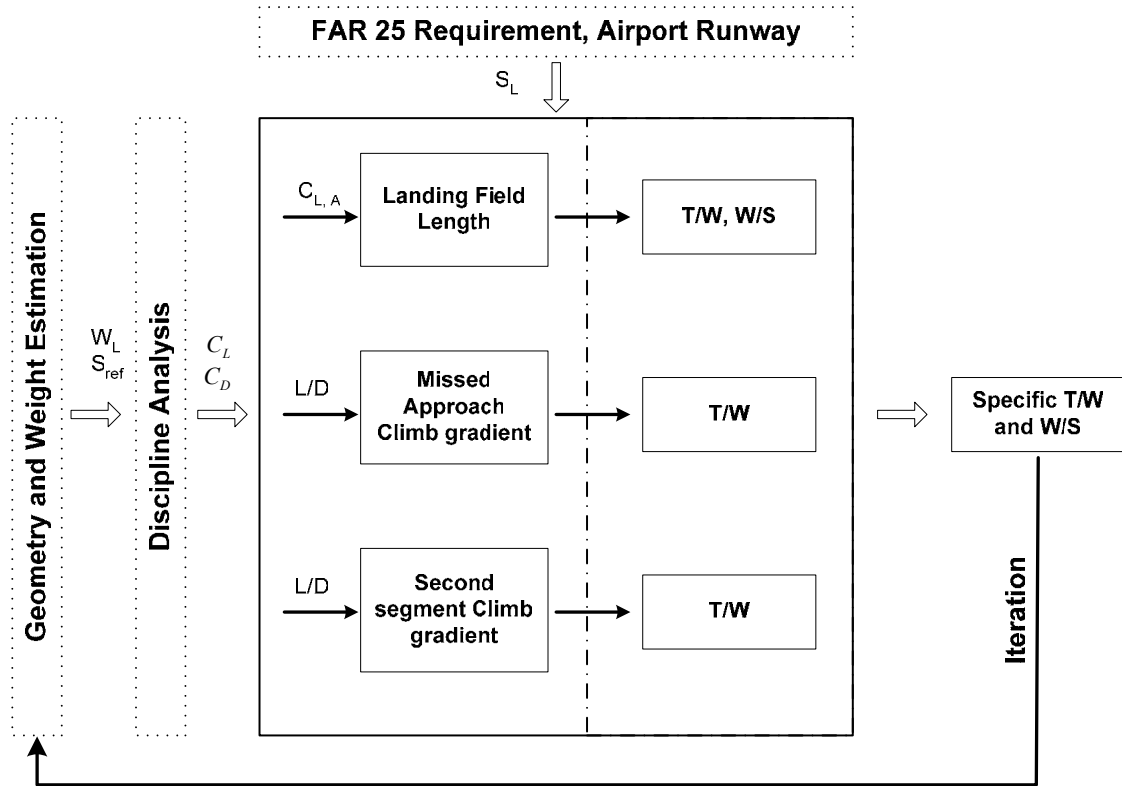


Figure 119: Multidisciplinary design analysis of landing segment

Two programs (**SAV_LANDE** based on empirical methods and **SAV_LANDA** based on analytical methods) were developed to determine the variation of the key design parameters throughout the landing phase. Figure 120 shows a screen shot of these Excel programs to estimate landing field length, wing loading (W/S), and thrust to weight (T/W) ratio under different landing conditions. In accordance with the particular characteristics of the conceptual design (CD) phase, emphasis was placed on overall simplicity and minimum data input requirements. As a consequence, the key design parameters can be evaluated quickly and efficiently.

Missed Approach Climb gradient

Landing Missed Approach Climb Gradient				
Missed Approach Climb				
	T/W	=	1/LD + γ	
	γ	=	0.021	Engine # 2
	γ	=	0.024	3
	γ	=	0.027	4
Horizontal Tail (HT)	L/D	=	5.160	
Canard	L/D	=	7.790	
				Engine #
Horizontal Tail (HT)	T/W	=	0.215	2
	T/W	=	0.218	3
	T/W	=	0.221	4
				Engine #
Canard	T/W	=	0.149	2
	T/W	=	0.152	3
	T/W	=	0.155	4
	W/S (psi)	=	0	50
				100
Horizontal Tail (HT)	T/W	=	0.215	0.215
Canard	T/W	=	0.149	0.149

T/W and W/S requirement

FAR25

Figure 121: T/W requirement for missed approach climb

(a) Landing Field Length:

The variations of wing loading (W/S) with maximum lift coefficient for different FAR landing field length requirements is shown in Figure 122. It can be clearly seen that the *OU XP* design satisfied the 8,000 ft landing field length and it would be able to land at a shorter distance if the maximum landing lift coefficient, $C_{L_{Landing}}$ were increased.

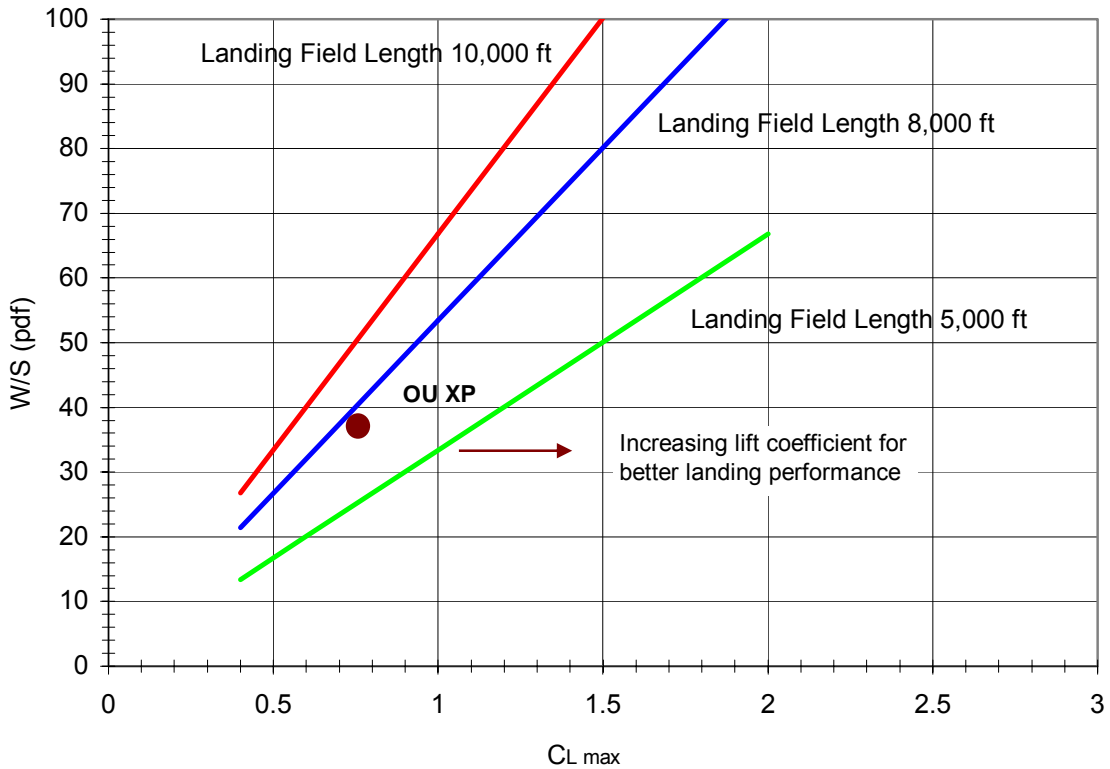


Figure 122: Wing loading vs. maximum lift coefficient

(b) Missed Approach Climb Gradient:

The lift to drag (L/D) ratio of the *OU XP* with the canard configuration is 7.79 and 5.16 for the horizontal tail configuration. The thrust to weight (T/W) ratios for both 'landing missed approach climb gradient requirements' are shown in Figure 123. As can be seen, the horizontal tail configuration required a larger T/W due to its lower L/D .

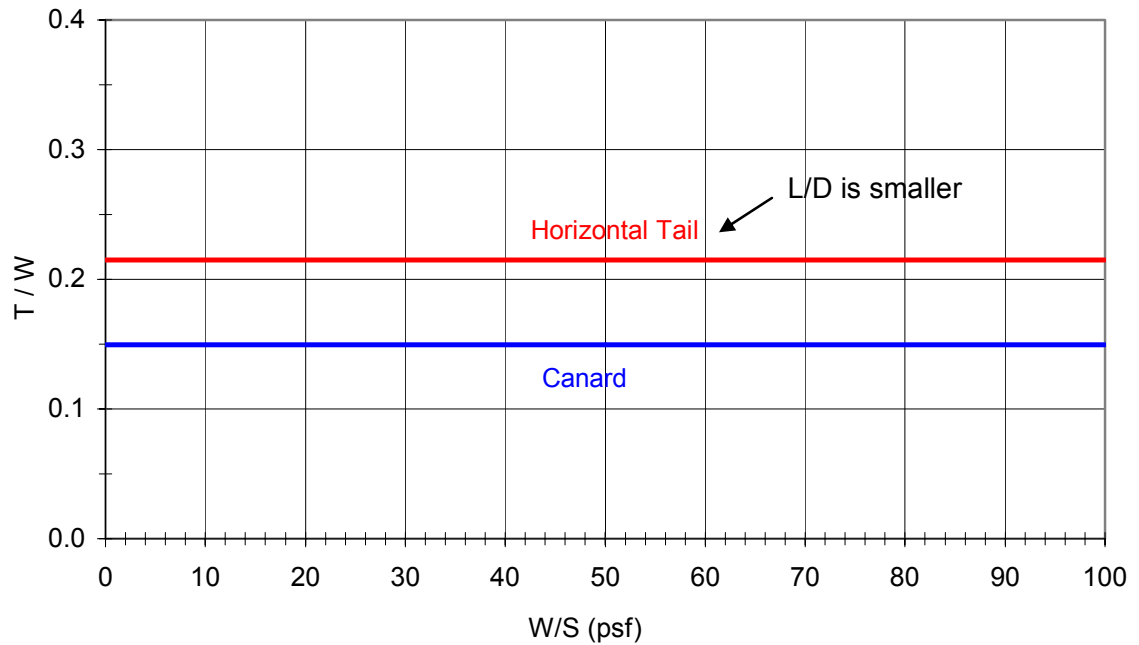


Figure 123: Landing missed approach climb gradient requirement

5.3.5 Design Space Screening

After key design parameters had been determined from the sub-synthesis design analysis throughout the flight loop, various configurations were analyzed at the master-synthesis level. The boundaries of the feasible design space were identified by design space screening as shown in Chapter 4.4. Figure 124 shows the program (**SAV_DSC**) to evaluate the Industrial Capability Index (ICI) and technology indexes (I_p and I_{str}) for the *OU XP*. This process of screening the available design space resulted not only in a single fully converged vehicle, but a range of converged vehicles, of which the best (optimum) vehicle for the design requirements was arrived at during the final step of the methodology.

Design Space Screening				
OU XP with 70 LE sweep				
Swet	=	1063.0	ft ²	
Splan	=	382.6	ft ²	
wing area	=	245.0	ft ²	
gross weight	=	19779.0	lb	
fuel weight	=	9890.0	lb	
Structure weight	=	4467.0	lb	
max payload	=	1200.0	lb	
cabin volume	=	380.0	ft ³	
Volume	=	634.5	ft ³	
tau	=	0.08		
thrust	=	5520.0	lb	
T/W	=	0.28		
propellant density	=	4.0	lb/ft ³	
WR	=	2.2	2.0 - 2.4	
I_p	=	3.3		
I_{str}	=	4.2		
ICI	=	0.8		

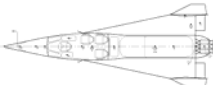
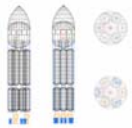
Key Design Parameters

Evaluate the technology index and Industrial capability index for design space screening

Figure 124: Excel program for design space screening

Based on the above program **SAV_DSC**, the Industrial Capability Index (ICI), and technology indexes (I_p and I_{str}) of the *OU XP* and the *TGV Michelle-B* were obtained and are shown in Table 36.

Table 36: Industrial capability index, technology indices of OU XP and TGV Michelle-B

Configurations	Parameters	Concepts	τ	S_{plan}	I_p	I_{str}	ICI
		Horizontal Takeoff and Horizontal Landing	0.081	383 ft ²	3.33 lb/ft ³	4.17 lb/ft ²	0.8
		Vertical Takeoff and Vertical Landing	0.3556	303.54 ft ²	3.33 lb/ft ³	5.4 lb/ft ²	0.62

The design space screening process presented in Chapter 4 was used to place the various indices (ICI , I_p , and I_{str}) in the solution space. Figure 125 shows the location of

these two concepts in the technology design space. The red point represents the design point of the *OU XP*, the blue point is the design point of the TGV *Michelle-B*. As can be seen, both of them are located in the feasible design regions of the wing-body and circular cone solution areas, respectively. Both of them have a maximum design margin, which means, both designs are converged for the given design requirements.

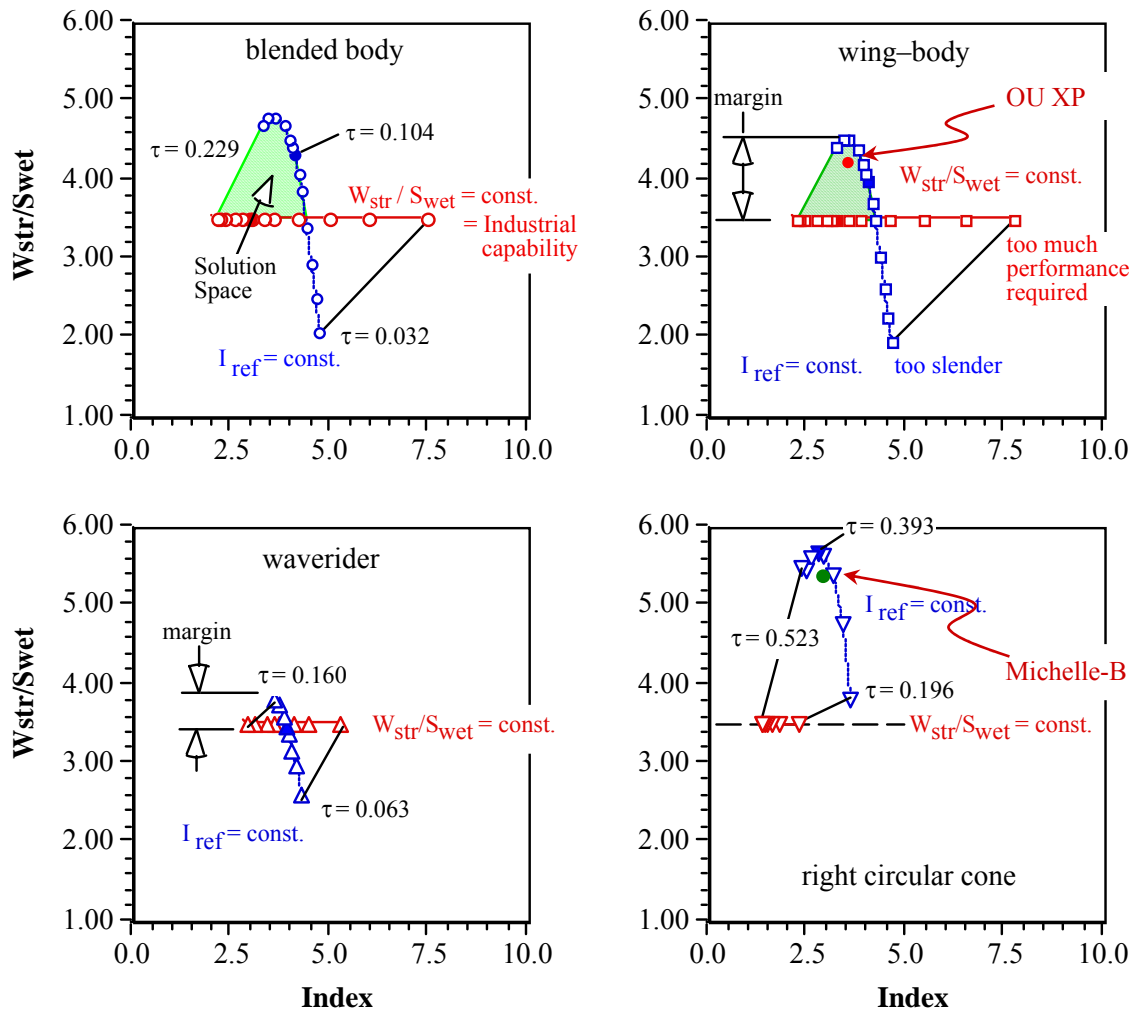


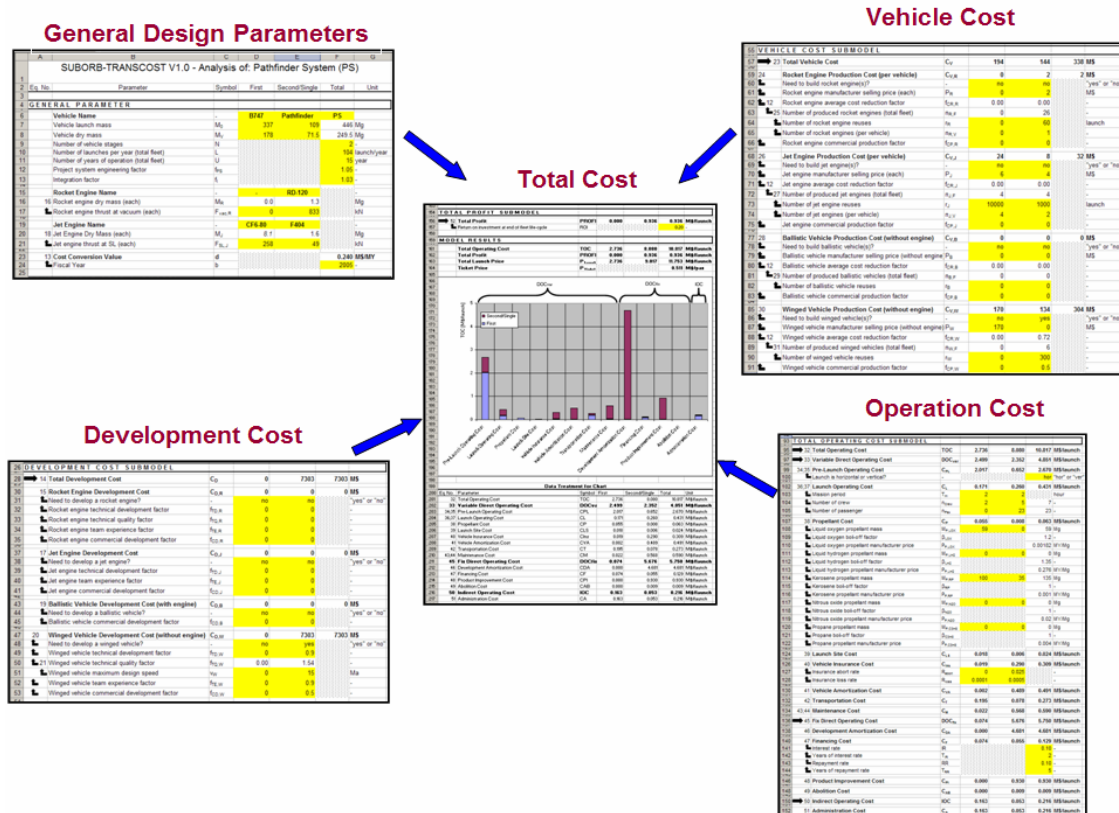
Figure 125: Design space of two possible SAV concepts

5.4 Cost Analysis

Until today, a large number of suborbital flight vehicles have been proposed. In order to illustrate the cost sensitivity of such suborbital vehicle, cost calculations were performed for several selected suborbital flight vehicle case studies to enable a fair basis for comparison. This cost analysis was performed by using the statistical-analytical model called SUBORB-TRANSCOST¹²⁰, see Figure 126. The suborbital flight vehicle case studies presented in Table 37 were selected because of availability of technical data and similarity in mission objectives (sub-orbital, reusable) compared to the *OU XP* design. It should be mentioned that the Ascender, Eclipse Astroliner, Kitten, and Pathfinder systems have been competing for the X Prize. This comparison will serve as an independent ‘first-order validation’ of the cost analysis results.

Table 37: Some suborbital flight vehicles

Vehicle	Developer	Country	Passenger	Launch Mass [Mg]	Apogee Altitude [km]
Micelle-B	TGV	USA	2	27.8	100
Ascender	Bristol Spaceplanes	UK	2	4.5	100
Eclipse Astroliner	Kelly Space and Technology	USA	40	327	162
Kitten	CFFC	USA	2	2.1	150
Pathfinder	Pioneer Rocketplane	USA	23	109	133
Roton C-9	Rotary Rocket Company	USA	14	181	>100
Space Cruiser	Vela Technology Development	USA	6	12.5	100



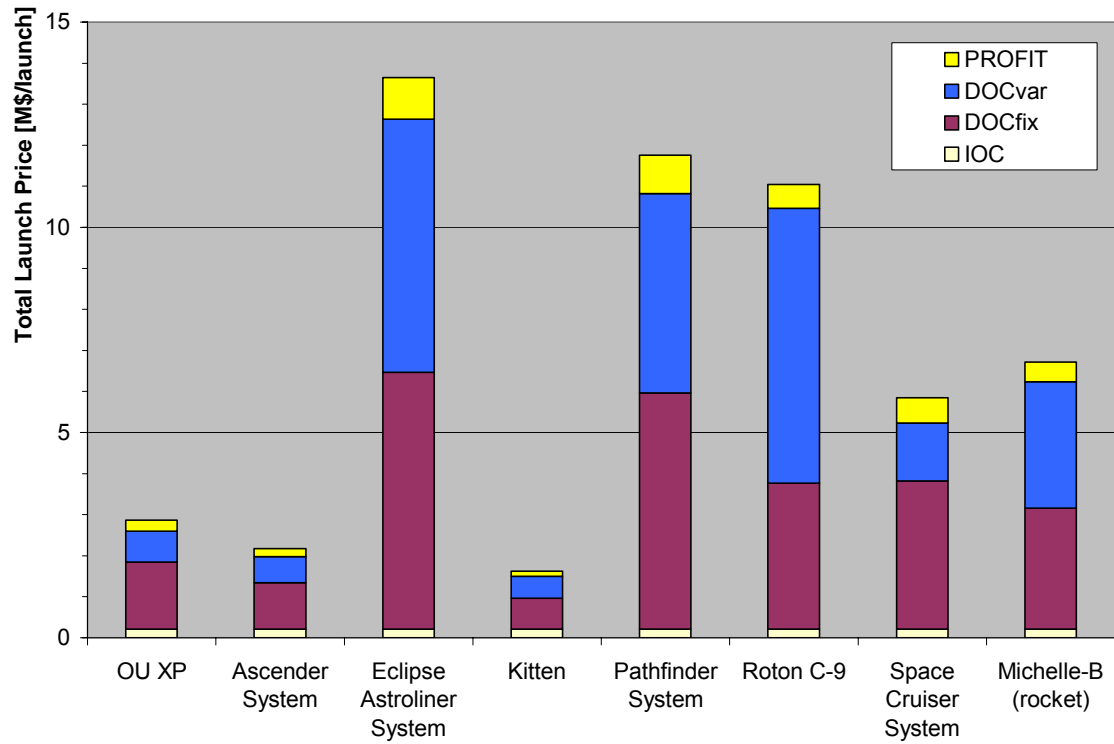


Figure 127: Total launch prices for several suborbital vehicles

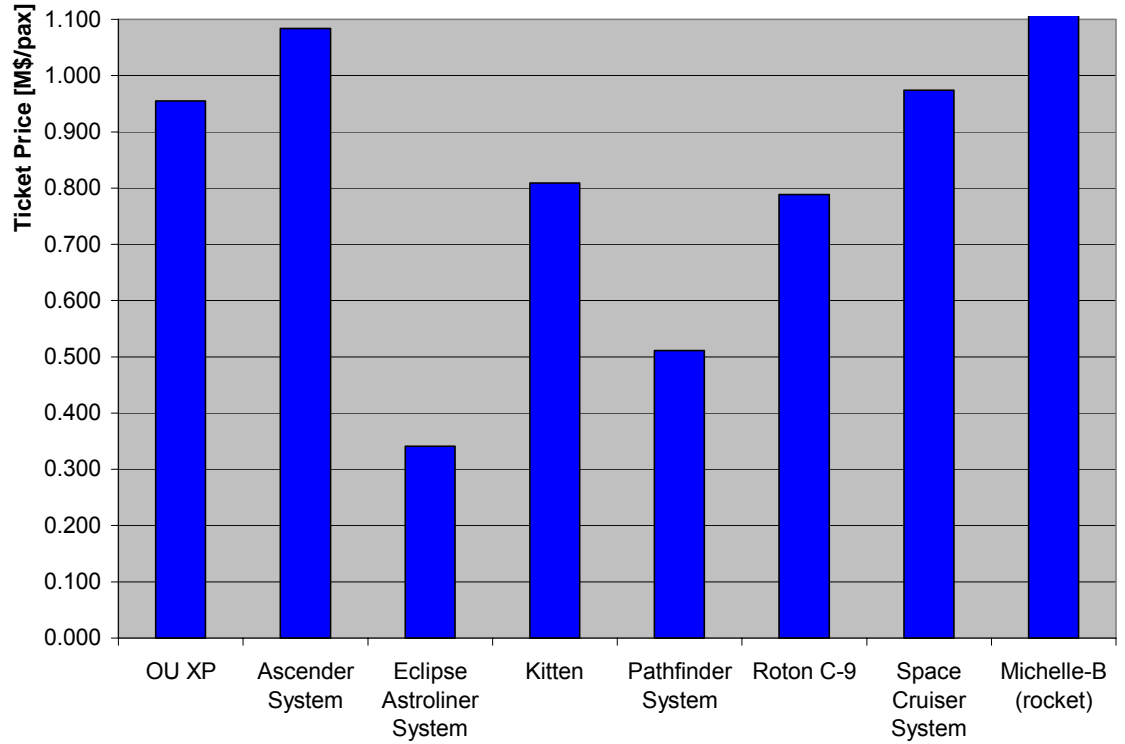


Figure 128: Ticket prices for several suborbital vehicles

Based on the above figures, the following conclusions can be drawn:

(1) As seen from these figures, the calculated ticket price per passenger for the *Michelle-B* is relatively high among the suborbital vehicles because it not only carries crew and passengers but also a 700-kg payload to the same altitude. By converting the 700 kg payload into passengers, the ticket price would drop. However, the *Michelle-B* design has no space provision for additional passengers.

(2) The ticket prices shown indicate that the higher the passenger capacity the lower the ticket price. The *Eclipse Astroliner* carries 40 passengers, whereby the *Pathfinder System* is able to carry 23 passengers. However, smaller scale development programs such as the *Michelle-B*, *Ascender*, and *Kitten* require less investment, thus, could begin service sooner. It should be noted that the smaller the initial investments the better the chances of finding an investor.

(3) The important design parameter direct operating cost (DOC) for *Michelle-B* shows that a large effort is required for the pre-launch operations. The higher risk levels of the vertical takeoff architecture become apparent, a fact assumed in the current version of SUBORB-TRANSCOST.

(4) The above studies clearly indicate the limitations of applying SUBORB-TRANSCOST directly to particularly the *Michelle-B* design. In order to apply this code efficiently to the *Michelle-B* design, the model needs to be improved by including that the airframe development cost and the assumed pre-launch cost require adjustment. In addition, SUBORB-TRANSCOST is currently taking Reference 119 (based on cost data published until 2003) into account; the additional revised 2003-2005 data need to be added.

Figure 129 is an overview of the entire ‘hands-on’ design synthesis methodology. It summarizes the design process, design components and all the programs developed for this ‘hands-on’ design methodology.



Figure 129: Overview of hands-on HTHL SAV design synthesis methodology

6. Contribution Summary and Recommendations

6.1 Summary

The future generation of reusable space access vehicles requires a paradigm shift away from Cayley's Design Paradigm. The second century of flight will see the emergence of true multi-disciplinary flight vehicle design resulting from generic synthesis methodologies. However, research clearly indicates that the current generation of synthesis systems is mainly used for aircraft design, both civil and military. Only a few computer-based space access vehicle design synthesis systems are known. To even complicate matters, most of these SAV synthesis systems are only developed for a specific type of vehicle and don't have the potential for being extended to other applications; J.L. Hunt's design methodology is only applicable to air-breathing vehicles, K.D. Wood's design methodology is only valid for expendable launch vehicles (Titan, Atlas and Delta), and SSSP only works for the Space Shuttle configuration concept, overall eliminating the opportunity to compare those vehicle concepts against each other using a consistent toolset. Such a dilemma poses a particular problem to today's SAV designer. As a consequence, inconsistent high fidelity tools are used during the conceptual level, tools not capable of visualizing the multi-disciplinary design space or being able to offer a proof of design convergence. The anatomy of the failure of all proposed RLV configuration concepts until today warrants the development of a generic synthesis SAV design methodology with the key features multi-disciplinary conceptual design capability, solution space visualization, proof of convergence capability, and the integration of a dedicated SAV knowledge-based system. This research idea has been

assessed and confirmed by design experts from NASA, Boeing, and Lockheed Martin to have a promising future and make a solid contribution to aerospace science.

As the discussion in Chapters 1 and 2 shows, a computer-based synthesis methodology is the key technology required to successfully size, synthesize, and converge the next generation of highly integrated low-cost space access transportation vehicles. Such a development will take place gradually but it will happen. One of the incremental steps is the development of the configuration independent (generic) ‘hands-on’ design methodology presented in this research thesis. This highly organized and transparent design process will be of help to those design environments which do not have access to an expensive computer-based synthesis system. Still, the capability to efficiently screen the design space ‘by hand’ should not be underestimated when done correctly. Clearly, during the conceptual design phase, a low-fidelity design space screening procedure like the one presented here can easily outperform expensive high-fidelity analysis tools because the deliverable during the CD level has to be correctness rather than accuracy. Moreover, it identifies how to get started. In particular, the presented methodology differentiates itself from other processes because it not just evaluates a configuration with its determining characteristics, but it sizes the configuration concept to a mission. The AVD Lab is utilizing the manual design sequence as a stepping stone towards the true space access vehicle synthesis environment AVDS-PrADO^{SAV}.

The research presented emphasizes the systematic organization of the SAV design process to minimize the design randomness usually seen during the conceptual design phase. In addition, the integration of a dedicated database and knowledge-based into either the manual or computer-based design sequence is inevitable for any serious design environment. We have surveyed too many past and in-progress SAV design projects which give a blind eye to the lessons supposedly learned from past experience. Still, the secret is to remember the past! The engineer's capability to screen the design space, to visualize the design space, and to converge the total design according to pre-defined figures of merit is at the heart of a true synthesis methodology.

The key original contribution of this research investigation is the development of a prototype hands-on synthesis methodology capable of identifying the convergence design space of a range of SAV design alternatives. The main activities of the researcher's effort to develop this prototype design synthesis methodology for generic SAV conceptual design are summarized as follows:

1. It is the first time that a comprehensive survey of 115 synthesis systems has been performed and evaluated. As a consequence, an informed specification for a future dedicated generic SAV conceptual design synthesis methodology has been defined. This specification clearly describes the path towards an integrated synthesis engineering approach for the multi-disciplinary design of SAVs.
2. Various research and development strategies leading to a generic space access vehicle conceptual design level methodology have been proposed. For the highly demanding multi-disciplinary task of arriving at a generic conceptual design SAV

synthesis methodology, only a systematic research strategy can ensure successful development of this *Class V* SAV synthesis system.

3. The different design configurations and physical aspects of various SAVs are investigated. The generic characteristics of various SAVs' mission profiles show the applicability of the proposed generic mission profile. As a consequence, the HTHL configuration, itself offering the most comprehensive mission profile, has been selected as a baseline vehicle for the development of the generic design synthesis methodology. The initial framework for a dedicated SAV design knowledge-based system KBS^{DESIGN} (*Data Domain, Engineering Domain, and Process Domain*) has been developed. This particular strength of the system enables the user to quickly gain fundamental understanding of solution concepts realized in the past which will lead to informed decision making. Throughout the flight mission profile, the design constraints and primary key design parameters are identified for the major design disciplines (e.g., aerodynamics, structures) which are of relevance during the conceptual design stage. A prototype design methods library for those major design disciplines has been developed and integrated into the hands-on SAV design methodology.

4. A "hands-on" design methodology and algorithm for HTHL SAVs has been developed based on an abstract mission profile consisting the takeoff, ascent, reentry, approach, and landing segments. For each mission segment, the result of the multidisciplinary design analysis (e.g., geometry, weight and balance, aerodynamics, stability and control, aerothermodynamics, propulsion, etc.) is imported into the sub-synthesis module which determines and visualizes design constraints. The sub-synthesis constraints for each mission segment are then input into the master synthesis level which

discusses the resulting design space for the entire mission profile. Vehicle design convergence leading to a SAV design proposal is sought based on sub-synthesis and master-synthesis design spaces. This “hands-on” design methodology helps the engineer visualize the physical design space leading to a converged total design. Synthesis tools and disciplinary computer codes have been developed for each flight segment. The associated algorithms have been validated with selected supersonic vehicles and SAV vehicles (wing body, lifting body, and cone concepts). Table 38 summaries the overall development contributions for the generic SAV design synthesis methodology.

Table 38: Overall development contributions for the generic SAV design synthesis methodology.

Development Contributions	AVD	Developer - Xiao Huang
Synthesis systems evaluation	Literature papers	Survey and evaluations
Knowledge-Based	Aircraft	Space access vehicles
Database	Aircraft	Space access vehicles
Generic concept	A generic approach for the stability and control of conventional and unconventional aircraft configurations	A generic approach for the SAV conceptual design is proposed and implemented based on the mission profile.
Design synthesis methodology for HTHL SAVs		Multidisciplinary design synthesis methodology for the takeoff, ascent, reentry, landing phases are developed and validated.
Programs	AVDS-PrADO	SAV_HASA, SAV_BFL, SAV_CLM, SAV_TSSP, SAV_REENTRY, SAV_LANDE, SAV_LANDA, SAV_DSC

5. The feasible design solution space for HTHL vehicles has been identified. The activity that identifies the topography of the design solution space is essential to ensure worthwhile detailed multi-disciplinary optimization studies of the more refined vehicle. The process of design space screening incorporates the KBS^{DESIGN} , historical and empirical information, and current technology limitations, all contributing to the definition of the design space. In addition, system level design space screening eliminates gross mistakes due to existing SAV design knowledge available ‘at the fingertips’. This

process helps the design engineer to iterate the baseline configuration towards a final converged design. Overall, the methodology has been devised to ensure safe, successful, and profitable space access vehicles.

6. An outlook towards the implementation of the VTVL logic into this ‘hands-on’ HTHL design methodology has been presented. This research undertaking has, for the first time, outlined an approach to arrive at a generic SAV methodology.

6.2 Recommendations

The development of a multi-disciplinary conceptual design capability for SAVs requires a highly systematic and consistent approach. Since it is a demanding task to develop a generic multi-disciplinary SAV design system within a Ph.D. research time frame, it has been the objective from the outset to develop a functioning prototype system with focus on overall simplicity and correctness in the context of ‘how to get started’. This approach contrasts the usual design approach, where accuracy is substituted for correctness with the adaptation of preliminary to detail design methods.

The following work is recommended in order to continue the presented research towards a more complete and advanced, thus, generic prototype SAV design methodology:

(1) The dedicated SAV design knowledge-based system KBS^{DESIGN} needs to be continually updated and organized in a systematic way.

(2) A detailed investigation of the takeoff and landing segment for the VTVL vehicle is necessary. The development of new sub-synthesis modules for both segments is required to complete the design methodology for VTVL vehicles.

(3) The integration of appropriate multidisciplinary design optimization techniques and tools has to be considered. As soon as the SAV design concepts have been identified within the feasible design solution space, multidisciplinary design optimization needs to be applied to identify the final design proposal complying with the pre-defined objective function like minimum gross weight or minimum direct operating cost.

(4) In a follow-on step, the generic SAV ‘hands-on’ design algorithm needs to be integrated into the computer-based system AVDS-PrADO. Having validated the generic SAV modules in a stand-alone mode, it is planned to integrate the SAV algorithm into the existing AVDS-PrADO synthesis system at the AVD Lab, The University of Texas. The baseline synthesis system PrADO²² has been under development since 1986 by Dr. Heinze at the Technical University of Braunschweig, Germany. The design capability of the baseline PrADO system is shown in Table 39. Its design synthesis capabilities are: (1) Data Input and Representation of the Results [Data Visualisation]; (2) Disciplinary Analysis, Single-Point Analysis, Parameter Variation, Optimisation; (3) Iterative Design Process [Convergency-Check, Program Execution]; (4) Problem-Oriented Program Libraries [Disciplinary Analysis Models], (5) Data Management System [Computer-Based Management System]. Also, the successful application of PrADO in industry (aerospace, automobile), research organizations, and academia shows the flexibility, integration capability, and growth potential of the system.

Table 39: Design capability of PrADO

PrADO	Capabilities	
Configuration	TAC (Tail-Aft Configuration)	
	TFC (Tail-First Configuration)	
	TSC (Three-Surface Configuration)	
	FWC (Flying-Wing Configuration)	
Speed Range	Subsonic Design	
	Transonic Design	
	Supersonic Design	
	Hypersonic Design	
Design Applications	UAV (Unmanned Aerial Vehicle)	[Subsonic Design]
	High-Performance Glider	[Subsonic Design]
	Transport/Freighter (TAC/BWB)	[Transonic Design]
	Cryogenic Aircraft (Cryoplane)	[Transonic Design]
	‘Green’ Aircraft	[Transonic Design]
	Global Range Aircraft	[Transonic Design]
	Elastic Aircraft	[Transonic Design]
	SCT (Supersonic Com. Transport)	[Supersonic Design]
	Two-Stage-to-Orbit (TSTO)	[Hypersonic Design]
	Airship	
	Automobiles	

Reference

¹SBA ISG, Simulation Based Acquisition Industry Steering Group., “*SBA Functional Description*,” URL: <https://www.msiac.dmsomil/sba/generalinfo.asp> [cited 24 February 1999].

²Chudoba, B., “*Managerial Implications of Generic Flight Vehicle Synthesis*,” Invited Lecture, New Airplane Product Development, The Boeing Company, Renton, Seattle, 17 December 2004.

³Cayley, G., “On Arial Navigation,” *Nicholson’s Journal*, Vol. 24, 1809, pp 164–174, Vol. 25, 1810, pp 81-87, 161-173.

⁴Czysz, P. A., “*Hypersonic Convergence – Volume 1*,” AFRL-VA-WP-TR-2004-3114, Air Force Research Laboratory, December 2004.

⁵Shishko, R., “*NASA Systems Engineering Handbook*,” SP-6105, NASA, June 1995.

⁶Chudoba, B., “*Stability and Control of Conventional and Unconventional Aircraft Configurations – A Generic Approach*,” First Edition, Books on Demand, April 2001 [ISBN 3-8311-2982-7].

⁷Chudoba, B., “*Managerial Implications of Generic Flight Vehicle Design Synthesis*,” AIAA Paper, AIAA-2006-1178, 44th AIAA Aerospace Sciences Meeting and Exhibit, Reno, 9-12 January 2006

⁸Hirschel, E. H., “*Towards the Virtual Product in Aircraft Design*,” Fluid Dynamics and Aeronautics New Challenges, CIMNE Handbooks on Theory and Engineering Applications of Computational Methods, Barcelona, Spain 2003, pp 453–464.

⁹Chudoba, B., “*Energy for Cruising Flight*,” AME 4593/5593, Lecture Notes *Space Systems & Mission Design*, Spring Semester 2005, The University of Oklahoma, May 2005.

¹⁰Wood, D., “*Project Cancelled – British Aircraft That Never Flew*,” First U.S. Printing, The Bobbs-Merrill Company, Indiana, 1975.

¹¹Huang, X., Chudoba, B., and Coleman, G., “*A Generic Hands-On Conceptual Design Methodology Applied to a Tourist Space Access Vehicle*,” AIAA Paper, AIAA-2006-1242, 44th AIAA Aerospace Sciences Meeting and Exhibit, Reno, 9-12 January 2006.

¹²Hammond, W. E., “*Design Methodologies for Space Transportation Systems*,” First Edition, AIAA Education Series, 2001.

¹³Straub, W. L., “*Managerial Implication of Computerized Aircraft Design Synthesis*,” *Journal of Aircraft*, Vol. 11, No. 3, 1974, pp 129 - 135.

¹⁴PACE, URL: <http://www.pacelab.com/en/newsdetail.php?myid=6&theid=572> [cited November 2004].

¹⁵Nickol, C., “*Vehicle Systems (VS) Program Efficient Aerodynamic Shapes & Integration (EASI) Project: Conceptual Design Shop (CDS) Sub-Project Overview*,” NASA Langley Research Center, September 2004.

¹⁶Hammond, W. E., “*Space Transportation: A Systems Approach to Analysis and Design*,” AIAA Education Series, 1999.

¹⁷Chudoba, B., Huang, X., Coleman, G. and Czysz, P. A., “*Future Space Tourism Transportation Design Requirements*,” AIAA Paper, AIAA-2005-3445, AIAA/CIRA International Space Planes and Hypersonic System and Technologies Conference, Capua, Italy, 16-20 May 2005

¹⁸Torenbeek, E., “*Synthesis of Subsonic Airplane Design*,” Second Printing, Delft University Press, Kluwer Academic Publisher, Netherlands, 1982.

¹⁹Chudoba, B., and Huang, X., “*Development of a Dedicated Aerospace Vehicle Conceptual Design Knowledge-Based System*,” AIAA Paper, AIAA-2006-0225, 44th Aerospace Sciences Meeting and Exhibit, Reno, 9-12 January 2006

²⁰Roberts, K., Mixon, B., Chudoba, B., and Huang, X., “*A Unique Conceptual Design Approach: Generic Design Space Screening and Convergence of Hypersonic Vehicles*,” AIAA Paper, AIAA-2006-1241, 44th AIAA Aerospace Sciences Meeting and Exhibit, Reno, Nevada, 9-12 January 2006

²¹Huang, X., “*A Prototype Computerized Synthesis Methodology for Generic Space Access Vehicle (SAV) Conceptual Designs*,” Invited Student Paper, AIAA-2005-2539, 1st Space Exploration Conference, January 2005.

²²Chudoba, B., and Pouillard, S., “*Aircraft Conceptual Design Tool Development – Qualitative User-Assessment of the Aircraft Conceptual Design Software PrADO*,” E02-011/2001, Future Projects & Technologies E02, Fairchild Dornier GmbH, 19 February 2001.

²³Soanes, C., and Stevenson, A., “*The Concise Oxford English Dictionary*,” Oxford University Press, 11th Edition, October 7, 2004.

²⁴Moore, W. F., “*A Model for the Configuration Integration Process*,” AIAA Paper 95-3905, Aircraft Engineering, Technology, and Operations Congress, Los Angeles, September 1995.

²⁵Lee, V. A., Ball, H. Glenn, Wadsworth, E.A., Moran, W.J., and McLeod, J.D., “*Computerized Aircraft Synthesis*,” Journal of Aircraft, Vol. 4, No. 5, Sept.-Oct. 1967, pp 402-408.

²⁶David, J. S., and Wisniewski, J. S., “*User’s Manual for HESCOMP the Helicopter Sizing and Performance Computer Program*,” Boeing Vertol Company, Philadelphia, PA, September 1973.

²⁷Powell, R. W., Striepe, S. A., Desani, P. N., Braun, R. D., Brauer, G. L., Cornick, D. E., Olson, D. W., Peterson, F. M. and Stevenson, R., “*Program To Optimize Simulation Trajectories (POST): Volume II, Version 5.2, Utilization Manual*,” NASA Langley Research Center, Hampton, VA, October 1997.

²⁸McCullers, L. A., “*Flight Optimization System, Computer Program and Users Guide*,” Version 5.7, NASA Langley Research Center, Hampton, Va., December 1994.

²⁹Ardema, M. D., and Williams, L.J., “*Automated Synthesis of Transonic Transports*,” AIAA Paper 72-794, Los Angeles, August 1972.

³⁰Kossira, H., Bardenhagen, A., and Heinze, W., “*Investigations on the Potential of Hypersonic Waveriders with the Integrated Aircraft Design Program PrADO-Hy*,” AIAA Paper 93-5098, 5th International Aerospace Planes and Hypersonics Technologies Conference, München, November - December 1993.

³¹Wallace, R. E., “*A Computerized System for the Preliminary Design of Commercial Airplanes*,” AIAA Paper 72-793, Los Angeles, August 1972.

³²Dovi, A. R., Wrenn, G. A., and Barthelemy, J.-F.M., “*Multidisciplinary Design Integration System for a Supersonic Transport Aircraft*,” AIAA Paper 92-4841, 4th Multidisciplinary Analysis and Optimization, Cleveland, 1992.

³³Dirk V. R., “*Technology Assessment with Multi-Disciplinary Aircraft Design Tools on the Next Generation Supersonic Commercial Transport*,” ICAS 96-3.5.1, Naples, 1996.

³⁴Convair Aerospace Division of General Dynamics., “*Space Shuttle Synthesis Program (SSSP)- Volume I, Part I, Engineering and Programming Discussion Final Report*,” Report No. GDC-DBB70-002, December 1970, Presented by Contract NAS9-11193, Submitted to National Aeronautics and Space Administration, Manned Spacecraft Center, Houston, Texas.

³⁵Szedula, J. A., “*FASTPASS: A Tool for Launch Vehicle Synthesis*,” AIAA Paper 96-4051-CP, Symposium on Multidisciplinary Analysis and Optimization, 6th, Bellevue, WA, 1996.

³⁶Huang, X., “*AVD-004-2003 Synthesis Systems Evaluation Reports*,” AVD Reports, AVD Laboratory, The University of Oklahoma, 15, December, 2003.

³⁷Nicolai, L. M., and Carty, A., “*Role of the Aerodynamicist in a Concurrent Multi-Disciplinary Design Process*,” Paper Presented at the Symposium of the RTO (Research and Technology Organization) Applied Vehicle Technology Panel (AVT) held in Ottawa, Canada, October 1999.

³⁸Wood, K. D., “*Aerospace Vehicle Design Volume II: Spacecraft Design*,” Johnson Publishing Company, Boulder, Colorado, 1964.

³⁹Czysz, P. A., and Mruthy S. B., “*Energy Management and Vehicle Synthesis*,” Developments in High-Speed-Vehicle Propulsion Systems, Progress in Astronautics and Aeronautics, 1996, ISBN 1-56347-176-0, Vol. 165, PP 581-686.

⁴⁰Hunt J. L., “*Hypersonic Airbreathing Vehicle Design (Focus on AERO-SPACE PLANE)*,” Hypersonics, Volume I: Defining the Hypersonic Environment, Birkhäuser Boston, 1989, pp 205-262.

⁴¹Rau, T. R., and Decker, J. P., “*ODIN: Optimal Design Integration System for Synthesis of Aerospace Vehicles*,” AIAA Paper 74-72, Aerospace Sciences Meeting, 12th, Washington, D.C., 1974.

⁴²Dirks, G., and Schneegans, A., “*Scenario Based Aircraft Design Using Knowledge Based Software Methods*,” ICAS 2000 Congress, Toronto, 2000, pp 5103.1-5103.10.

⁴³Hale, M. A., Mavris, D. N., and Carter, D. L., “*The Implementation of a Conceptual Aerospace Systems Design and Analysis Toolkit*,” SEA/AIAA 1999-01-5639, 1999.

⁴⁴Wennagel, G. J., Mason, P. W., and Rosenbaum, J. D., “*Ideas, Integrated Design and Analysis System*,” Paper 680728, Society of Automotive Engineers, October 1968.

⁴⁵Stanley, T. T., Alexander, R., and Landrum, D. B., “*A Collaborative Analysis Tool for Integrating Hypersonic Aerodynamics, Thermal Protection Systems, and RBCC Engine Performance for Single Stage to Orbit Launch Vehicles*,” AIAA Paper 99-4808, International Space Planes and Hypersonic Systems and Technologies Conference, 9th, Norfolk, November 1999.

⁴⁶AIAA MDO Technical Committee, <http://www.aiaa.org/portal/index.cfm?GetComm=80>, 2006.

⁴⁷Bartholomew, P., “*The Role of MDO within Aerospace Design and Progress Towards an MDO Capability*,” AIAA-98-4705, Symposium on Multidisciplinary Analysis and Optimization, 7th, St. Louis, 1998.

⁴⁸Sobieski, J., and Haftka, R. T., “*Multidisciplinary Aerospace Design Optimization: Survey of Recent Developments*,” AIAA 96-0711, Aerospace Sciences Meeting and Exhibit, 34th, Reno, 1996.

⁴⁹Malone, B., and Mason, W. H., “*Multidisciplinary Optimization in Aircraft Design Using Analytic Technology Models*,” Journal of Aircraft, Vol. 32, No. 2, March-April 1995, pp. 431-438.

⁵⁰Tejtel, D., “*Conceptual Aircraft Design Environment: Case Study Evaluation of Computing Architecture Technologies*,” AIAA Paper 98-4844, Symposium on Multidisciplinary Analysis and Optimization, 7th, St. Louis, 1998.

⁵¹Siegers, F., and Smith, H., “*Numerical Synthesis Methodology for Conceptual Design of New Generations of Combat Aircraft*,” AIAA Paper 95-3881, Aircraft Engineering, Technology, and Operations Congress, Los Angeles, 1995.

⁵²Schneider, G., Dalen, F. C., Krammer, J., and Stettner, M., “*Multidisciplinary Wing Design of a Regional Aircraft Regarding Aeroelastic Constraints*,” Optimization In Industry Conference, Banff, 1999.

⁵³Korte, J. J., Weston, R. P., and Zang T. A., “*Multidisciplinary Optimization Methods for Preliminary Design*,” NASA Langley Research Center, Multidisciplinary Optimization Branch, 2003.

⁵⁴Hollowell, S., and Bitten, R., “*Application of Multidisciplinary Optimization to Conceptual Aircraft Design at Rockwell International – A Status Report*,” AIAA Paper 92-1196, Aerospace Design Conference, Irvine, 1992.

⁵⁵Simos, D., *"Piano - Competitor Evaluation and Project Definition of Commercial Aircraft. At your desktop,"* Lissys Research Ltd., United Kingdom, 1991.

⁵⁶Kroo, I., and Takai, M., *"A Quasi-Procedural, Knowledge-Based System for Aircraft Design,"* AIAA Paper 88-4428, Aircraft Design, Systems and Operations Meeting, Atlanta, 1988.

⁵⁷Roskam, J., Malaek, S. M., and Anemaat, W., *"AAA (Advanced Aircraft Analysis): A User-Friendly Approach to Preliminary Aircraft Design,"* ICAS Paper 90-2.10.2, September 1990.

⁵⁸Phoenix Integration, URL: <http://www.phoenix-int.com>, 2005.

⁵⁹Hallion, R. P., *"The Hypersonic Revolution – Volume I: From Max Valier to Project PRIME (1924-1967),"* Air Force History and Museums Program, Bolling AFB, DC 20332-1111, 1998.

⁶⁰Hallion, R. P., *"The Hypersonic Revolution – Volume II: From Scramjet to the National Aero-Space Plane (1964-1986),"* Air Force History and Museums Program, Bolling AFB, DC 20332-1111, 1998.

⁶¹Schweikart, L., *"The Hypersonic Revolution – Volume III: The Quest for the Orbital Jet: The National Aero-Space Plane Program (1983-1995),"* Air Force History and Museums Program, Bolling AFB, DC 20332-1111, 1998.

⁶²Jenkins, D. R., Landis, T., and Miller, J., *"American X-Vehicles: An Inventory – X-1 to X-50,"* Centennial of Flight Edition, Monographs in Aerospace History No.31, SP-2003-4531, June 2003.

⁶³NASA *"Space Shuttle Synthesis Program /SSSP/. Volume 1 - Part 1 – Engineering and Programming Discussion Final Report,"* NASA-CR-114986; GDC-DBB70-002-VOL-1-PT-1, 19701201, December, 1970.

⁶⁴NASA *"Space Shuttle Synthesis Program /SSSP/. Volume 1 - Part 2 - Program Operating Instructions Final Report,"* NASA-CR-114984; GDC-DBB70-002-VOL-1-PT-2, 19701201, December, 1970.

⁶⁵NASA *"Space Shuttle Synthesis Program /SSSP/. Volume 1 - Part 2 - Program output Final report,"* NASA-CR-114985; GDC-DBB70-002-VOL-1-PT-3, 19701201, December, 1970.

⁶⁶Heinze, W., and Bardenhagen, A., *"Waverider Aerodynamics and Preliminary Design for Two-Stage-to-Orbit Missions, Part 2,"* Journal of Spacecraft and Rockets, Vol. 35, No. 4, pp 459-466, 1998.

⁶⁷HOTOL, <http://www.daviddarling.info/encyclopedia/H/HOTOL.html> , 2006.

⁶⁸Glatt, C. R., *"WATTS - A Computer Program for Weights Analysis of Advanced Transportation Systems,"* NASA CR-2420, 1974.

⁶⁹Harloff, G. J., and Berkowitz B. M., *"HASA – Hypersonic Aerospace Sizing Analysis for the Preliminary Design of Aerospace Vehicles,"* NASA Lewis Research Center, NASA CR-182226, November, 1988.

⁷⁰NASA, <http://www.nasa.gov/centers/dryden/research/X43/index.html>, Dryden Flight Research Center, 2006.

⁷¹Anderson D. J., *"Airplane Performance and Design,"* Kluwer Academic Publishers, Netherlands, 1982.

⁷²AIAA System Engineering Technical Committee., *"AIAA Aerospace Design Engineers Guide,"* American Institute of Aeronautics and Astronautics, Reston, Virginia, September, 2003.

⁷³Mattingly, J. D., Heiser, W. H., and Pratt, D. T., *"Aircraft Engine Design,"* AIAA Education Series, 2nd Edition, 2002.

⁷⁴Sutton, G. P., *"Rocket Propulsion Elements,"* 7th edition, John Wiley & Sons, New York, 2001.

⁷⁵Jenkins, D., *"Hypersonics Before the Shuttle: A Concise History of the X-15 Research Airplane,"* NASA Report SP-2000-4518, 2000.

⁷⁶Johnston, E. W., *"Current and Advanced X-15,"* Journal of Aircraft, Vol. 2, No. 6, 1965.

⁷⁷Stillwell, W. H., *"X-15 Research Results with a Selected Bibliography,"* NASA SP-60, 1965.

⁷⁸Williams, John E., and Vukelich, S. P., *"The USAF Stability and Control Digital DATCOM,"* Vol. I, User's Manual, AFFDL-TR-79-3032, April, 1979.

⁷⁹Magnus, A. E., and Epton, M. A., *"PAN AIR-A Computer Program for Predicting Subsonic or Supersonic Linear Potential Flows About Arbitrary Configurations Using A Higher Order Panel Method,"* Vol. 1. Theory Document (Version 1.0), NASA CR-3251, 1980.

⁸⁰Gentry, A. E., *"Hypersonic Arbitrary-Body Aerodynamic Computer Program,"* Douglas Report DAC 61552, Vol. 1 and 2, April 1968.

⁸¹Bonner, E., Clever, W., and Dunn, K., *"Aerodynamic Preliminary Analysis System II, Part I – Theory,"* Rockwell International Corporation, NASA Contractor Report 182076, April 1989.

⁸²Sova, G., and Divan, P., *"Aerodynamic Preliminary Analysis System II, Part II – User's Manual,"* Rockwell International Corporation, NASA Contractor Report 182077, April 1989.

⁸³Küchemann, D., *"The Aerodynamic Design of Aircraft,"* Pergamon Press Ltd., Cambridge, 1978.

⁸⁴Schlichting, H., Truckenbrodt, E., and Ramm, H.J., *"Aerodynamics of the Airplane,"* McGraw-Hill International Book Company, New York, ISBN 0070553416, 1979.

⁸⁵Anderson, J. D., *"Fundamentals of Aerodynamics,"* 3rd Edition, McGraw-Hill, New York, 2001.

⁸⁶Bertin, J. J., *"Aerodynamics for Engineers,"* 4th Edition, Prentice Hall, Englewood Cliffs, NJ, December 2001.

- ⁸⁷Hoerner, S. F., *"Fluid-Dynamic Lift,"* Hoerner Fluid Dynamics, Vancouver, WA, 1985.
- ⁸⁸Hoerner, S. F., *"Fluid-Dynamic Drag,"* Hoerner Fluid Dynamics, Vancouver, WA, 1965.
- ⁸⁹Pamadi, B. N., *"A Simple Analytical Aerodynamic Model of Langley Winged-Cone Aerospace Plane Concept,"* NASA Contractor Report 19341, 1994.
- ⁹⁰Mehta, U. B., and Bowlers, J.V., *"A Two-Stage-to-Orbit Spaceplane Concept with Growth Potential,"* Journal of Propulsion and Power, Vol. 17, No. 6, November-December 2001.
- ⁹¹Nelms, W. P., *"Effects of Body Shape on the Aerodynamic Characteristics of an All-Body Hypersonic Aircraft Configuration at Mach Numbers from 0.65 to 10.6,"* NASA Technical Report TN D-6821, 1972.
- ⁹²McCandless, R. S., and Cruz, C. L., *"Hypersonic Characteristics of an Advanced Aerospace Plane,"* NASA Langley, AIAA paper 85-0346, 1985.
- ⁹³Whitford, R., *"Design for Air Combat,"* Janes, London, 1987.
- ⁹⁴Heffley, R. K., and Jewell, W. F., *"Aircraft Handling Qualities Data,"* NASA CR-2144, December, 1972.
- ⁹⁵SpaceshipOne Data, *"Aviation Week,"* pp 28-30, Jun 28, 2004 and pp 34-36, October 11, 2004.
- ⁹⁶SpaceshipOne Data, *"Time,"* November 29, 2004.
- ⁹⁷Lan, C. E., *"User's Manual for VORSTAB Code (Version 3.2),"* Department of Aerospace Engineering, The University of Kansas, May 1999.
- ⁹⁸Saltzman, E. J., Wang, K. C., and Iliff K. W., *"Aerodynamic Assessment of Flight-Determined Subsonic Lift and Drag Characteristics of Seven Lifting-Body and Wing-Body Reentry Vehicle Configurations,"* NASA TP-2002-209032, 2002.
- ⁹⁹Walker, H. J., *"Performance Evaluation Method for Dissimilar Aircraft Designs,"* NASA Reference Publication 1042, September, 1979.
- ¹⁰⁰Corning, G., *"Supersonic and Subsonic Airplane Design,"* University of Maryland, College Park, 1979.
- ¹⁰¹Etkin, B., *"Dynamics of Atmospheric Flight,"* John Wiley & Sons, Inc., New York, 1972.
- ¹⁰²Rich, B. R., *"F-12 Series Aircraft Aerodynamic and Thermodynamic Design in Retrospect,"* Journal of Aircraft, Vol. 11, No. 7, 1974.
- ¹⁰³Lyndon, B., *"Space Shuttle,"* NASA Johnson Space Center, SP-407, 1976.
- ¹⁰⁴Astronautix, <http://www.astronautix.com/craft/dynasoar.htm>, Dyna—Soar, 2006.
- ¹⁰⁵Bertin, J. J., *"Hypersonic Aerothermodynamics,"* AIAA Education Series, September 1993.

¹⁰⁶Allen, H. J., and Eggers, A. J., "*A Study of the Motion and Aerodynamic Heating of Ballistic Missiles Entering the Earth's Atmosphere at High Supersonic Speeds*," NACA Report 1381, 1958.

¹⁰⁷Miele, A., "*Flight Mechanics*," Vol.v1 Theory of Flight Paths, Addison-Wesley Publishing, Reading, Mass., 1962.

¹⁰⁸Rutowsky, R. S., "*Energy Approach to the General Aircraft Performance Problem*," Journal of Aerospace Sciences, Vol. 21, 1954, pp 187-195.

¹⁰⁹Bryson, A. E., Desai, M. N., and Hoffman, W. C., "*Energy-State Approximation in Performance Optimization of Supersonic Aircraft*," Journal of Aircraft, Vol. 6, 1969.

¹¹⁰Paris, S. W., and Hargraves, C. R., "*OTIS 3.0 Manual*," Boeing Space and Defense Group, Seattle, WA, 1996.

¹¹¹Huang, X., and Chudoba, B., "*A Trajectory Synthesis Simulation Program for the Conceptual Design of a Suborbital Tourism Vehicle*," AIAA 2005-6023, AIAA Modeling and Simulation Technologies Conference and Exhibit, San Francisco, August 2005.

¹¹²Olds, J. R., "*Cost Estimation for Spacecraft and Launch Vehicles*," School of Aerospace Engineering, Georgia Institute of Technology, October 1997.

¹¹³Stephenson, A., Smith, D., and Cook, S., "*Revolutionizing Space Transportation for the 21st Century*," NASA Marshall Space Flight Center Presentation, June 2001.

¹¹⁴Chudoba, B. and Huang, X., "*A Conceptual Design Assessment of the Vertical Riser 'Michelle-B'*," AVD/TGV-CD1-2004, Final Contract Report to TGV Rockets, AVD Laboratory, Norman, April 2004.

¹¹⁵Parametric Estimating Handbook, <http://www.jsc.nasa.gov/bu2/handbooks/index.htm>, 2002, 2004.

¹¹⁶PRICE H, http://www.pricesystems.com/solutions/solutions_overview.html, 2004.

¹¹⁷London, J. R., "*LEO on the Cheap – Methods for Achieving Drastic Reductions*," USAF Research Report No. AU-ARI-93-8, 1994.

¹¹⁸Eisman, M., and Gonzales, D., "*RAND: Life Cycle Cost Assessments for Military Transatmospheric Vehicle*," Project AIR FORCE, Published by RAND, 1997.

¹¹⁹Koelle, D., "*Transcost – Statistical-Analytical Model for Cost Estimation and Economic Optimization of Space Transportation Systems*", Ottobrunn, Germany, 1991, 1999, 2003.

¹²⁰Goehlich, A. R., "*Space Tourism: Economic and Technical Evaluation of Suborbital SPACE Flight for Tourism*," Der Andere Verlag, 2002, ISBN 3-936231-36-2.

¹²¹Diaz-Calderon, A., Paredis J. J., and Khosla, P. K., "Organization and Selection of Reconfigurable Models," In Proceedings of the 2000 Winter Simulation Conference, Orlando, FL, 386-392, 2000.

¹²²Steele, J. M., Mollaghasemi, M., Rabadi, G., and Cates, G., "Generic Simulation Models of Reusable Launch Vehicles," In Proceedings of the 2002 Winter Simulation Conference, San Diego, 747-753, 2002.

¹²³Cope, D., Mollaghasemi, M., Ruiz-Torres, J.A., Kaylani, A., Steele, J. M., and Cowen, L. M., "*An Integrated Estimation and Modeling Environment for the Design of the Orbital Space Plane*," In Proceedings of the 2004 Winter Simulation Conference, Washington, DC, 459-465, 2004.

¹²⁴Nassi, I., and Shneiderman, B., "*Flowchart Techniques for Structured Programming*," SIGPLAN Notices 12, Technical Contributions, August 1973.

¹²⁵Chudoba, B., Coleman, G., Huang, X., and Czysz, P. A., "*Conceptual Design Assessment of a Suborbital Tourist Space Access Vehicle (SAV)*," AIAA-2006-1242, 44th AIAA Aerospace Sciences Meeting and Exhibit, Reno, Nevada, January 2006.

¹²⁶Chudoba, B., Czysz, P. A., Ferguson, A., and Baird, B., "*Model XP 'Space Sooner' Wind Tunnel Campaign – Phase 1*," AVD/RLI-WT1-2005, Contract Report, AVD Laboratory, The University of Oklahoma, February 2005.

¹²⁷Chudoba, B., Huang, X., and Coleman, G., "*Model XP Conceptual Design Methodology – Phase 2*", AVD/RLI-CD2-2005, Final Phase 2 Contract Report, AVD Laboratory, The University of Oklahoma, January 2005.

¹²⁸Chudoba, B., Coleman, G., and Huang, X., "*Model XP Conceptual Design Wing Planform Selection – Phase 2*", AVD/RLI-CD2-2004, Final Phase 2 Contract Report, AVD Laboratory, The University of Oklahoma, October 2004.

¹²⁹Chudoba, B., Striz, F., Huang, X., *et al*, "*Conceptual Design Support for Rocketplane Limited, Inc. Model XP 'Space Sooner' – Phase I*", AVD/RLI-CD1-2004, Final Phase 1 Contract Report, AVD Laboratory, The University of Oklahoma, September 2004.

¹³⁰Airworthiness Standards: Transport Category Airplanes, FAR Pt. 25, FAA, February 1965.

¹³¹Loftin, L. K., "*Subsonic Aircraft: Evolution and the Matching of Size to Performance*," NASA RP 1060, August 1980.

¹³²Roskam, J., "*Airplane Design Part I: Preliminary Sizing of Airplanes*," The University of Kansas, Lawrence, Kansas, 1989.

¹³³Shevell, R. S., "*Fundamentals of Flight*," 2nd Edition, Prentice Hall, Inc, New Jersey, 1989.

¹³⁴Taylor, D., and Czysz, P. A., "*McDonnell Aircraft Company Takeoff Analysis Methods*," McDonnell Aircraft Company, St Louis, 1996.

¹³⁵Nguyen, V. X., "*Flight Mechanics of High-Performance Aircraft*," Cambridge University Press, New York, 1993.

¹³⁶Mair, W. A., and Birdsall, D. L., "*Aircraft Performance*," Cambridge University Press, New York, 1992.

- ¹³⁷“*The USAF Prediction of Aircraft Drag due to Lift*,” AFFDL-TR-71-84, August 1971.
- ¹³⁸Miller, J., “*Convair B-58*,” Aerograph 4, Aerofax Inc., Arlington, Texas, 1985.
- ¹³⁹Davies, D. P., “*Concorde: Air Flight Test Report*,” Air Registration Board, 1969, 1972, 1975.
- ¹⁴⁰Janes., “*Concorde*,” 1972, 1975.
- ¹⁴¹Reddy, R. J., “*An Analog Computer Study of the F-106A*,” US Air Force Flight Test Center, Edwards Air Force Base, California, 1959.
- ¹⁴²Saxey, E., and David W. L., “*F-106A Performance Evaluation with 360-Gallon External Fuel Tanks*,” US Air Force Flight Test Center, Edwards Air Force Base, California, 1967.
- ¹⁴³Rivers, R. A., Jackson, E. B., Fullerton, C. G., Cox, T. H., and Princen, N. H., “*A Qualitative Piloted Evaluation of the Tupolev Tu-144 Supersonic Transport*,” NASA TM-200-209850, 2000.
- ¹⁴⁴Larson, T. J., and Schweikhard W. G., “*Verification of Takeoff Performance Predictions for the XB-70 Airplane*,” NASA Flight Research Center, NASA TM X-2215, 1971.
- ¹⁴⁵Berry D, T., and Powers B. G., “*Handling Qualities of the XB-70 Airplane in the Landing Approach*,” NASA TN D-5676, 1970.
- ¹⁴⁶Sick, T. R., Irwin, K. S., and McKay, J. M., “*Review of the XB-70 Flight Program*,” NASA Flight Research Center, 1965.
- ¹⁴⁷Whitford, R., “*Design for Air Combat*,” Janes, London, 1987.
- ¹⁴⁸Whitford, R., “*Fundamentals of Fighter Design*,” Airlife, London, 2000.
- ¹⁴⁹Ojha, S. K., “*Flight Performance of Aircraft*,” AIAA Aerospace Educational Series, Washington, DC, 1995.
- ¹⁵⁰Lynn, S., “*Summary Report for an Undergraduate Research Project to Develop Programs for Aircraft Takeoff Analysis in the Preliminary Design Phase*,” Virginia Polytechnic Institute and State University, Blacksburg, VA, 1994.
- ¹⁵¹Gunston, B., “*Bombers of the West*,” Charles Scribner’s Sons, New York, 1973.
- ¹⁵²Lan, C. T. E., and Roskam, J., “*Airplane Aerodynamics and Performance*,” Roskam Aviation and Engineering Corp., Ottawa, Kansas, 1981.
- ¹⁵³Miller, L. E., and Koch, P. G., “*Aircraft Flight Performance Methods*,” AFFDL-TR-75-89, Wright-Patterson Air Force Base, Dayton, Ohio, 1976.
- ¹⁵⁴Space Shuttle, <http://spaceflight.nasa.gov/shuttle/reference/shutref/sts/profile.html>, NASA, 2005.

¹⁵⁵Allen, H. J., and Eggers, A. J., “*A Study of the Motion and Aerodynamic Heating of Missiles Entering the Earth’s Atmosphere at High Supersonic Speeds*,” NASA Rep. 1381, 1958.

¹⁵⁶Eggers, A. J., Allen, H. J., and Neice S. E., “*A Comparative Analysis of the Performance of Long Range Hypersonic Vehicles*,” NASA TN-4046, October 1957.

¹⁵⁷Chapman, D. R., “*An Approximate Analytical Method for Studying Entry into Planetary Atmospheres*,” NASA TN-4267, May 1958.

¹⁵⁸Lecture Notes in Space Course 91, RWTH Aachen, Germany, 1991.

¹⁵⁹Fortescue, P., Stark, J., and Swinerd, G., “*Spacecraft Systems Engineering*,” Third Edition, John Wiley & Sons, Ltd, Hoboken, NJ, 2003.

¹⁶⁰Angelici, A. A., “*Minimum Environmental Control & Lift Support Guidelines for Manned Commercial Suborbital Reusable Launch Vehicles*,” FAA-CAMI, NRC Grant Proposal, May 2004.

¹⁶¹Anderson, J. D., “*Modern Compressible Flow with Historic Perspective*,” 1st ed., McGraw-Hill, New York, 1982.

¹⁶²Van Buren, M. A., and Mease, K. D., “*Aerospace Plane Guidance Using Geometric Control Theory*,” Proceedings of the 1990 American Control Conference, San Diego, Ca, May 23-25, 1990.

¹⁶³Harris R. V. Jr., “*On the Threshold – The Outlook for Supersonic and Hypersonic Aircraft*,” Journal of Aircraft, Vol. 29, No.1, pp 10-19, January – February 1992.

¹⁶⁴Herman, J. A., and Schmidt, D. K., “*Fuel-Optimal Single-Stage-to-Orbit Mission Analysis of a Generic Hypersonic Vehicle*,” AIAA Paper 95-3372, AIAA Guidance, Navigation, and Control Conference, Baltimore, MD, August 1995.

¹⁶⁵Ardema, M. D., Bowles, J. V., and Whittaker, T., “*Optimal Trajectories for Hypersonic Launch Vehicles*,” Dynamics and Control, No. 4, pp 337-347, 1994.

¹⁶⁶Matlab Version 7.0, The MathWorks, 2004.

¹⁶⁷Sacle Composite, <http://www.scaled.com/projects/tierone>, 2005.

¹⁶⁸Nguyen, V. X., Busemann, A., and Culp R. D., “*Hypersonic and Planetary Entry Flight Mechanics*,” University of Michigan Press, Ann Arbor, 1980.

¹⁶⁹NLoh, W. H. T., “*Reentry and Planetary Entry – Volume II*,” Springer-Verlag Inc., New York, 1968.

¹⁷⁰Martin, J. J., “*Atmospheric Reentry – An Introduction to Its Science and Engineering*,” Prentice-Hall, Inc., Englewood Cliffs, NJ, 1966.

¹⁷¹Tsuchiya, T., and Mori, T., “*Optimal Conceptual Design of Two Stage Reusable Rocket Vehicles Including Trajectory Optimization*,” Journal of Spacecraft and Rockets, Vol. 41, No. 5, pp 770-778, September-October 2004.

¹⁷²Tsuchiya, T., and Mori, T., "*Optimal Conceptual Design of Two Stage to Orbit Space Planes with Airbreathing Engines*," Journal of Spacecraft and Rockets, Vol. 42, No. 1, pp 90-97, January-February 2005.

¹⁷³Harpold, J. C., and Graves, C. A., "*Shuttle Entry Guidance*," The Journal of the Astronautical Sciences, Vol. XXVII, No. 3, pp 239-268, July-September 1979.

¹⁷⁴Anderson, J. D., "*Introduction to Flight*," McGraw-Hill Inc., Boston, 1985.

¹⁷⁵Freeman, D. C., Powell, R. W., Naftel, J. C., and Wurster, K. E., "*Definition of an Entry Research Vehicle*," Journal of Spacecraft and Rocket, Vol. 24, No. 3, pp 277-281, 1987.

¹⁷⁶Powell, R. W., Naftel, J. C., and Cunningham, M. J., "*Performance Evaluation of an Entry Research Vehicle*," Journal of Spacecraft and Rocket, Vol. 24, No. 6, pp 489-495, 1987.

¹⁷⁷Gregory, T. J., Williams, L. J., and Wilcox, D. E., "*Airbreathing Launch Vehicle for Earth Orbit Shuttle – Performance and Operation*," Journal of Aircraft, Vol. 8, No. 9, pp 724-731, 1971.

¹⁷⁸Petersen, R. H., Gregory, T. J., and Smith, C. L., "*Some Comparisons of Turboramjet-Powered Hypersonic Aircraft for Cruise and Boost Missions*," Journal of Aircraft, Vol. 3, No. 5, pp 398-405, 1966.

¹⁷⁹Walberg, Gerald D., "*A Survey of Aeroassisted Orbit Transfer*," Journal of Spacecraft and Rocket, Vol. 22, No.1, pp 3-18, 1985.

¹⁸⁰Tauber, M. E., Meness, G. P., and Adelman, H. G., "*Aerothermodynamics of Transatmospheric Vehicles*," Journal of Aircraft, Vol. 24, No. 9, pp 594-602, September 1987.

¹⁸¹Surber, T. E., and Olsen, D. C., "*Space Shuttle Orbiter Aerodynamic Development*," Journal of Spacecraft and Rockets, Vol. 5, No. 1, 1978.

¹⁸²Space shuttle, <http://science.ksc.nasa.gov/shuttle/resources/orbiters/columbia.html>, NASA, 2005.

¹⁸³Miller, J., "*The X-Planes: X1 to X-31*," Aerofax, Inc., New York, 1998.

¹⁸⁴X-15, Landing Speed, http://www.sierrafoot.org/x-15/adventures/flight_001/flight_1.html.

¹⁸⁵Butrica, A. J., "*Single Stage to Orbit: Politics, Space Technology, and the Quest for Reusable Rocketry*," The Johns Hopkins University Press, Baltimore, Maryland, 2003.

¹⁸⁶Urie, D., "Rocketplane XP – An Advanced Space Transportation Concept," Presentation to FAA/AST, March 1, 2004.

¹⁸⁷Carmichael, R., "*Public Domain Computer Program for the Aeronautical Engineer*," Version 9.0, Jan 2004.

¹⁸⁸The United States Committee on Extension to the Standard Atmosphere, "*U.S. Standard Atmosphere, 1976*," National Oceanic and Atmospheric Administration, National Aeronautics and Space Administration, United States Air Force, Washington D.C., 1976.

¹⁸⁹Soderman, P. T., and Aiken, T. N., “*Full-Scale Wind-Tunnel Tests of a Small Unpowered Jet Aircraft with a T-Tail*,” NASA Technical Note, NASA TN D-6573, November 1971.

¹⁹⁰Kroo, I., “*LinAir Version 3.4: A Nonplanar, Multiple Lifting Surface Aerodynamics Program*,” Desktop Aeronautics, Inc., Stanford, CA, 1997.

¹⁹¹Chudoba, B., Coleman, G., Huang, X., Huizenga, A., Czysz, P. A., and Butler, C. M., “*A Feasibility Study of a Supersonic Business Jet (SSBJ) Based on the Learjet Airframe*,” AIAA Paper, AIAA-2006-0028, 44th AIAA Aerospace Sciences Meeting and Exhibit, Reno, Nevada, 9-12 January 2006.

¹⁹²Goodell, R. M., and Elrod, C. W., “*Suborbital Launch Trajectories for Satellite Delivery*,” Journal of Spacecraft and Rockets, Vol. 32, No. 3, May-June 1995.

¹⁹³Windhorst, R., Ardema, M. D., and Bowles, J. V., “*Minimum Heating Entry Trajectories for Reusable Launch Vehicles*,” Journal of Spacecraft and Rockets, Vol. 35, No. 5, September-October 1998.

¹⁹⁴Lu, P., “*Analytical Solutions to Constrained Hypersonic Flight Trajectories*,” Journal of Guidance, Control, and Dynamics, Vol. 16, No. 5, September-October 1993.

¹⁹⁵Ardema, M. D., Bowles, J. V., Terjesen, E.J., and Whittaker, T., “*Approximate Altitude Transitions for High-Speed Aircraft*,” Journal of Guidance, Control, and Dynamics, Vol. 18, No. 3, May-June 1995.

¹⁹⁶Ardema, M. D., Bowles, J. V., and Whittaker, T., “*Near-Optimal Propulsion-System Operation for an Air-Breathing Launch Vehicle*,” Journal of Spacecraft and Rockets, Vol. 32, No. 6, November-December 1995.

¹⁹⁷Ardema, M. D., Chou, H. C., and Bowles, J. V., “*Near-Optimal Operation of Dual-Fuel Launch Vehicle*,” Journal of Guidance, Control, and Dynamics, Vol. 19, No. 5, 1996.

¹⁹⁸Chou, H. C., Ardema, M. D., and Bowles, J. V., “*Near-Optimal Re-Entry Trajectories for Reusable Launch Vehicle*,” Journal of Guidance, Control, and Dynamics, Vol. 21, No. 6, 1998.

¹⁹⁹Gregory, T. J., Petersen, R. H., and Wyss, J. A., “*Performance Tradeoffs and Research Problems for Hypersonic Transports*,” Journal of Aircraft, Vol. 2, No. 4, July-August 1965, pp 266-271.

²⁰⁰McCandless, R. S., and Cruz, C. I., “*Hypersonic Characteristics of an Advanced Aerospace Plane*,” AIAA Paper 85-0346, Reno, NV, January 1985.

²⁰¹Tauber, M. E., and Yang, L., “*Performance Comparisons of Maneuvering Vehicles Returning from Orbit*,” Journal of Spacecraft and Rockets, Vol. 25, No. 4, pp 263-270, July-August 1988.

²⁰²Booher, C., “*Man-System Information Standard (MSIS)*,” NASA Johnson Space Center, NASA-STD-300, July 1995.

²⁰³Tartabini, P. V., Wurser, K. E., Korte, J. J., and Lepsch R. A., “*Multidisciplinary Analysis of a Lifting Body Launch Vehicle*,” Journal of Spacecraft and Rockets, Vol. 39, No. 5, pp 788-795, September-October 2002.

²⁰⁴Messerschmid, E., and Schöttle, U., “*Atmospheric Reentry of Capsules and Winged Vehicles*,” Space Course, Aachen, 1991.

²⁰⁵Boylan, D. E., and Potter, J. L., “*Aerodynamics of Typical Lifting Bodies under Conditions Simulating Very High Altitude*,” AIAA Journal, Vol. 5, No. 2, pp 226-232, 1967.

²⁰⁶Windhorst, R., Ardema, M.D., and Bowles, J.V., “*Minimum Heating Entry Trajectories for Reusable Launch Vehicles*,” Journal of Spacecraft and Rockets, Vol. 35, No. 5, September-October 1998.

²⁰⁷Ardema, M. D., and Bowers, J. V., Terjesen, E. J., and Whittaker, T., “*Approximate Altitude Transitions for High-Speed Aircraft*,” Journal of Guidance, Control, and Dynamics, Vol. 18, No. 3, May-June 1995.

Appendices

Appendix A Geometric Characteristics of OU XP Configuration

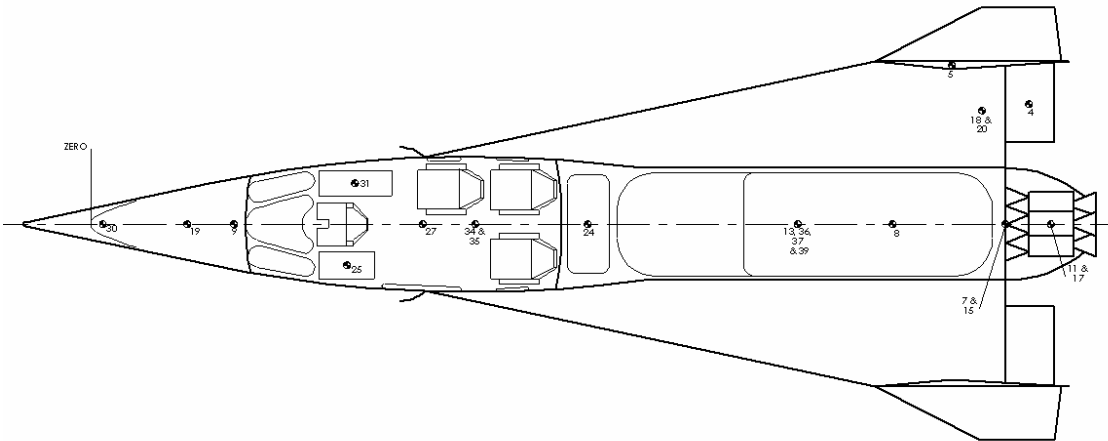


Fig. A.1: Plane View of the CG distribution of each component of OU XP.

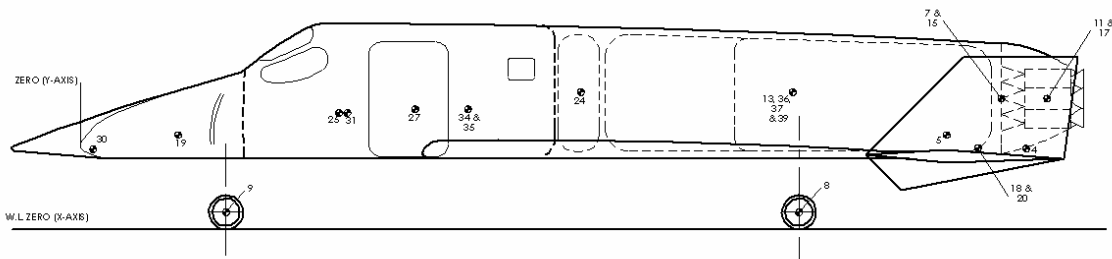


Fig. A.2: Side View of the CG distribution of each component of OU XP.

TABLE A.1: The Geometry of OU XP Model.

Parameters		OU XP Jet and Rocket
Dimensions		
Wing span	(ft)	24
Wing chord at root	(ft)	35.1
Wing chord at tip	(ft)	4.2
Wing aspect ratio	(ft)	1
Leading edge angle	(degree)	78
Length overall	(ft)	41
Height overall	(ft)	7.94
Fuselage max diameter	(ft)	5.25
Landing gear height	(ft)	2.69
LNG and LOX tank length	(ft)	14.1
LNG and LOX tank diameter	(ft)	4.26
Area		
Wings, gross	(ft ²)	245
Flap	(ft ²)	10.1
Elevon	(ft ²)	6.8
Vertical control surface	(ft ²)	29.7

TABLE A.2: The OU XP Jet Engine and Rocket Engine.

Aircraft Model			
Parameters	GE CJ - 610	F3-IHI-30	OU Rocket Engine
Thrust (lb)	2950	3680	27900
Weight (lb)	411	750	2325

In our study, four wings were selected with varying leading edge sweep angles: 78°, 70°, 60°, and 45°. A comparative study of these four wings was performed to assess their aerodynamics, stability and control and performance characteristics during the takeoff. At the design point, all four wings were sized to have the same induced drag. Thus, these wings were comparable at the same drag level. The aim of our study was to find out which wing offers the best performance and s&c design potential coupled with a safe trim mechanism. The results from this study suggested which wing planform should be selected based on performance, s&c, and flight safety. Table A.3 shows the design

parameters of four wings which were selected based on keeping the induced drag coefficient constant. The geometries of four wings are shown in Figure A.3 to A.6.

TABLE A.3. Parameters of Wing Planform with Varying Leading Edge Sweep Angles.

Parameter		78° LE sweep angle	70° LE sweep angle	60° LE sweep angle	45° LE sweep angle
c/4 sweep degree		74.3	64.5	52.3	36.9
Span	ft	19.8	22.0	25.5	25.7
mac	ft	30.7	24.4	17.0	12.2
S _{plan}	ft ²	394.5	339.4	283.6	278.0
AR		1.01	1.45	2.31	2.40

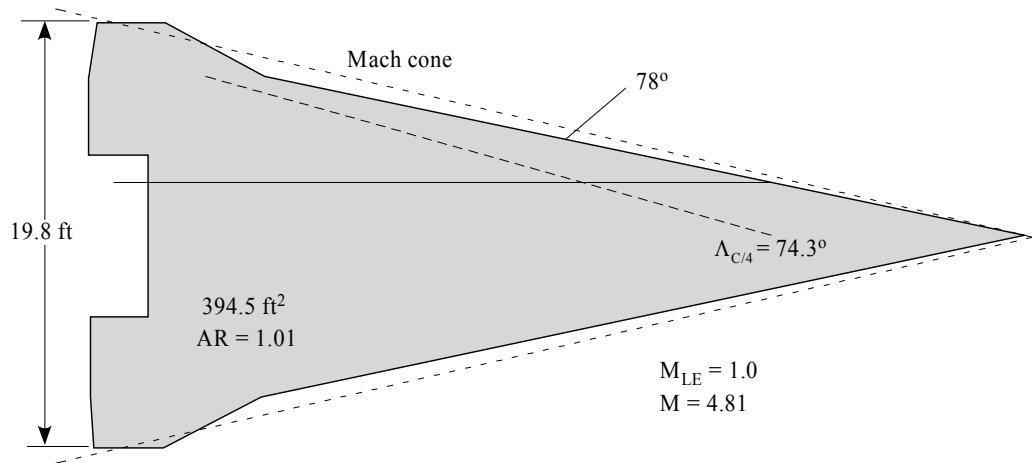


Fig. A.3: Wing planform with 78° leading edge sweep angle

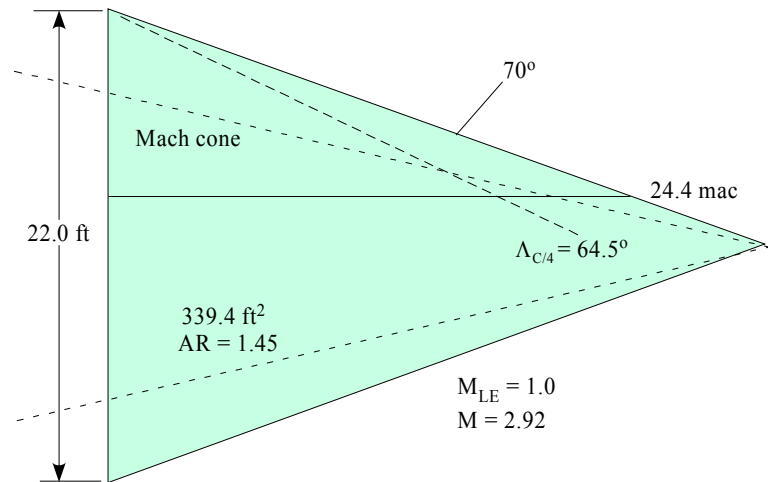


Fig. A.4: Wing planform with 70° leading edge sweep angle

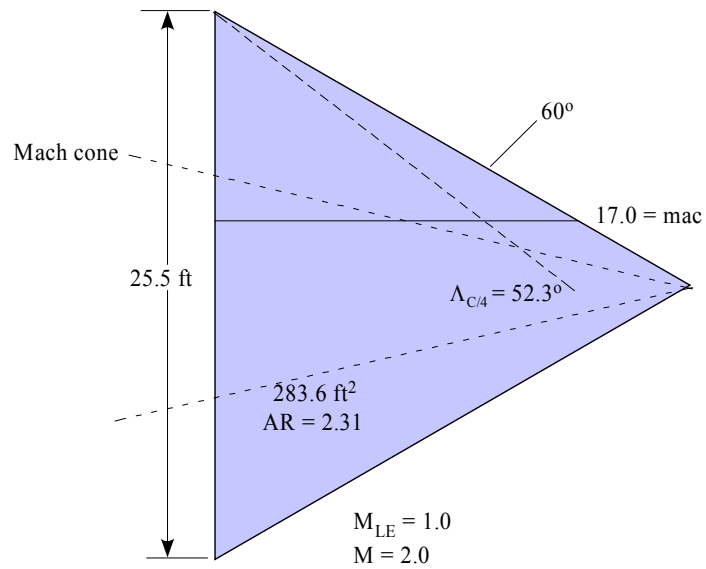


Fig. A.5: Wing planform with 60° leading edge sweep angle

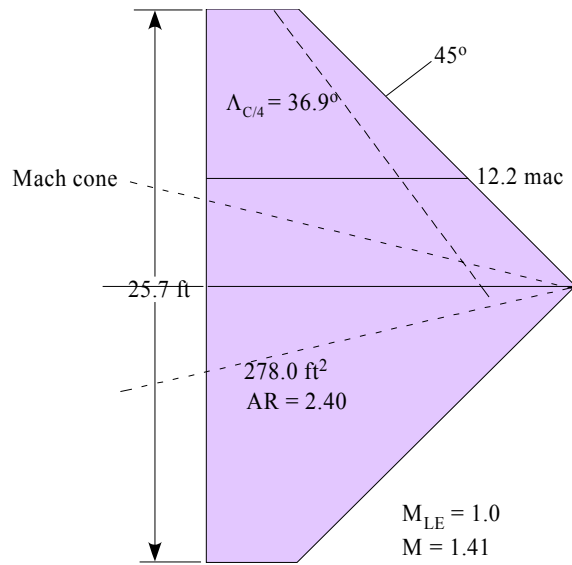


Fig. A.6: Wing planform with 45° leading edge sweep angle

Appendix B SAV Design Methodologies

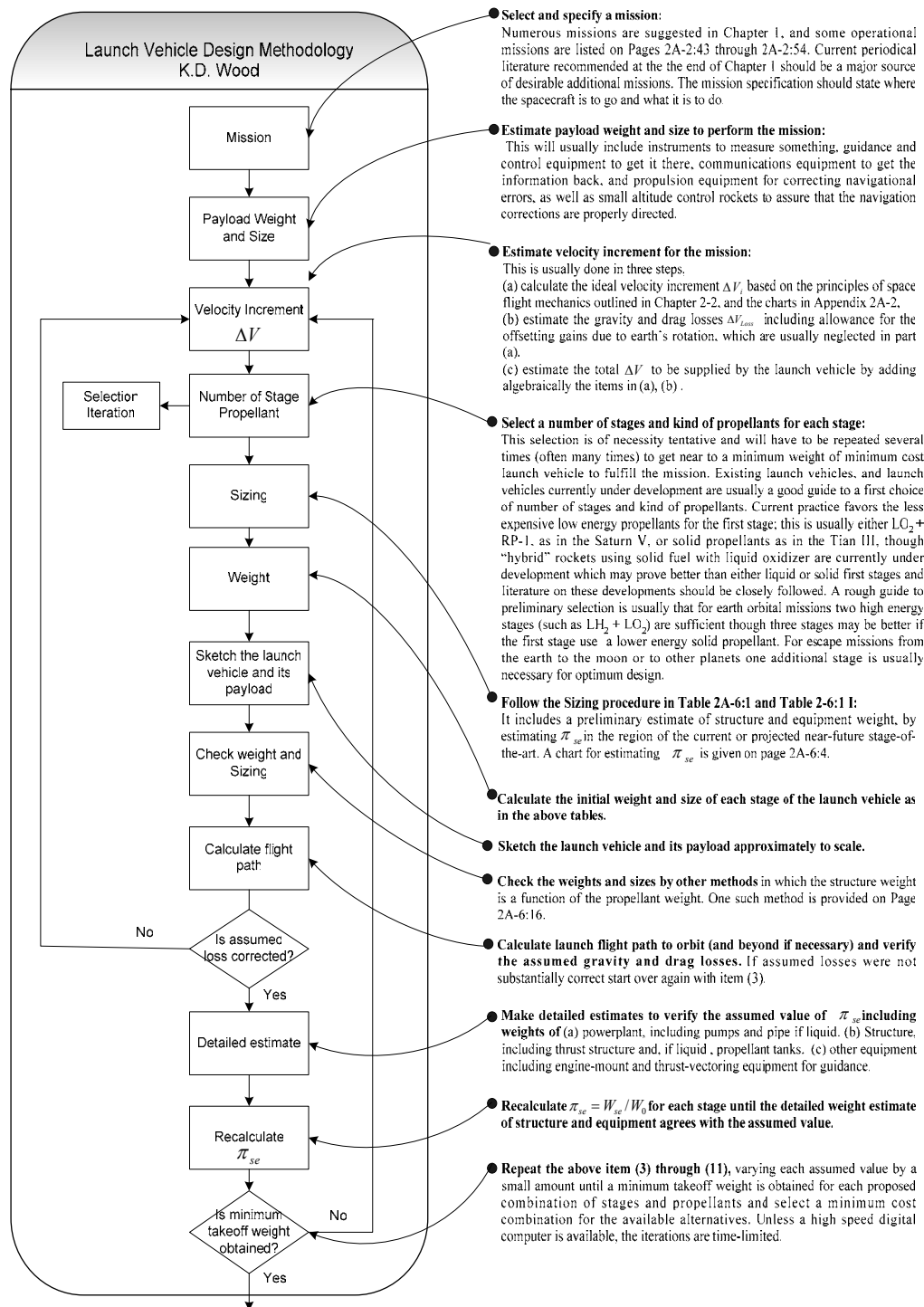


Fig. B.1: Design methodology of spacecraft and its launch vehicle by K.D. Wood. ¹

The space shuttle synthesis program automates the trajectory, weights and performance computations essential to predesign of the space shuttle system for earth-to-orbit operations

The SSSP is strictly for use in predesign, with layout drawings of baseline vehicles and separate analyses of dynamics and thermodynamics as essential companions

SSSP's primary job is to determine the implications of the design change on system performance, gross weight, etc., consistent with vehicle and mission constraints

The program is not sufficient but is intended to reduce the work and time required for the predesign cycle, from point design to new point design, by providing fast, reliable sensitivities data

The weight / Volume portion of the SSSP (abbreviated WTVOL) is a library of weight and volume equations for the components of space shuttle vehicles. It uses existing weight data, plus inputs describing the thermal protection system, propulsion and other subsystems, as well as performance mass ratios and other mission requirements derived from the trajectory subprogram.

The WTVOL subprogram solves the following basic problem: for a specified payload weight and mass ratio, find the stage gross weight and volume. This problem is solved separately for the orbiter and booster stages, then iterations are performed to satisfy specified mission constraints or specified relationships between the booster and orbiter

The General Trajectory Simulation Module (GTSM) program is a general purpose high speed, precision flight program which simulates the flight for an aerospace vehicle in the gravitational field of a central body. It utilizes the efficient Kutta-Merson variable stepsize numerical integration technique to integrate with respect to time the twelve state equations. These equations define the time rate of change of the three degree of freedom vehicle motion, the vehicle mass, the ideal velocity and velocity losses, and a heating parameter. The vehicle motion equations consist of three kinematic and three kinetic equations and are expressed in a natural applied force coordinate system which minimizes the extent of matrix coordinate transformations common to other simulations.

The SSSP is a highly useful tool in conceptual design studies where the effects of various trajectory configurations and shuttle subsystem parameters must be evaluated relatively rapidly and economically

The program furnishes sensitivity and tradeoff data for proper selection of configuration and trajectory predesign parameters.

Emphasis is placed upon predesign simplicity and minimum input preparation. Characteristic equations for describing aerodynamic and propulsion models and for computing weights and volumes are kept relatively simple.

The synthesis program is designed for a relatively large number of two-stage space shuttle configurations and mission types, but avoids the complexity of a completely generalized computer program that would be unwieldy to use and/or modify.

The computational flow is summarized as follows:

(1) Input data to basic data blocks: fixed input quantities and estimates for IDVEL, main impulse mass ratios for the booster and orbit (u_B , u_O), and gross stage weight for the booster and orbiter.

(2) Process input data and adjust mass ratio u_B estimate to agree with IDVEL estimate

(3) In WTVOL, size the vehicle:

- Compute the gross stage weight for the orbiter, using fixed T/WB or thrust, mass ratio and payload;
- compute the gross stage weight for the booster using fixed T/WB or thrust, mass ratio u_B and booster payload W_{BO}
- Compare vehicle with sizing constraints imposed by input options if utilized and, if not within specified tolerances, adjust control parameters and repeat step a cycle
- Prepare GTSM data from WTVOL

(4) In GTSM, simulate ascent trajectory with fixed u_B determine u_O^* required to reach the specified terminal velocity at orbit insertion

(5) In synthesis driver, test the error $u_O - u_O^*$ with specified tolerance

- if acceptable, set termination flag and cycle through WTVOL and GTSM for printout.
- if not acceptable, adjust u_B and repeat step 3 cycle.

Fig. B.2: SSSP design methodology for the Space Shuttle.²

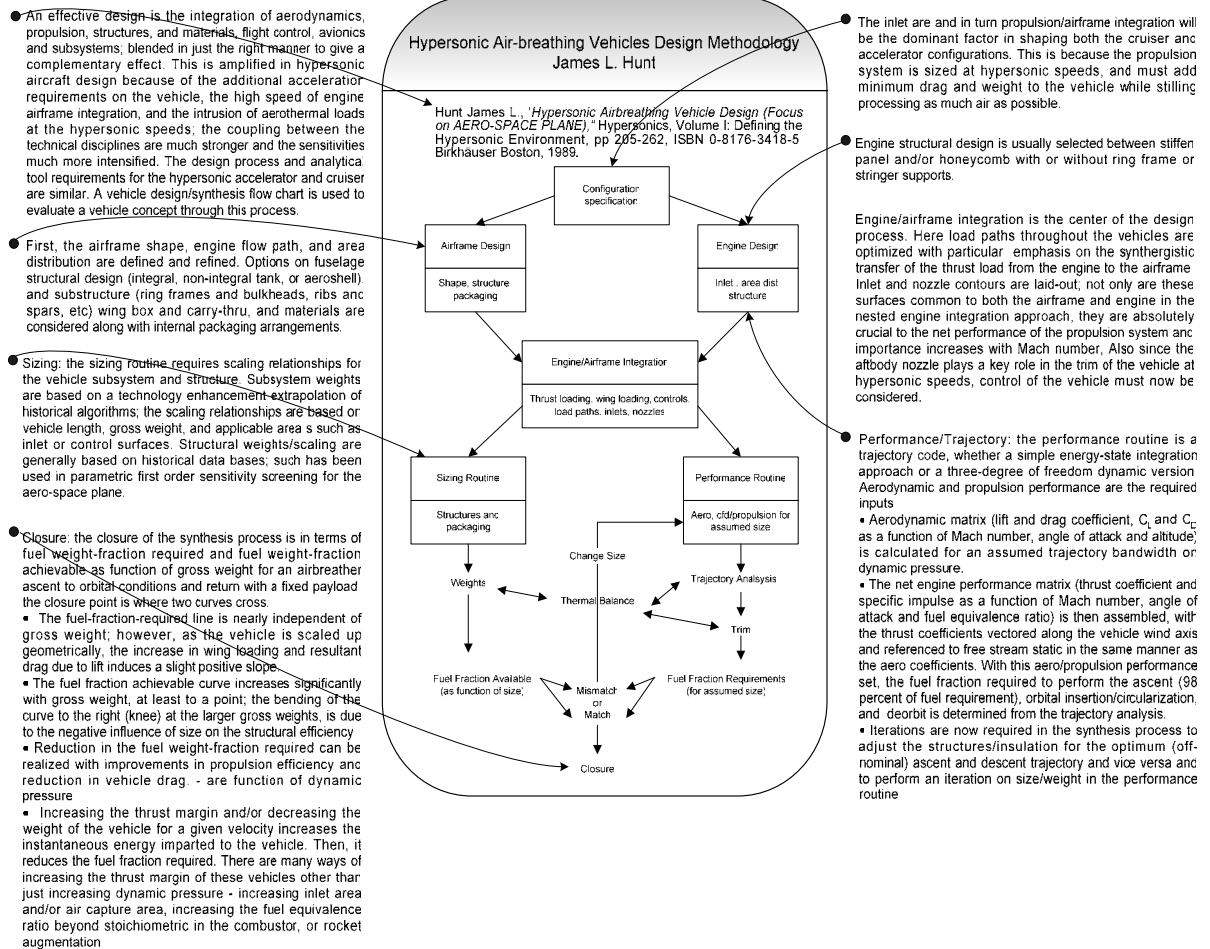


Fig. B.3: Hypersonic air-breathing vehicle design methodology by James L. Hunt.⁵

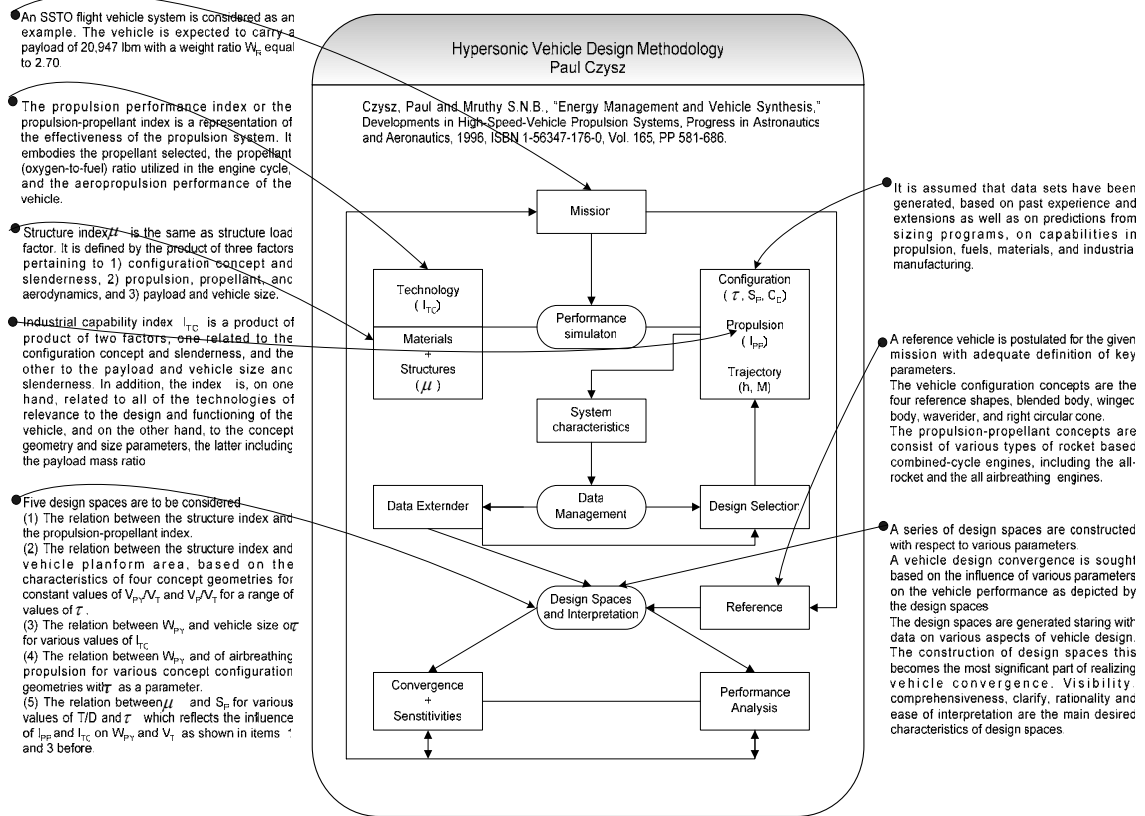


Fig. B.4: Hypersonic vehicle design methodology by Paul Czysz.⁶

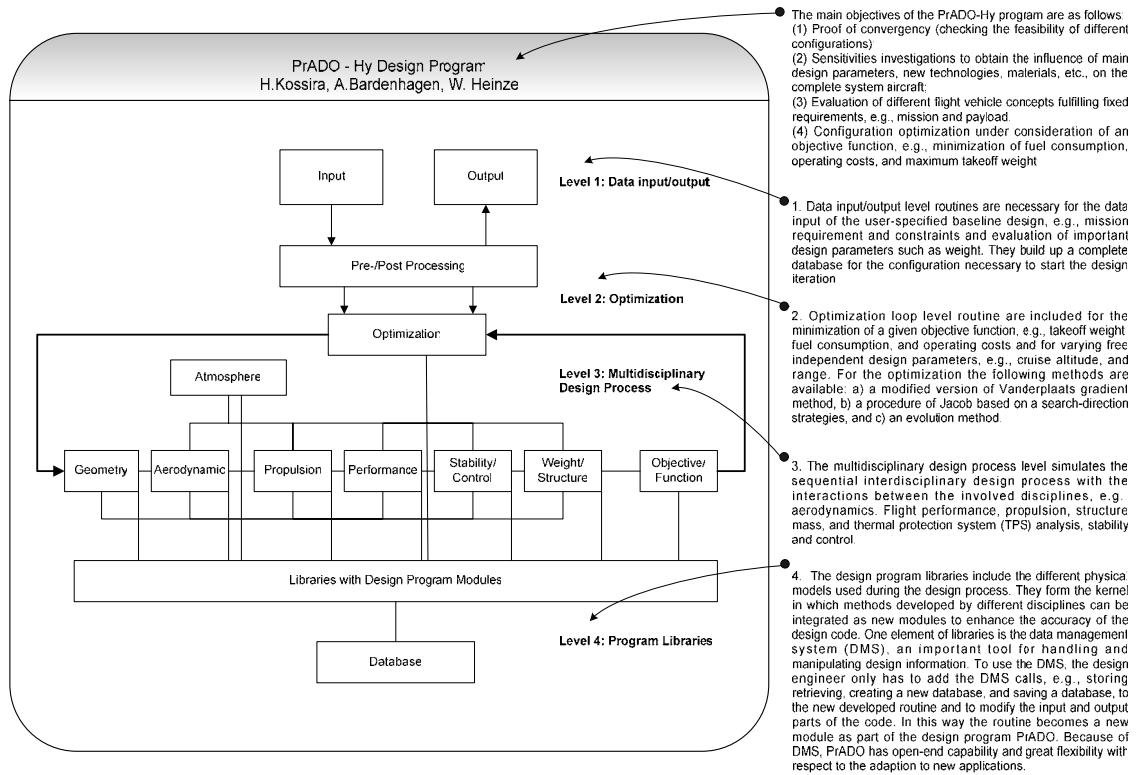


Fig. B.5: PrADO-Hy design methodology for TSTO by W. Heinze.⁷

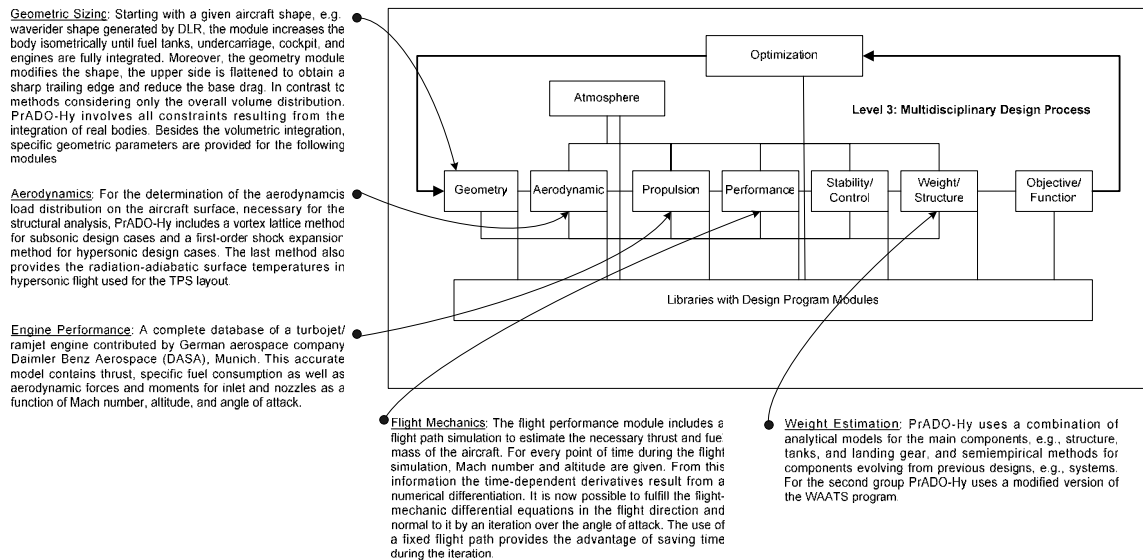
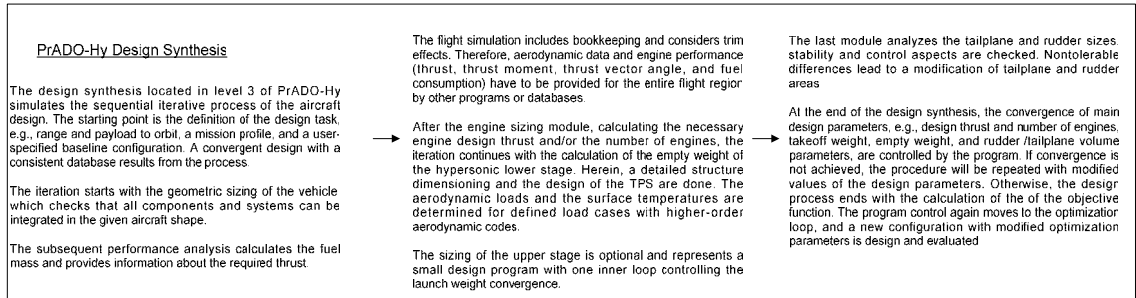


Fig. B.6: Design synthesis of PrADO-Hy design methodology.⁷

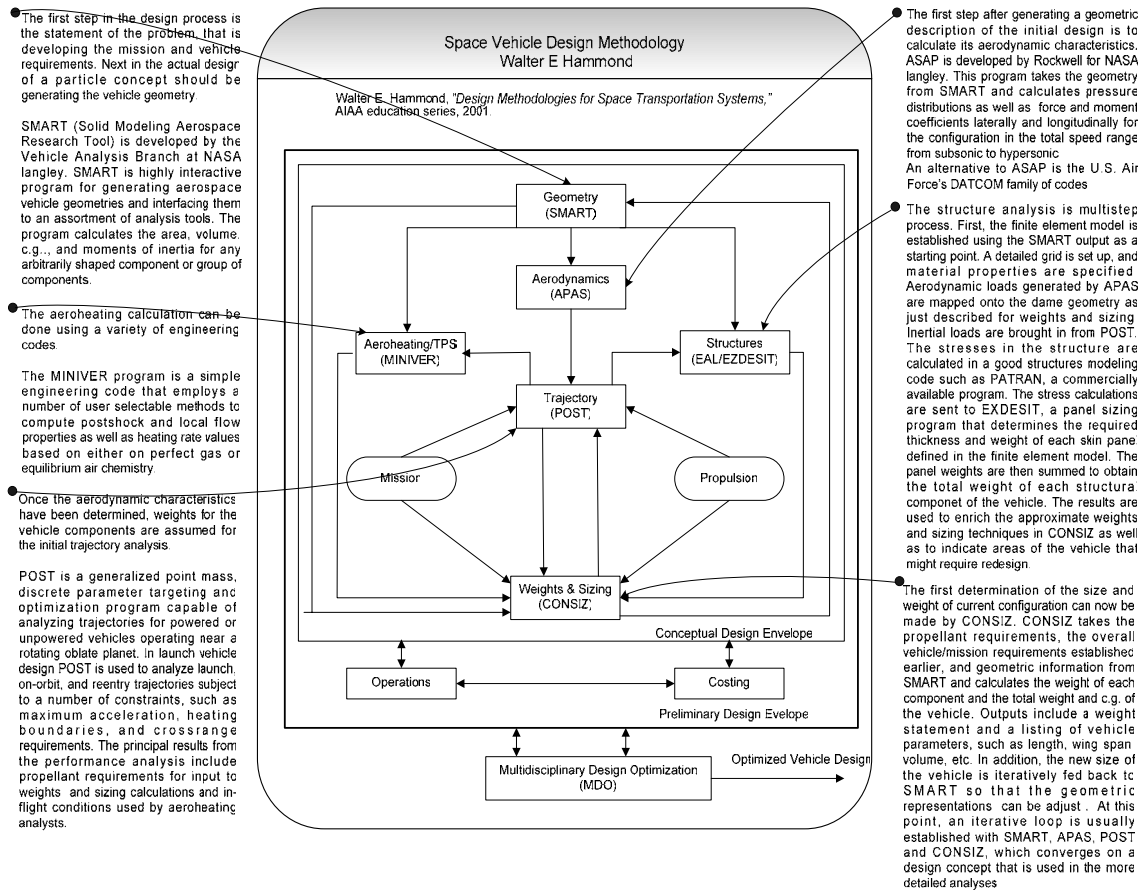


Fig. B.7: Design methodology for space transportation systems by Walter E. Hammond.⁸

REFERENCE

¹Wood, K. D., “*Aerospace Vehicle Design Volume II: Spacecraft Design*,” Johnson Publishing Company, Boulder, Colorado, 1964.

²NASA, “*Space Shuttle Synthesis Program /SSSP/. Volume 1 - Part 1 – Engineering and programming discussion Final report*”, NASA-CR-114986; GDC-DBB70-002-VOL-1-PT-1 , 19701201; December, 1970.

³NASA, “*Space Shuttle Synthesis Program /SSSP/. Volume 1 - Part 2 - Program operating instructions Final report*”, NASA-CR-114984; GDC-DBB70-002-VOL-1-PT-2 , 19701201; December, 1970.

⁴NASA, “*Space Shuttle Synthesis Program /SSSP/. Volume 1 - Part 2 - Program output Final report*”, NASA-CR-114985; GDC-DBB70-002-VOL-1-PT-3 , 19701201; December, 1970.

⁵Hunt J. L., “*Hypersonic Airbreathing Vehicle Design (Focus on AERO-SPACE PLANE)*,” Hypersonics, Volume I: Defining the Hypersonic Environment, Birkhäuser, Boston, 1989, pp 205-262.

⁶Czysz, P., and Mruthy, S.N.B., “*Energy Management and Vehicle Synthesis*,” Developments in High-Speed-Vehicle Propulsion Systems, Progress in Astronautics and Aeronautics, 1996, ISBN 1-56347-176-0, Vol. 165, PP 581-686.

⁷Heinze, W., and Bardenhagen, A., “*Waverider Aerodynamics and Preliminary Design for Two-Stage-to-Orbit Missions, Part 2*”, Journal of Spacecraft and Rockets, Vol. 35, No. 4, pp 459-466, 1998.

⁸Hammond, W. E., “*Design Methodologies for Space Transportation Systems*,” AIAA Education Series, 2001.

Appendix C Aerodynamic Method

The National Aero-Space Plane (NASP) program envisaged the development of a manned, single-stage-to-orbit vehicle capable of horizontal takeoff and landing using conventional runways. A simple analytical aerodynamic model of Langley winged-cone aerospace plane concept is based on both empirical DATCOM methods and several theoretical methods (e.g., Prandtl-Meyer Shock expansion, Tangent wedge/Tangent cone Newtonian, etc.). It is desired to program and integrate this simple analytical method into the SAV design synthesis methodology in a continuous study. Analytical expressions are presented in the following tables for the estimation of drag, lift, and pitching moment coefficients for subsonic, transonic, supersonic, and hypersonic Mach numbers and angles of attack from 0 to 20 deg.¹

Estimation of Drag Coefficient

Skin Friction

Mach	Body	Wing	Vertical Tail
M < 1.0			
1.0 < M < 1.4			
1.4 < M < 4.0	$C_{Df,B} = C_{f,B} \left[1 + \frac{60}{(l_B/d)^3} + 0.0025 \left(\frac{l_B}{d} \right) \right] \frac{S_s}{S_w}$	$C_{Df,W} = C_{f,W} \left[1 + L \frac{t}{c} + 100 \left(\frac{t}{c} \right)^4 \right] R_{LS} \frac{S_{wet}}{S_w}$	$C_{Df,V} = C_{f,V} \frac{S_V}{S_w}$
4.0 < M < 6.0			
M > 6.0			

Wave Drag

Mach	Body	Wing
$M < 1.0$	Ignore	$C_{DW,W} = \frac{0.000585\Lambda(M-0.6)}{1.05-0.6\sqrt{\Lambda}} M^6$
$1.0 < M < 1.4$	$C_{DW,B} = \theta^2 (8.0101 - 2.431M + 0.2443M^2) \frac{S_B}{S_W}$	$C_{DW,W} = c_1 M + c_2$
$1.4 < M < 4.0$	$C_{DW,B} = \theta^2 (8.0101 - 2.431M + 0.2443M^2) \frac{S_B}{S_W}$	$C_{DW,W} = k \cot \Lambda_{le} \left(\frac{t}{c} \right)^2$
$4.0 < M < 6.0$	$C_{DW,B} = (c_1 M + c_2) \frac{S_B}{S_W}$	$C_{DW,W} = c_1 M + c_2$
$M > 6.0$	$C_{DW,B} = 2 \sin^2 \theta \left(\frac{S_B}{S_W} \right)$	$C_{DW,W} = 0.0064$

Induced Drag

Mach	Body	Wing	Canard
$M < 1.0$		$C_{Di,W} = \left[\frac{(1-M^4)}{\pi e_{av}} + 0.4M^4 \right] C^2_{L,W}$	$C_{Di,C} = 0.909 C_{N,C} \alpha \frac{S_C}{S_W}$
$1.0 < M < 1.4$		$C_{Di,W} = (0.35699257M + 0.94479781) C^2_{L,W}$	$C_{Di,C} = (c_1 M + c_2) \frac{S_C}{S_W}$
$1.4 < M < 4.0$	$C_{Di,B} = C_{N,N} \alpha$	$C_{Di,W} = \left[\frac{0.4010 + \sqrt{M^2 - 1}}{4.1887} \right] C^2_{L,W}$	0
$4.0 < M < 6.0$		$C_{Di,W} = a C_{Di,W4} + b C_{Di,W6}$	0
$M > 6.0$		$C_{Di,W} = C_{L,W} \alpha \frac{S_{eff}}{S_W}$	0

Base and aft body Drag Coefficient

Mach	Aft Body
$M < 1.0$	$C_{Db} = [0.139 + 0.419(M - 0.161)^2] \frac{S_{base}}{S_W}$ $C_{D, aft} = C_{D, aft1} M^4$
$1.0 < M < 1.4$	$C_{Db} = c_1 M + c_2$ $C_{D, aft} = -0.0002M^3 + 0.003M^2 - 0.016M + 0.0342$
$1.4 < M < 4.0$	$C_{Db} = \left[\frac{1}{M^2} - \frac{0.570}{M^4} \right] \left(\frac{S_{base}}{S_W} \right)$ $C_{D, aft} = -0.0002M^3 + 0.003M^2 - 0.016M + 0.0342$
$4.0 < M < 6.0$	$C_{Db} = \left[\frac{1}{M^2} - \frac{0.570}{M^4} \right] \left(\frac{S_{base}}{S_W} \right)$ $C_{D, aft} = -0.0002M^3 + 0.003M^2 - 0.016M + 0.0342$
$M > 6.0$	$C_{Db} = \left[\frac{1}{M^2} - \frac{0.570}{M^4} \right] \left(\frac{S_{base}}{S_W} \right)$ $C_{D, aft} = C_{D, aft6} e^{-(M-0.6)}$

Estimation of Lift Coefficient

Mach	Body	Wing
$M < 1.0$	$C_{N,N} = 2(k_2 - k_1)\alpha \frac{S_B}{S_W}$ $k_2 - k_1 = 0.92$	$C_{N\alpha,e} = \frac{3.1428}{1 + 0.5\sqrt{9 - M^2}}$ $C_{N,aa} = 4.7783 - 1.4504C_{N\alpha,e}$
$1.0 < M < 1.4$	$C_{N,N} = \frac{1.84\alpha S_B}{S_W} + 1.6766511(M - 1)\alpha^2$	$C_{N\alpha,e} = 0.35699257M + 0.94479781$ $C_{N,aa} = -0.8467277M + 3.736911 + 0.3333(M - 1)\sin \alpha$
$1.4 < M < 4.0$	$C_{N,N} = 2(k_2 - k_1)\alpha \frac{S_B}{S_W} + \frac{C_{d,e}S_p\alpha^2}{S_W}$ $C_{d,c} = c_1M^3 + c_2M^2 + c_3M + c_4$ $c_1 = 0.16018212e - 01$ $c_2 = -0.212232216,$ $c_3 = 0.83332039,$ $c_4 = 0.48085365,$	$C_{N\alpha,e} = K_f(1.56250 - 0.140620\sqrt{M^2 - 1})$ $K_f = -0.0086M^2 - 0.0385M + 1.08470$ $C_{N,aa} = -0.8467277M + 3.736911 + 0.3333(M - 1)\sin \alpha$
$4.0 < M < 6.0$	$C_{N,N} = a_1\alpha^3 + a_2\alpha^2 + a_3\alpha + a_4$ $a_1 = 0.24197221M - 0.9678888$ $a_2 = -0.32024002M + 2.0393596e - 01$ $a_3 = -0.55238185e - 01M + 0.48702338$ $a_4 = 1.5351068e - 04M - 6.1404271e - 04$	$C_{N\alpha,e} = \frac{4.0K_f}{\sqrt{M^2 - 1}}$ $K_f = 0.25245975e - 01M^2 - 0.15027659M + 0.97881773$ $C_{N,aa} = -0.17500M + 1.05 + (1.90M - 6.6)\sin \alpha$
$M > 6.0$	$C_{N,B} = a_1\alpha^3 + a_2\alpha^2 + a_3\alpha + a_4$ $a_1 = 4.8394443e - 01,$ $a_2 = 1.1791944e - 01,$ $a_3 = 1.5559427e - 01,$ $a_4 = 3.0702135e - 04,$	$C_{N,W} = \left[\frac{4 \sin \alpha \cos \alpha}{M} + 0.8M \sin^3 \alpha \right] \frac{S_{eff}}{S_W}$

REFERENCE

¹Pamadi, B. N., "A Simple Analytical Aerodynamic Model of Langley Winged-Cone Aerospace Plane Concept," NASA Contractor Report 19341, 1994.

Appendix D Cost Models – Transcost and Suborb-Transcost

A statistical-analytical model called TRANSCOST has been developed by Dr Dietrich Koelle¹ which is widely used and accepted throughout the aerospace industry. This model is based on a 30 year database from US and European space vehicle projects. It assumes that the primary cost contributors are the engines, propellant, and the airframe. The validation study of the Koelle cost model shows a costing accuracy of about +/- 25%.¹ Therefore, this model is considered at least sufficient for a rough estimation of life-cycle cost. The cost model structure and equations have been modified and extended by Dr.-Ing. Robert A. Goehlich² so that they can be applied to suborbital tourism vehicles. As a consequence, a modified computer-based cost model called SUBORB-TRANSCOST has been provided by Dr. Goehlich for our research study. The SUBORB-TRANSCOST model is applicable for the following combinations of reusable space transportation systems to suborbit:

- | | |
|----------------------------------|--|
| • Single stage winged vehicle | used for Ascender, Kitten |
| • First stage winged vehicle | used for B747, Sky Lifter |
| • Second stage winged vehicle | used for Eclipse Astronliner,
Space Cruiser, Pathfinder |
| • Single stage ballistic vehicle | used for Roton |
| • First stage ballistic vehicle | not applicable |
| • Second stage ballistic vehicle | not applicable |

Due to the fact that there does not exist any reusable ballistic vehicle, the cost model results are not considered fully accurate for those applications but rather a sufficient cost model for the conceptual design analysis. By using this program, Dr. Goehlich² attempts

to verify whether suborbital vehicles are economically feasible by estimating the ticket price for a realistic space-tourist scenario in the near future. A comparison of calculated ticket prices of several suborbital vehicles (Ascender, Eclipse Astroliner, Kitten, Pathfinder, Roton C-9 and Space Cruiser) is presented in his book.

Cost Model Structure

Koelle's cost model¹ defines life-cycle cost consisting of development cost, vehicle cost, operating cost, and abolition cost. As a consequence, the SUBORB-TRANSCOST model² is subdivided into four interconnected submodels as shown in Figure D.1:

- Development Cost Submodel: The development cost is nonrecurring. It includes the cost of testing as well as the fabrication of rigs and tools, since normally, at least a prototype unit is included in a development program requiring tools and rigs.
- Vehicle Cost Submodel: The vehicle cost is recurring. It includes the prototype manufacturing as well as the follow-on production.
- Total Operating Cost Submodel: The total operating cost is recurring. It includes management, pre-launch operations, launch operations, mission control, propellants, and ground transportation.
- Total Profit Submodel: Includes the profit for the shareholders for the total fleet life-cycle.

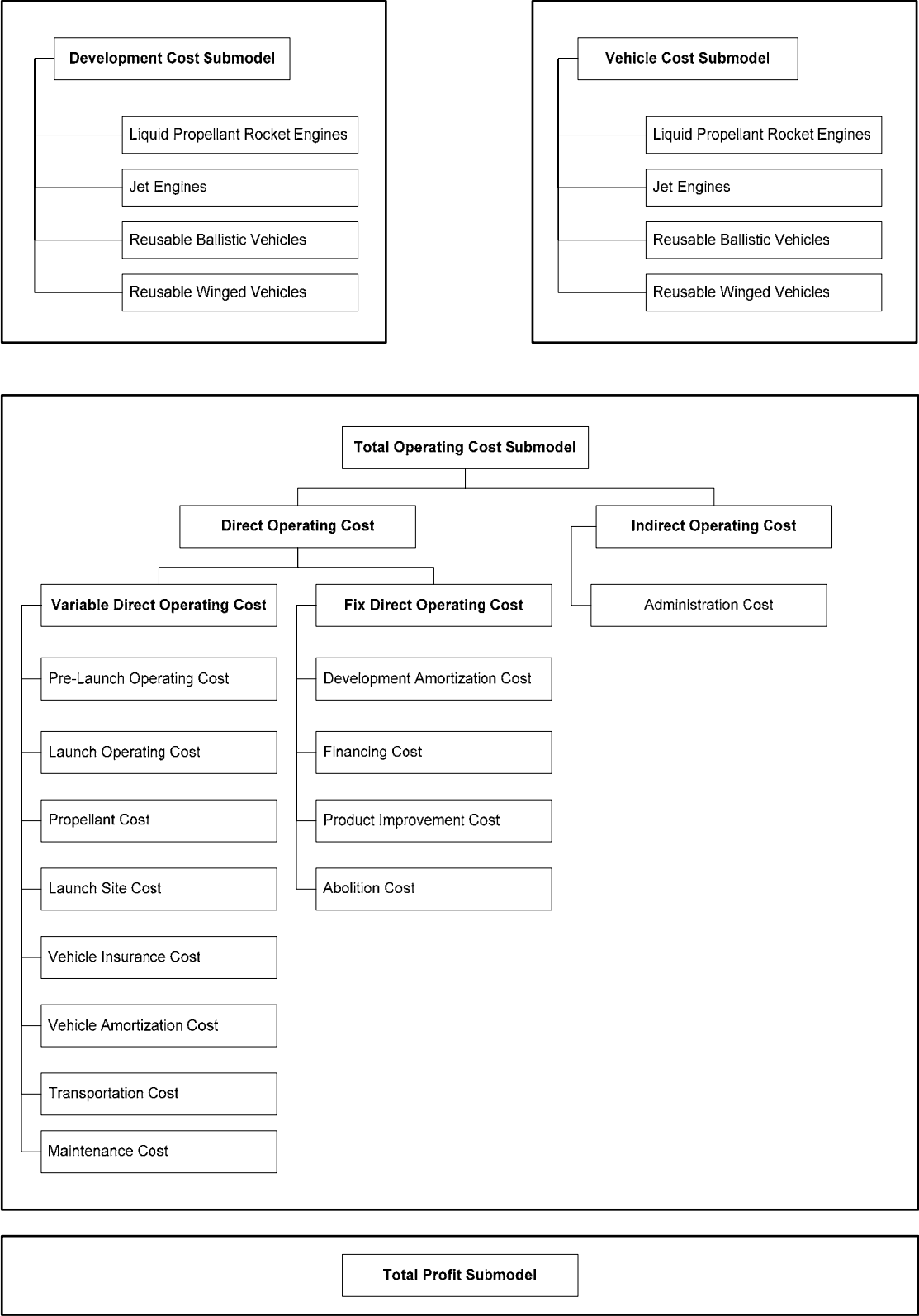


Fig. D.1: Model structure of SUBORB-TRANSCOST.²

REFERENCE

¹Koelle D., “*Transcost – Statistical-Analytical Model for Cost Estimation and Economic Optimization of Space Transportation Systems*”, Ottobrunn, Germany, 1991, 1999, 2003.

²Goehlich, A. R., “Space Tourism: Economic and Technical Evaluation of Suborbital SPACE Flight for Tourism,” Der Andere Verlag, 2002, ISBN 3-936231-36-2.

Appendix E VDK Sizing Code

An airbreathing launcher version sizing code is presented. This program is used to specify the range of “ τ ” mission requirements. The non-dimensional volume index, “ τ ”, has been introduced by Küchemann as a volume parameter. It can also be considered a slenderness parameter. “ τ ” is an essential parameter to relate configuration concept geometric properties across a diverse spectrum of configurations and to the sizing process.

The structure of the program is shown in Figure E.1 and Figure E.2. Figure E.1 shows the initial input and calculation of the sizing program. The sizing iteration process is shown in Figure E.2. It can be seen from these figures that trajectory, aerodynamics, and propulsion analyses are included in this sizing program. Among these discipline, propulsion is a dominator factor.

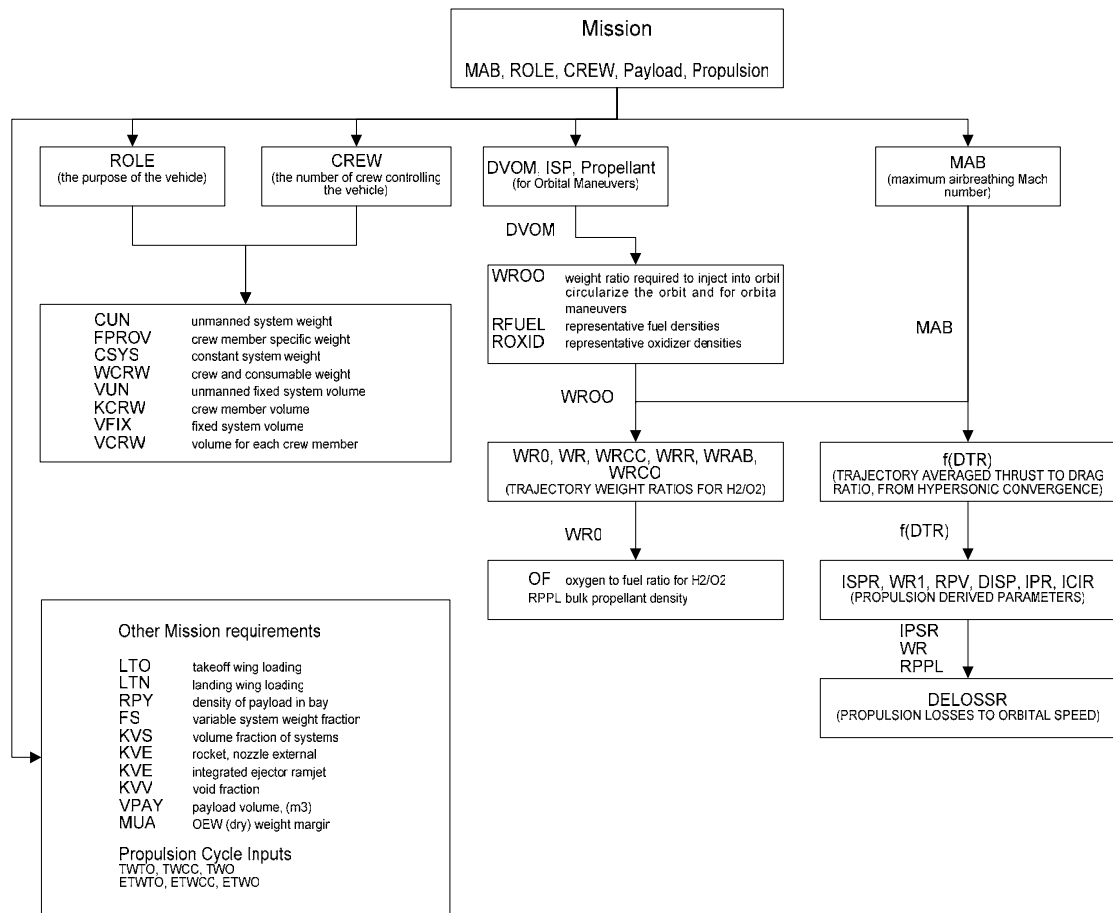


Fig. E.1: Initial inputs and calculation of the airbreathing sizing program.

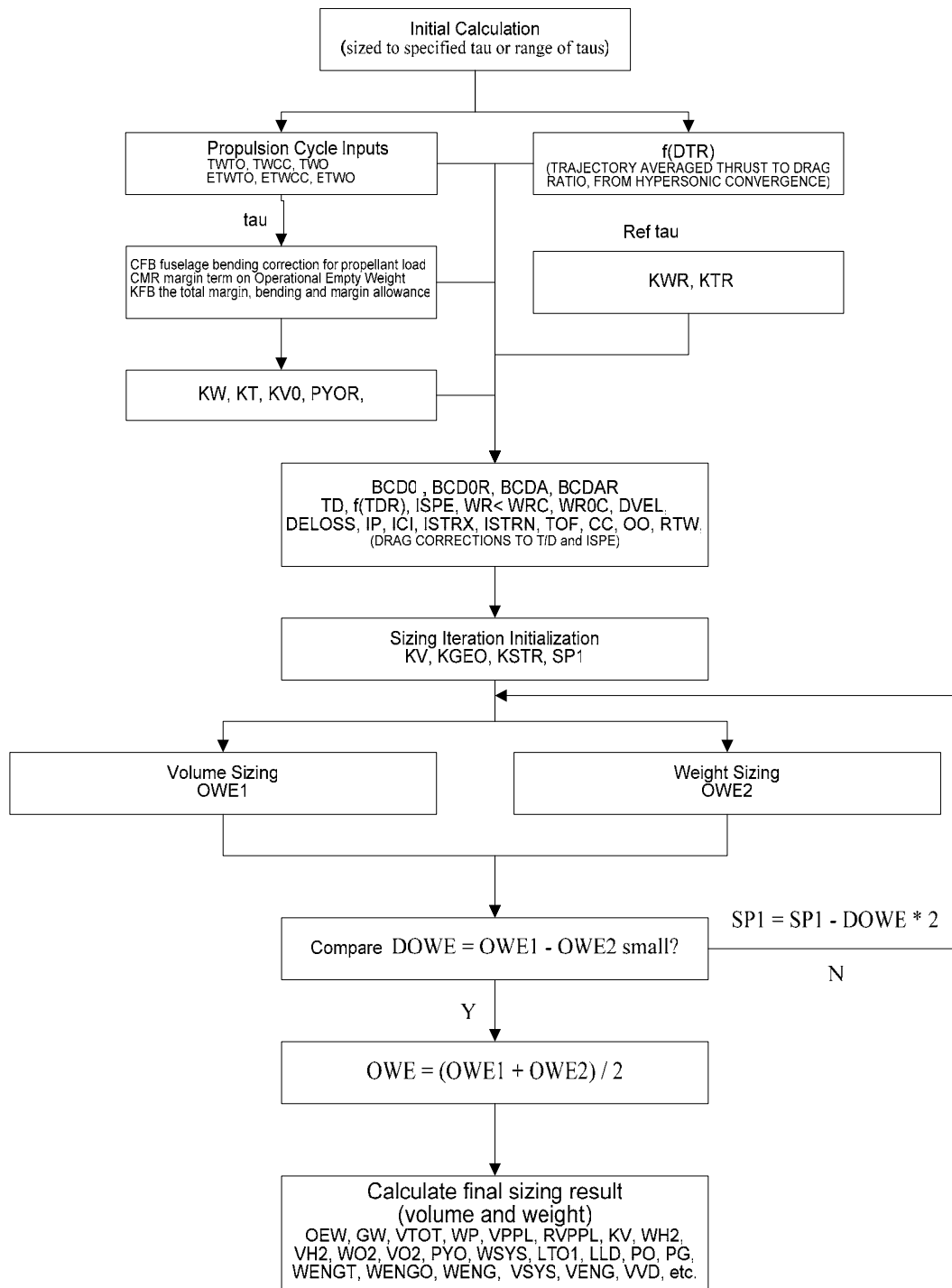


Fig. E.2: Iteration process of the airbreathing sizing program.

In Figure E.3, the geometry value of the *Michelle-B* is represented in green point, *DC-X* in orange point and OU XP in blue point. As can be seen, *Michelle-B*, *DC-X*, and *OUXP* fit this trend line very well. Thus, it is concluded that these vehicles are properly sized. The *Michelle-B* and *DC-X* lie in the lower corner of Figure E.3. In fact, the observation by Paul Czysz shows that this is the region of SAV with rocket engines only.

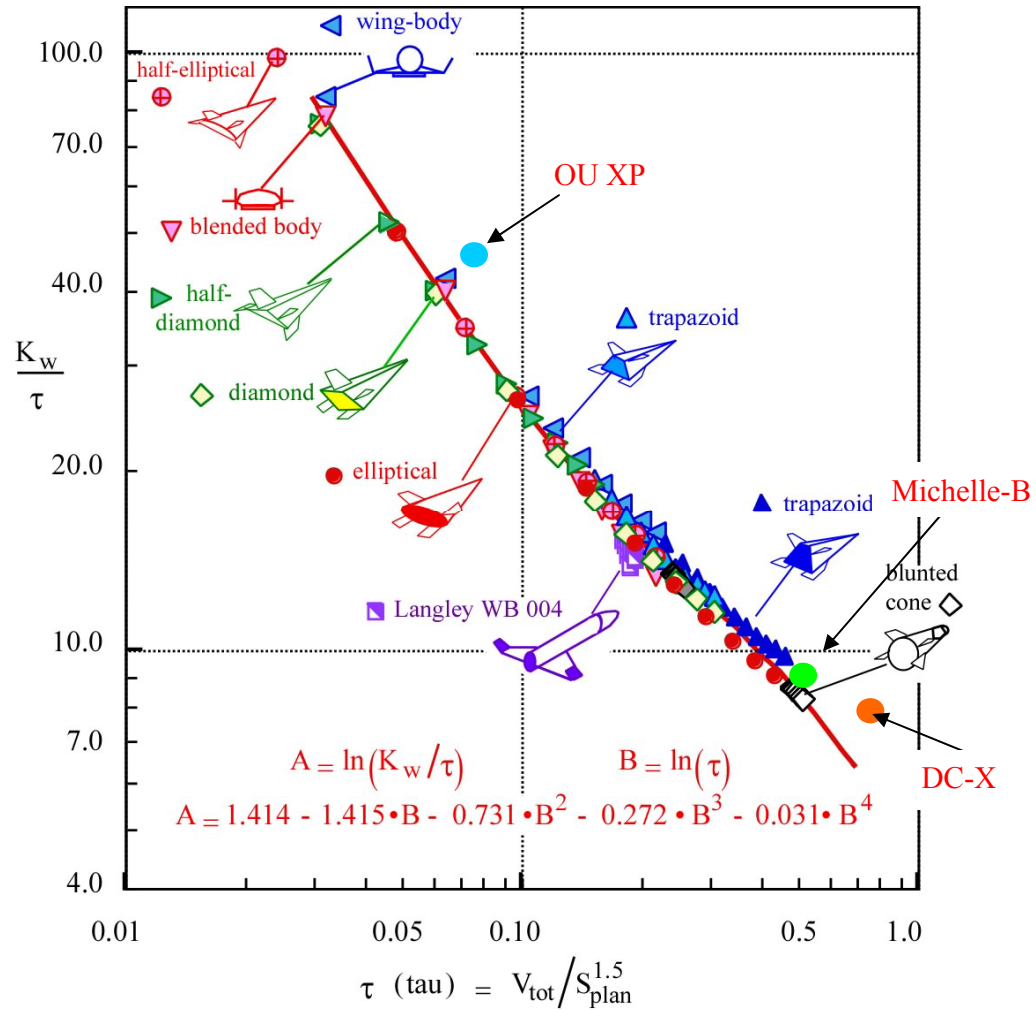


Fig. E.3: The variation of sizing geometry parameter (K_w / τ) with τ .¹

REFERENCE

¹Czysz, P. A., "Hypersonic Convergence," Parks College of Engineering and Aviation, Saint Louis University, St. Louis, Missouri, 2004.

Appendix F SpaceShipOne Case Study

In this section, the sub-synthesis design methodology for the reentry phase is used for the design analysis of the reentry flown by SpaceShipOne. The results are then compared with data collected during the record setting flight of SpaceShipOne on October 4, 2004.¹ Since the published data related to the SpaceShipOne flights are from the general press only, it is not possible to quantify the associated error throughout this validation; still, the case study is highly instructive. Clearly, due to the uncertainty of the data, the study can only be considered approximate to illustrate the capability of the design methodology. All the flight data of SpaceShipOne have been derived from articles published by Aviation Week & Space Technology¹ and Times². Table F.1 presents some SpaceShipOne vehicle data and flight input data required for the case study.

Table F.1: SpaceShipOne Data. ^{1,2}

Parameters	Data Input from Source
Weight	3086 kg
Flight Path Angle	80-90 degree
Altitude (start to glide)	57,000 ft - 80,000 ft
Max Deceleration	4 -5 g
Down Range	25 miles – 35 nm

The ballistic parameter of SpaceShipOne is estimated as,

$$z = \frac{g_0}{RT} = \frac{9.8}{(287)(288)} = 0.000118 \text{ m}^{-1}$$

$$\left. \frac{dV}{dt} \right|_{Max} = -\frac{1}{2} V^2 Z \sin \gamma = -3.26g$$

$$V = 741.51 \text{ m/s}^2$$

$$\frac{m}{C_D S} = 1040 \text{ kg/m}^2$$

$$\rho = \frac{m}{C_D S} \left(\frac{2g \sin \gamma}{V^2} + Z \sin \gamma \right) = 0.1574 \text{ kg/m}^2$$

This can be translated to an altitude h ,

$$\frac{\rho}{\rho_0} = e^{-g_0 h / RT} = e^{-Zh}$$

$$h = -\frac{1}{Z} \ln \left(\frac{\rho}{\rho_0} \right) = 17.39 \text{ km}$$

The first flight data of SpaceShipOne show that the altitude at which SpaceShipOne starts to glide, is around 57,000 ft (17.37 km).¹ According to those flight data, the above analysis showed that the ballistic parameter of SpaceShipOne is around 1040 kg/m².

References 1 and 2 show that SpaceShipOne wears thermal protection coating (carbon composite) on the nose, belly, and leading edges, which show no signs of real damage in two flights. If the stagnation temperature of SpaceShipOne during reentry is over 600°F,^{1,2} composite materials such as metal matrix and carbon fiber are required for a thermal protection system. As can be seen in Figure F.1, under these thermal constraints (e.g., the stagnation temperature is 600°F), SpaceShipOne is required to start to glide at an altitude above 50,000 ft. Also, since the glide ratio (L/D) of SpaceShipOne is around 7, from Eq. (4-44), the cross range (25 miles from launch point) can easily be achieved as soon as the vehicle starts to glide at an altitude of 4 miles.

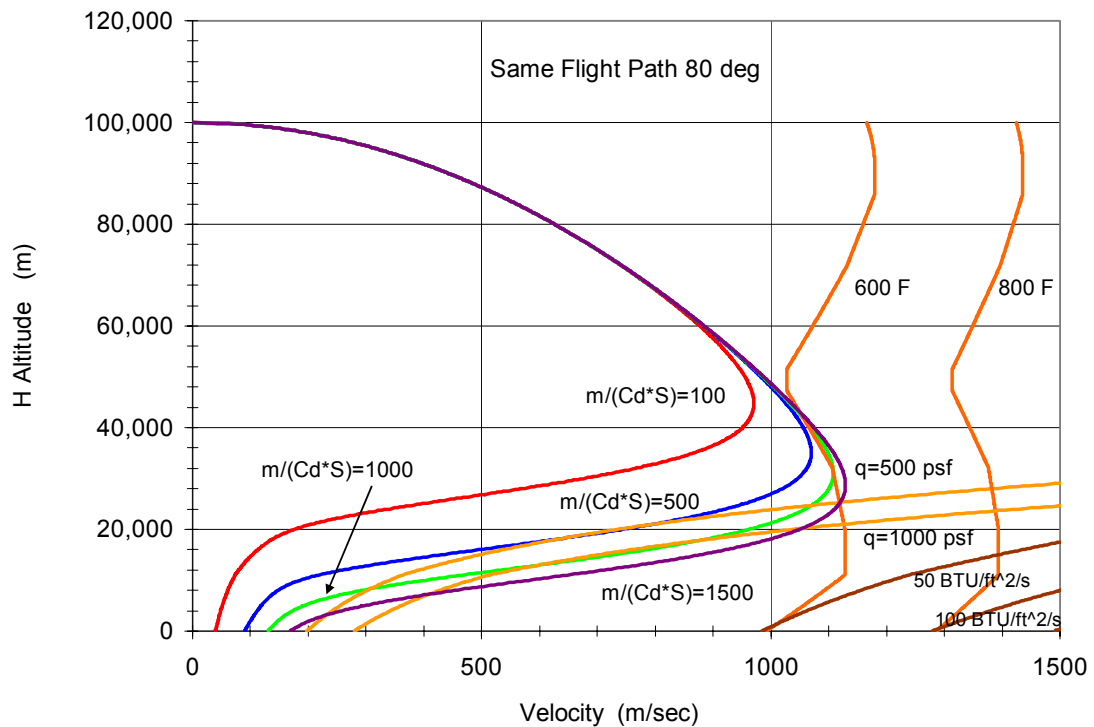


Figure F.1: Design space for the ballistic entry of a suborbital vehicle.

In summary, while a highly swept wing is usually applied to high speed vehicles to reduce wave drag, the wing shape of SpaceShipOne is strongly driven by the subsonic glide conditions (high L/D) and landing capability. The high lift coefficient ($C_{L_{max}}$) is the main driver for the wing shape of SpaceShipOne with little consideration of supersonic aerodynamic drag. Therefore, it is desired to find a balance between low speed and high speed design drivers.

REFERENCE

¹ SpaceShipOne Data, “*Aviation Week*,” pp 28-30, Jun 28, 2004 and pp 34-36, October 11, 2004.

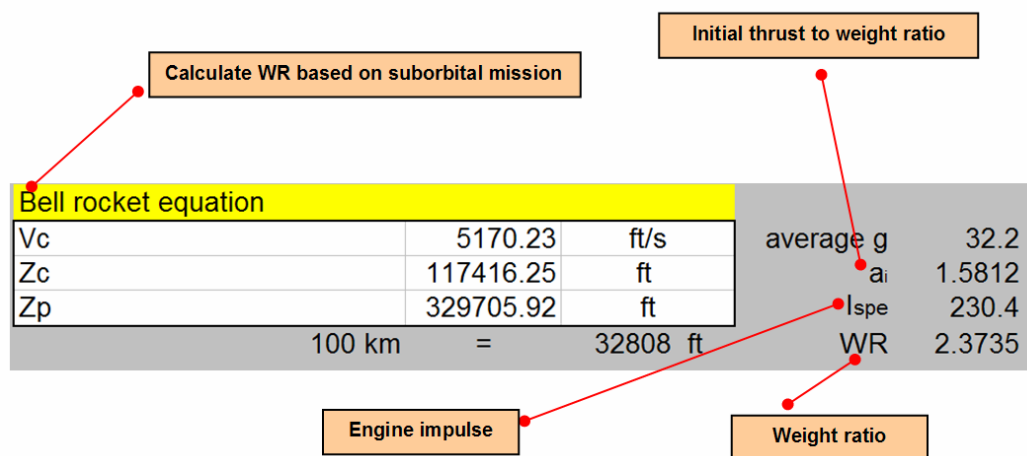
²SpaceShipOne Data, “*Time*,” November 29, 2004.

Appendix G Program User's Guide

This section provides a quick tour of all the programs developed for the “Hands-on” design methodology of SAV conceptual design. It includes performing some basic pre- and post-processing activities. The aim of this user's guide is only to provide the user a feel for how to routinely execute the program from program start to output visualization.

Weight and Sizing Program (SAV_ HASA): The user can follow the steps below for a quick tour of the program for an initial estimation of space vehicle weight and size.

- 1) Enter mission requirement - max altitude (100 km) and solve three Bell rocket equations simultaneously for the weight ratio (WR), I_{SP} (depending on the fuel combinations) and initial acceleration.



- 2) Define all design requirements, design constraints, and initial empirical engine data.

Mission and Design Requirement				
Maximum dynamic pressure	Q	=	500	psf
Payload	W _{pay}	=	1200	lb
Ultimate load factor	n	=	4	
Altitude	H	=	100	km
Thrust	T _{totrk}	=	27900	lb
Weight ratio	WR	=	2	
Total takeoff weight	W _{gtot}	=	19783	lb
Average TPS weight	W _{ins}	=	2	lb/sqft
Modifying factor	mf	=	1.25	
Rocket expansion ratio	A _{ratio}	=	25	
Engine number	N _{engrt}	=	1	

3) Estimate the vehicle geometry (e.g., based on the Learjet 25 fuselage) and wing configuration proposed for the design trade study.

Vehicle Configuration Sizing (HASA)			
GEOMETRY			
Vehicle Length, Forward Cone		12	ft
Vehicle Length, Cylinder		36	ft
Vehicle Length, Aft Cone		1.5	ft
Total Vehicle Length		49.5	ft
Fuselage diameter		5.25	ft
Equivalent Body Diameter		3.8	ft
Length/Diameter		15.94	
Body Wetted Area		500	ft ²
Nose radius			
Wing Area, S _{ref}		344	ft ²
Wing Span, b		22	ft
Wing taper ratio		0	
Wing sweep angle		35	
Wing thickness ratio		0.06	
Aspect Ratio, AR		1.44	
Wing Loading			lb/ft ²
Vertical Tail Area		30	ft ²
Horizontal Tail Area			ft ²
Volume Required		600	ft ³
Volume Payload			ft ³

4) Estimate space vehicle weight for different categories (such as payload, propulsion, structure, fuel, and subsystem). The process of geometry and weight estimations is an iterative process to configure an initial size of the vehicle to meet both mission and design requirements.

WEIGHTS			
Crew	400		
PAX	1200	lb	
Payload	1600	lb	
Fuel Tank	450	lb	
Turbojet	800	lb	
Ramjet		lb	
Scramjet		lb	
Rocket	390	lb	
Propulsion	1640	lb	
Body	1356	lb	
Wing	1032	lb	
Horiz., Vert Tail	204	lb	
Thermal Protection System	1188	lb	
Landing Gear	618	lb	
Thrust Structure	70	lb	
Structure	4467	lb	
Hydrogen		lb	
Oxygen		lb	
Other CH4, etc			
Fuel	9890	lb	
Avionics	383	lb	
Hydraulics	115	lb	
Electronics	402	lb	
Equipment	1282	lb	
Subsystems	2182	lb	
Operation Weight Empty	9890	lb	
Total Takeoff Gross Weight	19779	lb	

Weight estimation for different groups

HASA value is not good. Some modifications are made based on the more realistic statistical data for the similar mission.

Takeoff Analysis (SAV_BFL, SAV_CLM)

1. Calculation of Takeoff Field Length and Nose Liftoff Speed (SAV_BFL): The user can follow the steps below for a quick tour to calculate takeoff field length and nose liftoff speed.

1) Define the geometry and aerodynamics data of different wing configurations used for the takeoff study.

Wing geometry and Aerodynamics data						
	A	B	C	D	E	F
1	LE Sweep	78.0	70.0	60.0	45.0	
2	c/2 Sweep	39.0	35.0	30.0	22.5	
3	span	19.8	22.0	25.5	25.7	
4	mac	30.7	24.4	17.0	12.2	
5	S _{plan}	393.0	344.0	283.6	278.0	
6	S _{wet}	1,517.0	1,281.0	1,164.0	1,147.0	
7	K _w	3.860	3.724	4.104	4.126	
8	ϵ	0.990	0.986	0.982	0.998	
9	AR	1.01	1.44	2.31	2.40	
10	AR _{wet}	0.258	0.378	0.559	0.576	
11	AR*tan Λ_{LE}	4.752	3.956	4.001	2.400	
12	N	0.318	0.224	0.140	0.133	
13	K	0.05	0.05	0.05	0.05	
14	L'	0.368	0.274	0.190	0.183	
15	f/c	0.010	0.010	0.010	0.010	
16	taper ratio	0.00	0.00	0.00	0.25	
17	cos $\Lambda_{c/4}$	0.52250	0.60876	0.70711	0.83147	
18		0.27301	0.37059	0.50000	0.69134	
19	C _{Do}	0.0135	0.0132	0.0142	0.0144	
20	C _{LB}	0.768	0.714	0.657	0.587	
21	C _{Lo}	0.150	0.150	0.150	0.150	
22	M _B	0.57	0.49	0.42	0.36	
23		0.132	0.132	0.132	0.132	
24	C _{L TO}	0.450	0.527	0.635	0.648	
25	C _L *S	176.9	181.3	180.1	180.1	
26	q _{TO}	125.5	122.5	123.3	123.2	
27	q _{TO}	111.7	108.9	109.7	109.6	
28	C _{La}	0.0351	0.0437	0.0559	0.0574	
29	alpha ZL	4.27	3.43	2.68	2.62	
30	alpha	8.5	8.6	8.7	8.7	
31		0.47	0.55	0.64	0.75	
32	C _{LiB}	0.90	0.90	0.90	0.90	
33	W/S	56.23	64.24	77.93	79.50	
34	T/W	0.343	0.300	0.273	0.293	

2) Enter basic geometry of the baseline vehicle and airport runway condition.

	A	B	C	D	E	F
1						
2	c =	1.00	Z =	13.70	K1 =	1.04
3	d =	5.80	Z _T =	13.70	K2 =	0.45
4	b =	13.70	X =	12.70	CL =	0.70
5	μ _n =	0.025	n =	13.70	CD =	0.131
6	μ _m =	0.025	ξ =	12.70		
7	μ _{eff} =	0.025	β =	3.30		
8						
9			mac =	24.40		
10			Splan =	344.00		
11			Cm =	0.0253		
12			CL =	0.527		
13			W/S =	64.24		
14						

Basic geometry

Airport runway condition

3) Then, the climb gradient is calculated according to different lift coefficients. Select a reasonable combination of lift coefficient and climb gradient for the takeoff BFL analysis.

G	H	I	J	K
C _L	sin γ	sin γ	sin γ	sin γ
0.00	0.00	0.00	0.00	0.00
0.05	16.92	14.82	13.51	14.65
0.10	16.67	14.68	13.45	14.59
0.15	16.18	14.39	13.31	14.46
0.20	15.46	13.95	13.07	14.24
0.25	14.51	13.36	12.76	13.95
0.30	13.34	12.63	12.36	13.58
0.35	11.94	11.75	11.87	13.12
0.40	10.33	10.73	11.30	12.59
0.450	8.49	9.57	10.65	11.98
0.50	6.44	16.38	9.91	11.29
0.526		7.50		
0.55	4.17	6.81	9.09	10.53
0.60	1.69	5.23	8.19	9.69
0.635			7.51	
0.648				8.81
0.65	-1.02	3.50	14.87	15.99
0.70	-3.95	1.63	6.14	7.78
0.75	-7.11	-0.38	5.00	1.78
0.80	-10.53	-2.54	3.77	-2.13
0.85	-14.21	-4.84	2.46	-6.72
0.90	-18.19	-7.30	1.07	-12.03
	78	70	60	45

Lift coefficients

Climb gradient

Wing configurations

4) Finally, the takeoff field length and nose liftoff speed are estimated.

L	M	N	O	P	Q	R	S	T	U	V	X	Y	Z
C_L	$\sin \gamma$	$\sin \gamma$	$\sin \gamma$	$\sin \gamma$	C_L	V_{to}	V_{to}	V_{to}	V_{to}	C_L	XTO	XTO	XTO
0.40	8.49				0.40	334				0.50	9,205		
0.50		7.50			0.50		332			0.55		10,078	
0.70			7.51	8.81	0.70			333	332	0.80		10,842	9,764
C_L	Xgto	Xgto	Xgto	Xgto	C_L	X50	X50	X50	X50	Denom	23.6	17.1	10.0
0.40	1,793				0.40	593				Num	73	65	61
0.50		1,773			0.50		405			VNWLO	226	269	372
0.70			1,788	1,770	0.70			407	364	Cmcg	0.148	0.134	0.113
	numerator												
C_L	Xgto	Xgto	Xgto	Xgto	C_L	XR	XR	XR	XR	C_L			
0.40	0.2355				0.40	1,001				0.50			
0.50		0.2044			0.50		996			0.55			
0.70			0.1895	0.2106	0.70			1,000	995	0.80			
	denominator												
C_L	Xgto	Xgto	Xgto	Xgto	C_L	Vvert	Vvert	Vvert	Vvert	C_L			
0.40	7,611				0.40	2,957				0.50			
0.50		8,677			0.50		2,599			0.55			
0.70			9,436	8,405	0.70			2,614	3,047	0.80			
	78	70	60	45		78	70	60	45		78	70	60

2. T/W requirement for climb gradient (SAV_CLM): The user can follow the steps below for a quick tour to calculate T/W requirement for the initial climb.

1) Check the FAR 25 handbook to get climb gradient requirements for initial climb and second segment climb with different engine numbers. Enter the requirements into the related box as shown in the following figure.

	A	B	C	D	E	F	G	FAR 25 Climb Gradient Requirements
1								
2								
3		Takeoff Climb Gradient						
4		Initial Climb						
5								
6			T/W	=	1/LD + γ			
7								
8							Engine #	
9			γ	=	0.012		2	
10			γ	=	0.015		3	
11			γ	=	0.017		4	
12								
13		Horizontail Tail (HT)	L/D	=	5.160			
14		Canard	L/D	=	7.790			
15								
16							Engine #	
17		Horizontail Tail (HT)	T/W	=	0.206		2	
18			T/W	=	0.209		3	
19			T/W	=	0.211		4	
20								
21		Canard					Engine #	
22			T/W	=	0.140		2	
23			T/W	=	0.143		3	
24			T/W	=	0.145		4	
25			W/S (psi)	=	0	50	100	
26								
27		Horizontail Tail (HT)	T/W	=	0.206	0.206	0.206	
28		Canard	T/W	=	0.140	0.140	0.140	

2) Enter L/D ratio which is obtained from previous aerodynamic analysis.

	A	B	C	D	E	F	G	H
1								
2								
3		Takeoff Climb Gradient						
4		Initial Climb						
5								
6			T/W	=	1/LD + γ			
7								
8							Engine #	
9			γ	=	0.012		2	
10			γ	=	0.015		3	
11			γ	=	0.017		4	
12								
13		Horizontail Tail (HT)	L/D	=	5.160			
14		Canard	L/D	=	7.790			
15								
16							Engine #	
17		Horizontail Tail (HT)	T/W	=	0.206		2	
18			T/W	=	0.209		3	
19			T/W	=	0.211		4	
20								
21		Canard					Engine #	
22			T/W	=	0.140		2	
23			T/W	=	0.143		3	
24			T/W	=	0.145		4	
25			W/S (psi)	=	0	50	100	
26								
27		Horizontail Tail (HT)	T/W	=	0.206	0.206	0.206	
28		Canard	T/W	=	0.140	0.140	0.140	

3) Then, T/W requirements for the initial and second climb gradient are calculated.

	A	B	C	D	E	F	G	H
1								
2								
3		Takeoff Climb Gradient						
4		Initial Climb						
5								
6			T/W	=	1/LD + γ			
7								
8							Engine #	
9			γ	=	0.012		2	
10			γ	=	0.015		3	
11			γ	=	0.017		4	
12								
13		Horizontal Tail (HT)	L/D	=	5.160			
14		Canard	L/D	=	7.790			
15								
16							Engine #	
17		Horizontal Tail (HT)	T/W	=	0.206		2	
18			T/W	=	0.209		3	
19			T/W	=	0.211		4	
20								
21		Canard					Engine #	
22			T/W	=	0.140		2	
23			T/W	=	0.143		3	
24			T/W	=	0.145		4	
25			W/S (psi)	=	0	50	100	
26								
27		Horizontal Tail (HT)	T/W	=	0.206	0.206	0.206	
28		Canard	T/W	=	0.140	0.140	0.140	

Output T/W required

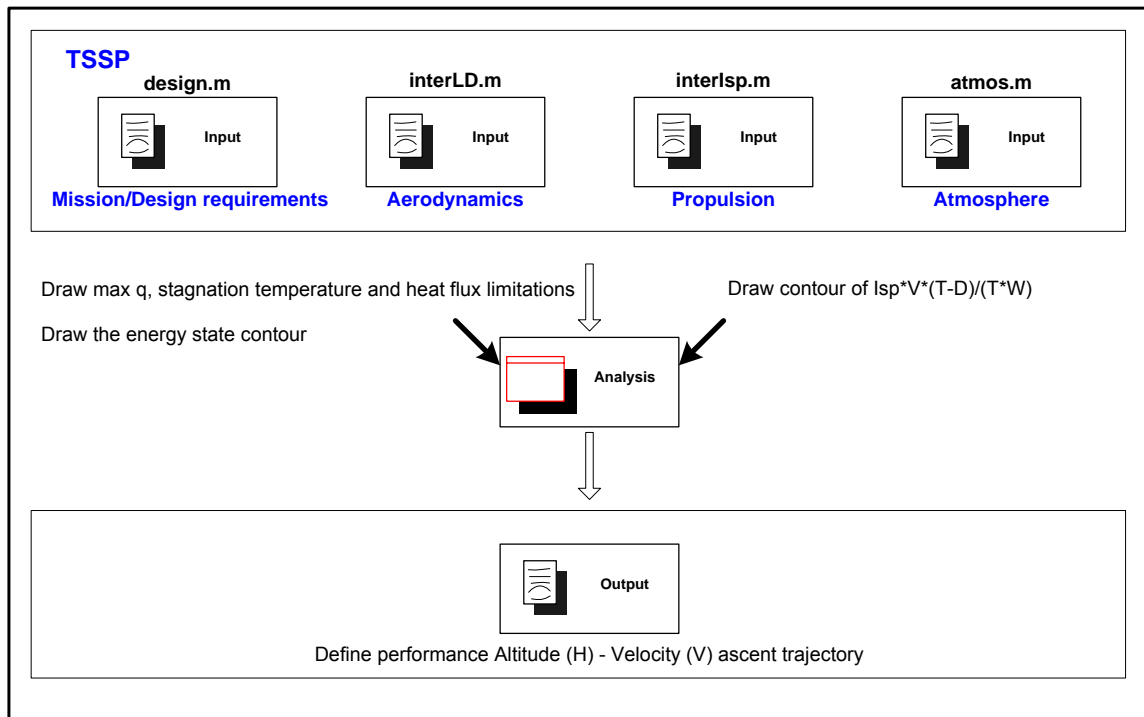
Ascent Trajectory Analysis Program (SAV_TSSP): The user can follow the steps below for a quick tour of **SAV_TSSP** to determine a near optimal ascent trajectory for the space mission.

1) Define the design constraints and mission requirements (energy contour lines) in a Matlab function file design.m.

2) Enter aerodynamic analysis data (e.g., lift and drag coefficient estimation using MDC wind tunnel data) in the Matlab function file interLD.m.

3) Enter propulsion design data (e.g., engine I_{sp} as a function of altitude) in the Matlab function file interIsp.m.

4) Enter the atmospheric condition (density, pressure, temperature) for the space mission in the Matlab function file atmos.m..



5) Execute the analysis module. It will draw the constraint lines for maximum dynamic pressure, stagnation temperature, and heat flux limitations. Also, the contour lines for the energy state and $I_{sp} \cdot V \cdot (T-D)/(T \cdot W)$ will be drawn.

6) Based on ESA technique and all the contour lines drawn in step 5, a near optimal altitude (H) – velocity performance diagram can be obtained.

Reentry Analysis (SAV_REENTRY): The user can follow the steps below for a quick tour of the following program to calculate the reentry performance.

- 1) Enter the vehicle mass, reference wing area, reentry flight path angle, and ballistic parameter.

The diagram shows a table titled 'Design Parameters' with the following data:

Design Parameters			
m	4050	kg	
Sw	245	ft^2	
γ	80	deg	
SIN	0.98		
COS	0.17		
m/Cd*A	1200	kg/m^2	
Cd*A	4.1666667		
an	0.17		
Z=g/RT	0.000118	m-1	

Callouts point to the following values in the table:

- Vehicle mass:** 4050 kg
- Wing area:** 245 ft^2
- Reentry flight path angle:** 80 deg
- Ballistic parameter:** 1200 kg/m^2

- 2) Enter the design constraints: the maximum dynamic pressure and temperature.

The diagram shows a table titled 'Design Constraints' with the following data:

Design Constraints			
q	500	psf	
	23939.48	pa	N/m^2
	1000	psf	
	47878.96	pa	N/m^2
	500	psf	
	23939.48	pa	N/m^2
Temperature	500	F	
	959.67	R	
	533.15	K	
	800	F	
	1259.67	R	
	699.82	K	
	1000	F	
	1459.67	R	
	810.93	K	

Callouts point to the following values in the table:

- Maximum dynamic pressure constraint:** 500 psf, 23939.48 pa, 1000 psf, 47878.96 pa
- Maximum temperature constraint:** 500 F, 959.67 R, 533.15 K, 800 F, 1259.67 R, 699.82 K, 1000 F, 1459.67 R, 810.93 K

3) Calculate the velocity, deceleration rate, load factor for the reentry phase.

The screenshot shows a table titled "Performance Data" with columns for various flight parameters. Four orange callout boxes with red arrows point to specific data points in the table:

- Altitude:** Points to the "h" column, specifically the value 100 in the first row of the first section.
- Load factor:** Points to the "n" column, specifically the value 0.94 in the first row of the second section.
- Reentry velocity:** Points to the "V" column, specifically the value 101.54 in the first row of the third section.
- Reentry deceleration:** Points to the "Z" column, specifically the value -2.53 in the first row of the fourth section.

The table data is as follows:

Performance Data						
g	h	s	V	a	"g"	an + at
	m	m				
9.8	100	101.54				
9.8	100	101.54				
9.8	100	101.54				
9.8	100	101.54				
9.8	100	101.54				
9.8	100	101.54				
9.8	100	101.54				
9.8	100	101.54				
9.8	100	101.54				
9.8	100	101.54				
9.8	100	101.54	0		0.94	
9.8	100	101.54	44.2718872	9.65	0.98	1.00
9.8	100	101.54	62.6099026	9.65	0.98	1.00
9.8	100	101.54	76.6811561	9.65	0.98	1.00
9.8	100	101.54	88.5437711	9.65	0.98	1.00
9.8	100	101.54	98.9949443	9.65	0.98	1.00
9.8	100	101.54	108.443527	9.65	0.98	1.00
9.8	100	101.54	117.132395	9.65	0.98	1.00
9.8	100	101.54	125.219795	9.65	0.98	1.00
U	V	W	X	Y	Z	AA
9.8	100	101.54	1014.31996	-24.78	-2.53	2.53
9.8	100	101.54	1011.79763	-25.16	-2.57	2.57
9.8	100	101.54	1009.23016	-25.55	-2.61	2.61
9.8	100	101.54	1006.61711	-25.94	-2.65	2.65
9.8	100	101.54	1003.95803	-26.33	-2.69	2.69
9.8	100	101.54	1001.25251	-26.71	-2.73	2.73
9.8	100	101.54	998.500132	-27.10	-2.77	2.77
9.8	100	101.54	995.700431	-27.49	-2.81	2.81
9.8	100	101.54	992.852967	-27.88	-2.85	2.85
9.8	100	101.54	989.95732	-28.27	-2.88	2.89
9.8	100	101.54	987.013091	-28.66	-2.92	2.93
9.8	100	101.54	984.01985	-29.05	-2.96	2.97
9.8	100	101.54	980.97719	-29.44	-3.00	3.01
9.8	100	101.54	977.884726	-29.83	-3.04	3.05
9.8	100	101.54	974.741996	-30.22	-3.08	3.09
9.8	100	101.54	971.548614	-30.60	-3.12	3.13
9.8	100	101.54	968.304215	-30.99	-3.16	3.17

Landing Analysis (SAV_LANDE, SAV_LANDA): The user can follow the steps below for a quick tour to calculate the landing performance.

1) **SAV_LANDE:** Enter the FAR landing field length, landing lift coefficients, and derive the wing loading requirements.

FAA Landing field Length - Empirical Method (Roskam)									
OU XP with 70 LE sweep									
OU XP with 70 LE sweep		Landing Field Length	=	10000	ft				
		SFL	=	$0.3VA^2$					
		VA	=	182.57	kts				
		VSL	=	140.44	kts				
		W/S	=	66.82					
		W/S	=	66.82	Climax	Climax	=	0.8	
TO		W/S (Low)	=	53.46				1.2	
		W/S (High)	=	80.19					

2) **SAV_LANDA**: Enter the gliding altitude, gliding path angle, approach speed, lift to drag ratio, ground coefficient, landing weight, wing area, landing lift/drag coefficients, and landing speed to calculate the gliding distance, flaring distance, and ground run distance.

Landing Performance Analysis - Analytical Method									
Space shuttle landing									
Glide		flaring		Ground run					
6.9	nm	=	41925.23	ft	6.9	nm	=	41925.23	ft
0.86	nm	=	5225.46	ft	0.86	nm	=	5225.46	ft
190	knot	=	320.72	ft	190	knot	=	320.72	ft
	H	=	10000	ft		CL	=	0.67	
	Y	=	17	deg		CD	=	0.15	
						V	=	320.72	ft/s
						u	=	0.40	0.4-0.6
						S	=	2690.00	ft*2
						W	=	187000.00	lb
						q	=	$1/2\rho V^2$	
						q	=	122.302108	
						L	=	220096.10	
						D	=	49348.90	
						a/g	=	0.19	
						Sg	=	$VL^2/(2ao)$	
						Sg	=	8271.32	ft
Flight data		Results		Flight data		% Difference			
SGL	=	34199.76	ft	34939	34199	-2.16			
SF	=	7725.46	ft	7700	7725	0.32			
S	=	50825.23	ft	8271	8900	7.07			
				50910	50824	-0.17			

Ground run		Ground distance		
6.9	nm	=	41925.23	ft
0.86	nm	=	5225.46	ft
190	knot	=	320.72	ft
CL	=	0.67		
CD	=	0.15		
V	=	320.72	ft/s	
u	=	0.40	0.4-0.6	
S	=	2690.00	ft^2	
W	=	187000.00	lb	
q	=	$1/2\rho V^2$		
q	=	122.302108		
L	=	220096.10		
D	=	49348.90		
a_0/g	=	0.19		
SG	=	$VL^2/(2a_0)$		
SG	=	8271.32	ft	

Comparison of flight data and analysis results			
Results		Flight data	% Difference
34939		34199	-2.16
7700		7725	0.32
8271		8900	7.07
50910		50824	-0.17

3) **SAV_LANDA**: Enter the FAR 25 missed approach climb gradient requirements and lift to drag ratio to obtain the T/W requirements.

Landing Missed Approach Climb Gradient					
Missed Approach Climb					
	T/W	=	1/LD + γ		
				Engine #	
	γ	=	0.021	2	
	γ	=	0.024	3	
	γ	=	0.027	4	
Horizontaltail Tail (HT)	L/D	=	5.160		
Canard	L/D	=	7.790		
				Engine #	
Horizontaltail Tail (HT)	T/W	=	0.215	2	
	T/W	=	0.218	3	
	T/W	=	0.221	4	
Canard				Engine #	
	T/W	=	0.149	2	
	T/W	=	0.152	3	
	T/W	=	0.155	4	
	W/S (psi)	=	0	50	100
Horizontaltail Tail (HT)	T/W	=	0.215	0.215	0.215
Canard	T/W	=	0.149	0.149	0.149

FAR 25 Climb Gradient Requirements

L/D ratio input from Aerodynamics Analysis

Output T/W required